The role of acute ambient hypoxia in the regulation of myostatin

Elliott, B.

The Role of Acute Ambient Hypoxia in the Regulation of Myostatin

Bradley Thomas Elliott

A thesis submitted in partial fulfilment of the requirements of the University of Westminster for the degree of Doctor of Philosophy

February 2015

"The significance of experiments on organisms as individual wholes, as leading towards the proper object and final purpose of biological investigation, - the discovery of the laws of life. Growth, anabolic and accumulating, has its reverse in all forms of katabolism [*sic*]."

As written by Stewart (1898; page 40) in the American Journal of Physiology, volume 1, issue 1, during an examination on the effects of barometric pressure on activity levels of rats.

Abstract

When exposed to chronic hypoxia by pathophysiological or environmental causes humans show muscle atrophy, challenging homeostasis and increasing mortality rate. Chronic hypoxia also presents with elevated myostatin peptide, a negative regulator of muscle size. This work induced acute hypoxia in healthy individuals; hypothesizing hypoxia would increase myostatin expression in both muscle and plasma in a concentration- and time-dependent manner. Hypoxia (1 % O_2) reduced C2C12 myoblast migration and myotube size *in vitro*. Myotube atrophy was time-dependent, longer exposures showed greater atrophy. Intracellular myostatin peptide was decreased at every time point measured. Myostatin and downstream signalling pathways in muscle showed a high degree of percentage similarity between mouse and human, when amino acid sequences were directly compared. Healthy males (N = 8) were exposed to 20.9 % O_2 or 11.9 % O_2 for 2 hours. Following hypoxic exposure myostatin peptide was reduced in muscle but not plasma, relative to control conditions. A second cohort (N = 8) was exposed to 12.5 % O_2 for 10 hours. Plasma myostatin was decreased following hypoxia, muscle myostatin trended towards increasing. A third cohort (N = 9; n = 8 lowlander, n = 1 Sherpa) was exposed to 10.7 % or 12.3 % O_2 for 2 hours. Plasma myostatin was reduced at both concentrations with no difference between concentrations noted. In response to chronic hypoxia, individuals lose muscle mass. Counter to the hypothesis of an increase in myostatin in both muscle and plasma, here a consistent decrease in plasma myostatin following acute hypoxia is seen. Muscle myostatin shows a variable response, with decreasing intracellular expression seen following a 2 hour hypoxic exposure, and trends towards an increase following 10 hours of hypoxia. Decreases in plasma and muscle myostatin may represent myostatin's movement towards peripheral compartments in these acute timeframes. Hypoxia alone is capable of altering myostatin in healthy individuals; the effects of hypoxia on myostatin appear to differ between the acute timeframes examined here and chronic exposures in environmental or disease models.

Acknowledgments

This work would not have been possible without the support and supervision of my Director of Studies, Dr Richard Mackenzie, and my co-supervisors Dr Derek Renshaw and Dr Stephen Getting. The balance of supervision and academic freedom allowed me to pursue a topic of interest and develop it into a complete thesis. A number of Westminster staff and students contributed, with particular thanks to Ms Maggie DePiero for blinded analysis, Ms Anna Kerékgyártó for assistance with Western blotting, Dr M. Gulrez Zariwala for assistance with *in vitro* techniques and Dr Paul Curley for tutelage in, and discussions surrounding, various bioinformatic approaches.

The projects described herein were collaborative in nature, and as such, involved a number of collaborators. My thanks therefore to Dr Peter Watt, University of Brighton, for use of laboratory spaces, discussions surrounding hypoxia and protein synthesis, as well as assistance with the gas chromatography-mass spectrometry methods. Professor Stephen Harridge of Kings College London, for the kind gift of the C2C12 cell line used herein. Professor David Howard, formally of the Centre for Altitude, Space and Extreme Environmental Medicine, University College London (amongst others), for collection of muscle biopsies as well as insightful discussions regarding human performance at extreme altitudes. Dr Tatum Simonson and Professor Peter Wagner of the University of California, San Diego, for my time there, discussions regarding human physiological responses to hypoxia, and individual variation in these responses. Dr Mark Kerrigan of Anglia Ruskin University for discussions surrounding rapid changes in cell morphology, as well as ongoing academic mentorship.

As a self-funded project, this work would not have been possible without external research funding. The Society for Endocrinology and Santander Banking Corporation provided financial support for research costs and consumables. The Society for Endocrinology and the Physiological Society also provided travel grants, training courses and opportunity to build the above mentioned collaborative links. Finally, the University of Westminster provided financial support to offset the cost of my studies.

All of my doctoral researcher colleagues within the Faulty of Science and Technology, University of Westminster, for their assistance and support throughout my studies.

My family for ongoing support throughout my studies, wherever in the world they continue to take me. Finally, my wife Melanie, who for some mad reason is still willing to read, correct and critique my work, as well as putting up with and supporting me during the production of this thesis.

Author's Declaration

I declare that the present work was carried out in accordance with the Guidelines and Regulations of the University of Westminster. The work is original except where indicated by special reference in the text.

The submission as a whole or part is not substantially the same as any that I previously or am currently making, whether in published or unpublished form, for a degree, diploma or similar qualification at any university or similar institution.

Until the outcome of the current application to the University of Westminster is known, the work will not be submitted for any such qualification at another university or similar institution.

Any views expressed in this work are those of the author and in no way represent those of the University of Westminster.

Signed: **Date:** 20 / 02 / 2015

Contents

Communications Arising

Peer Reviewed Publications

Accepted

1) **Elliott, B.**, Renshaw, D., Getting, S. & Mackenzie, R. (2012). *The Central Role of Myostatin in Skeletal Muscle and Whole Body Homeostasis.* Acta Physiol (Oxf), 205(3):324-40.

Representing theoretical discussions form within Chapter Two.

In Review

1) **Elliott, B.,** Renshaw, D., Getting, S., Simonson, T., Wagner, P., Watt, P. & Mackenzie, R. (submitted). *Acute hypoxia reduces plasma myostatin concentrations in otherwise healthy males.* J. Cachexia Sarcopenia Muscle. (in review).

Conference Oral Presentations

1) **Elliott, B.,** Debigare, R., Maltais, F., Getting, S., Renshaw, D. & Mackenzie, R. (2011). *Characterisation of a commercial human skeletal muscle cell line.* SSHB, Loughborough, UK.
2) **Elliott, B.,** Renshaw, D., Getting, S. & Mackenzie, R. (2012). *Hypoxia induces myotube atrophy in a time-dependent manner via NF-κB.* Proc Physiol Soc 2012.
3) **Elliott, B.,** Renshaw, D., Getting, S., Watt, P & Mackenzie, R. (2014). *Acute hypoxia alters myotube size in vitro and myostatin signalling in vivo.* FASEB J. vol 28 no. 1 Suppl. 1167.1.

Conference Poster Presentations

1) **Elliott, B**., Renshaw, D., Getting, S. & Mackenzie, R. (2012). *Myostatin and its downstream signalling pathways are well maintained between Mus musculus and Homo sapiens*. Proc Physiol Soc 2012.
2) **Elliott, B**., Renshaw, D., Getting, S., Watt, P. & Mackenzie, R. (2013). *Effect of acute hypoxia upon myostatin expression in healthy individuals.* Proc Soc Endo 2103 (P136).
3) **Elliott, B**., Renshaw, D., Getting, S., Watt P. & Mackenzie, R. (2013). *Plasma myostatin does not show a diurnal rhythm.* Endocr Rev, Vol. 34, MON-400.
4) **Elliott, B**., Renshaw, D., Getting, S., Watt, P., Howard, D., & Mackenzie, R. (2014) *The role of acute hypoxia in skeletal muscle atrophy.* Proc Physiol Soc 2014. PCB125.
5) **Elliott, B.,** Simonson, T., Getting, S., Renshaw, D., Wagner, P. and Mackenzie, R. (2015). Acute hypoxia reduces plasma myostatin independent of hypoxic dose. J Cachexia Sarcopenia Muscle. 6(4), 2-10.

List of Abbreviations

ActRIIB	Activin receptor type two B
ADH	Antidiuretic hormone
AMF	Autocrine motility factor (also known as GPI)
ALK4	Activin like kinase type 4
AMPK	Adenosine monophosphate kinase
AMS	Acute mountain sickness
ANOVA	Analysis of variance
ATCC	American Type Cell Culture
ATP	Adenosine triphosphate
AUC	Area under the curve
BLAST	Basic local alignment search tool
BMI	Body mass index
BSA	Bovine serum albumin
CHO	Chinese hamster ovary cell line
COPD	Chronic obstructive pulmonary disease
CHF	Chronic heart failure
CSA	Cross sectional area
DEC1,2	Deleted in oesophageal cancer 1, 2
DM	Differentiation media

DMEM	Dulbecco's modified Eagle media
DMSO	Dimethyl sulfoxide
DNA	Deoxyribonucleic acid
dPBS	Dulbecco's phosphate buffered saline
ECL	Enhanced chemiluminescence
EGLN1	Egl nine homolog 1
ELISA	Enzyme linked immunosorbent assay
ENO1	Enolase 1
EPAS1	Endothelial PAS domain-containing protein 1
EPO	Erythropoietin
ET1	Endothelin 1
ETS-1	E26 transformation-specific
FBS	Foetal bovine serum
FBR	Fractional breakdown rate
FEV_1	Forced expiratory volume in 1 s
FIH-1	Factor inhibiting hypoxia-inducible factor
FoxO	Forkhead box protein, O sub-family
FSR	Fractional synthesis rate
FVC	Forced vital capacity
GAPDH	Glyceraldehyde 3-phosphate dehydrogenase

GDF-8	Growth and differentiation factor 8 (more commonly myostatin)
GLUT1	Glucose transporter type 1
GM	Growth media
GPI	Glucose phosphate isomerase (also known by AMF)
GSK-3β	Glycogen synthase kinase three beta
HIF	Hypoxia inducible factor
HIV	Human immunodeficiency virus
HK1, 2	Hexokinase 1, 2
HR	Heart rate
IFN-ɣ	Interferon gamma
IGF	Insulin-like growth factor
IL	Interleukin
IGF-BP	Insulin-like growth factor binding protein
KRT14,18,19	Keratin 14, 18, 19
LAP	Latency associated peptide (specifically the myostatin latency associated peptide in this work)
LDH	Lactate dehydrogenase
LDHA	Lactate dehydrogenase A
LEP	Leptin
LLAMS	Lake Louise acute mountain sickness questionnaire
LPS	Lipopolysaccharide

LRP1	Low density lipoprotein receptor-related protein 1
MDR1	Multidrug resistance protein 1
MHC	Myosin heavy chain
MIC2	Transmembrane glycoprotein p30/32
mLLAMS	Modified Lake Louise acute mountain sickness questionnaire
NF-κB	Nuclear Factor Kappa light-chain enhancer of B cells
NIH	National Institute of Health
NIP3	Nineteen kDa interacting protein-3
NIX	Bcl-2 homology only protein
NOS	Nitric oxide synthase
NUR77	Nerve growth factor IB
OSA	Obstructive sleep apnoea
P#	Passage number
p35srj	Protein 35, serine rich junction
$p70^{s6k}$	Kinase phosphorylating S6 protein
PBS	Phosphate buffered saline
PFKBF3	6-phosphofructo-2-kinase/fructose-2, 6-bisphosphatase-3
PFKL	6-phosphofructokinase - liver type
PGK	Phosphoglycerate kinase
PKM	Pyruvate kinas M

PPARA	Peroxisome proliferator-activated receptor alpha
RER	Respiratory exchange ratio
RNA	Ribonucleic acid
RTP80	Regulated in development and DNA damage responses
SD	Standard deviation
SDS	Sodium dodecyl sulfate
SEM	Standard error of the mean
SNP	Single nucleotide polymorphism
SaO_2	Arterial oxygen saturation
SpO_2	Peripheral capillary oxygen saturation
TBS-T	Tris-buffered Saline with tween
TGF	Transforming growth factor
TNFα	Tumour necrosis factor alpha
TPI	Triose-phosphate isomerase
VEGF	Vascular endothelial growth factor
VHL	von Hippel Lindau
VIM	Vimentin
WAF1	Protein p21

List of Figures

List of Appendix Figures

List of Tables

List of Appendix Tables

Chapter One – Introduction

1.1 Introduction

Skeletal muscle tissue is ubiquitously found throughout all members of the Kingdom Animalia. There is evidence for maintenance of muscle tissue throughout evolutionary history, with fossilized evidence for striated muscle tissue dating 560 million years (Liu et al., 2014). In the non-obese human, skeletal muscle is the largest tissue type by volume and the only tissue capable of producing locomotion via mechanical contraction (Janssen et al., 2000, Rennie et al., 2004). In the adult human, muscle mass shows sexual dysmorphism, with males (20 – 30 years of age) normally showing 40 – 45 % of body mass as lean muscle mass, while females of a matching age tend towards 30 – 35 % (Janssen et al., 2000). The proportion of lean muscle mass decreases with age, with males showing a more rapid decrease than females (Janssen et al., 2000). In addition to its role in locomotion, skeletal muscle is key in thermoregulation, metabolism and endocrinology (Rennie et al., 2004).

Muscle is a highly plastic tissue and adapts to external stimuli to better suit its altered environment. Galan (AD ca. 129 – 200) wrote of the hardening of tissues and increases in strength seen in exercised individuals. Further, Galen states that exercise is “extremely beneficial for health” increasing metabolism and respiration, and preventing sickness (Singer, 1997). It can be seen therefore that the plasticity of muscle mass and the importance of muscular tissue in the maintenance of health has long been recognised. Indeed, as will be examined in the literature review of this thesis, chronic pathophysiological disorders typically show losses in muscle mass and this loss of muscle mass correlates with reduction in quality of life and increased mortality.

Hypoxia is a challenging physiological stimulus to any obligate aerobe, which must therefore adapt to survive or perish. Hypobaric hypoxia results in a reduction of body mass (Hoppeler et al., 1990, Rose et al., 1988), alters activity levels (Stewart, 1898), inhibits regeneration following injury

(Chaillou et al., 2014), and as Robert Boyle demonstrated, can be detrimental to life. Small insects, birds and mice rapidly lose consciousness in a low pressure environment, but can be revived if returned to ambient atmospheric pressure quickly enough (Boyle, 1660). A similar effect was seen on the 1st of December, 1893 when Jacques Charles ascended to ~ 3,000 m in his new invention, a hydrogen balloon. He records feeling faint and dizzy, and experienced a painful popping in his ears. Panicked by this experience, he rapidly descended (Mainardi et al., 2013). Charles inadvertently put himself in the same position as Boyle's mice, experiencing hypobaric hypoxia without suitable time to adapt.

It is now well understood that oxygen is a necessary step for metabolism in obligate aerobes, for the oxidation of freed hydrogens from Krebs cycle (reviewed by Kalckar, 1991, Pollock et al., 2015, Harridge et al., 1999). Death, by the majority of causes, ultimately results from a lack of oxygen supply, either focally or globally. Individual tissues vary in resilience to hypoxic stressors. Neural and cardiac tissues are metabolically demanding, thus a lack of oxygen supply rapidly results in cellular death. In comparison, cartilage *in vivo* is avascular and metabolically undemanding; chondrocytes *in vitro* can survive at least 7 days without oxygen supply (Grimshaw and Mason, 2000). Muscular tissue is constantly stressed by variations in oxygen supply (Marshak and Maeva, 1956), and is capable of surviving to and adapting to moderate hypoxic insults. As will be discussed in detail below, repeated or prolonged exposure to hypoxic conditions result in adaptation, altering metabolic and structural factors to better cope with future hypoxic events.

Thus, the study of the consumption of oxygen by metabolic tissues and the response to a lack of oxygen is central to the understanding of physiology. A central premise of this thesis is that muscle tissue adapts rapidly to hypoxic stressors with hypoxia instigating processes that, if left unchecked, will result in a loss of muscle mass.

In the review of literature to follow, an examination of the research surrounding muscle and the regulation of muscle size will be conducted. Particular focus will be given to myostatin and its role in the regulation of muscle mass. Following this, this thesis will examine hypoxia and its effects on the human. The physiological differences between normobaric and hypobaric hypoxia are examined. Finally, interactions between hypoxia and muscle mass are discussed, before the central aims and hypothesis are presented.

Chapter Three of this work presents a series of experiments conducted in C2C12 myoblasts and myotubes *in vitro*. Cells were stimulated with 1 % O_2 for varying lengths of time and myoblast chemotaxis and myotube atrophy was directly quantified. Changes in myostatin and other downstream cell signalling markers of atrophy were examined and comparison of these variables between normoxic and hypoxic conditions performed. As *in vitro* work was performed in the murine C2C12 myoblast cell line (Yaffe and Saxel, 1977), and the following Chapters used hypoxia in healthy humans as a research model, a bioinformatic analysis is also presented in Chapter Three examining the structure differences and similarities between myostatin protein in the mouse and the human, as well as the cell surface receptors and intracellular signalling pathways associated with myostatin's activity.

In Chapters Four, Five and Six healthy humans were exposed to hypoxic environments of varying concentrations and durations in an attempt to extend those findings shown in Chapter Three into a human research model. Specifically, Chapter Four examines the effect of 2 hours hypoxia, Chapter Five extends this to 10 hours to examine the effect of time in hypoxia and Chapter Six uses 2 hours but varies concentration of O_2, to examine the effect of oxygen concentration. Plasma myostatin concentration is quantified by ELISA and intracellular myostatin peptide expression is semi-

quantified by Western blot from skeletal muscle biopsies. Downstream markers of proteasomal activity are investigated within muscle biopsies, with particular focus on ubiquitin binding.

Finally, Chapter Seven of this work draws comparisons of findings between experimental Chapters. As myostatin is a significant regulator of muscle mass, alterations in myostatin expression in response to hypoxia in the models researched here is likely to be relevant across a number of hypoxic conditions. A discussion of the meaning of these findings with relevance to hypobaric hypoxia in mountaineering, pathological hypoxia in disease states, and with regards to wider physiology follows. Limitations of this work are discussed then recommendations for future work are presented. Finally, conclusions are drawn. As proposed by Stewart (1898), and through the examination of 'organisms as individual wholes', this work aims to add to the knowledge of the regulation of homeostasis and further the understanding of the laws of life.

Chapter Two – Review of Literature

2.1 Scope of Review

In the review of literature to follow, the form and function of skeletal muscle and its plasticity will be examined, which will lead into a discussion of the regulation of muscle size by the hypertrophy or atrophy of myocytes, and the major intracellular signalling pathways involved in this. With the uncovering of myostatin as a key regulator of muscle mass (McPherron et al., 1997) and subsequent understanding of its importance in muscle homeostasis (Allen et al., 2011, Rodriguez et al., 2014), particular focus will be placed on the role of myostatin signalling in the regulation of the size of myocytes.

In conditions where oxygen supply to skeletal muscle is reduced, atrophy of this muscle subsequently occurs (Bernard et al., 1998, Hoppeler et al., 1990, Rose et al., 1988). Section 2.5.1 and 2.5.2 of this work therefore focus on different causes of peripheral tissue hypoxia, both in health and disease states, and the homeostatic reaction to hypoxic stimuli, both phenotypically and with reference to the cellular signalling response within myocytes. Tissue hypoxia as caused by decreases in barometric pressure, ambient oxygen concentration and pathophysiological impairments will be considered, and the comparisons between will be drawn. This review, and the greater thesis as a whole, concentrates on tissue hypoxia as caused by impairment of oxygen delivery (hypoxemic hypoxia). As such, histotoxic hypoxic disorders of oxygen usage, as caused by narcotics, cyanide and similar cytotoxic substances, are not considered.

Finally, some recent work examining the effect of hypoxia, both ambient and pathophysiological, on muscle mass and myostatin signalling will be examined. This will lead to an identification of current knowledge gaps within the field, before logically arising experimental aims and hypothesis driving the subsequent experimental Chapters of this thesis will be presented.

2.2 Skeletal Muscle

2.2.1 Form and Function

Individual skeletal muscles are typically found peripherally, superficial to the skeletal frame of the human body. In the human and other mammalian species, muscle can be sub-divided into three distinct tissue types; skeletal muscle, cardiac muscle and smooth muscle, each with differing phenotype and roles. Unless otherwise specified, in this work the term muscle is in reference to skeletal muscle. Mature myocytes in adult human muscle are found as multinucleate, terminally differentiated myofibers, arranged in striated bands (Figure 2.1A). Myofibers are terminally differentiated and increases in muscle mass are therefore primarily the result of cellular hypertrophy (Chambers and McDermott, 1996).

The internal structure of a myofiber is approximately 90 % sarcomeres by volume, formed into parallel strands of myofibrils. Within a sarcomere, myosin heads cycle in an ATP-dependent manner, applying force on actin filaments, and thereby contracting and shortening the sarcomere (Figure 2.1B and C), a process known as cross bridge cycling. Sarcomeric contraction, both in parallel and serial, thus results in contraction of muscle (Gordon et al., 2000).

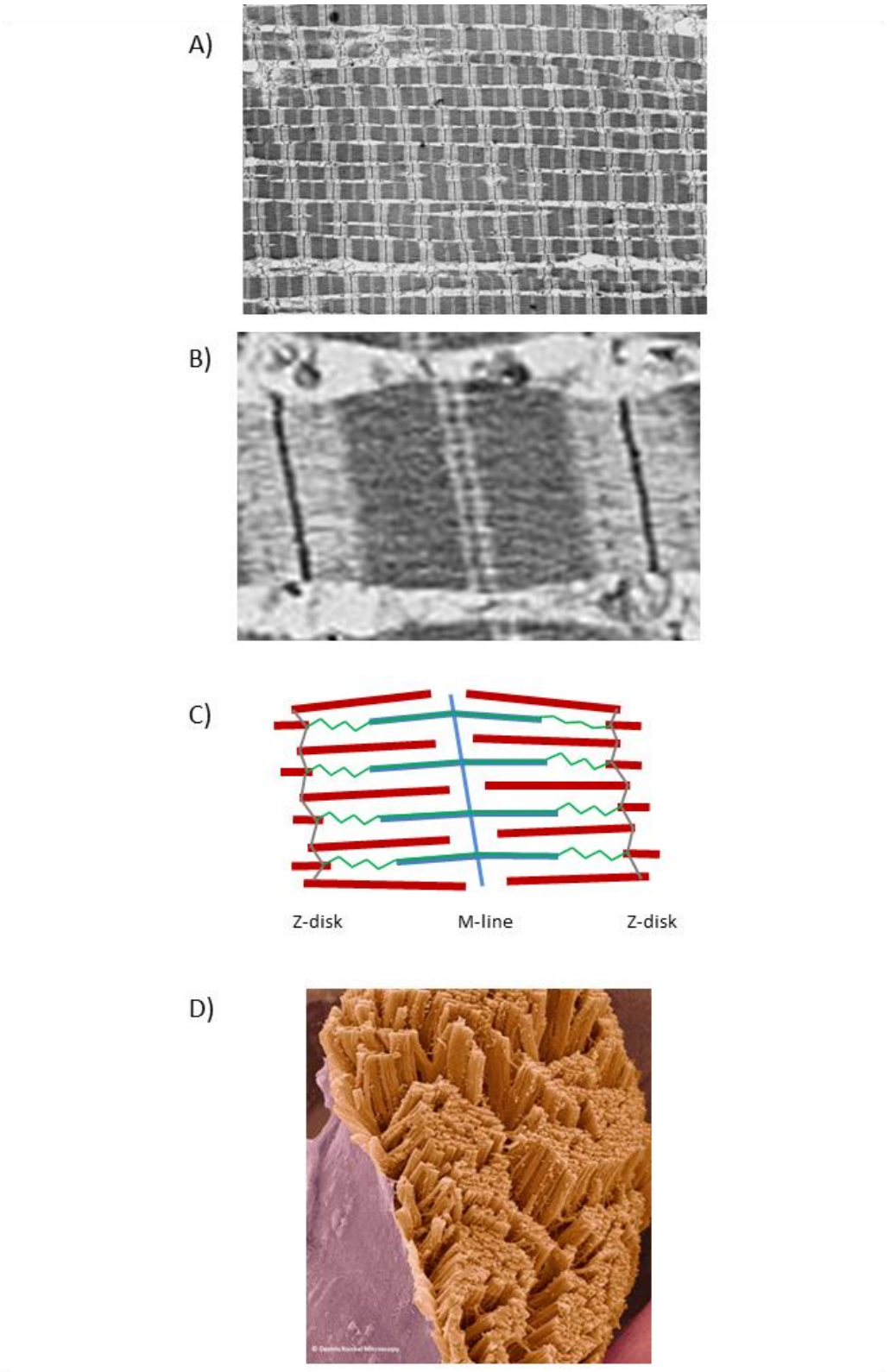

Figure 2.1: Sarcomere of skeletal muscle. A) Electron microscope image. B) A single sarcomere. C) Schematic of actin (red), myosin (blue), Titin (green) and α-actinin (grey). D) Individual myofiber shown, transversely sectioned and viewed by scanning electron microscope. Artificially coloured, yellow strands represent sarcomeres. Pink wall indicates the cellular sarcolemma. A) and B) taken from Sugi and colleagues (1998). D) taken from (Srivastava et al., 2012)

Whilst actin and myosin make up the large majority of sarcomeric proteins (Figure 2.1d), acting together to produce mechanical force, a number of other key structural proteins have been identified. Titin forms the third most abundant structural protein, after actin and myosin, and also forms the largest protein found in humans, with a mass of 3.5 MDa (Baranano and Hartman, 2008). Titan anchors to the M-line, extending from the end of a myosin filament, connecting to the Z-disk. Titin contributes to the electric property of muscle, acting as a molecular spring (Cox and Clarke, 2014). In cardiac muscle, loss of function mutations of titin results in restrictive cardiomyopathy, reflecting the role of titin in elasticity (Peled et al., 2014). Myomesin is primarily found on the M-line band of sarcomeres. It shows an affinity for both titin and myosin (Horscroft and Murray, 2014), and as such, is thought to play a role in anchoring titin to the M-line.

The lateral edge of each sarcomere (assuming convention of sarcomere aligned left-right, as shown in Figure 2.1a - c), primarily consists of overlapping actin filaments of two neighbouring sarcomeres cross-linked by α-actinin, allowing transmission of force between sarcomeres (Edwards et al., 2014). Four sub-grouping of α-actinin exists (1 - 4), with α-actinin-2 and -3 being found within sarcomeres of both cardiac and skeletal muscle (Lexell et al., 1983). Mutations of α-actinin-3 are common, suggesting some interchangeable roles between the α-actinins (Owen et al., 1974).

Dystrophin forms structural links between actin filaments and the sarcolemma, allowing the transfer of sarcomeric mechanical force from the interior of the cell to the exterior (Hoffman et al., 1987). Dystrophin nonsense or loss of function mutations are associated with myodystrophic disorders that result in reduction in muscle function, fragility of myofibers and death (Alchin, 2014).

Individual myofibers within a muscle express differences in metabolic consumption and force output. Historically, muscles were characterised as red or white; these visual differences in colour

arising through differences in internal myoglobin content. Red muscles, with a higher amount of myoglobin content are a more oxidative type than white muscle, which are more glycolytic in both characteristic and function (Cassens and Cooper, 1971). Muscles and their individual component myofibers can be distinguished by expression of myosin heavy chain (MHC) isoforms. Individual myofibers within muscle express different MHC isoforms (Figure 2.2A and B) and subsequently make up the muscle 'type', with slow type muscles having a higher proportion of type I fibres and fast fibres having a higher proportion of type II fibres (Josephson, 1993). Force production of individual myofibers varies, with stimulation of isolated type I fibres producing a twitch force less than type II (Close, 1965).

Current evidence suggests myofibers contain four different MHC isoforms. Rat muscle contains four detectable MHC isoforms that can be isolated by Western blot, type I, IIA, IIX and IIB (Schiaffino et al., 1989). Individual excised fibres from the rat have four different contraction phenotypes that correspond to these isoforms (Bottinelli et al., 1994a, Bottinelli et al., 1994b). In the human MHC type I, IIA and IIX have been identified, with IIX replacing the historically mislabelled IIB isoform (Ennion et al., 1995).

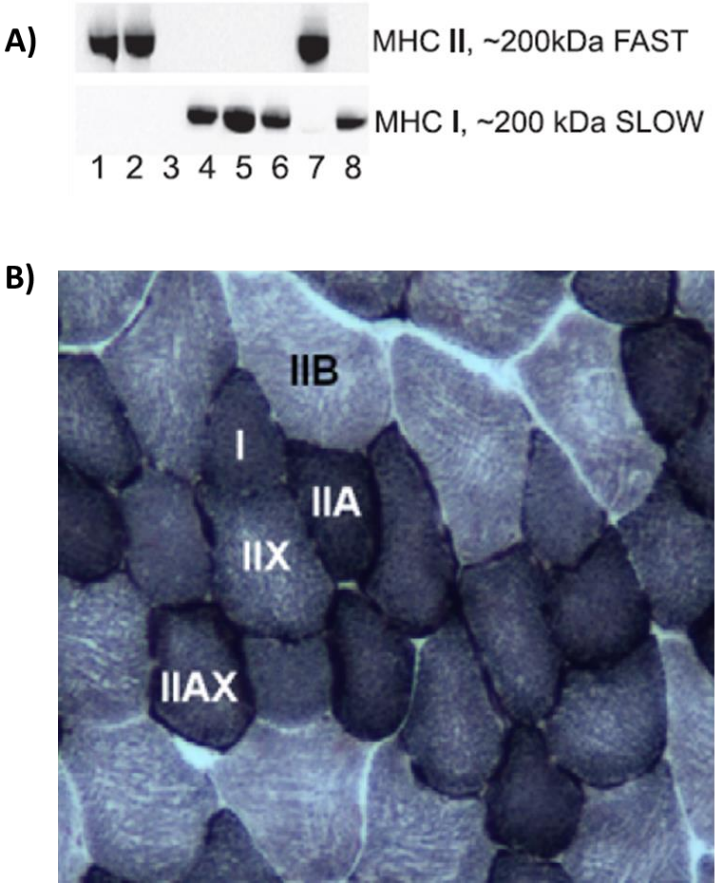

Figure 2.2: Myosin heavy chain differences between individual myofibers. A) Single fibre Western blot from human vastus lateralis, probed for MHC I and II. Individual gel lanes numbered 1 – 8, lane 3 shows negative control, no protein loaded (Murphy, 2011). B) Immunohistochemistry of rat tibialis anterior, stained for succinate dehydrogenase (Bloemberg and Quadrilatero, 2012).

The primary function of skeletal muscle is to induce movement. Voluntary stimulation from the somatic nervous system results in coordinated contraction of muscle to induce movement of one aspect of the body relative to another. Another function of skeletal muscle is thermoregulation, as human muscle is only ~ 25 % efficient in converting chemical potential energy into mechanical contraction (Andersen and Saltin, 1985), the majority of this remainder of energy is lost as heat which helps maintain the optimal internal body temperature for enzymatic reactions. Muscle also forms a major store of amino acids (AA) within the body, with atrophy of muscle releasing AA which can be used metabolically (Murray and Montgomery, 2014).

2.2.2 Plasticity

Skeletal muscle myofibers show a high degree of plasticity, and are capable of hypertrophy or atrophy as challenging environments or stimuli dictate. In the presence of available amino acids, the application of mechanical load over time results in an increase in the size of muscle mass (Goldspink et al., 1983, Koong et al., 1994b), resulting from hypertrophy of individual cell components, and is driven primarily by an Akt-mammalian target of rapamycin (mTOR) dependent pathway (Rennie et al., 2004; reviewed below).

Phenotypic increases in muscle mass results from increases in myofiber size (Goldspink, 1986). This increase in size results from increases in protein synthesis for the construction of new sarcomeres, which can be added in parallel, increasing force production, or in serial, increasing length and speed of myofiber contraction (Goldspink, 1986, Goldspink et al., 1983). Force production by individual myofibers is a function of cross sectional area (Figure 2.3), representing the increase in sarcomere number (Krivickas et al., 2011). Phenotypic atrophy results in a reverse process, with loss of sarcomeric proteins resulting in reductions in myofiber size and ultimately losses in muscle mass. One noted exception to this is in sarcopenia, where both hypoplasia and atrophy are noted (Lexell et al., 1983, Green et al., 1989).

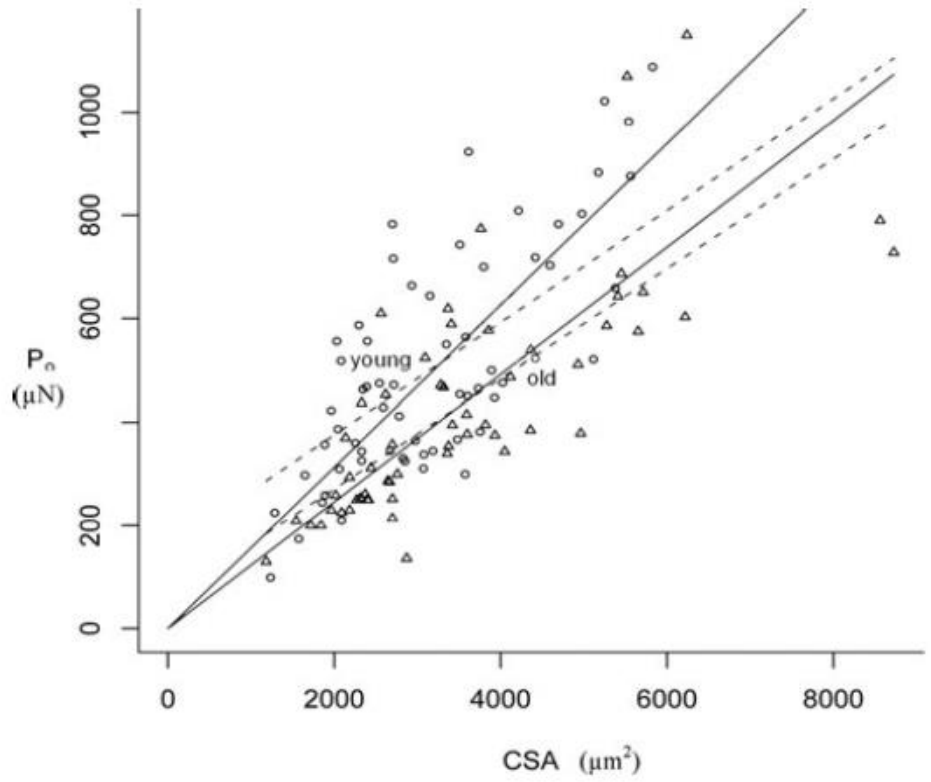

Figure 2.3: Force production in isolated myofibers as a function of cross-sectional area (CSA). Force production (μN) as a function of CSA (μm^{-1}) form young (circles) and old (triangles) individuals. Muscle biopsies taken from vastus lateralis. Taken from Krivickas and colleagues (2011).

This hypertrophy primarily occurs in a muscle specific manner in response to repeated mechanical loading, with loaded but not unloaded muscle groups showing adaptation (Housh et al., 1992, Wilkinson et al., 2006). Power lifters are noted to have larger myofiber cross-sectional area than control participants, however the hypertrophy is notably greater in the type IIa and IIb fibres (~ 100 % over control) than in type I (~ 50 % over control), and proportion of type II fibres is increased over type I (Kadi et al., 1999). These results are also found with short term resistance training in untrained humans (Widrick et al., 2002) and mice (Matsakas et al., 2006). These changes are stimulus dependent, as aerobic exercise training (60 minutes session, 4 × week, 5 months in untrained individuals) increases type I but not type II fibre cross sectional area (Gollnick et al., 1973). Adaption of muscle can be seen therefore to occur in a specific manner in response to specific stimuli.

During times of physiological stress, starvation or disease, losses in muscle mass often occur (Jackman and Kandarian, 2004). While all proteins in mammalian cells are constantly being degraded and replaced (Mitch and Goldberg, 1996), elevated protein degradation rates (above those of the rate of synthesis) result in losses of muscle mass, primarily via increased protein breakdown by the proteasomal pathway (reviewed below). Inhibition of proteasomal activity offsets muscle atrophy during denervation (Tawa et al., 1997). Disuse following lower limb surgery or fracture causes losses in both type I and II fibres size that are approximately equal in magnitude between fibres (MacDougall et al., 1991, Coyle, 2005, Hirofuji et al., 1992). With aging-induced muscle loss atrophy is fibre dependent, predominantly affecting type II fibres (Jobin et al., 1998, Lexell et al., 1988, Sullivan et al., 1997). This disparity between disuse atrophy and aging-induced atrophy suggests sarcopenic atrophy results from more than simple disuse alone.

Muscle can be seen therefore to have a high degree of plasticity in response to external stimuli. These adaptations can be seen phenotypically, decreasing organ size in response to physiological stressors, and increasing in size in response to repeated mechanical loading, and result from cellular alterations, with changes in fibre type, metabolic function and vasculation.

2.3 Regulation of the Size of Muscle

2.3.1 Amino Acid Liberation and Metabolism

Amino acids within muscle tissue, as with all tissues, are in constant flux (Mitch and Goldberg, 1996). Freed amino acids from muscle protein breakdown are either reused in the synthesis of new proteins locally, oxidised for the production of energy or released for either systemic usage or removal from the body (Figure 2.4). Entry of freed amino acids into Krebs cycle is either via direct deamination (such as glutamate), or in the majority of amino-acids, indirect transamination yielding a glutamate and ketone (Murray and Montgomery, 2014). The balance of protein turnover is governed by the rate of muscle protein degradation and muscle protein synthesis. The rate of each is altered dynamically, with the balance between the two placing an individual cell, tissue or whole body within a rate of net synthesis or breakdown (Phillips, 2004, Phillips et al., 1997).

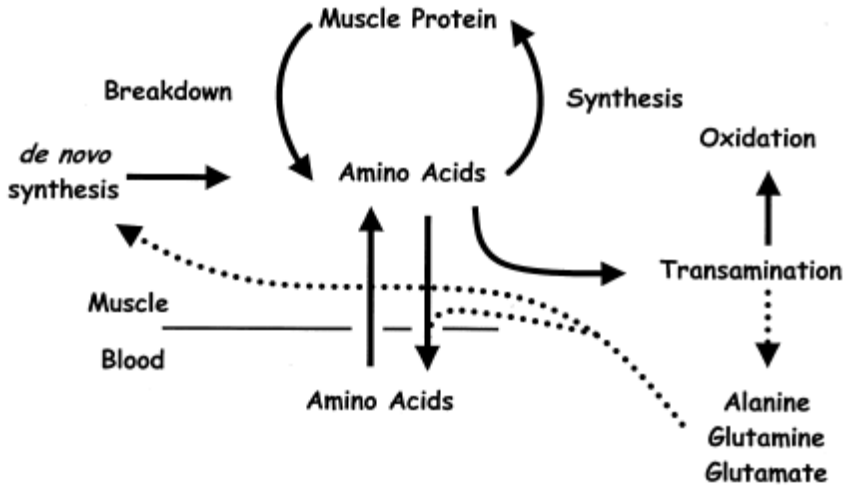

Figure 2.4: Protein turnover and metabolic fates of amino acids in skeletal muscle (Taken from Phillips, 2004).

Situations where muscle wasting occurs are noted to involve elevated liberation amino acids via muscle atrophy. Mice with implanted C26 adenocarcinoma cells show a progressive loss of both body mass, muscle mass and muscle total protein content (Bonetto et al., 2011). In otherwise

healthy humans, 14 days bedrest suppresses rate of protein synthesis without altering rate of protein breakdown, shifting individuals to a state of net catabolism (Ferrando et al., 1996). In a differing model of atrophy, 64 hours of cortisone (140 mg.kg.hour^{-1}) results in elevated protein breakdown (Darmaun et al., 1988). Cachexic COPD patients are noted to have reduced muscle mass and elevated concentration of multiple amino acids, suggesting liberation from muscle wasting (Pouw et al., 1998)

The quantification of the rate of protein synthesis and degradation relies on isotope tracer based methodologies. Rare but stable isotopes of elements are incorporated into amino acids then administered to individuals, with the rate of appearance or disappearance from bodily compartments monitored over known period of time. Traditionally, two techniques for the delivery of labelled isotopes amino acids have existed, either a continuous infusion at a constant rate or a bolus 'flooding' dose. Whilst a bolus approach does offer simpler experimental design of a single time point isotope infusion, it has been noted that bolus injections of essential amino acids can directly stimulate rate of protein synthesis (Smith et al., 1998). However, constant infusion protocols require long infusions protocols (3 -5 hours), and precludes the simultaneous measurement of fractional breakdown rate, unless a second isotope tracer is separately infused, as breakdown calculation relies on rate of decay on tracer enrichment on cessation of infusion (Wolfe, 1984). More modern bolus approaches have recently been developed that use a smaller total bolus of amino acids, thereby giving the benefits of shorter timeframe without affecting measures of protein synthesis (Tuvdendorj et al., 2014), which may allow for flexible experimental designs in future work.

2.3.2 Proteasomal Activity

The 26S proteasome represents the principal mechanism for the destruction of intracellular proteins (Saeki and Tanaka, 2008). The proteasome represent a large barrel shaped machine which contains proteolytic enzymes responsible for degradation of delivered proteins into their amino acid components (Kriegenburg et al., 2008, Rosenzweig and Glickman, 2008).

2.3.3 Proteasomal Activity

The 26S proteasome represents the principal mechanism for the destruction of intracellular proteins (Saeki and Tanaka, 2008). The proteasome represent a large barrel shaped machine which contains proteolytic enzymes responsible for degradation of delivered proteins into their amino acid components (Kriegenburg et al., 2008, Rosenzweig and Glickman, 2008).

Destruction of proteins is a carefully regulated process which involves, in order, an E1 (activating), E2 (conjugating) and E3 (ligating) enzyme with the end result being a transfer and tagging of targeted protein with the ubiquitin protein marker (Figure 2.5). Ubiquitin is found throughout eukaryote cells (Goldstein et al., 1975), and is required for protein degradation (Hershko et al., 1980). Subsequent polyubiquitinated targets are recognized by the proteasome and are subsequently broken down into resultant amino acids for reuse in the synthesis of new proteins or entry into metabolic pathways (Coux et al., 1996, Schreiner et al., 2008).

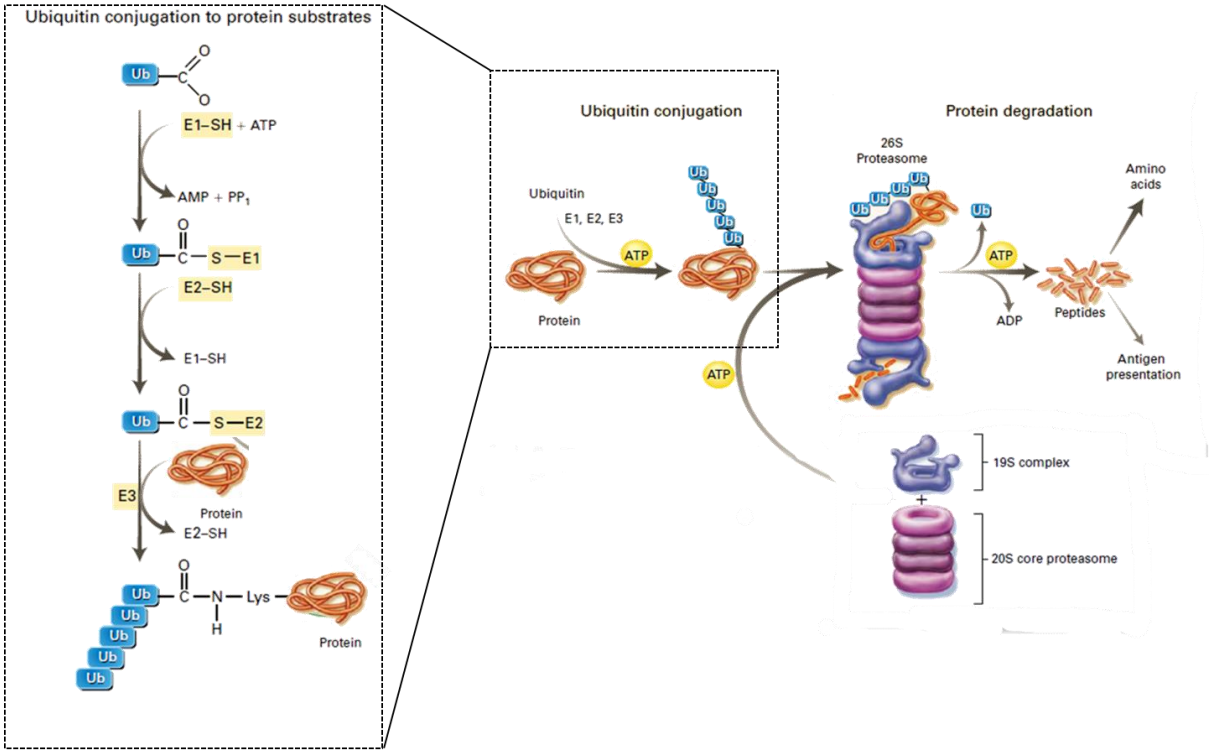

Figure 2.5: The ubiquitin-proteasomal pathway of proteolysis. Taken from Mitch and Goldberg (1996).

Where the proteasomal system is ubiquitous throughout different cell types, the E3 stage of ubiquitination allows for the regulation of target protein specific degradation. Within muscle at least two specific E3 ligases exist, namely atrogin and MuRF1 (Bodine et al., 2001a, Gomes et al., 2001). Atrogin and MuRF1 are only found within heart and muscle tissue, and induction of skeletal muscle atrophy via denervation, immobilization or hind limb suspension in rat results in rapid increases in expression of both ligases within muscle (Bodine et al., 2001a). Stimulation of muscle cells with E1, E2 or MuRF1 in isolation results in no increase in ubiquitin binding rate, but combination of all three results in increased ubiquitin expression. Conversely, genetic knockout (-/-) of atrogin or MuRF1 results in mice that are resistant to muscle wasting in response to denervation or septic shock (Bodine et al., 2001a). Combined, the necessary role of the E3 ligases for proteasomal activity can be seen.

Transcription factor Forkhead box protein, O sub-family, (FoxO1) is capable of binding to and increases atrogin and MuRF1 expression (Waddell et al., 2008). Transgenic overexpression of FoxO1 in mice results in increased atrogin expression and muscle atrophy (Southgate et al., 2007). Inhibition of FoxO transcription factors specifically within muscle prior to injection with carcinoma cells prevents tumour induced atrophy and in control mice (sham tumour injection), induces hypertrophy (Reed et al., 2012).

2.3.4 Akt-mTOR Signalling

Insulin and insulin-like growth factor (IGF) act to promote protein synthesis, increase glucose uptake and inhibit apoptosis in muscle, thereby regulating growth and regeneration (Dent et al., 1990, Fryburg and Barrett, 1993, Lawlor and Rotwein, 2000, Le Roith et al., 2001). IGF binds to and induces activity of the IGF-Akt pathways via the IGF receptor (IGF-R) while mutation of this receptor prevents IGF-induced increases in myoblast differentiation (Cheng et al., 2000). Binding of IGF to the IGF-R induces phosphorylation of the phosphoinositide 3-kinase (PI3-K) into an active state, phosphorylating cell surface molecule phosphatidylinositol-(3,4,5)-bisphosphate (PIP_2) to phosphatidylinositol-(3,4,5)-trisphosphate (PIP_3). PIP_3 binds with the Akt Pleckstrin homology domain, rotating and positioning it within the cell membrane to allow for phosphorylation by phosphoinositide-dependent kinase-1 at Threonine 308 (Thr308) and Serine 473 (Ser473), putting Akt into its fully active state (Alessi, 2001, Alessi et al., 1997, Li et al., 2006).

Akt phosphorylation promotes phosphorylation of glycogen synthase kinase 3β (GSK-3β) on its N-terminus regulatory domain, promoting cellular protein synthesis (Cross et al., 1995) and upregulates mTOR complex 1 (mTORC1) activity, which promotes two downstream signalling factors, an S6 kinase of 70 kDa ($p70^{S6K}$) and 4E-BP1. Inhibition of either mTOR phosphorylation or $p70^{S6K}$ in the presence of phosphorylated Akt prevents cellular protein synthesis that Akt phosphorylation alone promotes (Ohanna et al., 2005). Inhibition of $p70^{S6K}$ does not prevent GSK-

3β phosphorylation, suggesting divergence of this signalling at this point (Cross et al., 1995), however phosphorylation of GSK-3β can selectively inactivate 4E-BP, showing further negative control of synthesis (Sharples et al., 2012).

Knock-down of Akt signalling in mice results in a reduction in body mass relative to wild type mice, and a reduction in lean muscle mass, but not fat mass. This global loss of total muscle mass is mirrored in atrophy across individual muscles (Goncalves et al., 2010). Alternatively, functional overload in mice induce muscular hypertrophy and increases pAkt (Ser473) expression, while inhibition of mTOR reduces hypertrophy but maintains pAkt (Ser473), showing the role of mTOR downstream of Akt (Bodine et al., 2001b). Similarly, conditionally over-activation of Akt in mice results in rapid (~2 weeks) hypertrophy of peripheral muscle (Borsi et al., 2015).

This effect of Akt activity on muscle protein synthesis appears to be driven by the above mentioned effects on mTORC1 and GSK-3β. Targeted mTOR inhibition via rapamycin treatment of myotubes *in vitro* decreases $p70^{S6K}$ activation in the presence of IGF and activated Akt, and offset muscle hypertrophy in the rat (Zhang et al., 2010). Similarly, phosphorylation and inhibition of GSK-3β results in myotube hypertrophy, either via Wnt1 stimulation (McFarland, 1971) or GSK-3β inhibitor stimulation (Vyas et al., 2002).

Impairment of IGF-R offsets IGF-1 driven atrophy. Wild-type mice show ~ 25 % increase in myofiber diameter in muscle from the quadriceps following IGF-1 infusion, while mice with a deletion of the IGF-R associated protein myoferlin show a lack of muscle hypertrophic response following a matching IGF-1 infusion. Mice with a muscle specific deletion of the IGF-R show muscle atrophy relative to wild type mice, but show a maintained muscular hypertrophy response following 7 days of functional overload relative to wild type mice, while pAkt (Ser473) phosphorylation is maintained

(Spangenburg et al., 2008). These results suggest that while important for normal growth of muscle mass *in vivo*, IGF-R activity is not necessary for mechanical load-induced hypertrophy.

Finally, links between proteasomal activity and Akt-mTOR signalling have been noted, suggesting cross-regulation between the two pathways. Phosphorylation of Akt induces phosphorylation and exclusion of the FoxO transcription factors to the cytoplasm, preventing FoxO1 dependent increases in atrogin and MuRF1 in response to atrophic stimuli (Stitt et al., 2004), while alternatively mTOR activation increases proteasomal activity (Zhang et al., 2014). FoxO1 overexpression is also capable of inhibiting 4E-BP1 via mTOR inhibition, demonstrating some cross talk between FoxO and Akt pathways (Southgate et al., 2007).

2.3.5 Inflammation and Cytokine Activity

In response to challenge from an external pathogen, the innate immune response follows a well-characterized response involving canonical pro-inflammatory cytokines such as tumour necrosis factor alpha (TNFα), the interleukins and interferon gamma (IFNγ). Common to several pro-inflammatory cytokines pathways is the nuclear signalling factor kappa beta (NF-κB), which is held in an inactive state in the cytosol by its inhibitor (inhibitor of kappa B alpha [IκBα]) . In response to external signalling and activation, NF-κB is released from IκBα by a specific kinase Iκk (Traenckner et al., 1994). Freed of IκBα by IκK, NF-κB can translocate to the nucleus, binding promoter regions and increasing transcription of multiple pro-inflammatory cytokines, including TNFα and IFNγ (Frost et al., 2002), which may then act in an auto/paracrine manner or enter the circulation and act in an endocrine manner.

Pro-inflammatory models show rapid atrophy of skeletal muscle. Induction of sepsis in rats decreases muscle protein synthesis and reduces muscle weight, while pre-treatment with TNFα

inhibitors prevents this (Cooney et al., 1999), which may in part act via Akt-mTOR signalling, as septic rats have depressed mTOR activity, which is again prevented with pre-treatment by TNFα inhibitors (Lang and Frost, 2007). These effects are NF-κB dependent, overexpression of IκBα prevents NF-κB activation in response to TNFα, and stimulated cells do not show atrophy (Li and Reid, 2000). Conversely, overexpression of a muscle specific IκK causes NF-κB to be constitutively active within muscle and substantial muscle atrophy (Cai et al., 2004)

2.3.6 Satellite Cells

During an examination of the sarcolemma of myocytes excised from frogs, Mauro (1961) noted the presence of a previously unknown type of cell embedded superficially to the plasma membrane (Figure 2.6A). As myofibers are terminally differentiated, Mauro (1961) hypothesized that activation of these cells induces proliferation of precursor myoblasts that are capable of fusing to pre-existing myofibers to provide new or replacement nuclei (Figure 2.6B).

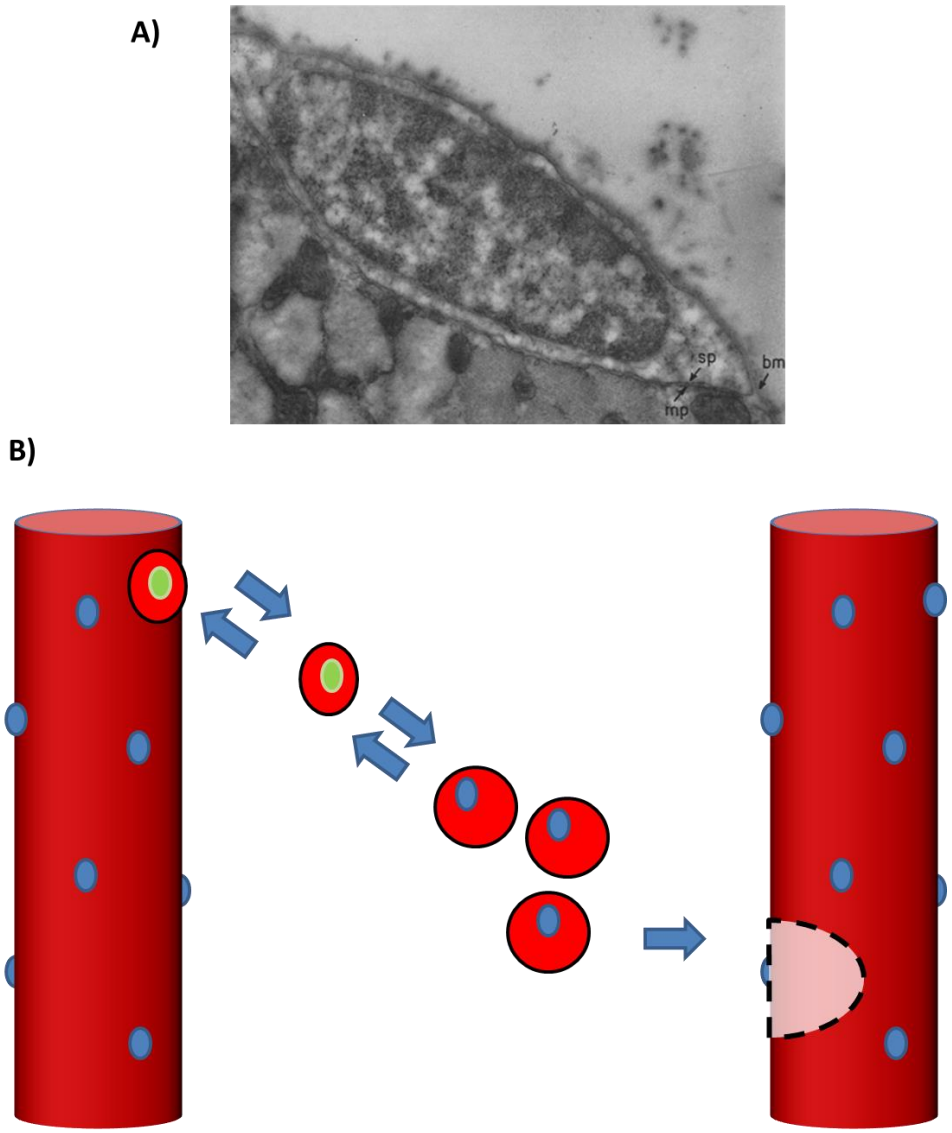

Figure 2.6: Satellite cells and their function. A) Visualisation of satellite cell, showing placement below the basement membrane but separate to the myofiber. sp = satellite cell membrane, mp = muscle cell membrane, bp = basement membrane. Taken from Mauro (1961). **B)** Schematic of satellite cell replication and fusion. On activation (top left), satellite cells proliferate (middle) and migrate to site of action, fusing to existing myofiber (bottom right) and increasing myofiber nuclear number.

Satellite cell differentiation is regulated by MyoD and Pax7, with quiescent cells staining positive for Pax7, proliferating cells positive for both Pax7 and MyoD, and differentiating cells positive for MyoD only (Motohashi and Asakura, 2014, Seale et al., 2000). Pax7 -/- mice show smaller muscle mass than wild type mice, and lack of satellite cells within muscle (Seale et al., 2000). Biopsies from human vastus lateralis suggest satellite cells are typically found in the quiescent state (Beauchamp

et al., 2000). In humans, increased satellite cell activity (as indicated by MyoD activation) is seen following resistance training (Kadi et al., 2004). The impaired muscle mass of Pax7 -/- mice and the activation of satellite cells following resistance training in humans is suggestive for a role for satellite cell activity in load induced hypertrophy.

In response to stretch or exercise in the rat, satellite cells are activated and proliferate (Rosenblatt and Parry, 1992, Smith and Merry, 2012), then migrate to their fusion site via chemotaxis (Hawke and Garry, 2001). It was initially proposed that satellite cells are required for the inducement of muscular hypertrophy. Low doses of gamma-radiation in mice cause reproductive death of satellite cells without perceivable damage to myofibres. Subsequent mechanical overload of muscles does not induce measurable hypertrophy (Rosenblatt and Parry, 1992, Rosenblatt et al., 1994), suggesting satellite cell activity is a necessary step in muscle hypertrophy.

The role of satellite cells in muscular hypertrophy in the healthy human has recently been questioned by McCarthy and colleagues (2011), who used an adult-onset knock-down model to inactivate satellite cells in adult mice, paired with a synergist ablation model, and showed similar hypertrophy of agonist muscles in both control and knock-down mice. As would be expected, myonuclei domain increased, indicating that no increase in myonuclei number was seen (McCarthy et al., 2011).

2.4 Myostatin

2.4.1 Discovery and Phenotypic Effects

McPherron and colleagues (1997) first identified the role of myostatin while investigating the effect of previously uncharacterized growth and differentiation factor (GDF) family members. Generated myostatin (previously GDF-8) knockout mice were viable and showed a 30 % increase in body weight over wild type mice at 2 months of age. This phenotype appears to result from increases in muscle mass. Myostatin -/- mice showed significant muscle hypertrophy of 200 – 260 % across different muscles and reductions in subcutaneous fat mass. Mass gained appeared to be via cellular hypertrophy, with no visible evidence of hyperplasia.

The phenotypic effect of myostatin deletion appears to be maintained throughout Mammalia. Belgium blue cattle naturally present with significant increases in muscle mass and reduced subcutaneous fat over other bovine species. Multiple research groups simultaneously identified that Belgium blue cattle naturally presented with an 11 nucleotide deletion resulting in a lack of mature muscle myostatin peptide expression (Grobet et al., 1997, Kambadur et al., 1997, McPherron and Lee, 1997). 'Bully whippets', a subset of the whippet breed of dog, show significant muscular hypertrophy over common whippets due to a mutation of the myostatin gene, with both homozygous and heterozygous mutations presents, and hypertrophy greatest in the homozygous variant (Mosher et al., 2007). This role of myostatin on muscle size appears to be maintained in humans. A spontaneously occurring myostatin -/- infant has been reported; this individual showed heightened amounts of muscle mass relative to normative values when measured 6 days post birth, which was maintained up to at least 4.5 years of age (Schuelke et al., 2004).

The myostatin protein is coded for by the myostatin gene, a 7,033 base pair, located on chromosome 2, position q32.2. Baseline myostatin transcription is higher in fast twitch muscles, relative to slow twitch muscles (Allen and Unterman, 2007), which may link to the fibre type specific roles of myostatin.

The myostatin promotor region contains binding sites for FoxO and SMAD transcription factors. Myostatin transcription appears directly controlled by FoxO1, over-activation of FoxO1 induces a ~100 fold increase in myostatin mRNA in myoblasts and ~500 fold increase in myotubes (Allen and Unterman, 2007). SMAD transcription factors 2 and 3 (SMAD 2/3) both increase myostatin mRNA expression in C2C12 myotubes (Allen and Unterman, 2007), in a similar manner to other TGF- β family members. Inhibition of myostatin transcription can occur via binding of micro-interfering RNA-27a (miR-27a), which can direct bind and block the myostatin promotor region. Overexpression of miR-27a reduces myostatin mRNA expression and muscle hypertrophy, whilst miR-27a targeted degradation increases myostatin expression and muscle atrophy (McFarlane et al., 2014).

Myostatin is initially translated as a 376 amino acid prepropeptide in the human (375 in the mouse). In a similar manner to other TGF-β family members, two cleavage events at amino acid 240 – 243 produce a C-terminus signalling peptide (Figure 2.7A, yellow) and a larger latency associated propeptide (Figure 2.7A, dark blue) that is capable of binding to, and inhibiting the C-terminus myostatin peptide (McPherron et al., 1997). The peptide cleavage protease appears to be a member of the metalloproteinase family as stimulation of C2C12 myotubes with metalloproteinase inhibitors promotes cellular hypertrophy, the accumulation of unprocessed prepropeptide myostatin (denoted in Figure 2.7A-1) and a decrease in myostatin peptide (Figure 2.7A-4 and Figure 2.7B) expression (Huet et al., 2001).

A three dimensional structural ribbon diagram (Figure 2.7B) demonstrates the dimerization of two myostatin peptide monomers post cleavage of the inhibitory propeptide. To date, no x-ray crystallography data for the full length myostatin prepropeptide has been published, precluding visualisation of the full length myostatin precursor.

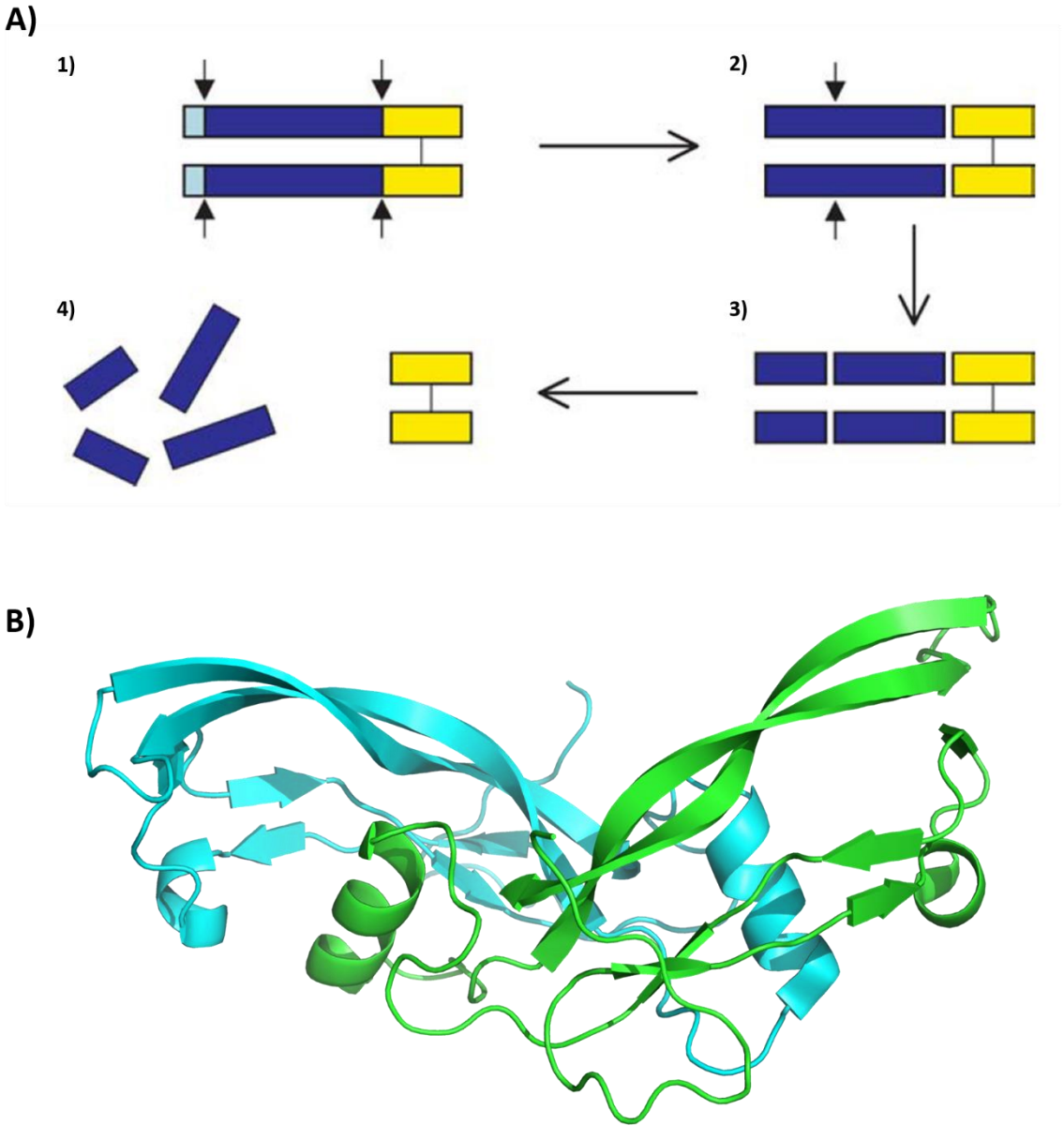

Figure 2.7: Processing of the myostatin protein. A) Schematic of myostatin homodimer formation, showing cleavage events**.** Following synthesis of the full length protein, **1)** myostatin undergoes two proteolytic events, removing the N-terminus (light blue) and cleaving the C-terminus (yellow). The C-terminus peptide forms a disulphide-linked homodimer. **2)** The cleaved C-terminus remains inactive (latent) in a non-covalent bond with the propeptide (dark blue), preventing activity. Cleavage of this latency associated propeptide (**3 - 4**) results in a bioactive peptide with receptor binding abilities (Lee, 2004). **B)** Ribbon diagram of myostatin peptide homodimer, with individual monomers coloured. (blue and green; sequence data modified from Cash et al., 2012). UniProt sequence access #O08689-mouse myostatin peptide

Three major compartments exist for the myostatin peptide *in vivo*. A 26 kDa band, representing the myostatin peptide is detected by Western blot, and this band size is halved in size under strong reducing conditions, representing the myostatin peptide monomer (disulphide bond broken; McPherron et al., 1997, Zimmers et al., 2002). Under non-reducing conditions, a further band at 100 kDa can be seen representing unprocessed myostatin. An antibody raised against the myostatin LAP will detect a band at ~40 kDa. Antibodies with a paratope crossing the C-terminus have been reported in the literature, resulting in Western blots that detect both the 26 kDa, the 40 kDa and the 100 kDa bands in muscle tissue (McFarlane et al., 2005).

Myostatin peptide is also detected circulating in plasma at 26 kDa and 40 kDa (Gonzalez-Cadavid et al., 1998, Walker et al., 2004), which again is halved in size under reducing conditions (Zimmers et al., 2002), and this 26 kDa band is absent in myostatin -/- animals (Szulc et al., 2012). Myostatin is also found in the intercellular space, where is primarily expression appears to be in an inactive form, with the myostatin peptide not witnessed by Western blot (Anderson et al., 2008).

Myostatin DNA as measured by Southern blot is present in muscle samples from multiple species, including humans, and faintly present in chicken, but is not seen in either zebrafish or frog (McPherron et al., 1997, Palstra et al., 2010). Rainbow trout show two separate myostatin coding regions (MSTN-1a and -1b, respectively), and unlike mammalian species, myostatin is ubiquitous in tissues, with expression highest in brain, testes, eyes, spleen and muscle. Thus, it would appear that myostatin's evolutionary conservation and function may differ outside of Mammalia.

In the Human, the myostatin protein is found in both muscle and plasma. Plasma myostatin concentration negatively correlates with muscle mass in healthy and sarcopenic older individuals (Yarasheski et al., 2002) and also in healthy and cachexic HIV patients (Gonzalez-Cadavid et al.,

1998). Muscle myostatin peptide is elevated in sarcopenic older individuals, relative to younger control participants (Leger et al., 2008). Humans undergoing 10 weeks of resistance training show decreased plasma myostatin (Walker et al., 2004) and 9 weeks of a similar resistance training program reduces muscle myostatin mRNA (Roth et al., 2003). Combined these results suggest anabolic stimuli-induced changes in myostatin may underlie muscle mass growth in the heathy human. Conversely, 25 days of bed-rest induces loss of muscle mass and increases plasma myostatin concentration (Zachwieja et al., 1999), and disuse due to osteoarthritis increases muscle myostatin mRNA (Reardon et al., 2001). It would seem therefore that myostatin plays a role in the adaptation of muscle mass to both hypertrophic loading and atrophic disuse.

Myostatin appears to alter muscle size via a direct regulation of myofiber size. Incubation of C2C12 myotubes with myostatin *in vitro* induces cellular atrophy in a dose-dependent manner (McFarlane et al., 2006). These effects are maintained *in vivo*, mice with a Chinese hamster ovary (CHO) implanted tumour modified to generate and secrete myostatin show elevated systemic myostatin and muscular atrophy at muscles distal to the tumour implantation site, while those animals with a control CHO tumour do not (Zimmers et al., 2002). Myostatin -/- mice show a reduced representation of type I fibres compared to wild type mice (Gentry et al., 2010, Savage and McPherron, 2010), and a reduced aerobic exercise capacity relative to wild type mice (Matsakas et al., 2010, Savage and McPherron, 2010). Myostatin expression and activity is thought to act primarily on type II (fast) fibres, myostatin -/- mice are noted to have a higher representation of type II muscle fibres (Matsakas et al., 2010) and myostatin mRNA is higher in type II muscles of normal mice (Allen and Unterman, 2007). While not noted by McPherron and colleagues (1997) in the initial description of myostatin -/- mice, it has since been reported that adult myostatin -/- mice may show some indication of increased muscle fibrosis (Gentry et al., 2010).

A number of proteins act to inhibit or modulate the activity of myostatin. The mature myostatin peptides own propeptide competitively binds to and prevents receptor binding of myostatin (Thies et al., 2001), in a similar way to that of several TGF-β family members. Overexpression of the myostatin propeptide induces muscle growth in mice, increased muscle fibre area and an increase in total body weight that is greater in males than female mice (Jiang et al., 2004, Wang et al., 2013). Indeed, myostatin peptide expression is reduced in male mice relative to female mice of matching age, suggesting myostatin regulation may be involved in sexual dysmorphism. Despite these differences at the muscular level, no alteration in plasma myostatin is seen by gender (Oldham et al., 2009). However, the gene expression of part of the myostatin receptor (ALK4), is increased in human females relative to males (Welle et al., 2008), suggesting a higher sensitivity to myostatin may also exist in females. Titin-cap is capable of binding to and inhibiting myostatin's activity (Nicholas et al., 2002), as does Follistatin (Lee and McPherron, 2001, Nakatani et al., 2008), follistatin related gene protein (FLRG; Hill et al., 2002) and growth and differentiation factor-associated serum protein-1 (GASP-1; Hill et al., 2003).

Finally, it should be recognized that myostatin is not the only factor regulating muscle size. Follistatin overexpressing mice show muscular hypertrophy (Lee, 2007), as expected due to the above mentioned role of follistatin in myostatin inhibition (Nakatani et al., 2008). Myostatin -/- mice crossed with follistatin overexpressing mice showing significant hypertrophy over that of myostatin -/- mice alone (Lee, 2007), suggesting follistatin interacts with other muscle size regulating mechanisms besides myostatin. These 'off-myostatin' effects may involve activin, another TGF-β family member, as follistatin is recognised to bind and inhibit activin's actions (Patel, 1998, Sugino et al., 1997). Further, inhibition of follistatin's activin-binding ability prevents hypertrophy in myostatin -/- mice (Parslow, 2014).

2.4.2 Mechanisms Underlying Myostatin's Atrophic Effect

In the unstimulated myotube *in vitro*, the myostatin protein is localized to the nucleus. Application of an atrophic stimulus increases myostatin expression and induces translocation into the cytoplasm and then into the intracellular media (Artaza et al., 2002). In the cytoplasm, myostatin is found cleaved into its C-terminus biologically active peptide and bound to its inhibitory propeptide (Hill et al., 2002). *In vivo,* myostatin is found in three compartments; in the intracellular space, intercellularly and within the plasma (Anderson et al., 2008, Gonzalez-Cadavid et al., 1998, McPherron et al., 1997), where it is suspected to have an endocrine role (section 2.4.7).

The myostatin peptide induces an intercellular signalling cascade by binding to the external portion of the target cells transmembrane receptor activitin receptor IIB (Rebbapragada et al., 2003), which induces ActRIIB homodimerization with either activity receptor-like kinase-4 or -5. Blockage of the myostatin receptor ActRIIB increases body mass and decreases fat mass (Goncalves et al., 2010), similar to the phenotype seen in myostatin -/- mice (McPherron et al., 1997).

Internally to the muscle cell, myostatin signalling appears to target three separate mechanisms in the regulation of cellular size. Myostatin activation down regulates satellite cell activity, increasing proteasomal activity and decreases Akt-mTOR complex activity (sections 2.4.2 – 2.4.5). Degradation of protein is a metabolically expensive process (Mitch and Goldberg, 1996). Myostatin appears to also directly increase glucose metabolism, as direct stimulation of C2C12 myotubes with myostatin increases glucose transporter type 1 and 4 (GLUT1 and GLUT4) mRNA, increases glucose uptake in a concentration dependent manner, decreases intracellular ATP and increases AMPK activity (Chen et al., 2010), potentially to help offset the metabolic cost of its actions.

2.4.3 Regulation of Satellite Cell Activity by Myostatin

As an *in vitro* model of satellite cells, myoblast differentiation into mature myotubes is offset in the presence of endogenous myostatin in a dose-dependent manner (Rios et al., 2002, Taylor et al., 2001, Thomas et al., 2000). Satellite cell differentiation is regulated by MyoD and Pax7, with quiescent cells staining positive for Pax7, proliferating cells positive for both Pax7 and MyoD, and differentiating cells positive for MyoD only (Motohashi and Asakura, 2014). As mentioned above, myostatin signals via activated SMAD2,3,4 complex, which decreases MyoD expression (Langley et al., 2002). Stimulation of myoblasts with myostatin prevents Pax7-MyoD co-localization, maintaining cells in a quiescent state (McFarlane et al., 2008). Myostatin -/- mice show a decreased number of satellite cells per fibre, and hypertrophy of muscle in adult mice does not alter satellite cell number. Furthermore, satellite cells from adult wild type mice do not appear to express ActRIIB (Amthor et al., 2009), suggesting, at least in the adult, that myostatin's atrophic effects are not via satellite cell inhibition, or myostatin's' effects on satellite cells is not a direct one. However, a role in developmental influences cannot be ruled out.

Under physiologically normal conditions, proliferating satellite cells fuse to existing myotubes to aid hypertrophy. Differentiating myoblasts *in vitro* that overexpress myostatin show a reduction in MyoD expression and a reduced rate of differentiation in satellite cells derived from both mice and sheep muscle (Langley et al., 2002, Liu et al., 2012), the effect of which is reversed dose-dependently if the cells are co-cultured in the presence of suramin (1 – 100 $\mu g.mL^{-1}$), a peptide which appears to down-regulate myostatin activity via an undescribed mechanism (Nozaki et al., 2008).

In response to myostatin binding to the ActRIIB receptor, phosphorylation of intracellular signalling proteins SMAD2 and SMAD3 occurs, which then induces binding with SMAD4. The SMAD2,3,4 complex then translocates to the nucleus where it directly binds to and blocks the MyoD promoter

region (Zhu et al., 2004). However, counter to what may be expected, SMAD4 -/- mice show significant muscle atrophy that is fibre-type independent, a reduction in force output, and notable hyperplasia (Sartori et al., 2013), which outlines the joint role of SMAD signalling not just in myostatin signalling, but across TGF-β family members as a common intracellular signalling pathway (Corrick et al., 2015).

2.4.4 Regulation of Degradative Pathways by Myostatin

Stimulation of C2C12 myotubes with myostatin sufficient to induce ~ 50 % atrophy increases atrogin but not MuRF1 and increases ubiquitin binding, while inhibition of FoxO1 prevents these increases (McFarlane et al., 2006). Injection of dexamethasone into mice *in vivo* induces rapid atrophy and increases in atrogin and MuRF1 expression. This atrophy is reduced in myostatin -/- mice, as is the increases in atrogin and MuRF1 (Gilson et al., 2007). Conversely, atrogin or MuRF1 -/- mice maintain muscle mass in response to disuse atrophy relative to wild type mice (Bodine et al., 2001a). This consistent and necessary role of atrogin and MuRF1 for muscle atrophy makes them useful markers of muscle catabolism. In what appears to be a feedback mechanism, the myostatin promoter region contains a FoxO1 binding site, and FoxO1 activation increases myostatin expression (Allen and Unterman, 2007).

Following injury of myofibers *in vivo*, elevated myostatin protein expression is co-localized with necrotic fibres, suggesting a role in the necrotic process. Conversely, zones of myoblast fusion show a lack of myostatin expression and reduced myostatin expression during hypertrophy (Kirk et al., 2000), suggesting an acute and time-dependent role of myostatin in regeneration following injury.

2.4.5 Regulation of Akt-mTOR Dependent Anabolism by Myostatin

Synthesis of structural proteins within a number of cells, including muscle cells, is governed primarily by the Akt-mTOR signalling pathway, as described above (Section 2.3) and visualised below (Figure 2.8). Myostatin stimulation of C2C12 myoblasts inhibits proliferation, and this process is dependent on activity of myostatin receptor ActRIIB and phosphorylation of Akt at Ser473, but not SMAD3 (Yang et al., 2007), indicating the intracellular signalling pathway by which myostatin alters Akt activity is independent of its SMAD2,3,4 pathway. Increased Akt-mTOR activity regulates p300 expression, a transcriptional co-activator necessary for cell cycle progression (Ogryzko et al., 1996). Myostatin decreases p300 expression via targeted ubiquitination, and both IGF-1 stimulation and constitutively active Akt rescues this effect, suggesting myostatin is capable of inhibition of IGF-1 activity, and this effect is upstream of Akt (Ji et al., 2008). Such an activity could be of interest in the balance of synthesis and degradation pathways, an inhibition of synthesis via differentiation of new myoblasts in parallel with increased degradation would result in the efficient loss of muscle mass.

Mice overexpressing myostatin following plasmid promoter electro-transfer into tibialis anterior show down-regulation of Akt phosphorylation (Ser473) and downstream Akt targets $p70^{S6k}$ (Ser235/236) and 4E-BP1 (Thr37/46; Figure 2.8). Interestingly, ubiquitin binding was not changed in these animals (Amirouche et al., 2009). Blockage of the myostatin receptor ActRIIB increases body mass while showing a trend towards decreased fat mass in both wild type and Akt knockdown mice, suggesting the effects of myostatin on Akt-mTOR are not the only way by which myostatin alters muscle size (Goncalves et al., 2010).

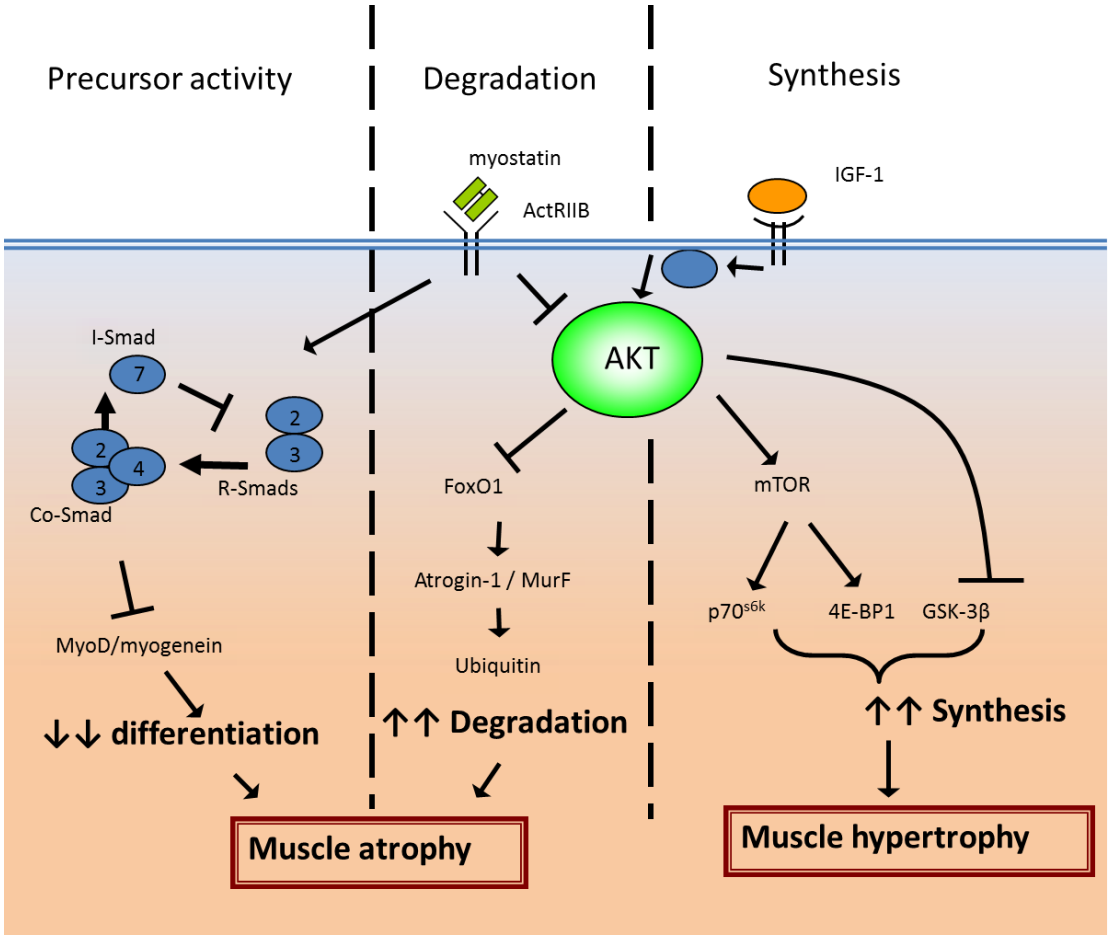

Figure 2.8: Summary of Myostatin intercellular signalling pathways. MyoD, myogenic determination; ActRIIB, activin receptor type two beta; FoxO1, Forkhead box protein type O one; MuRF1, muscle ring finger protein 1;IGF-1, insulin-like growth factor one; mTOR, mammalian target of rapamycin; $p70^{s6k}$, ribosomal protein S6 kinase; 4E-BP1, 4E Binding protein; GSK-3β, glycogen synthase kinase 3 beta. Taken from Elliott et al. (2012).

2.4.6 Alteration of Myostatin *in vivo*

Myostatin protein concentration is decreased in plasma of human participants following 6 weeks of resistance exercise training (Walker et al., 2004), but not in the muscle following a similar exercise training intervention, despite a decrease in mRNA transcription (Jespersen et al., 2011). Inhibition of myostatin, via a systemically administered monoclonal antibody targeting the myostatin peptide, increases muscle mass and exercise capacity in aged mice, which is further enhanced by exercise training (LeBrasseur et al., 2009).

Individual variation in the myostatin gene may alter muscle phenotype. Coding differences in the myostatin gene is associated with muscle function and force production, particularly the K153R polymorphism. An analysis of 286 older (70 – 79 years of age) females suggested that R polymorphism containing individuals tend to show lower force production than K individuals (Seibert et al., 2001). In human males of Han Chinese origin, opposing findings are seen, with the presence of the R polymorphism associated with greater muscle size, and greater gains in muscle mass in both biceps and quadriceps following 8 weeks resistance training (Li et al., 2014). A link between maintenance of muscle mass and myostatin isoforms may be seen with aging; the R polymorphism displays an increased association with centenarians from Spanish and Italian populations than the K polymorphism (Garatachea et al., 2013).

The myostatin response to disuse is less well defined. No change in myostatin mRNA expression is seen following lower limb casting in healthy individuals for 14 or 23 days (de Boer et al., 2007), nor with lower limb casting for 4 – 11 days following lower limb fracture (Chen et al., 2007). Counter to these results, 5 days casting induces increases in myostatin mRNA expression (Dirks et al., 2014) as does chronic disuse (as induced by total hip arthroplasty) in elderly female patients (Reardon et al., 2001). Plasma myostatin is increased following 25 days head-down bed rest amongst healthy young males (Zachwieja et al., 1999). An unclear picture emerges as to the role of myostatin in disuse atrophy therefore. The length of disuse may be key with regards to myostatin mRNA changes, with increased transcription seen in the shortest study (Reardon et al., 2001), but not in the longer term studies (de Boer et al., 2007, Chen et al., 2007) resulting in an increased basal concentration of plasma myostatin, as is seen by Zachwieja and colleagues (1999).

While inhibition of myostatin offsets disuse atrophy in mice (Murphy et al., 2011), absence of myostatin does not preclude loss of muscle mass. It is noted that 7 days of hind-limb unloading in

myostatin -/- mice induces greater loss of muscle mass than in wild-type mice (McMahon et al., 2003b). Myostatin -/- mice who undergo 7 days hind-limb unloading show elevations in atrogin and MuRF1 relative to control unloaded mice, however after 7 days of reloading these effects are dissipated, and myostatin -/- mice show greater recovery (Smith et al., 2014). Conversely, atrophy as a result of glucocorticoid injection is seen in wild-type mice, but not in myostatin -/- mice (Gilson et al., 2007), suggesting the atrophic mechanism underlying the two processes is different, where glucocorticoids require myostatin signalling activity to induce atrophy, disuse does not.

A number of chronic disorders are associated with loss of muscle mass and may involve myostatin-dependent regulation. Myostatin is elevated in patients with chronic heart failure and exercise training can decrease muscle myostatin expression in this population (Lenk et al., 2012). Mouse models of chronic heart failure present with elevated plasma myostatin, and genetic deletion of myostatin expression in cardiomyocytes reduces heart failure induced muscle atrophy in mice (Breitbart et al., 2011). Myostatin is increased in the muscle of chronically hypoxemic COPD patients (Hayot et al., 2011), and elevated in the muscle of a rat model of cancer cachexia (Costelli et al., 2008). The findings of Hayot and colleagues (2011) may be clouded by differences in physical activity behaviours between the patient population and healthy controls. Further, Hayot and colleagues (2011) make no mention of treatment regimens of the COPD population, potentially confounding as glucocorticoids induce muscle atrophy via myostatin signalling (Gilson et al., 2007). Starvation of sheep involves both a loss of muscle mass and increase in muscle myostatin expression (Jeanplong et al., 2003). The most common interpretation of these findings is for a causative role of myostatin in the muscle atrophy seen in these disorders. Conversely, as plasma myostatin concentration is noted to correlate with muscle mass (Gonzalez-Cadavid et al., 1998), a reversal of causality could be suggested, where pathology reduces muscle mass thereby altering basal myostatin concentration.

2.4.7 Myostatin as an Endocrine Hormone

Myostatin's actions are both paracrine and endocrine. While the control of secretion of myostatin is not well understood, it appears to involve the protein titan-cap; titan-cap is capable of binding the myostatin peptide and C2C12 myoblasts that overexpress titin-cap show reduced myostatin secretion, but not altered myostatin production or processing intracellularly (Nicholas et al., 2002).

Early evidence for myostatin having an endocrine role came from Gonzalez-Cadavid and colleagues (1998), who noted a negative correlation between plasma myostatin and muscle mass across a cohort of healthy individuals, non-cachexic and cachexic HIV patients. Similar results are seen in aging individuals where muscle mass negatively correlates with serum myostatin (Yarasheski et al., 2002). Conversely, Ratkevicius and colleagues (2011) show no variation in serum myostatin concentration between young and elderly men. Differences in the ELISA protocol between publications may explain these results, while both groups generated custom ELISA for their work, Ratkevicius and colleagues (2011) do not report a plasma acidification step, the function of which is to break any antigen – binding protein bonds that may prevent antigen – antibody interaction.

An interventional model examining the endocrine hypothesis was completed by Zimmers and colleagues (2002), implanting mice with Chinese hamster ovary (CHO) myostatin expressing tumours. Subsequently mice showed significant atrophy relative to control (tumour only) mice and this atrophy was seen globally. Introduction of a soluble form of the ActRIIB systemically into the plasma binds circulating myostatin and results in increased strength and muscle function in mice (Whittemore et al., 2003), and can delay the atrophy of muscle in disuse models in mice (Murphy et al., 2011). In healthy mice, injection of an anti-myostatin antibody increases mass of tibialis anterior, quadriceps and gastrocnemius while injection of recombinant myostatin decreases muscle mass (Stolz et al., 2008).

Interaction between 'classical' hypertrophic pathways and myostatin appear to exist. Stimulation of C2C12 myotubes with increasing doses of growth hormone induces a decrease in myostatin expression in a dose-dependent manner, while treatment with a growth hormone antagonist gives the opposite effect (Liu et al., 2003). Further, growth hormone deficient adults show a decrease in myostatin expression with growth hormone stimulation (Liu et al., 2003). Growth hormone deficient animals show increased myostatin expression relative to control animals, but a larger decrease in myostatin mRNA expression following 3 days of compensatory muscle overload (Yamaguchi et al., 2006). While no relationship is seen between myostatin mRNA and growth hormone in men (Marcell et al., 2001), it should be remembered that there is a poor relationship between muscle myostatin peptide and mRNA in male mice (McMahon et al., 2003a), potentially clouding these results.

2.4.8 Acute Alterations in Myostatin

Examinations of changes in myostatin protein in acute timeframes (less than 24 hours) are lacking in the published literature. A lack of reliable tools for the measurement of plasma ELISA may have historically precluded the study of systemic myostatin, while the difficulties associated with repeated muscular biopsies (both scientifically and logistically) increase the difficulty of examining muscle peptide changes. One report exists that managed to collect eight muscle biopsies over a period of 24 hours following an acute resistance or endurance exercise session (Louis et al., 2007). These authors demonstrated a time-dependent decrease in myostatin mRNA, but did not examine the myostatin peptide (Louis et al., 2007). Alternative results were shown in rats following an eccentric exercise protocol, with an increase in myostatin mRNA expression peaking at 3 – 6 hours following exercise (Peters et al., 2003). These results suggest an exercise dependent effect, whereby complex multi-muscle exercise induces a differential result on muscle myostatin transcription than eccentric exercise alone. A single bout of resistance exercise decreased the expression of vastus lateralis myostatin mRNA one hour post and 48 hours post exercise in healthy

humans (Hulmi et al., 2008). Again, no attempt to measure myostatin peptide was made. No examinations examining myostatin peptide alterations in response to atrophic or hypertrophic stimuli over acute time-frames have taken place, leaving a clear gap in the literature.

2.5 Hypoxia

Within the human, transfer of oxygen (O_2) from the external environment into the mitochondria as a key ingredient of oxidative metabolism involves coordinated responses of the mechanical act of breathing, diffusion of O_2 across the alveolar membrane, O_2 transfer via circulation, capillary perfusion of peripheral tissue, O_2 dissociation from haemoglobin and diffusion into the cellular and then mitochondria for mitochondrial respiration (Figure 2.9), before metabolically produced CO_2 is expelled in a reversal of this process.

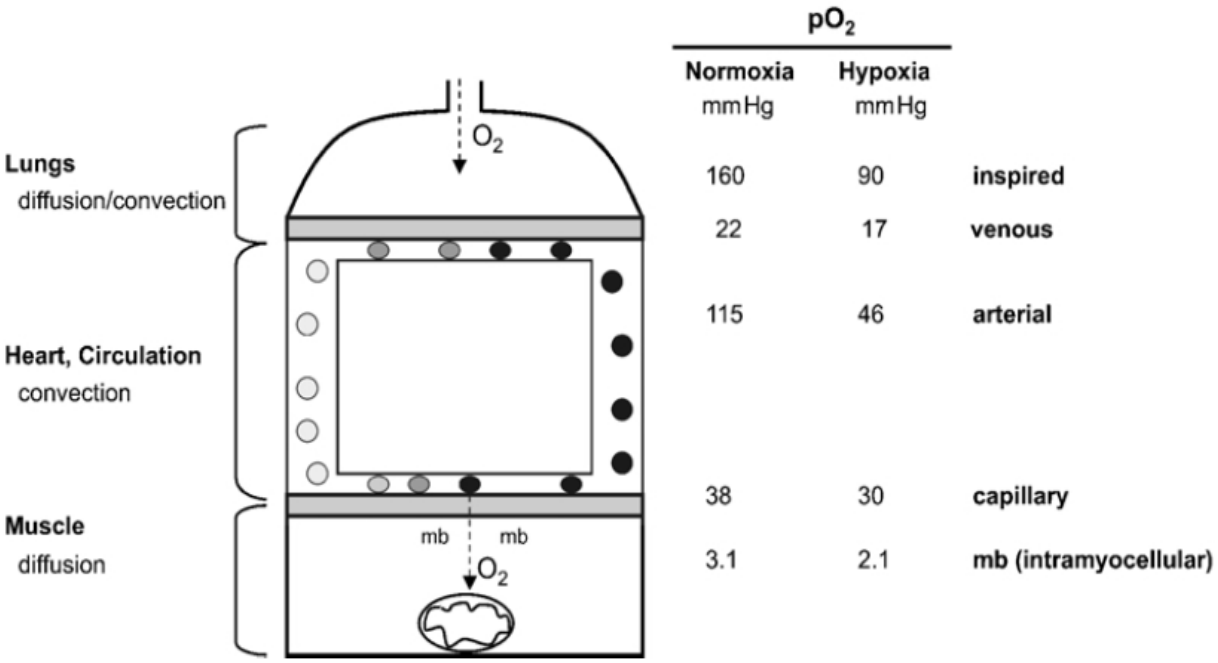

Figure 2.9: Oxygen partial pressure from the external environment to muscle mitochondria. Simplified model of oxygen transport and partial pressures of oxygen (PO_2) in either normoxic or hypoxic conditions (~ 4000 m). Taken from Hoppeler and colleagues (2003).

A reduction in the tissue oxygen supply (hypoxia) can result either from an alteration in ambient oxygen concentration (normobaric hypoxia) or a reduction in ambient pressure (hypobaric hypoxia; Figure 2.9). A reduction in barometric pressure reduces alveolar partial pressure O_2 (P_AO_2), and subsequently PO_2 at every stage of the O_2 delivery cascade, thereby reducing availability of O_2 to peripheral tissue mitochondria. Hypobaric hypoxia primarily occurs in situations where individuals are exposed to high altitude, such as mountaineering sojourns, but can result from specialised work

environments such as astronomy or high-altitude mining (West, 2002). Reductions in ambient oxygen concentration do not normally occur outside of research settings in the human, but do form a useful research model. Hypoxia in a research setting as induced by normobaric and hypobaric stimuli may produce differences in physiological response. Further, a diverse set of disorders where cardiorespiratory function is impaired results in reductions in arterial oxygen content (hypoxemia) also presents with peripheral hypoxia. Hypoxia is associated with loss of body mass that appears to preferentially targets muscle mass, evidence for this and possible reasons underlying hypoxic-induced atrophy are discussed in the following sub-sections. Finally, possible links between the myostatin signalling system and hypoxic conditions are presented.

2.5.1 Normobaric & Hypobaric Hypoxia

Induction of hypoxia in a research laboratory setting can be done either by a reduction of ambient O_2 (normobaric hypoxia) or by a reduction of ambient atmospheric pressure (hypobaric hypoxia), such as is experienced during increases in altitude. Both normobaric and hypobaric hypoxia result in a reduction in arterial oxygen supply (hypoxemia) leading to peripheral tissue hypoxia, however these two techniques can have difference in their physiological effect. For the comparison between the two models of hypoxia, a mathematical equivalency can be maintained (Figure 2.10; Appendix Thirteen).

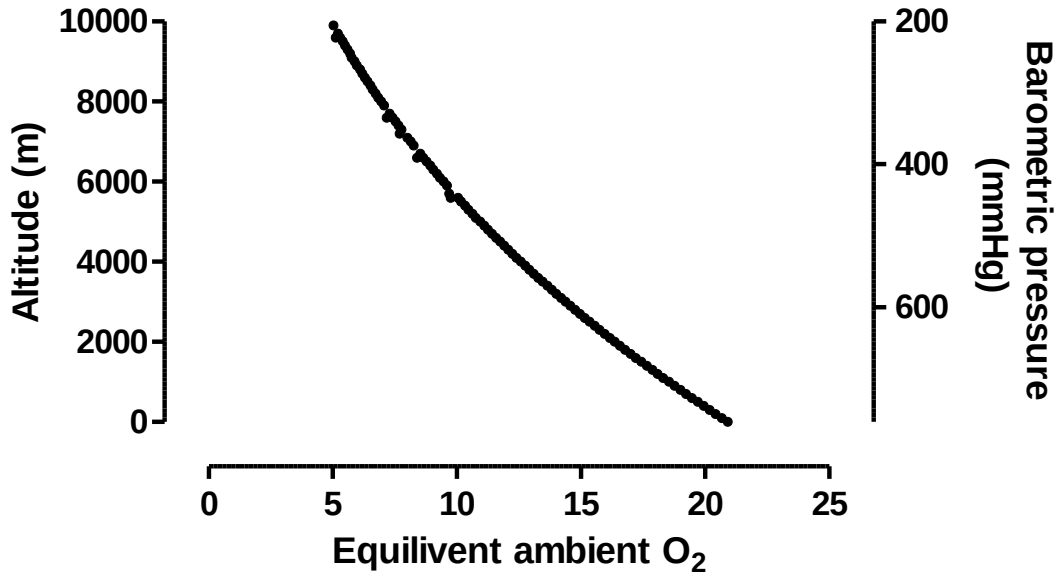

Figure 2.10: Equivalency between normobaric and hypobaric hypoxia. Modelled by Wagner (personal communications), the relationship between altitude and equivalent atmospheric O_2 intake under normoxic barometric pressure (mmHg) within normal human habitation is approximately logarithmic. Mathematical proof provided in Appendix Thirteen.

Normobaric (14.7 % O_2) or hypobaric (3,000 m, PO_2 ~ 102 mmHg) hypoxic exposure for 24 hours in healthy young males induces similar responses in saturation of capillary haemoglobin with oxygen (SpO_2), blood pressure (systolic or diastolic), heart rate, breath frequency, RER, or partial pressure of end tidal O_2. Expired ventilation rate (V_E) is not altered in hypobaric hypoxia compared to normobaric hypoxic before 8 hours but is reduced in hypobaric hypoxia between 8 and 24 hours (Faiss et al., 2013). Similar results were shown by Richard and colleagues (2014) who showed no difference in V_E, heart rate or SpO_2 between hypobaric and normobaric hypoxia. Heyes and colleagues (1982) examined urine production and cortisol, antidiuretic hormone (ADH) and prolactin in males following normobaric (n = 4) or hypobaric hypoxic (n = 8) exposure (10.5 % O_2 at 745 mmHg or ambient O_2 at 400 mmHg), each of 1 hour. A variable response was noted following hypobaric hypoxia with one subgroup (n = 4) showing no alteration in urine production, cortisol or plasma ADH concentrations, whilst the second hypobaric subgroup showed substantially increased ADH and cortisol production and decreased urine output. Normobaric hypoxic individuals showed

a decrease in urine production and increased cortisol expression, but not of the same magnitude of the hypobaric responders (Heyes et al., 1982).

Partial pressure of end tidal CO_2 ($P_{ET}CO_2$), while lower relative to baseline, is elevated at every time point (1, 8, 16, 24 hours) in hypobaric hypoxia, when compared to normobaric hypoxia (Faiss et al., 2013). This difference appears to results from a reduced respiratory drive in hypobaric hypoxia, the same work showed decreased V_E at rest under hypobaric hypoxia, relative to normobaric hypoxia. Differences in end tidal PCO_2 are unlikely to result from metabolic alterations; VO_2 and RER show no difference between hypoxic conditions (Faiss et al., 2013). Symptoms of acute mountain sickness (AMS), as measured by the Lake Louise AMS questionnaire, are lower in normobaric hypoxic relative to hypobaric hypoxic during altitude exposure (Roach et al., 1996), suggesting the effect of both reduced hypobaric pressure and ambient hypoxia combine during AMS at altitude.

2.5.2 Pathological Hypoxemia

Hypoxemia can result from a number of conditions, summarized below (Table 2.1) and in further detail in subsequent sub-sections. Where present, evidence for muscle atrophy co-presenting with hypoxia is also given.

Table 2.1: Hypoxic pathologies.

Condition	Brief description	Presence of atrophy	Reference
Chronic obstructive pulmonary disease	Non-reversible loss of lung function via emphysema, bronchitis or both	✓	(Bernard et al., 1998, Di Francia et al., 1994)
Chronic heart failure	Progressive reduction in cardiac output via loss of cardiac contractile force	✓	(Libera and Vescovo, 2004)
Lung Cancer	Loss of lung function due to tumour mass	✓	(Op den Kamp et al., 2013)
Obstructive sleep apnoea	Intermittent pharyngeal collapse during sleep	✗	

2.5.2.1 Chronic Obstructive Pulmonary Disease

Patients with chronic obstructive pulmonary disease (COPD) present with a decrease in lung function, as measured by forced expiratory volume over 1 s relative to forced vital capacity (FEV_1 / FVC ratio), resulting from emphysema, bronchitis or a combination of the two. This loss of function is not reversible (Maltais et al., 2014). This disorder also presents with increased systemic inflammation, reductions in aerobic capacity and peripheral tissue hypoxia (Wagner, 2008) and with loss of muscle size and strength in approximately 25 % of patients (Bernard et al., 1998, Di Francia et al., 1994). This loss of size and function correlates with a reduction in quality of life and is predictive of mortality (Marquis et al., 2002, Plant et al., 2010, Swallow et al., 2007). Protein expression of FoxO1, atrogin and MuRF1 within vastus lateralis is elevated in COPD patients relative to age matched controls, but in a counterintuitive finding, pAkt (Ser473) is also increased, and activity of this pathway was higher amongst COPD patients with muscle wasting than those without. The authors speculate this represents a failed protective response attempting to counter the increased proteasomal activity (Doucet et al., 2007).

As is described in the following section (2.5.6 Environmental Hypobaric Hypoxia), peripheral hypoxia can also result from ascent to high altitudes, due to the decrease in ambient PO_2. Epidemiological studies suggest COPD patients who reside at high altitudes show increased mortality (Sauer, 1980, Cote et al., 1993, Moore et al., 1982), suggesting additional hypoxic negatively affects disease progression. During acute and mild hypoxic exposures, such as travel by airline, decreased PaO_2 is witnessed in COPD, without obvious hypoxemia symptoms (Schwartz et al., 1984). However, variation in resting PaO_2 and SpO_2 are noted in COPD patients, and prior screening is recommended before flight, with the requirement for supplemental oxygen based on a combination of SpO_2 measured during rest and 6 minute walk test (Edvardsen et al., 2012).

2.5.2.2 Chronic Heart Failure

Chronic heart failure (CHF) presents with loss of muscle mass in 16 – 36 % of individuals (Anker et al., 2003, Tan and Fearon, 2008), reduced SpO_2 (Yoshihisa et al., 2011) and reduced oxidative metabolic capacity (Leyva et al., 1997). This population group also presents with reductions muscle mass (Libera and Vescovo, 2004), elevated expression of MuRF1 and atrogin within muscle (Kung et al., 2011). Plasma myostatin concentration is also elevated in CHF patients relative to sex-matched healthy controls (Gruson et al., 2011). However, CHF patients were notably older than controls (68 vs 57 years of age) and authors do not state if participants were matched for body composition. Thus, the age difference could contribute to the differences in muscle mass, and therefore the reduction in muscle mass may result in the observed increase in myostatin.

2.5.2.3 Lung Cancer

Lung cancer patients show significant cachexic atrophy, typically 5 – 10 kg lighter than non-cachexic cancer patients, with reduced fibre size from muscular biopsies of vastus lateralis and a reduction in isometric force output in both flexion and extension (Op den Kamp et al., 2013), however it is unclear whether the atrophy seen in this group is due to either the reduced lung function and

subsequent hypoxia or a tumour released factor. Indeed, cultured colon cancer cells (C26) express myostatin *in vitro* (Lokireddy et al., 2012). The data of Op den Kamp and colleagues (2013) also shows cachexic patients have a counterintuitive increase in p-Akt/Akt ratio, similar to that of Doucet and colleagues (2007) in cachexic COPD patients.

2.5.2.4 Obstructive Sleep Apnoea

Obstructive sleep apnoea (OSA) presents with intermittent pharyngeal collapse during sleep, resulting in intermittent hypoxemia and reduced quality of sleep (Malhotra and White, 2002). Intermittent hypoxic stimuli appear to differ with regards to the physiological effects seen in individuals. OSA patients do not appear to present with muscle wasting, with no reports in the published literature.

In a similar manner to the intermittent hypoxic stimulus seen in OSA, a number of intermittent hypoxic + resistance exercise studies suggest beneficial effects of intermittent hypoxia during mechanical loading. Muscle hypertrophy following 6 weeks training with and without intermittent local hypoxia (upper arm pressure cuff) is greater following the intermittent hypoxia condition (Nishimura et al., 2010), and acute resistance training stimuli under a similar intermittent hypoxia protocol induces greater GH response than exercise in normoxic conditions (Kon et al., 2010), as well as a decrease in myostatin mRNA expression (Drummond et al., 2008).

Thus, the consideration of hypoxia on any physiological response should differentiate between continuous and intermittent hypoxia, as the physiological response to intermittent hypoxia appear different than those of chronic hypoxia.

2.5.3 Environmental Hypobaric Hypoxia

Atmospheric pressure, and subsequent partial pressure of oxygen (PO_2), decreases as a function of altitude (Figure 2.11). With some notable exceptions (Figure 2.13, pg. 48), humans prefer habitation at or near sea level, and it is hypothesized that humanity evolved and developed at or near sea level conditions (Walter et al., 2000).

Lowlander individuals are capable of sojourning to the highest peak available, Mt Everest, at an altitude of 8,848 m, with prior time to allow for adaptation. Mt Everest does appear to be at, or about, the physiological limit for humanity (Figure 2.12), with individuals successfully summiting without external oxygen supply showing impaired physical function and severe hypoxemia (Grocott et al., 2009, West and Wagner, 1980). The arterial oxygen saturation (measured by direct arterial sampling) in functional humans at the Everest summit ranges from 68.1 % to 34.4 % (mean 54.0 %; Grocott et al., 2009), showing the problems with attempting to model the 'typical' response to hypoxia.

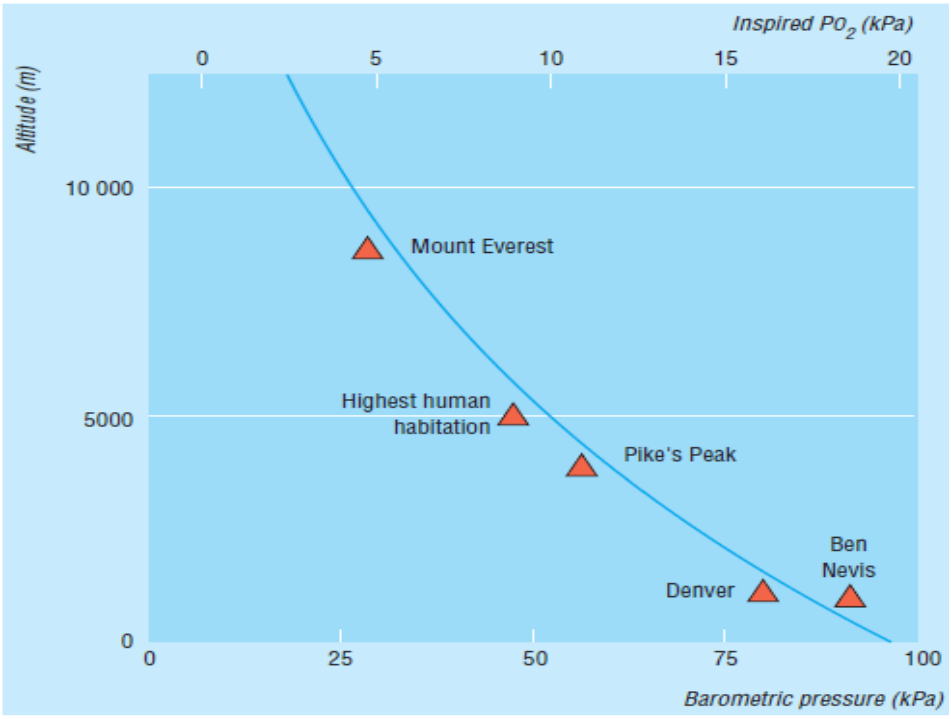

Figure 2.11: The relationship between altitude and pressure of oxygen in the atmosphere. Note barometric pressure and PO_2 are given in kilopascals (kPa). Taken from Peacock (1998).

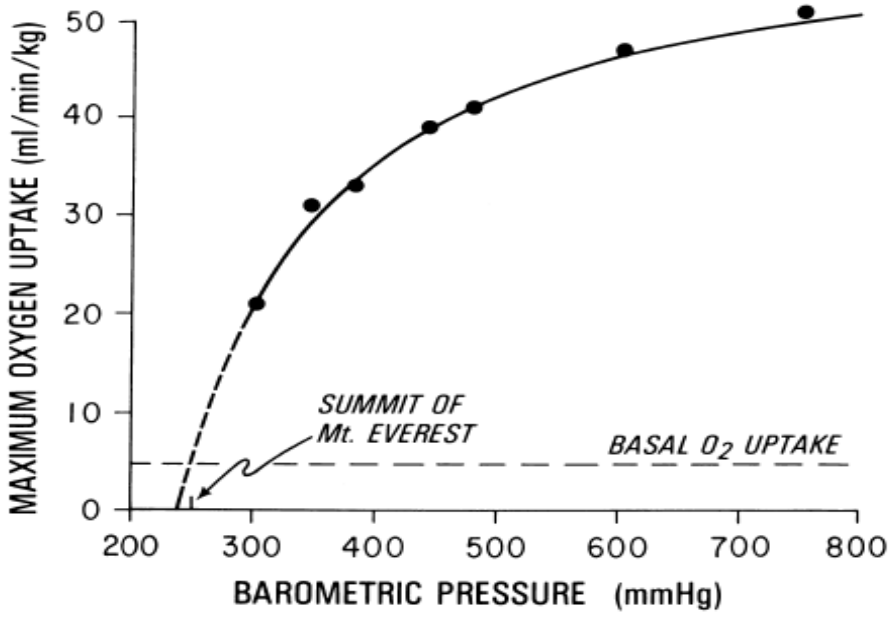

Figure 2.12: Prediction of VO_2max as a function of altitude. Horizontal dashed line indicates suggested minimal oxygen update for survival in the average man. Taken from West and Wagner (1980).

Exposure to hypobaric hypoxic environments at altitude greater than the Everest summit can occur during manned, unpressurised flight. Hoffman and colleagues (1946) demonstrated that individuals moving from a supra-maximal supply of oxygen (100 % oxygen via a nose and mouth covering non-rebreathing mask) to hypobaric hypoxic environments of between 8,000 – 12,000 m (as a simulation of aeroplane cabin depressurisation) demonstrate a rapid loss of mental function, reduced motor control and unconsciousness. The speed of this loss of function occurs as a function of degree of hypoxia, with decreasing atmospheric pressure resulting in more rapid loss of function. Specifically, 8,534 m (authors report 28,000 ft, or ~ 7.1 % O_2 equivalent) exposure leads to reduced mental function in 110 s, hand tremor after 106 s and loss of consciousness within 141 s while 11,582 m (38,000 ft, ~ 4.1 % O_2 equivalent) reduces mental function and increases hand tremor in 35 s, while loss of consciousness occurs in 47 s (Hoffman et al., 1946).

2.5.6.1 Adaptation to Hypoxia

Given sufficient time, humans can adapt to significant physiological extremes. Indeed, adaptation ultimately is *"gross physiological responses that attempt to maintain a constant intracellular environment"* (Murray, 2014). These adaptations differ as a result of duration of exposure, and are explored here first examining hours, days and then weeks, through to intergenerational adaptation as seen in Tibetan and Sherpa individuals.

Early research into adaptation to hypoxic exposure focused on phenotypic, metabolic or oxygen transport chain changes. Exposure to a hypobaric hypoxic chamber (equivalent to 4,300 m) for 2 hours increases plasma glucose clearance following an oral glucose tolerance test in healthy young males and females (Kelly et al., 2010) as does normobaric hypoxia at a similar concentration and time in type 2 diabetic individuals (Mackenzie et al., 2011). Similar effects are maintained after 9 days stay at 4,300 m (Brooks et al., 1991). These effects are enhanced by exercise in hypoxia

(Mackenzie et al., 2012b), and appear to be long lasting, with reductions in fasting glucose seen 24 hours after 2 hours of moderate hypoxic exposure (Mackenzie et al., 2012a).

Immediately on exposure to hypoxia (variable FiO_2, locked to 80 % SpO_2), depth and rate of breath increases. This hypoxic ventilatory response (HVR) occurs in two phases, with phase one (0 – 5 minutes) characterised by an immediately ventilation increase, whilst phase two (5 – 25 minutes) is characterised by a decline of the HVR back to normoxic baseline (Easton et al., 1986). Central respiratory drive is altered by long term, but not acute exposure. Carotid body chemoreceptor sensitivity is increased following 28 days of hypobaric hypoxia, but not 3 hours (Barnard et al., 1987). Despite an elevated respiratory rate, SpO_2 is reduced as a function of degree of hypoxia. Mäntysaari and colleagues (2011) note reductions in SpO_2 to 58 % within minutes of exposure to 8 % O_2. This effect is FiO_2 dependent; decreasing ambient O_2 % (21, 14, 12 and 10 % O_2) reduces SpO_2 and increases systolic BP (Duplain et al., 1999).

In response to hypoxic exposure, increased erythropoietin (EPO) concentrations are seen after 2 hours at 3,000 m simulated normobaric hypoxia (Mackenzie et al., 2008, Eckardt et al., 1989), and 90 minutes at 4,000 m simulated normobaric hypoxia, which continues for at least 5.5 hours (experimental duration; Eckardt et al., 1989), and between 6 – 24 hours at 2,454 - 2,800 m (Ge et al., 2002). Elevated EPO concentrations return towards baseline over 7 – 21 days (Richalet et al., 1994, Friedmann et al., 2005).

Elevated EPO directly contributes to hypoxia-induced haematopoiesis (Yoon et al., 2011). Erythroblasts cultured *in vitro* in the presence of EPO show EPO internalisation after 0.5 – 1 hour and erythrocyte-like morphology after 12 hours (Krantz, 1991). However, in acute timeframes of hours, this does not appear to effect haematological variables in the healthy human. Increases in

haemoglobin and haematocrit are not witnessed in passive assents to 4,541 m (reported as 14,900 ft) over 6 hours, but do occur following 48 hours (Reynafarje et al., 1959).

Reductions in plasma volume are witnessed after 3 – 12 days exposure to hypobaric hypoxia across a range of simulated altitudes (Surks, 1966, Hannon et al., 1969, Frayser et al., 1975, Singh et al., 1986), but not in an acute timeframe of 12 – 24 hours at an altitude of 4,350 m, despite an increase in renal filtration rate (Hansen et al., 1996), or at 4,500 m after 6 hours (Reynafarje et al., 1959).

Excluding the hyper-acute hypoxic ventilatory response, cardiorespiratory changes are noted in timeframes of days. Individuals show an increase in ventilatory equivalence (V_E / VO_2) after only 4 days of acclimatization to high altitude exposure (Lenfant and Sullivan, 1971). Haematocrit shows a time dependent increase in healthy young males at 3,800 m, increasing between days 3 - 8 and plateauing by day 10 (Jung et al., 1971). Changes in red cell mass are noted at 4 weeks with exposure to 2000 – 25000 m, but not 2 weeks (Rusko et al., 2004), and increases in VO_2max requires 4 weeks at 2500 m, but is not present at 2 weeks (Levine and Stray-Gundersen, 2006).

Exposure to a hypobaric hypoxic chamber (equivalent to 4,300 m) for 2 hours increases plasma glucose clearance following an oral glucose tolerance test in healthy young males and females (Kelly et al., 2010) as does normobaric hypoxia at a similar concentration and time in type 2 diabetic individuals (Mackenzie et al., 2011). Similar effects are maintained after 9 days stay at 4,300 m (Brooks et al., 1991). These effects are enhanced by exercise in hypoxia (Mackenzie et al., 2012b), and appear to be long lasting, with reductions in fasting glucose seen 24 hours after 2 hours of moderate hypoxic exposure (Mackenzie et al., 2012a). These changes are hypothesized to occur as the individual moves metabolic pathway usage to involve greater reliance on non-oxidative glycolytic mechanisms, providing ATP via less efficient means.

Short stays at altitude (9 - 11 days at 4,559 m) do not alter isolated mitochondrial function, despite substantial changes in systemic markers of adaptation (Jacobs et al., 2013). Longer stays (66 days summiting of Mt Everest) induce a 21 % loss of muscle mitochondrial density (Levett et al., 2012) and significant loss of body mass (Holloway et al., 2011). Over the course of 8 days at 3,800 m heart rate increases while stroke volume decreases, maintaining cardiac output at sea level values (Lenfant and Sullivan, 1971). Rats exposed to hypoxia for 3 – 14 days show a time dependent decrease in running endurance time on return to normobaric conditions, with greater decreases following longer exposures (Chaudhary et al., 2012). Rats exposed to moderate hypoxia (12.6 % O_2 for 44 days) show a fibre type shift in gastrocnemius from slow to fast (authors report shift from 'red to white'; Sillau and Banchero, 1977). Body weight of rats exposed to hypoxia for an extended period of time is consistently shown to be lower, when controlling for hypoxic induced impairments to satiety (El-Khoury et al., 2012, Sillau and Banchero, 1977). These losses in body mass, and especially muscle mass, may be linked to the alterations in metabolism seen, as muscle tissue is a relatively metabolically expensive tissue (Murray and Montgomery, 2014).

Haemoglobin concentration increases with increases in altitude during a summit sojourn of Mt Everest up to 6,400 m, then plateaus with increasing altitudes up to the summit (8,848 m), despite continued drops in SaO_2 and arterial oxygen content (Grocott et al., 2009). Plasma volume changes are less consistent, with some individuals showing a decrease in plasma volume, while other participants showed no change (Stokke et al., 1986), however it is worth noting that plasma volume is a variable measure amongst individuals and dependent on hydration status.

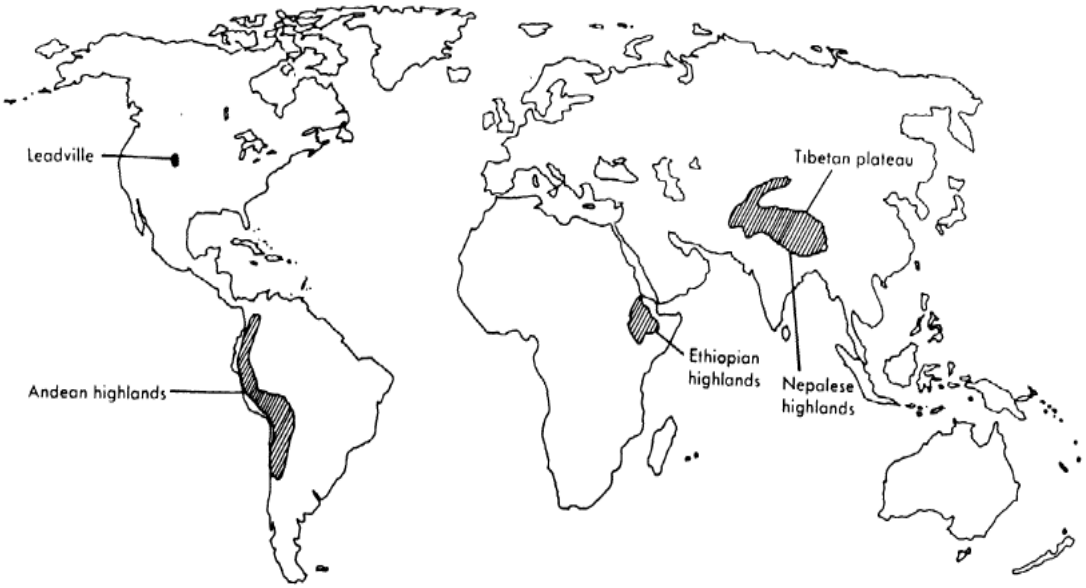

Figure 2.13: Populated high altitude regions of the world. Taken from Moore and Regensteiner (1983). Note also the Antarctic plateau, which could be considered for inclusion on this figure, as Amundsen-Scott Base has a semi-permanent population of 50 – 200, and an average elevation of ~ 3,000 m.

Distinct regions exist where permeant human habitation has allowed for chronic exposure and adaptation to hypobaric hypoxia (Figure 2.13). The highest permanent human settlement is currently La Rinconada, Peru at an altitude of 5,100 m, which has existed for 40 years (West, 2002). These regions have allowed for some of the most chronic examples of adaptation in humans, where Sherpa and Tibetans, who have had a sustained presence on the Tibetan plateau (average 4,500 m altitude) have lived for 7,000 to 20,000 years (Su et al., 2000, Zhao et al., 2009). Tibetans who have migrated to and live at sea level maintain an altered hypoxic response relative to Han Chinese, with a greater ventilatory increase and a decreased HIF response (Petousi et al., 2014). Tibetans show haemoglobin concentrations that are comparable with sea level individuals (Petousi et al., 2014, Simonson et al., 2010). Interestingly, Andean individuals who have also adapted to living at a similar high altitude, and do show elevated haemoglobin (Beall, 2007). Tibetans also show elevated capillarity of muscle, while Andeans do not (Beall, 2007, Hoppeler et al., 2003), suggesting divergent evolutionary adaptation to coping with high altitude.

Table 2.2: Adaptation of physiological systems as a function of time of exposure.

Timings	Adaptations	References
Minutes - Hours	↑ Respiratory rate and depth, EPO ↑,	(Lenfant and Sullivan, 1971, Mackenzie et al., 2008)
Days	↓ Oxidative metabolism, ↑ red cell mass, ↑ haematocrit	(Jung et al., 1971, Mackenzie et al., 2011)
Weeks	↓ body/muscle mass, ↓ mitochondrial density	(Hoppeler et al., 1990, Levett et al., 2012)
Generations	↑↓HIF sensitivity, ↑↓ haemoglobin, ↑↓capillary density	(Beall, 2007, Simonson et al., 2010)

EPO; Erythropoietin; HIF, hypoxic-inducible factor; ↑, increased;↓, decreased; ↑↓, increased or decreased (both witnessed).

2.5.4 Hypoxia Inducible Factor Activity

In response to hypoxic stimuli, activation of the hypoxia inducible factors (HIF) allows the cell to alter gene expression to adapt and survive the challenge. The HIF family consists of three major isoforms (HIF1, HIF2 and HIF3 [Table 2.3]).

HIF1 is a heterodimer formed of two constituent parts, HIF1α and HIF1β. Where HIF1β is stable in the cytosol, HIF1α, while consistently translated and expressed, is rapidly broken down via proteasomal degradation under physiological normal conditions (Figure 2.14). Under normal concentrations of oxygen, the HIF1α protein is hydroxylated by one of three prolyl hydroxylases (PHD1,2 or 3; Appelhoff et al., 2004) and factor inhibiting HIF (FIH-1; Zhang et al., 2010), allowing binding of the HIF1α-specific E3 ligase von Hippel-Lindau protein (pVHL). During cellular hypoxia, the rate of HIF1α hydroxylation is reduced, therefore reducing pVHL binding, allowing for increased binding of the HIF1β and HIF1α subunits and translocation of the complete HIF complex to the nucleus (Fandrey et al., 2006). Increased HIF1 translocation increases transcription of a number of

factors regulating adaptation and survival (Figure 2.15), including glucose metabolism, cellular survival, erythropoietin and angiogenesis (Semenza, 2003).

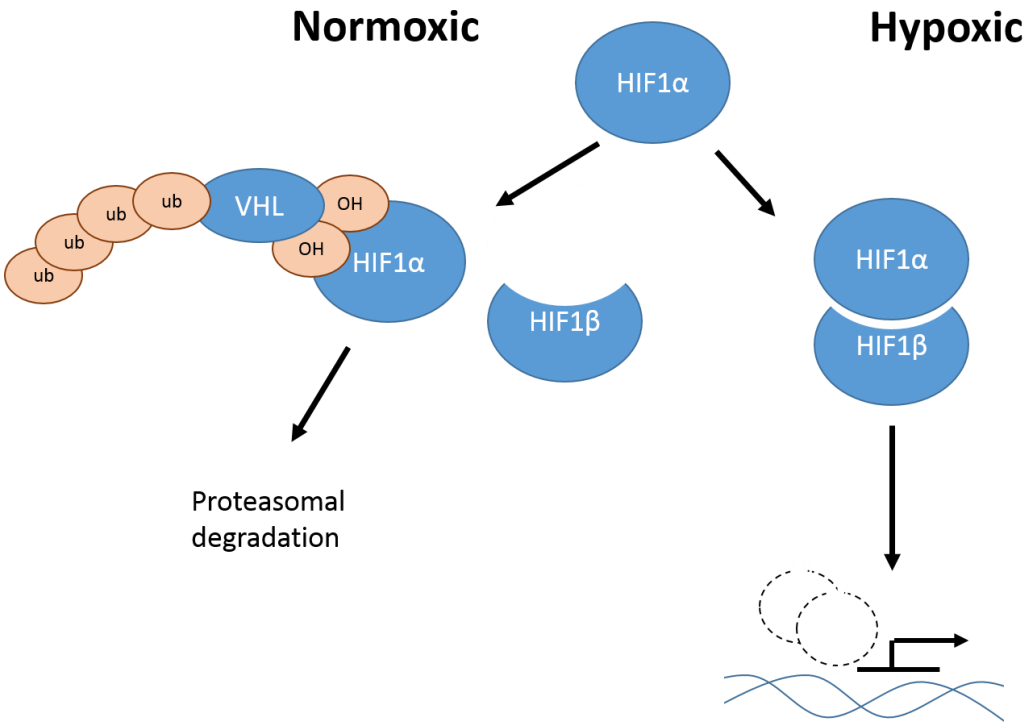

Figure 2.14: Regulation of HIF1 activity under normoxic and hypoxic conditions. HIF1α, Hypoxia inducible factor 1 alpha; HIF1β, hypoxic inducible factor 1 beta; OH, proline hydroxylation sites; VHL, von Hippel Lindau protein; Ub, ubiquitin. Hypoxic response elements outlined in Figure 2.15.

Table 2.3: HIFα isoforms, tissues of expression and known roles.

	Tissues	Roles	Reference
HIF1α	Ubiquitous	Activation of hypoxic regulated genes, apoptosis	(Raval et al., 2005, Stroka et al., 2001, Wang and Semenza, 1993a, Wang and Semenza, 1993b)
HIF2α	Placental, endothelium, lung, heart	↑ Proliferation, tumour role? ↑ VEGF mRNA expression	(Giatromanolaki et al., 2001, Raval et al., 2005, Wiesener et al., 2003)
HIF3α	Kidney, epithelial, endothelial, smooth muscle, brain	3 sub-isoforms characterized (HIF3α1,2,3), responsive to hypoxia. Suppression of hypoxic regulated gene expression	(Augstein et al., 2011, Hara et al., 2001)

HIF, Hypoxia inducible factor; VEGF, vascular endothelial growth factor.

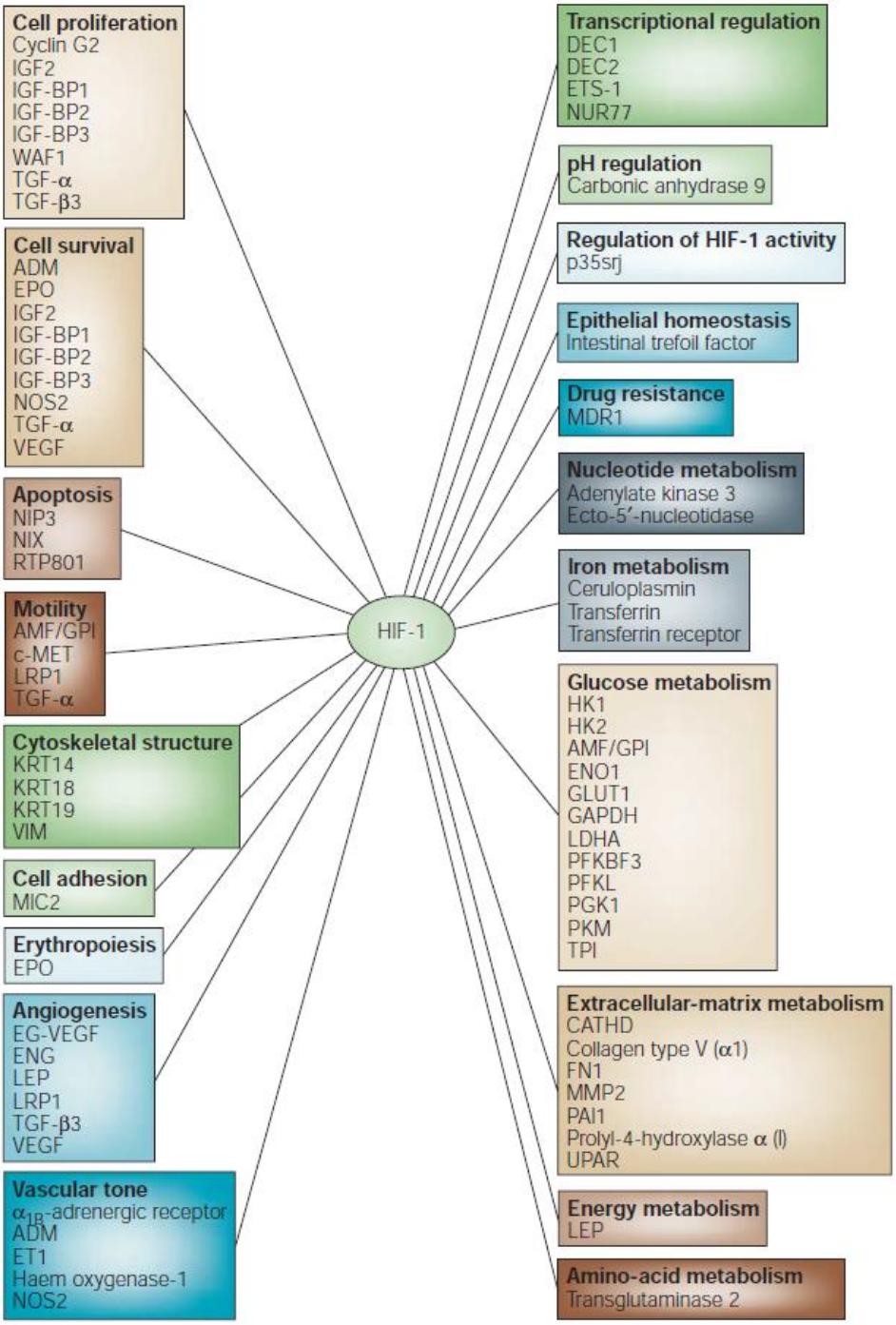

Figure 2.15: Factors transcriptionally activated by HIF1. Taken from from Semenza (2003). ADM, L-arginine; AMF/GPI, autocrine motility factor / glucose phosphate isomerase; c-MET, hepatocyte growth factor; DEC1, 2, deleted in oesophageal cancer 1, 2; EPO, erythropoietin; ENO1, Enolase 1; ET1, Endothelin 1; ETS-1, E26 transformation-specific; GAPDH, Glyceraldehyde 3-phosphate dehydrogenase; GLUT1, Glucose transporter type 1; HK1, 2, Hexokinase 1, 2; IGF-BP, Insulin-like growth factor binding protein; KRT14, 18, 19, Keratin 14, 18, 19; LDHA, Lactate dehydrogenase A; LEP, Leptin; LRP1, Low density lipoprotein receptor-related protein 1; MDR1, multidrug resistance protein 1; MIC2, Transmembrane glycoprotein p30/32; NIP3, nineteen kDa interacting protein-3; NIX, Bcl-2 homology only protein; NOS, Nitric oxide synthase; NUR77, nerve growth factor IB; p35srj, protein 35, serine rich junction; PFKBF3, 6-phosphofructo-2-kinase/fructose-2, 6-bisphosphatase-3; PFKL, 6-phosphofructokinase - liver type; PGK, Phosphoglycerate kinase; PKM, Pyruvate kinas M; RTP801, Regulated in development and DNA damage responses; TGF, Transforming growth factor; TPI, Triose-phosphate isomerase; VEGF, Vascular endothelial growth factor; VIM, Vimentin; WAF1, Protein p21.

Both HIF1α and HIF2α are expressed within skeletal muscle. While the role of HIF1α in response to hypoxic stimuli in muscle is well characterized (Lundby et al., 2009), the response of HIF2α is less well defined, with reports differing on its response to hypoxic stimuli within muscle (Ameln et al., 2005, Lundby et al., 2006), thus this review is focused on HIF1 and its roles within muscle tissue.

HIF1α -/- deletion in mice is fatal *in utero* (Iyer et al., 1998). Muscle-specific HIF1α -/- mice show reduced respiratory exchange ratio at rest relative to control mice (0.8 vs 0.85), with no differences noted in muscle fibre type from gastrocnemius, while in soleus HIF1α -/- mice showed a decrease in type IIa fibre expression (Mason et al., 2004), suggesting an increased reliance on glucose metabolism. Following endurance exercise training, control mice show a shift from fast to slow muscle phenotype, while this shift is blunted in HIF1α -/- mice (Mason et al., 2007).

Chuvash polycythaemia is seen in individuals primarily from the Chuvash regions of the Russian Caucasus. A single nucleotide polymorphism (SNP) of C → T in the VHL coding region results in an arginine-to-tryptophan shift in pVHL, thereby reducing the affinity of pVHL to HIF1α (Ang et al., 2002). Chuvash polycythaemic individuals present with increased EPO and elevated haemoglobin (Bushuev et al., 2006), but demonstrate reduced work rate during submaximal cycling, relative to age and body mass matched individuals (Formenti et al., 2010), suggesting a reduction in muscle mass as a ratio total body mass.

2.5.5 Hypoxia and Muscle Size

L6 myotubes exposed to 1 % O_2 for 12 or 24 hours show an elevation in actin breakdown, a marker of muscle protein degradation (Caron et al., 2009, Workeneh et al., 2006), paired with an increase in atrogin, but not MuRF1 expression. Rate of protein synthesis, as measured by labelled phenylalanine incorporation, is supressed at 24 hours and pAkt (Ser473) is decreased at 48 hours

(Caron et al., 2009), suggesting a suppression of protein synthesis is taking place following an acute hypoxic stimulus. Rats exposed to 6 hours of 11 % O_2 show depressed rates of protein synthesis in multiple tissues (heart, diaphragm, bone, skin, brain and kidney) but not in any peripheral muscle (gastrocnemius, soleus or plantaris) (Preedy et al., 1985). Combined, these results suggest, at least in the initial 24 hours, proteasomal pathways dominate, with decreases in synthesis requiring longer time frames.

Humans exposed to acute normobaric hypoxia (2 hours at 12 % O_2) show no alteration in fractional protein synthesis (FPS) or changes in phosphorylation of Akt (Ser473) at any time point measured, but do show a blunted response to post-resistance training increases in FPS (Etheridge et al., 2011). Conversely, following 4 hours of normobaric hypoxia (11 % O_2) pAkt (Ser473) is reduced in both hypoxia and control conditions, but the reduction following hypoxia is blunted (D'Hulst et al., 2013). Differences exist between these studies that may explain the disparity of findings. Where Etheridge and colleagues (2011) examined their participants in a fasted state, those of D'Hulst and colleagues (2013) consumed a meal 40 minutes prior to the start of the experimental trial. Thus, the results of D'Hulst and colleagues (2013) may suggest hypoxia blunts changes seen post feeding.

In endurance trained swimmers, 3 weeks at 2,300 m altitude does not alter muscle mass, but does reduce fat mass by 11.4 %, relative to pre-exposure mass (Chia et al., 2013). The effect appear to be maintained at 4,599 m, as a 9 day sojourn to the Margherita Hut of Mt Rosa, Italy, does not cause loss of muscle mass (Vigano et al., 2008) despite decreases in muscle mTOR expression. Stays at 5,300 m for 8 – 10 weeks interspersed with ascents to the summit of Lhotse (8,516 m) or Mt Everest (8,848 m) induces loss of muscle cross-sectional area and individual fibre size area, but do not change capillary-fibre ratio (Hoppeler et al., 1990). This atrophic effect is maintained if the exposure is reduced to 5,300 m, and the stay is only 13 days, without summiting attempts (Wing-

Gaia et al., 2014). Combined, these results may suggest an effect of altitude, and thus effective PO_2, where exposures of up to 4,500 m (equivalence ~ 12 % O_2) show no muscle atrophy, while greater than 5,000 m (equivalence ~ 10.7% O_2) induces atrophy. Alternatively, activity levels may account for differences seen, as the Mt Rosa cohorts ascent was partially by cable car, while access to the Everest base camp is a significant hike over multiple days, so differences in exercise stimuli have likely occurred.

Rats exposed to severe hypobaric hypoxia (~ 7000 m) show no difference in soleus muscle wet weight after 1 – 5 days, but do show significant atrophy after 13 days (Magalhaes et al., 2005). Rats exposed to 5,000 m equivalent of hypobaric hypoxia for 7 days show loss of body mass, with control rats weighing 196.0 (2.0) g and hypoxic treated rats weighing 184.9 (1.9) g. Although not measured at 7 days, a reduction in excised soleus mass is also seen at 14 days (Chaillou et al., 2014). Rats exposed to severe hypobaric hypoxia (7620 m) for 3 – 14 days show time-dependent decreases in muscle protein content, muscle wet weight / length ratio and an increase in protein degradation / synthesis ratio, paired with increases in Chymotrypsin-like and calpase-like activity and increased bound ubiquitin in dissected muscle (Chaudhary et al., 2012). Peak force output of excised soleus muscle from rats exposed to 6 weeks of hypobaric hypoxia (450 mmHg, ~ 4,500 m) is unchanged, but rate of fatigue is increased (El-Khoury et al., 2012). These rats showed a loss of body mass, however changes in muscle mass were not quantified (El-Khoury et al., 2012). It can be seen therefore that an effect of time may be seen, with 1 day insufficient to induce measurable muscle atrophy in rats. Further, 4,500 m does not appear to alter contractile properties of excised muscle suggesting no muscle atrophy had taken place, which, if true, suggests an effect of altitude, where at least 5,000 m equivalent is required for muscle atrophy to occur. While all performed in animal models, these studies are of interest in comparison to the above human studies, as they examine similar equivalent altitudes (4,500 m – 7000 m) as those seen during healthy human studies in mountaineering sojourns. Further, such animal models have a reduced effect of confounding

factors seen in these human studies, as they do not involve the heightened levels of physical activity and cold exposure required during mountaineering.

It can be seen therefore that in response to a chronic hypoxic stress of sufficient magnitude and time, muscle mass is lost as a result of cellular atrophy. This response has been proposed to be a protective response (Murray and Montgomery, 2014), both reducing metabolic cost of the individual by removal of metabolically costly muscle tissue, freeing of amino acid component for metabolic use, and also reducing diffusion distance for oxygen within individual myofibers. Indeed, as Harvey (1928) modelled, required PO_2 for diffusion is a function of the square of the radius supplied (Figure 2.16A). Thus, with a reduction of capillary PO_2 and reduction in supplied area, the most efficient solution is for a reduction of cellular cross sectional area (Figure 2.16B).

A)

$$PO_2 = VO_2 r^2 / 6K$$

(Where VO_2 indicates rate of oxygen consumption, r indicates radius and K the diffusion constant)

B)

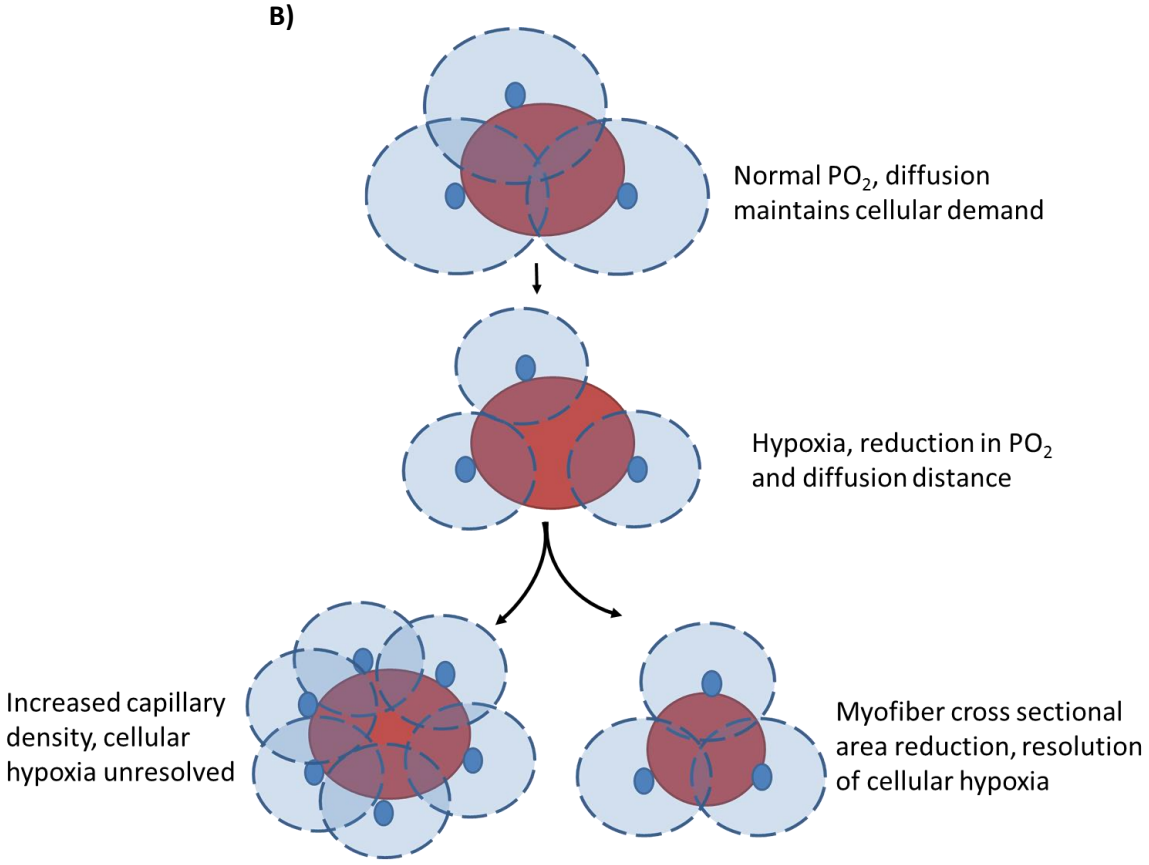

Figure 2.16: Modelling of cellular responses to reduced partial pressure of oxygen. A) Model of diffusion into the cell, as proposed by Harvey (1928), PO_2 refers to partial pressure of oxygen within supplying capillaries, r to radius and K a gas-specific diffusion constant. **B)** Visual representation of this model within a single myofiber (red circle) supplied by three capillaries (small blue circles) and their corresponding diffusible potential (dashed larger circle). A reduction in PO_2 reduces potential diffusion distance, thereby to maintain supply cellular atrophy must occur. The alternative, increasing capillary density in the absence of atrophy, cannot resolve cellular hypoxia.

2.5.6 Potential Atrophic Cell Signalling Pathways during Hypoxia

If hypoxia is directly altering muscle size, either as a dysregulatory or as a protective response, then alterations in HIF signalling may alter muscle phenotype. One commonly identified single nucleotide polymorphism (SNP) in the HIF1α gene is rs11549465 C > T, occurrence of which produces an amino acid substitution from proline to serine at position 582, and results in increased stabilisation of the HIF1α subunit (Yamada et al., 2005). Russian elite strength athletes (power lifters and wrestlers) show significantly increase expression frequency of the rs11549465 SNP (13.1 % and 15.7 % of respective sub-population) over a control group (7.5 % expression frequency) suggesting a selection advantage to this mutation (Gabbasov et al., 2013). However, this associative study does not suggest any causative reason for this finding.

HIF1α protein expression varies by muscle in the healthy male human at baseline normoxic conditions. Protein expression of HIF1α is similar in vastus lateralis and soleus, but notably lower in triceps brachii (Mounier et al., 2010). Care should be taken in the interpretation of HIF1α mRNA expression, as Mounier and colleagues (2010) notes a lack of correlation between HIF1α mRNA and protein expression across muscles.

2.5.7 Role of Myostatin

A link between regulation of myostatin and regulation of hypoxia may explain the response of humans to hypoxic environments; little work has been published to examine this hypothesis. However, a series of disparate models and experiments have reported alterations in myostatin expression with hypoxic conditions or models, which are noted below.

Chronically hypoxemic and cachexic COPD patients show elevated muscle myostatin peptide expression, as do otherwise healthy rats exposed to severe hypoxia (10 % O_2) for 5 weeks (Hayot et

al., 2011). Myostatin mRNA elevated in muscle of COPD patients (Plant et al., 2010) and in mice following a gradual exposure increasing from sea level to 8,200 m over 7 days, followed by 7 further days at this altitude (Hauerslev et al., 2014). Chronic smokers (≥ 20 cigarettes per day, ≥ 20 years) with reduced lung function show increased muscle myostatin, atrogin and MuRF1 mRNA and impaired muscle fractional protein synthesis (Petersen et al., 2007).

Cobalt chloride binds and stabilizes HIF1α expression, mimicking intracellular effects of hypoxia. Stimulation of myotubes *in vitro* with cobalt chloride increases myostatin peptide expression, and co-incubation of myotubes with the myostatin propeptide offsets the atrophy (Hayot et al., 2011), providing indirect evidence that myostatin and hypoxia may be linked.

Myostatin mRNA expression is noted to be present in cardiomyocytes taken from cardiac biopsies of sheep. Following a severe hypoxic insult (induced infarct) increases in myostatin protein expression are found 12 – 48 hours post infarct in the hypoxic zone surrounding the infarct site (Sharma et al., 1999). This finding suggests a role of myostatin either in cell atrophy or apoptosis surrounding the hypoxic infarct site, assuming similarity of the role of myostatin in closely related cardiomyocytes.

Severe pre-eclampsia can present with reduced SpO_2 and intrauterine hypoxia (Millman et al., 2011). Pre-eclampsia has been noted to present with elevated plasma myostatin, and plasma myostatin concentration increases as severity of pre-eclampsia increases (Guo et al., 2012). Whilst a link between reductions in SpO_2 and adverse birthing outcomes exists (Millman et al., 2011), any relationship between this and increased plasma myostatin concentrations is unclear, as is the role that myostatin may play.

Thus, a disparate group of conditions that present with alterations in oxygen uptake and transfer, HIF stabilisation, or respiratory function are also paired with alterations in myostatin expression. Hypoxia is linked with losses of muscle mass, it could be hypothesized that hypoxia regulates myostatin expression, thereby resulting in the observed muscle atrophy.

2.6 Summary

It is well established that individuals placed into a hypoxic state for a sufficient length of time, either due to hypobaric hypoxia or pathophysiological hypoxia, will lose muscle mass. This loss of muscle mass may represent a protective response, reducing cross-sectional area of individual myofiber to aid oxygen diffusion, however left unchecked causes significant mortality in chronic disorders such as COPD and CHF, independent of markers of disease progression. Losses appear to be a function of the concentration of hypoxia and time spent hypoxic. Whilst dependent on timing of hypoxia, atrophy appears to involve both pro-synthesis Akt-mTOR signalling and pro-degradative proteasomal signalling, with pro-degradation pathways dominating in the initial 24 hours.

Myostatin is a central regulating factor of the size of muscle mass. Myostatin decreases activity of the Akt-mTOR pathway while also increasing activity of the ubiquitin-proteasomal pathway. Further, evidence suggests that myostatin is elevated in the muscle of COPD patients with chronic hypoxemia, and is also elevated in a disparate group of conditions where hypoxia is also present.

If hypoxia alone is capable of inducing muscle loss, then hypoxia alone may be sufficient to increase myostatin expression. However, the effects of hypoxia on muscle atrophy may be additive when combined with other atrophy causing stimuli in chronic disease states as activity level, disease, inflammation or nutrition status. Care should be taken therefore to minimise these effects when investigating the effects of hypoxia.

It would appear therefore that an examination of the effect of hypoxia on myostatin signalling is required in the isolation of confounding factors due to environmental or disease factors. This work should examine the effect of time and magnitude of hypoxia on both myostatin and downstream markers of myostatin's atrophic actions with respect to both anabolic and catabolic mechanisms.

2.7 Aims & Hypotheses

The primary aim of this research project is to determine the role of acute hypoxia in the regulation of myostatin. Specifically, the objectives of this work are to;

1. determine the effects of hypoxia on the migration of myoblasts and the diameter of myotubes *in vitro*
2. ascertain the effect of acute hypoxic exposure on myostatin signalling *in vitro*
3. ascertain the presence or absence of a time-dependent effect of hypoxia on myotubes *in vitro*
4. determine the acute effect of hypoxia on myostatin signalling *in vivo* in healthy humans
5. ascertain the acute effect of hypoxia on whole body protein synthesis and degradation *in vivo* in healthy humans
6. demonstrate the presence or absence of a time dependent effect of hypoxia on myostatin signalling *in vivo* in healthy humans *and*
7. demonstrate the presence or absence of a concentration dependent effect of hypoxia on myostatin signalling *in vivo* in healthy humans.

The primary hypothesis presented here is that hypoxia will increase atrophy of muscle via increases in myostatin activity which subsequently activates proteasomal activity, independent of IGF-1-Akt pro-anabolic pathways. Specifically, it is hypothesized that;

1. hypoxia will decrease the migration of myoblasts and the diameter of myotubes *in vitro*
2. hypoxia will increase myostatin expression *in vitro*
3. the effect of hypoxia on myotubes diameter *in vitro* will be time-dependent
4. hypoxia will increase expression of intra-muscular myostatin and concentration of plasma myostatin *in vivo*

5. hypoxic exposure will increase whole body protein degradation but not alter protein synthesis *in vivo*
6. the effect of hypoxia on myostatin *in vivo* will be time-dependent, with increased myostatin both within muscle and in plasma with longer hypoxic exposure *and*
7. the effect of hypoxia on myostatin *in vivo* will be concentration dependent, with increased myostatin seen with lower concentrations of oxygen.

Chapter Three – The Effect of Hypoxia on Myoblast Migration and Myotube Size

3.1 Introduction

Myofibers *in vivo* are dependent on a near-continuous supply of oxygen from external vasculation, with a complete impairment of perfusion resulting in rapid cellular death (Pang et al., 1995). In times of partial restriction, such as during whole body hypobaric hypoxia, one adaption that muscle shows over chronic timeframes (days – weeks) is the loss of muscle mass. A chronic reduction in barometric pressure results in increased atrophy of skeletal muscle in otherwise healthy humans during mountaineering (Hoppeler et al., 1990) and extended stays in hypobaric chambers (Rose et al., 1988). In a similar manner, ~ 25 % of COPD and chronically hypoxemic chronic heart failure patients show atrophy of muscle mass (Anker et al., 2003, Bernard et al., 1998).

When resting healthy individuals are exposed to acute hypoxia (12 % O_2 for 2 hours) whole body protein synthesis is not altered, however the anabolic effect of an acute resistance exercise session appear to be blunted (Etheridge et al., 2011). Caron and colleagues (2009) demonstrated that myotubes exposed to hypoxia for 24 hours had reduced intracellular protein concentrations and increased expression of ubiquitin ligase atrogin, but no alteration in pAkt expression. Combined, this evidence suggests that acute hypoxia alone (< 24 hours) may preferentially target increased activity of atrophic pathways, and not suppression of hypertrophic pathways.

Exposure of C2C12 myoblasts *in vitro* to hypoxic conditions prevents differentiation into mature myotubes and increased proteasomal degradation of MyoD (Beall, 2006). Expression of HIF1α protein is increased under non-hypoxic conditions during C2C12 myoblast differentiation, and inhibition of HIF1α protein formation prevents myotube formation (Kallman et al., 1990), suggesting while HIF1α signalling is a necessary step in normal muscle function and growth, hypoxic exposure can prevent myoblast maturation. Variations in other atmospheric conditions may also alter cellular morphology and function. Where 5 % CO_2 is in mammalian cultures is standard *in vitro*,

increasing CO_2 towards 10 % results in suppression of myotube formation, whilst removal of atmospheric CO_2 results in increased time in G1 phase and delayed mitosis of precursor myoblasts (Przybylski et al., 1979). Similarly, enzymatic-dependent processes, such as ubiquitin-dependent protein degradation, is altered by temperature. C2C12 myotubes exposed to 40 °C show elevated proteasomal activity and protein degradation relative to myotubes at 37 °C (Morita et al., 1996). Thus, *in vitro* investigations standardize these variables where possible, whilst recognizing that metabolically active tissues, such as muscle, show minor variations around such standardized conditions *in vivo*.

Myostatin is a central regulator of muscle size (reviews by Lee, 2004, Rodriguez et al., 2014). Increases in myostatin expression can alter muscle mass by reducing protein synthesis pathways (Amirouche et al., 2009), increasing protein degradation via the ubiquitin-proteasomal pathway (McFarlane et al., 2006) and reducing the maturation of precursor satellite cells (McCroskery et al., 2003, McFarlane et al., 2008). Rats exposed to 10 % O_2 for 6 weeks show increased expression of myostatin in both soleus and gastrocnemius muscles and increased muscle atrogin expression (Hayot et al., 2011). Hypoxemic COPD patients also show an increase in muscle myostatin peptide expression relative to healthy controls (Hayot et al., 2011), suggesting myostatin may underlie atrophy in hypoxic conditions. Concentration of plasma myostatin correlates with muscle mass across healthy and cachexic patients (Gonzalez-Cadavid et al., 1998), thus a question of cause and effect arises. Either hypoxia increases myostatin concentration, thereby resulting in a loss of muscle mass, or, hypoxia decrease muscle mass, thereby increasing basal myostatin concentration. Evidence for a direct hypoxia – myostatin link was given by Hayot and colleagues (2011) who demonstrated that chemical hypoxia (cobalt chloride [$CoCl_2$] treatment) resulted in increased myostatin protein expression in a dose-dependent manner. This effect demonstrates an effect of HIF signalling, as $CoCl_2$ stabilises HIF1α expression (Epstein et al., 2001), but may not be a true representation of hypoxia *per se*.

The function of myostatin appears to be maintained between species, with myostatin deletion (either naturally occurring or experimentally induced, showing similar hyper-muscular phenotype in mice (McPherron et al., 1997), cattle (Grobet et al., 1997, Kambadur et al., 1997, McPherron and Lee, 1997), dogs (Mosher et al., 2007, Zou et al., 2015), sheep (Proudfoot et al., 2015) and one human case study (Schuelke et al., 2004). However, outside the case study of Schuelke and colleagues, there is limited direct evidence for the maintenance of myostatin's effect in the human, and no published examples to date examining myostatin differences between non-human and human species. Work examining myostatin between species may need to address this.

Cells from multiple cellular lineages, including myotubes, cultured in hypoxic conditions show elevated NF-κB activation relative to control cells (Koong et al., 1994a, Osorio-Fuentealba et al., 2009), whilst inhibition of TNFα activity prevents the hypoxia-induced loss of myotube protein content *in vitro* (Caron, M, personal communications) suggesting a hypoxia – inflammatory signalling link. Indeed, stimulation of myotubes with TNFα induces cellular atrophy, whilst NF-κB prevents this (Li and Reid, 2000). In alveolar macrophages, elevated TNFα expression is seen following hypoxic treatment (1.8 % O_2) (Leeper-Woodford and Detmer, 1999). In chronic disorders elevated pro-inflammatory signalling results in significant loss of muscle mass (Frost et al., 2007, Lang et al., 2006, Op den Kamp et al., 2013), and it has been suggested that hypoxia and inflammatory signalling pathways may interact during muscle atrophy in COPD (Wagner, 2008). Thus, any hypoxic induced atrophic effect may occur via the canonical NF-κB pathway.

3.1.1 Aims & Hypothesis

The aim of this Chapter was therefore to examine the acute temporal response of myocytes to hypoxic exposure. Further, to aid translation between these *in vitro* experiments utilizing a murine cell line and following Chapters *in vivo* in humans, a bioinformatic comparison between myostatin signalling pathways in both the human and mouse was planned. Specifically, this work aimed to;

1. determine the effects of hypoxia on the migration of myoblasts and the diameter of myotubes *in vitro,* and the relationship between NF-κB and myoblast migration / myotube size in response to hypoxia *in vitro*
2. establish what effect acute hypoxic exposure has on myostatin signalling *in vitro*
3. establish the presence or absence of a time-dependent effect of hypoxia on myotubes *in vitro and*
4. examine *in silico* similarities and differences between the structure of myostatin and downstream signalling proteins in the human and the mouse.

The hypothesis of this Chapter is that hypoxic exposure will result in reduced myoblast migration and increased myotube atrophy via a NF-κB dependent increase in myostatin activity. Specifically, it is hypothesized that;

1) hypoxia will decrease the migration of myoblasts and also decrease the diameter of myotubes *in vitro*, and inhibition of NF-κB activity will offset this
2) hypoxia will increase myostatin expression, inhibition of NF-κB will offset this
3) the effect of hypoxia on myotubes diameter and myostatin expression *in vitro* will be time-dependent *and*
4) myostatin and signalling proteins downstream of myostatin will show a high percentage similarity between humans and mice.

3.2 Methods

3.2.1 Initial Stock

Myoblasts from the well characterised murine muscle-derived C2C12 (Yaffe and Saxel, 1977) cell line (ATCC, # CRL 1772) were gifted by Professor Stephen Harridge, Centre for Human Aerospace Physiological Sciences, Kings College London. C2C12 cells were provided as 1,000,000 cells in a 1 mL volume containing 10 % foetal bovine serum (FBS) and 10 % Dimethyl sulfoxide (DMSO) for freezing, and were provided at passage 10 (p10). Cells were rapidly defrosted from – 196 °C to 37 °C and gently mixed in 10 mL of growth media (GM) consisting of Dulbecco's modified Eagle's media (DMEM ; Gibco, 22320), supplemented with 10 % FBS (Hyclone, 10175573), Penicillin and streptomycin (50 $\mu g.mL^{-1}$; Gibco, 15140) and seeded into a T175 flask. DMSO was removed 24 hours after seeding, cells were washed once in Dulbecco's phosphate buffered saline (dPBS) pre-heated to 37 °C and 10 mL GM replaced. Cells were incubated in standard conditions (37 °C, 5 % CO_2, 100 % humidity) with GM changed every 24 hours until cells reached 80 % confluence; typically taking 96 hours. Confluency was visually established by inverted light microscopy daily. Confluent cells were trypsinized (2 minutes, 2 mL TrypLE [Gibco, 12605.036] at room temperature), resuspended into 10 mL of GM + 10 % DMSO and aliquoted into 1 mL volumes. The majority (n = 7) were aliquoted into 1 mL cryogenic tubes (Nunc, 368632), slowly frozen to -80 °C (Thermo, 5100-0001 ['Mr Frosty']) over 24 hours before being stored at -196 °C while the remainder of the aliquots (n = 3) were reseeded into T175 flasks, grown to confluence again as described above before samples were aliquoted and storage as described above, to give a stock experimental bank of C2C12 myoblasts at p11-12, which were used for all experiments described below.

3.2.2 Growth

For experimental conditions, an aliquot was defrosted rapidly from -196 °C to 37 °C and gently mixed with 10 mL of GM before seeding into a T175 flask. After 24 hours, cells were washed once in dPBS after which GM was replaced, to remove excess DMSO. GM was changed every 48 hours until cells reached 80 % confluency, after which cells were trypsinized (2 mL TrypLE at room temperature), diluted 1:10 in GM and seeded for experimental conditions. All experiments were either run in 10 cm dishes or 6 - well plates. After seeding into plates for experimental conditions, myoblasts were grown to confluence for the scratch assays on precursor myoblasts (described below, section 3.2.2) or grown to 80 % confluency and differentiated (described below, section 3.2.4) for experiments on mature myotubes (sections 3.2.4 – 3.2.6). During this growth phase, cells were grown in standard conditions (37 °C, 5 % CO_2, 100 % humidity).

3.2.3 Differentiation

For experiments on mature myotubes, myoblasts at 80 % confluence in 10 cm dishes were washed once in dPBS then incubated in a differentiation media (DM) of DMEM with 2 % equine serum (Thermo, HYC-001-342B) penicillin and streptomycin (50 $U.mL^{-1}$ [Gibco, VX15140122]) for 96 hours with DM changed every 24 hours. After differentiation, DM was changed one final time prior to stimulation introduction.

3.2.4 Myotube Diameter Microscopy

The diameters of myotubes from collected photographs were quantified using open-source software ImageJ (NIH, version 1.48i). Diameter was quantified three times per myotube, perpendicular to the longitudinal sarcolemma of the cell; only cells with a long, thin morphology representative of myotubes were included in analysis. A total of 10 random myotubes were measured per photo, giving 30 myotubes measured per plate and time-point. The mean of 30 myotubes ± SEM is reported here. All experiments were done in triplicate in separate cultures.

Measurements were checked by a blinded individual, comparison by Pearson's correlation show a strong linear relationship (r = 0.651, $p < 0.001$ – Appendix Two).

3.2.5 Scratch Assay

For analysis of chemotaxis, confluent myoblasts in 6-well plates were scratched in a vertical straight line, using a single smooth motion, with a 200 µL sterile pipette tip, as described by Liang and colleagues (2007). Immediately after scratching, cells were washed once in dPBS to remove cellular debris then 10 mL GM replaced. Cells were stimulated with either control (no stimulation), hypoxic (1 % O_2 environment) or hypoxic + PS1145 (1 % O_2 environment plus addition of 10 µmol NF-κB inhibitor PS-1145 dihydrochloride [Sigma, P6624]).

After 15 hours, cells were removed and photographed three times per well in the same manner as above. Scratch diameter was quantified 50 times per photo and an average value taken, giving three measures per well. The regrown 'edge' was defined as those cells that maintained connection to the main body of seeded cells, isolated 'islands' of cells were ignored. All experiments were performed in triplicate in three separate cultures. The mean of three measures ± SEM are reported here. Hypoxic stimulation was provided using a separate standard incubator, pre-set to 1 % O_2, 5 % CO_2, with the balance of N_2, maintained at 37 °C. The concentration of O_2 used (1 % O_2) was chosen based on previous reports (Caron et al., 2009) which corresponds approximately to a PiO_2 of 7 mmHg, similar to that predicted within muscle of patients with peripheral arterial disease or healthy individuals in severe hypoxia (Landgraf et al., 1994).

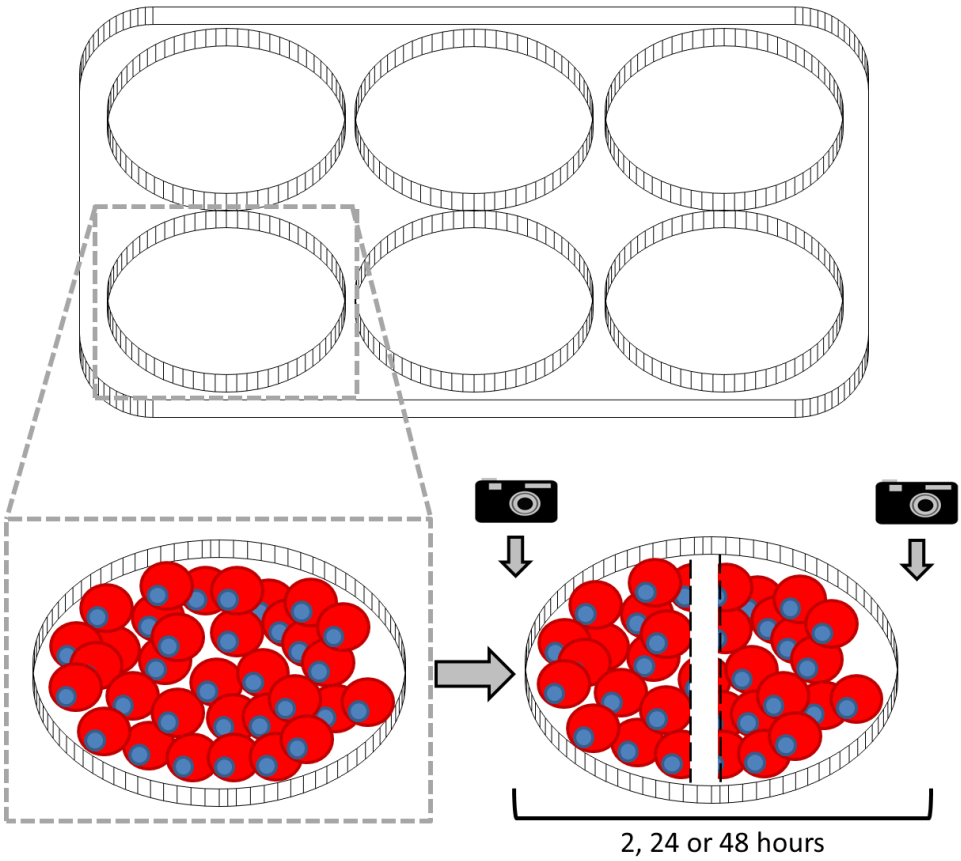

Figure 3.1: Scratch Assay Methodology Confluent C2C12 myoblasts were scratched and photographed pre- and post-treatment (± hypoxia [1 O_2] or hypoxia + PS1145 [10 µM], 15 hours).

3.2.6 Hypoxic stimulus

Differentiated mature myotubes (section 3.2.3) and precursor myoblasts (section 3.2.2) were stimulated ± hypoxia (1 % O_2) or hypoxia (1 % O_2) + PS1145 (10 µM). Hypoxic stimulation was provided with a standard incubator, pre-set to 1 % O_2, 5 % CO_2, with the remainder balance of N_2 from tanked supply, maintained at 37 °C, 100 % humidity throughout. The concentration of O_2 used (1 % O_2) was chosen based on previous reports (Caron et al., 2009).

Immediately prior to and post stimulation, myotubes were photographed at three random locations per plate using an inverted light microscope (2.5 × zoom, 1.3 megapixel digital camera

attachment) for quantification of cell size (section 3.2.5), then total protein was extracted in a standard manner. Cells were washed once with ice-cold dPBS then lysed in a lysis buffer (10 mmol Tris-HCl, 150 mmol NaCl, 2 mmol EDTA, 2 % Triton X-100, protease inhibitor [Sigma, P8340] & phosphatase inhibitor [Sigma, P6624], Appendix One) for 20 minutes on ice. Cells were then manually scraped with a sterile spatula, transferred into 1.5 mL eppendorf tubes and centrifuged at 6000 rpm for 6 minutes at 4 °C. Subsequent supernatant of total protein was aliquoted and frozen at -80 °C 1:4 in Laemmli's loading buffer (Appendix One) for future analysis by western blot (section 3.2.7). An aliquot of 30 µL was saved for analysis of total protein content, described below (3.2.7 Protein Quantification).

3.2.7 Protein Quantification

Quantification of total protein in cellular lysate was performed in the method of Lowry (Appendix Five; Biorad, 500-0116). Whole lysate aliquots were diluted 1:10 in lysis buffer and loaded in triplicate into a clear-bottomed 96 well plate. Bovine serum albumin (BSA) was used as a standard, with a range of 0.09 - 1.44 $\mu g.mL^{-1}$. Coefficient of variability of standards and samples were 0.086, and 0.084, respectively.

3.2.8 Western Blot

For all samples, 40 µg of total protein was analysed by Western blot in a standard manner. Collected lysate was run on precast 10 % polyacrylamide gels (Invitrogen, NP0301) and transferred to nitrocellulose membrane by electroblotting (3 hours, 25 V, on ice). Confirmation of successful loading was done by ponceau rouge stain (2 minutes, 2 mL with gentle agitation), an image of which was also digitised for later normalization. Membranes were blocked in 5 % BSA then probed with appropriate primary antibody. After a wash cycle (4 × 5 minutes, TBS-T), an anti-rabbit HRP-tagged secondary was applied, then visualised with 2 minutes treatment of enhanced chemiluminescence (ECL; Biological Industries, 20-5000-120). Individualized conditions for blocking, primary, and

secondary antibodies are given in Table 3.1. All primary antibodies were utilized in a 1:1,000 dilution, secondary antibodies were utilized 1:10,000. A wash stage from primary to secondary and secondary to developing was performed with tris-buffered saline with tween (TBS-T, 4 × 5 minutes, agitation, Appendix One). Films (Fujifilm, AUT-300-040D) were developed by hand, with 5 minutes treatment in developer (Kodak, P7042-1GA) with gentle agitation, 1 minute wash in running tap water, 5 minutes in fixer (Kodak, P7167-1GA), and a final 1 minute was performed in running tap water. Films were air dried and digitised before specific blot density was quantified with ImageJ open source software (NIH, version 1.45s). Blot density was normalized to the lanes total protein, as stained for by ponceau rouge, using the method of Romero-Calvo and colleagues (2010). Similar to the results of Romero-Calvo and colleagues (2010), this work found this method to produce repeatable, linear results for total protein per lane in the range of protein loading used here (Appendix Eight).

Table 3.1: Western blot characteristics by target protein. Blocking, primary and secondary conditions are diluted into tris-buffered saline with tween (TBS-T). Primary dilution 1:1000, secondary dilution 1:10,000.

Target	Supplier (code)	Blocking	Primary antibody	Secondary antibody
Myostatin	BIOSS antibodies (2227G)	5 % BSA, 1 hour, RT	0.5 % BSA o/n, 4 °C	0.5 % BSA, 1 hour, RT
Ubiquitin	Cell Signalling (3933)	5 % BSA, 1 hour, RT	0.5 % BSA o/n, 4 °C	0.5 % BSA, 1 hour, RT
TNFα	Sigma (T8300)	5 % BSA, 1 hour, RT	5 % BSA o/n, 4 °C	0.5 % BSA, 1 hour, RT

Bovine serum albumin (BSA). Room temperature (RT). Overnight (o/n).

3.2.9 Bioinformatic Analysis of Myostatin and Downstream Pathways

As a translational step from the *in vitro* work utilising the *Mus musculus* C2C12 cell line and the work done in *Homo sapiens* presented later in this work, a bioinformatic analysis was used to compare the percentage similarity of amino-acid sequence of myostatin and several downstream members of myostatin's signalling pathway. A basic local alignment search tool (BLAST) protein-protein analysis was performed using the technique of Altschul and colleagues (1997) and the National Centre for Biotechnology Information (NCBI) BLAST system. Specifically, the pathways examined were the specific proteins and accession numbers showed in Table 3.2. Results are expressed as a percentage similarity of candidate amino acid sequences.

Table 3.2: Proteins compared by BLAST and accession numbers.

Protein	*Homo sapiens*	*Mus musculus*
Myostatin	ABI48514	AAO46885
ActRIIB	NP_001097	NP_031423
ALK4	AAH40531	AAI45778
SMAD2	AAC39657	AAH89184
SMAD3	AAL68976	AAB81755
SMAD4	BAB40977	AAM74472
Akt	NP_001014432.1	NP_001103678
mTOR	NP_004949.1	NP_064393.2
GSK-3β	NP_001139628	NP_062801
p70^{S6k}	NP_003152	NP_001107806
4EBP-1	NP_004086	NP_031944
FoxO1	NP_002006	NP_062713
Atrogin	ABO37797	AAL49563
MuRF1	NP_115977	CAM25927
Ubiquitin	CAA28495	CAA35999

ActRIIB, Activin receptor type Two B; ALK4, Activin like kinase type 4; mTOR, mammalian target of rapamycin; GSK-3β, glycogen synthase kinase three beta; p70^{s6k}, kinase phosphorylating S6 protein; 4EBP1, binding protein 1 to 4E protein; FoxO1, Forkhead box protein, O sub-family; MuRF1, muscle ring finger type 1.

3.2.10 Statistical Analysis

Results are presented here as mean ± SEM or SD as appropriate, and written as 'mean (SEM / SD) units'. Significance was set at $p < 0.05$ throughout. Two-way or repeated measures analysis of variance (ANOVA) was used as appropriate, with *post hoc* analysis performed in the method of Bonferroni. Effect size is given by Cohen's d (*d*), magnitude of effect size is considered small (> 0.09), moderate (> 0.29) or large (> 0.49). Results from bioinformatic analysis comparing amino acid sequence similarity are expressed as a percentage value of *Homo sapiens* relative to *Mus musculus*.

3.3 Results

3.3.1 Effect of Hypoxia and NF-κB Inhibition on Myotube Size

The effect of hypoxia on myotube size was examined by two-way (condition [control, hypoxic] × time [2, 24, 48 hours]) ANOVA. A condition × time interaction was noted for the effect of hypoxia on myotube diameter ($p = 0.08$). *Post hoc* analysis reveals incubation of myotubes in 1 % hypoxia significantly reduced myotube diameter at 2 hours relative to matching control time point by 18.4 (0.7) arb. units to 15.6 (0.3) arb. units ($p = 0.013$, $d = 5.20$). Myotube diameter was further reduced at 24 and 48 hours relative to matched control time points by 7.0 arb. units ($p < 0.001$, $d = 8.26$) and 5.8 arb. units, respectively ($p = 0.001$, $d = 5.76$; Figure 3.2A). Further, an effect of time is noted during hypoxia, with myotube size decreasing between 2 hours and 24 hours by 3.2 arb. units ($p = 0.007$, $d = 3.58$). Similar effects are maintained when myotube diameter in hypoxic conditions is normalized to time point controls (14.2 %, 36.9 % and 34.2 % reduction relative to matching control, respectively, (Figure 3.2B) although *post hoc* analysis reveals the effect of hypoxia at 2 hours is removed ($p = 0.45$, $d = 2.89$). While not directly quantified, an increased number of undifferentiated myoblasts is visually noted in hypoxic treated conditions (Figure 3.2C), suggesting either impaired differentiation or increased apoptosis.

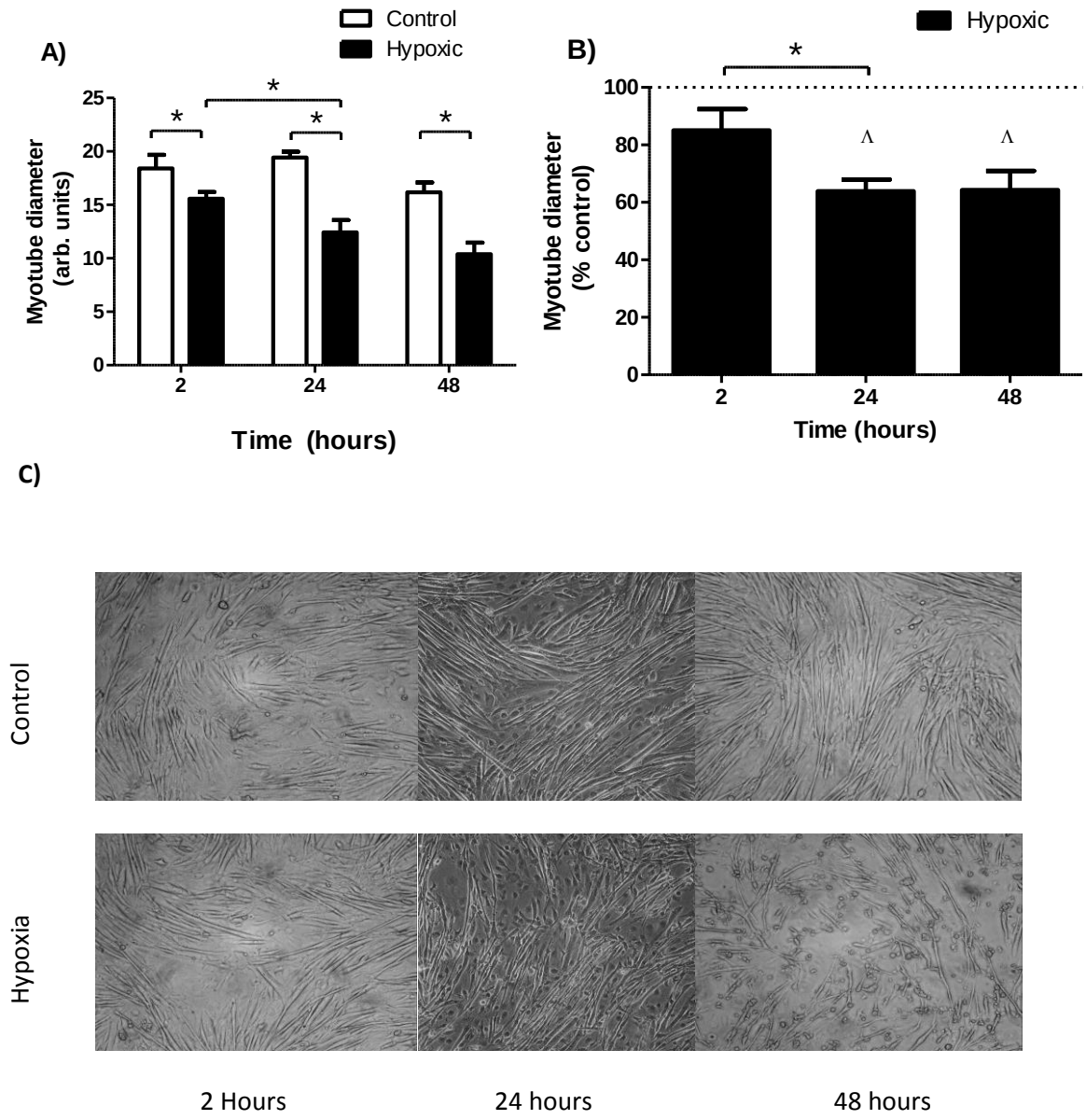

Figure 3.2: Effect of Hypoxia on myotube cross-sectional area. C2C12 myotubes were treated with control (20.9 % O_2) or hypoxic (1 % O_2) conditions for 2, 24 or 48 hours. Cells were photographed under light microscopy three times per plate with phase contrast. Cell diameter was quantified three times per cell, with 10 random cells per image measured, giving a total of 30 cells per plate, utilizing ImageJ. N = 3 separate cultures per condition. **A)** Results expressed as absolute data (Arb. Units) ± SEM. **B)** Results expressed as percentage of individual controls ± SEM. White bars represent control conditions, black stimulated with 1 % hypoxia. Significance is indicated by between conditions as marked (*), or from time point control (Λ; $p < 0.05$). **C)** Representative images of conditions and time points.

The effect of NF-κB inhibition on myotube diameter size during hypoxia was examined by two-way (condition [hypoxic, hypoxic + PS1145] × time [2, 24, 48 hours]) ANOVA. No condition × time interaction was noted on the effect of NF-κB inhibition on myotube diameter during hypoxic exposure ($p = 0.29$). A main effect of both time and group was noted (group $p = 0.001$, time $p < 0.001$, respectively), suggesting PS1145 consistently offset myotube atrophy in hypoxia (Figure 3.3A). When normalized to time point control, a similar effect is noted, with no group × time interaction ($p = 0.37$), but a main effect of group ($p = 0.005$; Figure 3.3B).

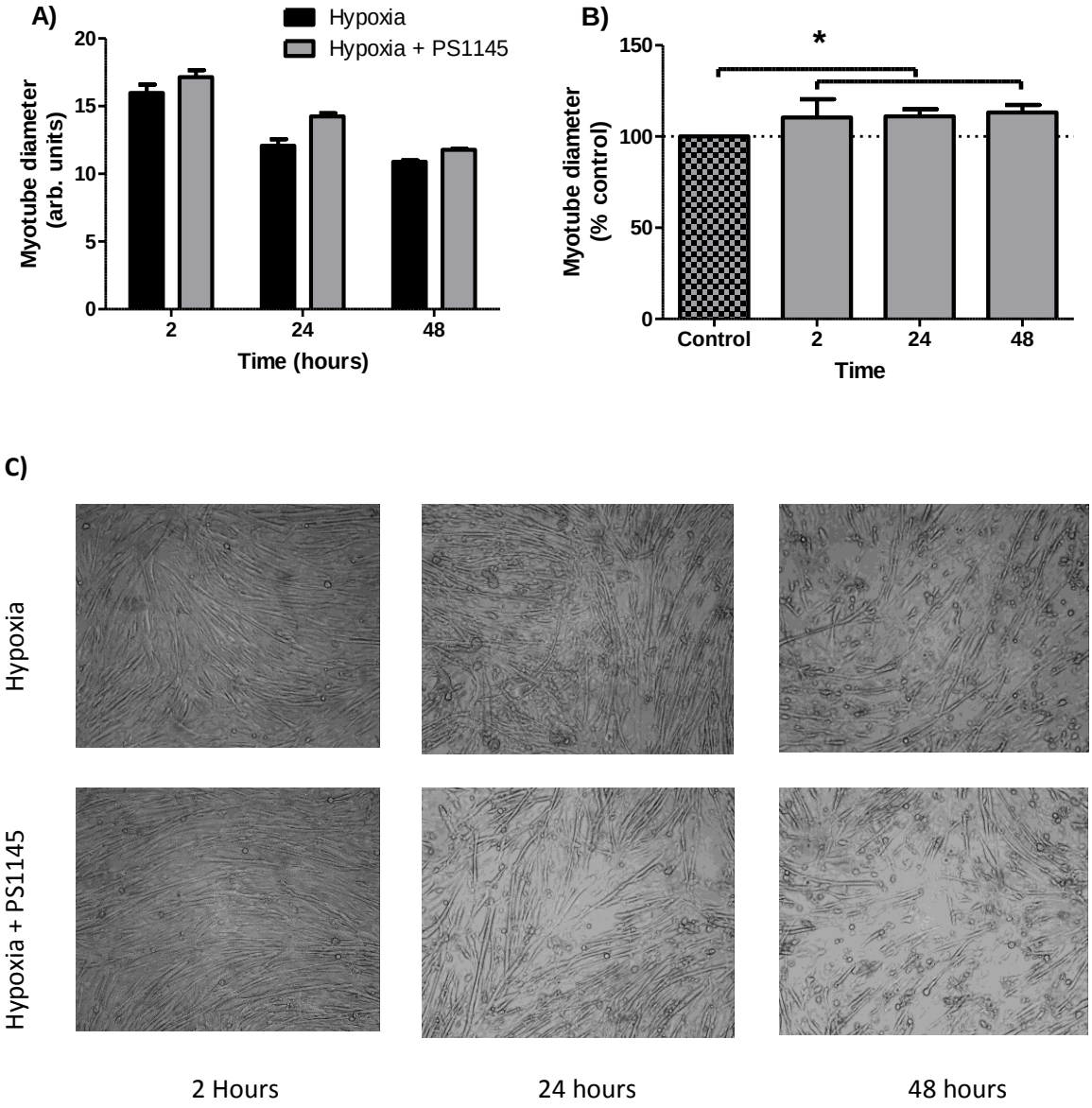

Figure 3.3: Effect of NF-κB inhibition on myotube cross-sectional area during hypoxia. C2C12 myotubes were incubated in hypoxic (1 % O_2) conditions for 2, 24 or 48 hours ± 10 µmol PS1145 (NF-κB inhibitor). Cells were photographed under light microscopy three times per plate with phase contrast. Cell diameter was quantified three times per cell, with 10 random cells per image measured, giving a total of 30 cells per plate, utilizing ImageJ. N = 3 separate cultures per condition. **A)** Results expressed as absolute data (Arb. Units) ± SEM. **B)** Results expressed as percentage of time point controls (%) ± SEM. Black bars represent hypoxia alone, grey stimulated with 10 µmol PS1145. **C)** Representative images of conditions and time points.

The effect of hypoxia on myotube cellular protein content was analysed by two way (condition [control, hypoxic] × time [2, 24, 48 hours]) ANOVA. A condition × time interaction was noted for the effect of hypoxia on myotube protein content ($p = 0.006$). In the control condition, p*ost hoc* analysis shows myotube total protein content was significantly increased (3.3 (0.6) $\mu g.mL^{-1}$ to 5.0 (0.8) $\mu g.mL^{-1}$) at 48 hours, relative to 24 hours ($p = 0.007$, $d = 1.36$). Conversely, in the hypoxic condition myotube total protein content was significantly reduced at 48 hours to 1.2 (0.4) $\mu g.mL^{-1}$, relative to both 2 hours hypoxic (4.5 (0.6) $\mu g.mL^{-1}$) and 48 hour control conditions ($p = 0.003$, $d = 3.77$ and $p = 0.03$, $d = 3.58$ respectively; Figure 3.4A). When results are expressed relative to matching time point controls, a condition × time interaction is maintained ($p = 0.021$), with *post hoc* analysis revealing a reduction of total protein content in hypoxia to 26.4 (10.0) % of matching control time point at the 48 hour point ($p = 0.009$, $d = 6.00$; Figure 3.4B).

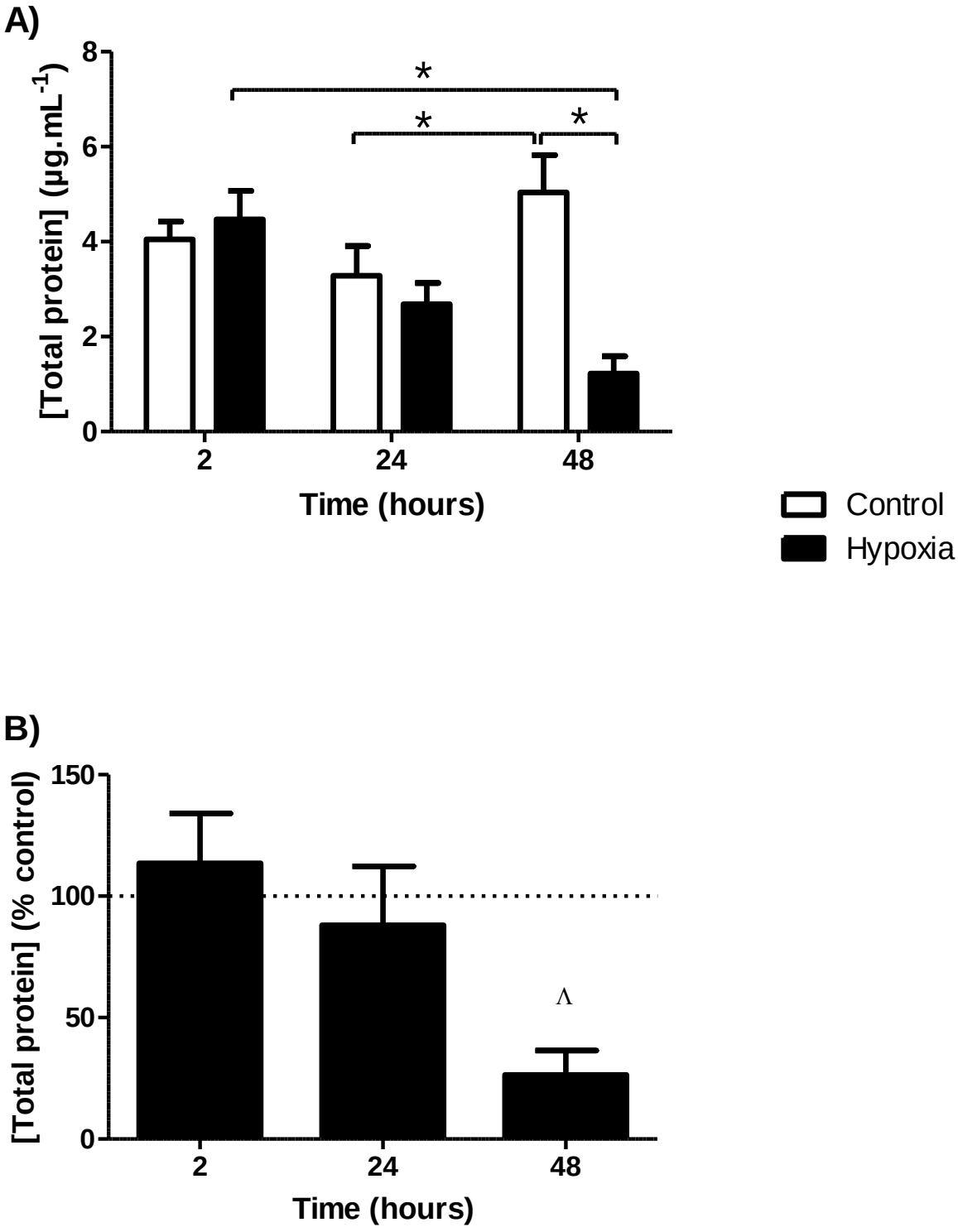

Figure 3.4: Effect of time in hypoxia on cellular total protein content. C2C12 myotubes were incubated in control (20.9 % O_2) or hypoxic (1 % O_2) conditions for 2, 24 or 48 hours. Total protein content of cell lysate was quantified in triplicate in the method of Lowry. N = 3 separate cultures per condition. Results are expressed as **A)** absolute concentrations ± SEM or **B)** change relative to matching time point control ± SEM. White bars represent control conditions, black stimulated with 1 % hypoxia. Significance between groups as marked (*) or from matching time point control (Λ; $p < 0.05$).

The effect of NF-κB inhibition on myotube total protein content in hypoxia was examined by two-way (condition [hypoxic, hypoxic + PS1145] × time [2, 24, 48 hours]) ANOVA. No condition × time interaction was noted on the effect of NF-κB inhibition (PS1145, 10 μM) on protein concentration from cultured myotubes ($p = 0.335$). Consistent with the results of Figure 3.4, a main effect of time on protein concentration was noted ($p < 0.001$), however, no effect of NF-κB stimulation was noted ($p = 0.242$), therefore hypoxia and hypoxia + PS1145 conditions were pooled for further analysis. Subsequent *post hoc* analysis on pooled groups reveals hypoxia has a time dependent effect on total protein concentration, with a (pooled) reduction from 3.9 (0.1) $\mu g.mL^{-1}$ to 2.7 (0.2) $\mu g.mL^{-1}$ then 1.7 (0.05) $\mu g.mL^{-1}$, at 2, 24 and 48 hours respectively (each $p < 0.001$, d = 3.28 and 3.04, respectively; Figure 3.5A). As would be expected, this effect is removed if results are expressed relative to time point controls, with no interaction ($p = 0.21$) or main effects being present.

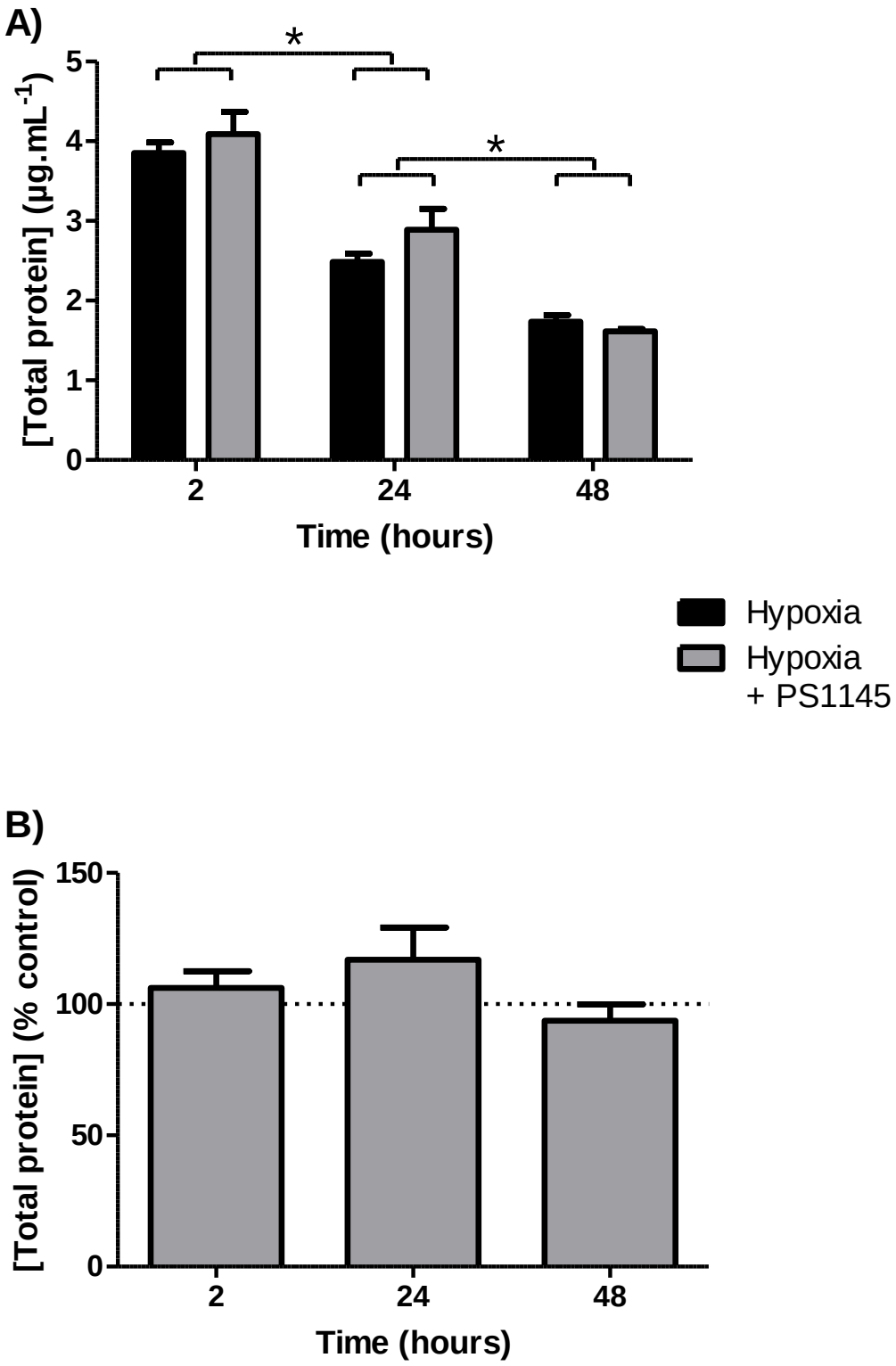

Figure 3.5: Effect of NF-κB inhibition on total protein content during hypoxia. C2C12 myotubes were incubated in hypoxia (1 % O_2) for 2, 24 or 48 hours ± 10 µmol PS1145 (NF-κB inhibitor). Total protein content of cell lysate was quantified in triplicate in the method of Lowry. N = 3 separate cultures per condition. Results are expressed as **A)** absolute concentrations ± SEM or **B)** change relative to matching time point. Black bars represent hypoxic conditions, grey hypoxia stimulated with 10 µmol PS1145. Significance is indicated by * between groups as marked ($p < 0.05$).

3.3.2 Effect of Hypoxia on Myostatin Peptide Expression and Downstream Signalling *in vitro*

The effect of hypoxia on myostatin peptide expression in myotubes was examined by two-way (condition [control, hypoxic] × time [2, 24, 48 hours]) ANOVA. No condition × time interaction was noted ($p = 0.07$). A main effect of condition was noted ($p = 0.04$), suggesting myostatin was reduced following hypoxic exposure in all time points. Pooled myostatin peptide response following hypoxic stimulus was 59.86 % of control ($p = 0.04$, $d = 1.64$; Figure 3.6A). No condition × time interaction was noted on with regards to the myostatin latency associated propeptide (LAP; $p = 0.10$), nor was any main effects noted (Figure 3.6B). No difference in LAP / myostatin peptide was noted at any time point ($p = 0.909$; Figure 3.6C).

The effect of NF-κB inhibition on myostatin expression was examined by two-way (condition [control, hypoxic] × time [2, 24, 48 hours]) ANOVA. No condition × time interaction was noted ($p = 0.23$). No main effect of condition was noted ($p = 0.32$) or group was noted (each $p = 0.64$; Figure 3.7A). In a similar manner, no condition × time interaction ($p = 0.4610$ or main effect of treatment (each $p = 0.147$) was noted for the effect of NF-κB inhibition on the myostatin LAP in hypoxia (Figure 3.7B). No difference in LAP / myostatin peptide was noted following NF-κB inhibitor treatment in hypoxia ($p = 0.315$; Figure 3.7C).

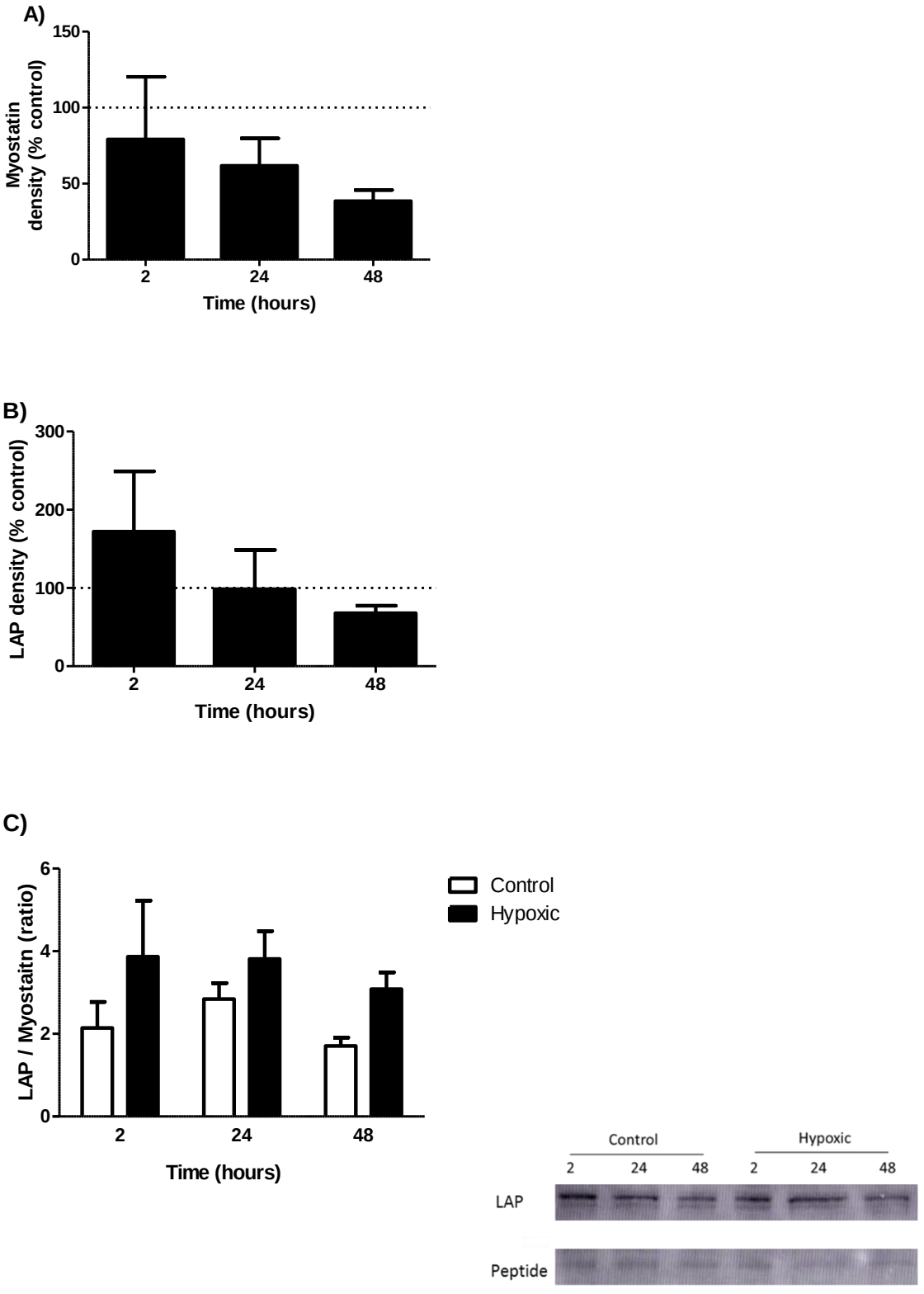

Figure 3.6: Effect of hypoxia on myostatin peptide expression *in vitro*. Western blots of myostatin **A)** peptide at 26 - 30 kDa, **B)** LAP at 45 kDa (bs1288R, BIOSS), and **C)** Ratio of LAP / Myostatin from C2C12 myotubes after 2, 24 or 48 hours in control (20.9 % O_2) or hypoxic (1 % O_2) environment. Blot density quantified in ImageJ and normalized to individual lane's total protein, detected by ponceau stain. All results expressed relative to matching time point control condition. N = 3 per condition. 40 µg total protein loaded per well. Error bars represent SD. **Insert**, Representative Western blot image, showing myostatin peptide (28 kDa) and LAP (45 kDa). Hypoxic condition shown in black (relative to control [white]), with exposure time (hours) as marked.

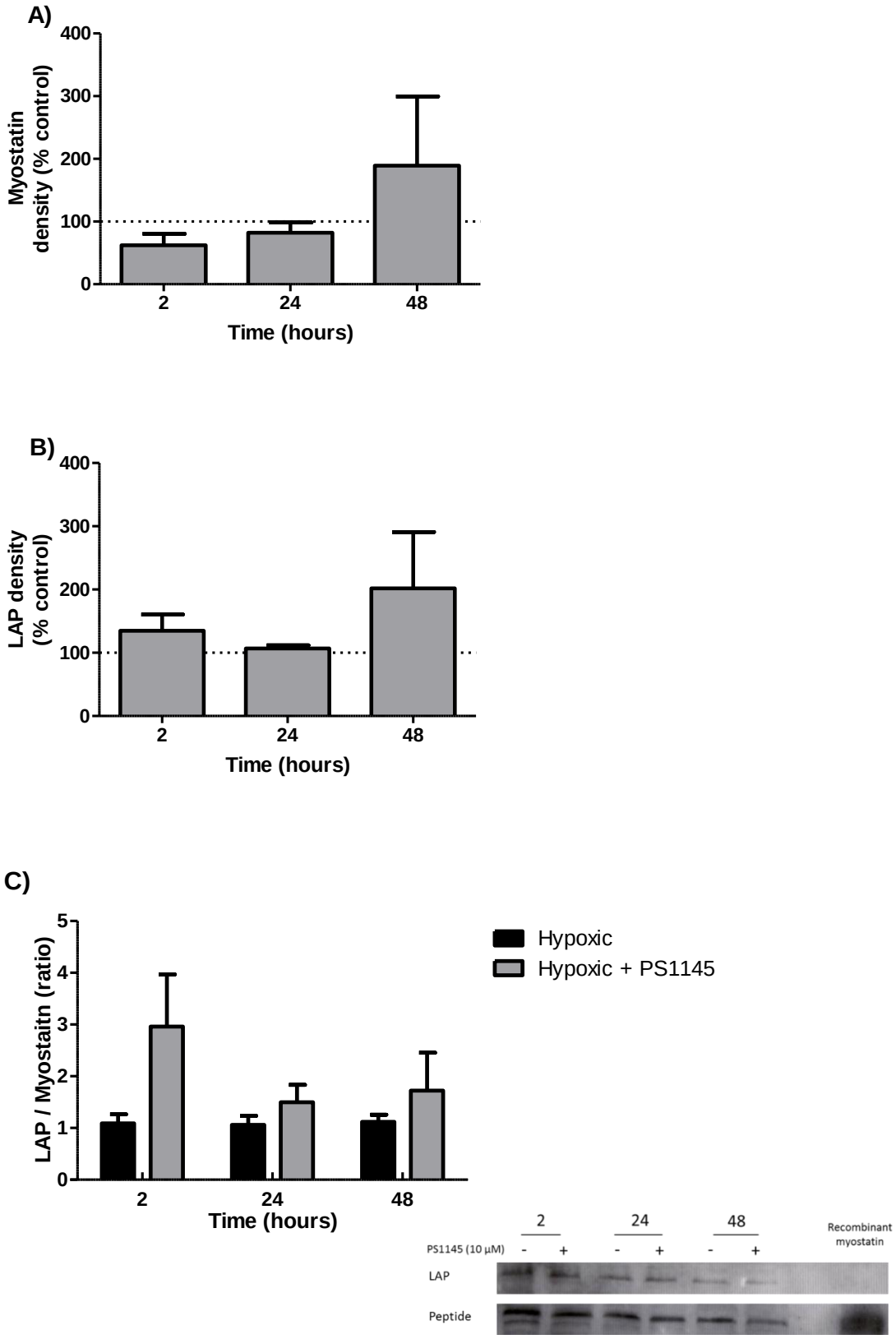

Figure 3.7: Effect of NF-κB inhibition on myostatin expression during hypoxia. C2C12 myotubes were incubated in 1 % O_2 for 2, 24 or 48 hours ± 10 µmol PS1145 (NF-κB inhibitor). **A)** Myostatin peptide at 26 - 30 kDa, **B)** LAP at 45 kDa, and **C)** Ratio of LAP / Myostatin. Hypoxic + PS1145 conditions shown in grey, relative to hypoxic only (control). All results are expressed as percentage of individual controls ± SD. **Insert)** Representative Western blot image showing myostatin peptide and LAP. Hypoxic and hypoxia + PS1145 conditions with exposure time (2, 24 or 48 hours) as marked. Recombinant myostatin peptide (RPB653Hu01, USCN). N = 3 per condition.

The effect of hypoxia on ubiquitin (both bound and free) was examined by two-way (condition [control, hypoxic] × time [2, 24, 48 hours]) ANOVA). No condition × time interaction was noted with respect to the effect of hypoxia on free ubiquitin ($p = 0.573$), nor was a main effect of group ($p = 0.573$) or condition ($p = 0.096$; Figure 3.8A). While a trend was noted towards a condition × time interaction respect to the effect of hypoxia on bound ubiquitin ($p = 0.08$; Figure 3.8B), no main effect of condition ($p = 0.175$) or time ($p = 606$) was noted.

Similarly, no condition × time interaction was noted with respect to the effect of NF-κB inhibition (10 μmol PS1145) in hypoxia on free ubiquitin ($p = 0.798$), nor was a main effect of condition ($p = 0.814$) or time ($p = 0.798$ – Figure 3.9A). With regards to the effect of NF-κB inhibition on bound ubiquitin (10 μmol PS1145) no group × time interaction ($p = 0.0758$), nor main effect of condition ($p = 0.974$) or time was noted ($p = 0.758$ – Figure 3.9B).

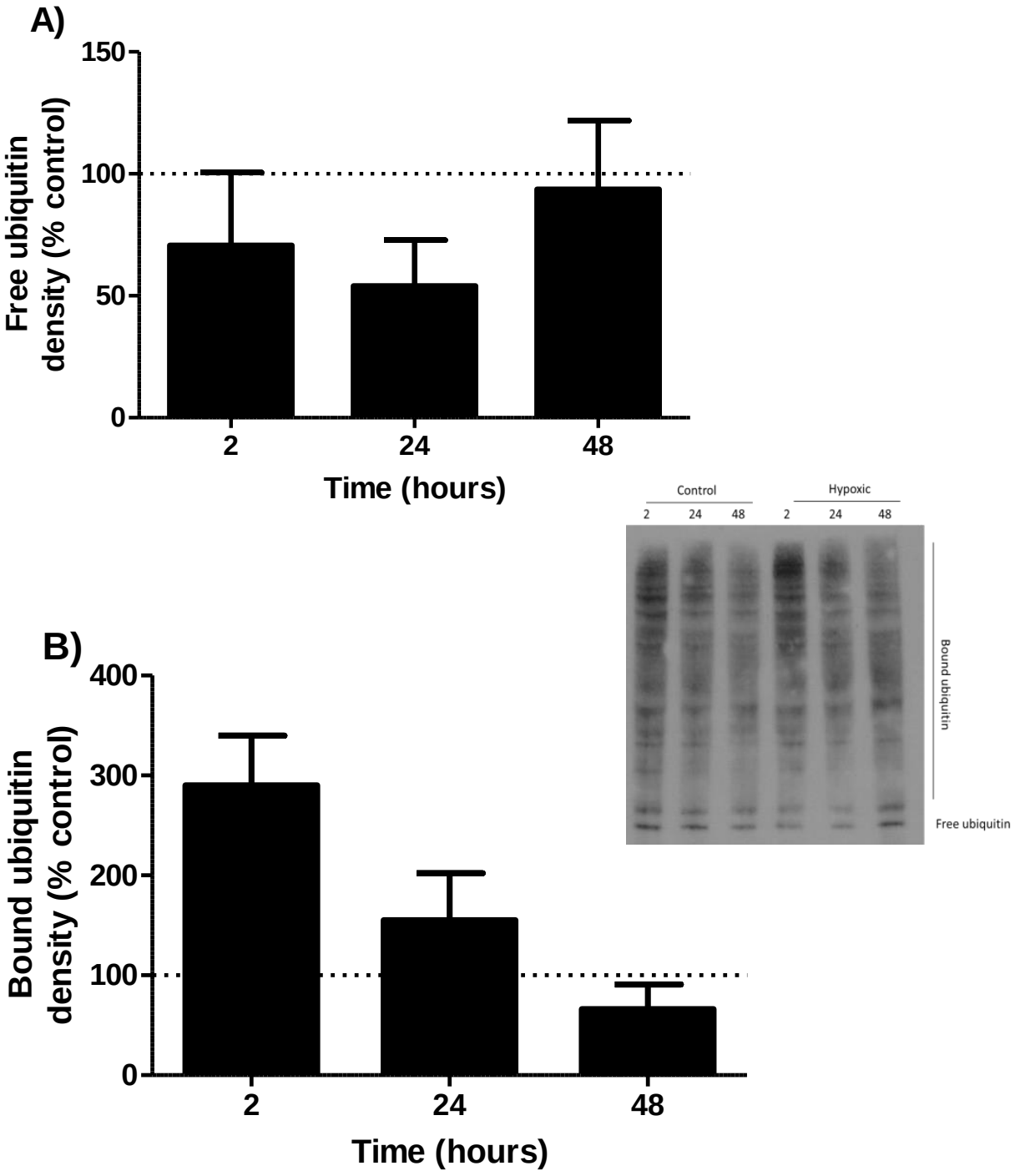

Figure 3.8: Effect of hypoxic exposure on ubiquitin expression. C2C12 myotubes were incubated in 20.9 % or 1 % O_2 for 2, 24 or 48 hours. **A)** Free ubiquitin (6 kDa), **B)** bound ubiquitin. Hypoxic condition in black, shown relative to matching control. All results are expressed as percentage of individual controls ± SD. **Insert**, Representative Western blot image showing free ubiquitin peptide (6 kDa) and total bound ubiquitin (remaining lane). Control and hypoxic conditions with exposure time (hours) as marked.

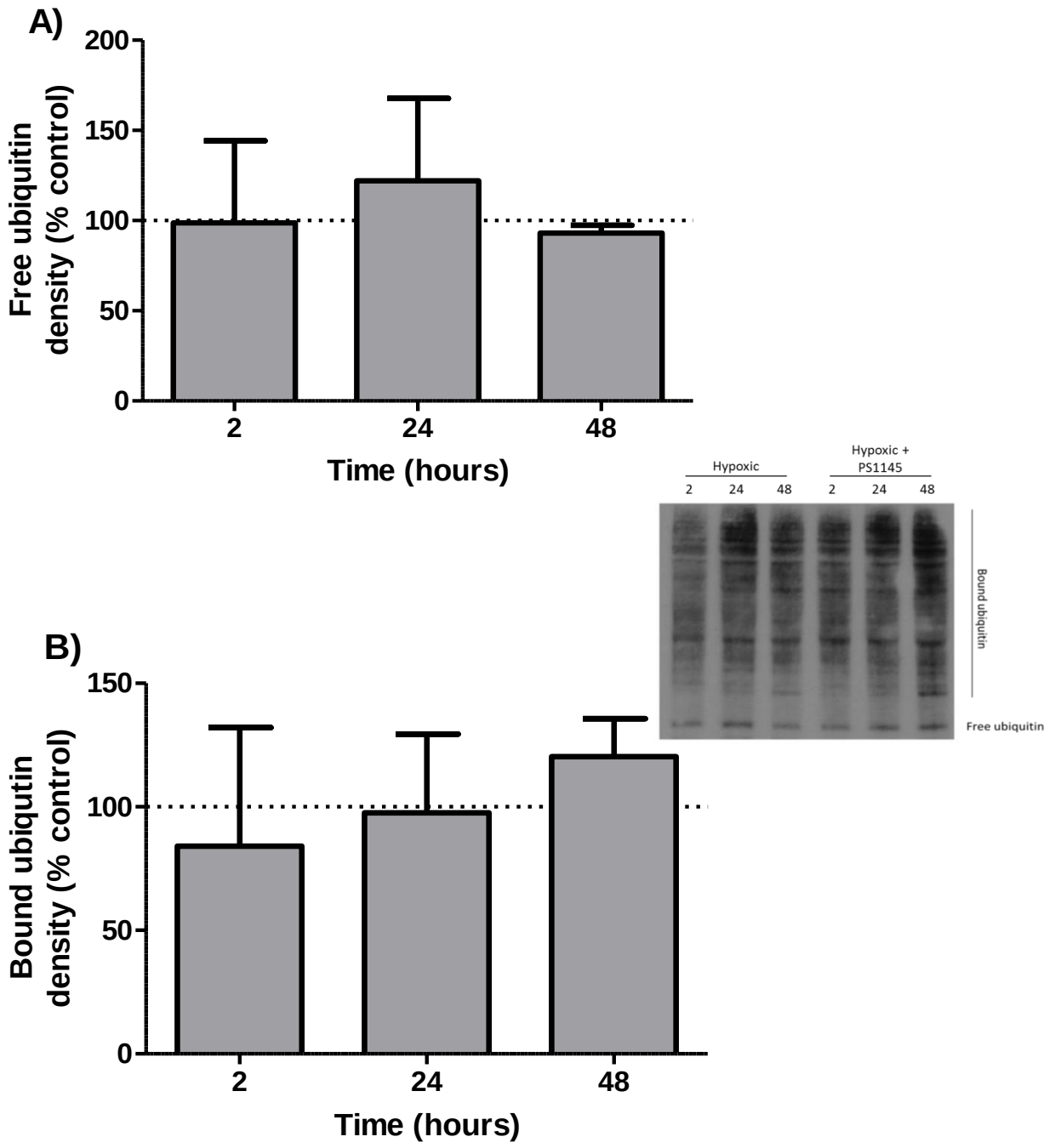

Figure 3.9: Effect of NF-κB inhibi on ubiquitin expression during hypoxia. C2C12 myotubes were incubated in 1 % O_2 for 2, 24 or 48 hours ± 10 µmol PS1145 (NF-κB inhibitor). **A)** Free ubiquitin (8.5 kDa), **B)** bound ubiquitin. Hypoxic + PS1145 condition shown in grey. All results are expressed as percentage of individual controls ± SD. **Insert**, Representative Western blot image showing free ubiquitin peptide (6 kDa) and total bound ubiquitin (remaining lane). Control and hypoxic conditions with exposure time (hours) as marked.

The effect of hypoxia on TNFα expression was examined by two-way (condition [control, hypoxic] × time [2, 24, 48 hours]) ANOVA. A condition × time interaction was noted with respect to the effect of hypoxia on TNFα expression ($p = 0.33$; Figure 3.10). *Post hoc* analysis reveals a time dependent effect of hypoxia on TNFα expression, with TNFα at the 2 hour time point 67.0 (15.79) %, and at the 48 hour time point 237.98 (50.91) % of control ($p = 0.041$, $d = 2.62$). No condition × time interaction was noted for the effect of NF-κB inhibition on TNFα expression ($p = 0.358$), nor was any main effects seen (condition $p = 0.80$, time $p = 0.36$; Figure 3.11).

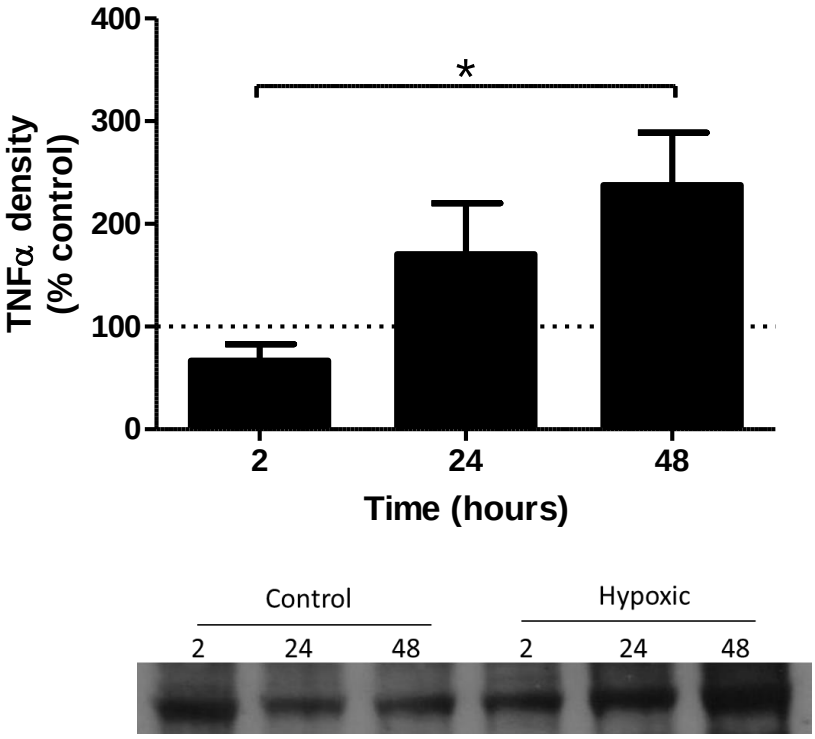

Figure 3.10: Effect of hypoxia on TNFα expression. C2C12 myotubes were incubated in 20.9 % or 1 % O_2 for 2, 24 or 48 hours. Hypoxic condition in black, expressed as percentage of individual controls ± SD. * indicates significant difference between marked conditions. **Insert**, Representative Western blot image showing TNFα control and hypoxic conditions with exposure time (hours) as marked.

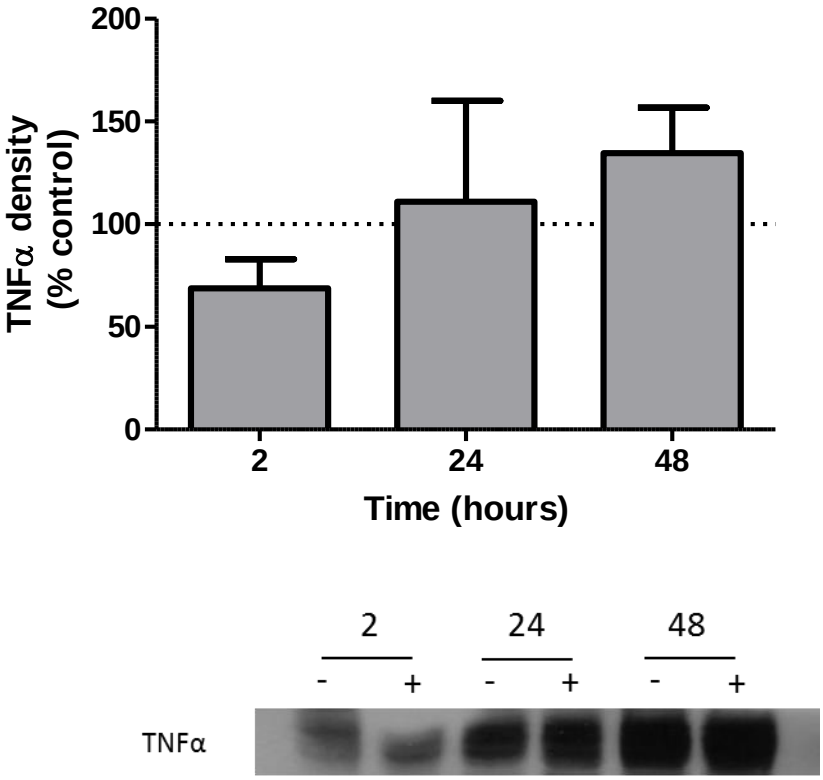

Figure 3.11: Effect of NF-κB inhibition on TNFα expression during hypoxia. C2C12 myotubes were incubated in 1 % O_2 for 2, 24 or 48 hours ± 10 µmol PS1145 (NF-κB inhibitor). Hypoxic + PS1145 condition grey, expressed as percentage of individual controls ± SD. **Insert**, Representative Western blot image with times as marked (hours) and absence (-) or presence (+) of PS1145.

3.3.3 Effect of Hypoxia on Myoblast Chemotaxis

The effect of hypoxia on myoblast chemotaxis was examined by two-way (condition [pre, post, post + ps1145) × (treatment [control, hypoxic] ANOVA. A significant condition × treatment interaction was noted ($p < 0.001$). *Post hoc* analysis revealed the control condition showed a large effect, reducing scratch diameter to 36.2 (1.59) % relative of the pre time point ($p = 0.0001$. $d = 32.75$). Control cells in the PS1145 condition did not show altered scratch diameter closure relative to pre time point ($p = 0.47$, $d = 0.65$; Figure 3.12A). Whilst exposure of scratched myoblasts to hypoxic condition still resulted in significant scratch closure, this effect was impaired relative to normoxic control [hypoxic 60.3 (0.63) % vs. control 36.2 (1.59) % closure, relative to individual baselines; $p = 0.003$, $d = 11.73$]. Furthermore, pre-treatment of hypoxic cells with PS1145 offset the effect of hypoxia on scratch closure [hypoxic 60.3 (0.63) % vs hypoxic + PS1145 51.0 % (0.29) % relative to individual baselines; $p = 0.0003$, $d = 3.61$; Figure 3.12A].

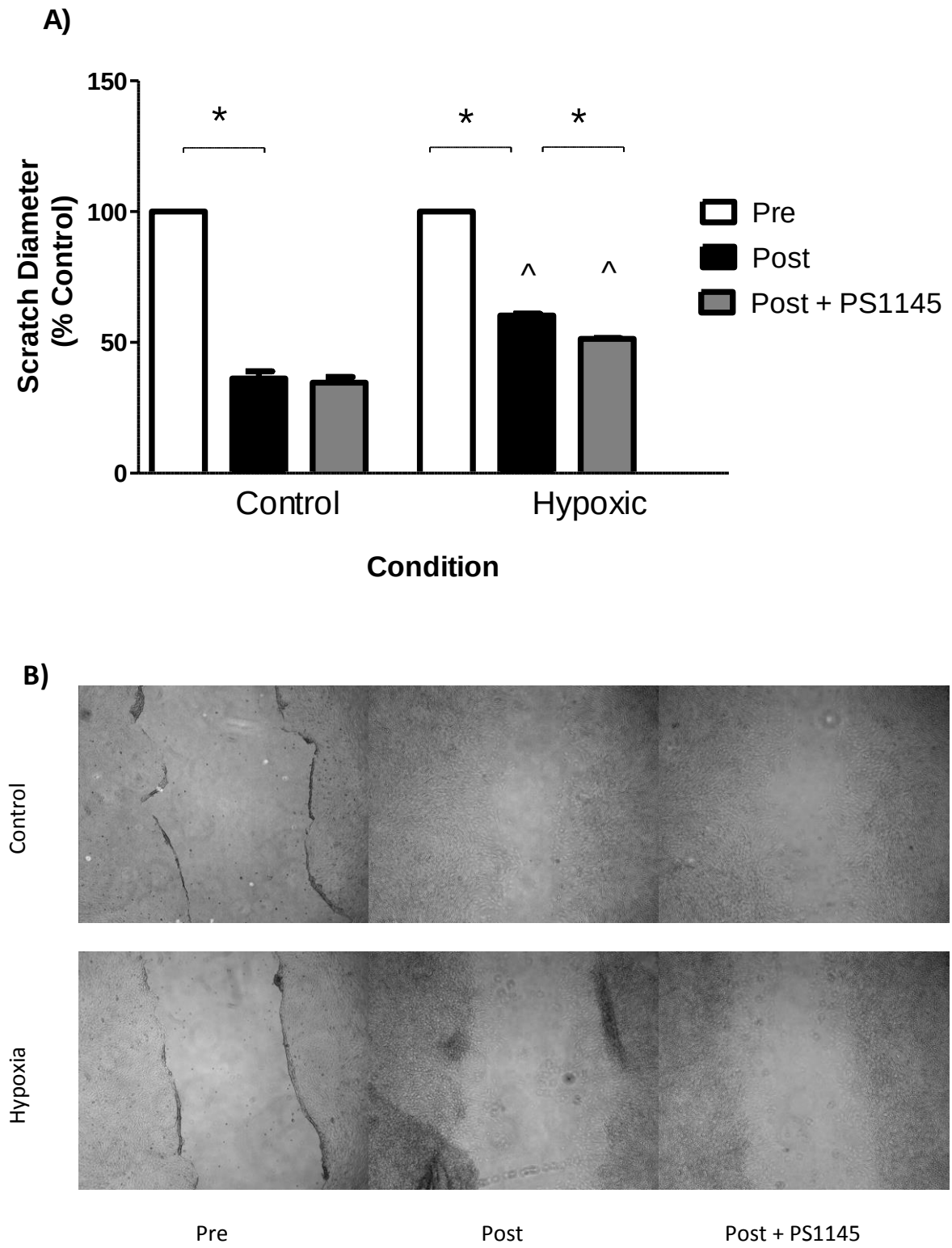

Figure 3.12: Effect of hypoxia on scratch diameter closure. C2C12 myoblasts were scratched, photographed (3 random locations per scratch) at 2.5× zoom (pre) with phase contrast filter and incubated for 15 hours in growth media (GM) in either control (20.9 % O_2), hypoxic (1 % O_2) conditions or hypoxic + PS1145 (10 µM). Scratch diameter was quantified 50 times per image, utilizing ImageJ. **A)** Bar graph of closure expressed as percentage of individual control condition ± SEM. Pre in white, post in black, post + PS1145. Significance is indicated either between groups as marked by asterisk (*) or between matching treatments across conditions by lambda (∧). N = 3 per condition. **B)** Representative images by condition and time point.

3.3.4 Structural comparison of Myostatin between Mus musculus and Homo sapiens

As a translational step between the preceding *in vitro* work completed in the mouse derived C2C12 line and the human work in following Chapters, a bioinformatic protein - protein BLAST analysis was performed on myostatin and members of its downstream signalling pathways to provide evidence supporting the hypothesized maintenance of myostatin function within humans.

```
Score = 760 bits (1963), Expect = 0.0, Method: Compositional matrix
adjust.Identities = 361/375 (96%),
Positives = 368/375 (98%), Gaps = 0/375 (0%)

Query 1 MMQKLQLCVYIYLFMLIVAGPVDLNENSEQKENVEKEGLCNACTWRQNTKSSRIEAIKIQI 60
        MQKLQ+#VYIYLFMLI#AGPVDLNE#SE++ENVEKEGLCNAC#WRQNT+#SRIEAIKIQI
Sbjct 2  MQKLQMYVYIYLFMLIAAGPVDLNEGSEREENVEKEGLCNACAWRQNTRYSRIEAIKIQI 61

Query 61 LSKLRLETAPNISKDVIRQLLPKAPPLRELIDQYDVQRDDSSDGSLEDDDYHATTETIIT 120
        LSKLRLETAPNISKD#IRQLLP+APPLRELIDQYDVQRDDSSDGSLEDDDYHATTETIIT
Sbjct 62 LSKLRLETAPNISKDAIRQLLPRAPPLRELIDQYDVQRDDSSDGSLEDDDYHATTETIIT 121

Query 121 MPTESDFLMQVDGKPKCCFFKFSSKIQYNKVVKAQLWIYLRPVETPTTVFVQILRLIKPM 180
         MPTESDFLMQ#DGKPKCCFFKFSSKIQYNKVVKAQLWIYLRPV+TPTTVFVQILRLIKPM
Sbjct 122 MPTESDFLMQADGKPKCCFFKFSSKIQYNKVVKAQLWIYLRPVKTPTTVFVQILRLIKPM 181

Query 181 KDGTRYTGIRSLKLDMNPGTGIWQSIDVKTVLQNWLKQPESNLGIEIKALDENGHDLAVT 240
         KDGTRYTGIRSLKLDM+PGTGIWQSIDVKTVLQNWLKQPESNLGIEIKALDENGHDLAVT
Sbjct 182 KDGTRYTGIRSLKLDMSPGTGIWQSIDVKTVLQNWLKQPESNLGIEIKALDENGHDLAVT 241

Query 241 FPGPGEDGLNPFLEVKVTDTPKRSRRDFGLDCDEHSTESRCCRYPLTVDFEAFGWDWIIA 300
         FPGPGEDGLNPFLEVKVTDTPKRSRRDFGLDCDEHSTESRCCRYPLTVDFEAFGWDWIIA
Sbjct 242 FPGPGEDGLNPFLEVKVTDTPKRSRRDFGLDCDEHSTESRCCRYPLTVDFEAFGWDWIIA 301

Query 301 PKRYKANYCSGECEFVFLQKYPHTHLVHQANPRGSAGPCCTPTKMSPINMLYFNGKEQII 360
         PKRYKANYCSGECEFVFLQKYPHTHLVHQANPRGSAGPCCTPTKMSPINMLYFNGKEQII
Sbjct 302 PKRYKANYCSGECEFVFLQKYPHTHLVHQANPRGSAGPCCTPTKMSPINMLYFNGKEQII 361

Query 361 YGKIPAMVVDRCGCS 375 (Homo Sapiens)
         YGKIPAMVVDRCGCS
Sbjct 362 YGKIPAMVVDRCGCS 376 (Mus musculus)
```

Figure 3.13: Amino acid sequence alignment of myostatin between *Homo sapiens* & *Mus musculus*. Top line indicates *Homo sapiens (*ABI48514), bottom *Mus musculus (*AAO46885), middle **bolded** and showing alignment where present. Non-aligned sequences identified by # symbol, conservative substitutions marked with a +. Note also RSRR region (underlined) indicating the end of the pro-peptide and start of the C-terminus peptide ('DFGLD….').

The full length myostatin protein shows a 96 % percentage identity between *Mus musculus* and *Homo sapiens* form (Access numbers, *Homo sapiens* ABI48514, *Mus musculus* AAO46885; Figure

3.13). The percentage identity of the bioactive C-terminus peptide is 100 % between *Mus musculus* and *Homo sapiens* (Figure 3.13 – beginning 'DFGLDC….' immediately post the RSRR region).

The receptor for myostatin is the Activin receptor type two B (ActRIIB), a 512 amino acid protein (Lee and McPherron, 2001). ActRIIB shares a similar percentage identity of 94 % with the mouse form (*Homo sapiens* NP_001097, *Mus musculus* NP_031423) with the only significant difference being a lengthening of the mouse form to 536 amino acids, occurring between positions 169 - 202 of the mouse form. On myostatin binding to ActRIIB, dimerization to ALK4 occurs in myocytes (Lee and McPherron, 2001). ALK4 shares 98 % identity between the human and mouse form (*Homo sapiens* AAH40531, *Mus musculus* AAI45778).

On binding of myostatin to ActRIIB, phosphorylation of signalling proteins SMAD2 and SMAD3, which subsequently induce binding with co-SMAD4 to induce nuclear translocation and activation (Zhu et al., 2004). BLAST analysis reveals SMAD2, SMAD3 and SMAD4 share 99 %, 99 % and 97 % identity, respectively (SMAD2 *Homo sapiens* AAC39657, *Mus musculus* AAH89184; SMAD3 *Homo sapiens* AAL68976, *Mus musculus* AAB81755; SMAD4 *Homo sapiens* BAB40977, *Mus musculus* AAM74472).

Myostatin can inhibit protein synthesis in muscle via its inhibitory effects on Akt (Trendelenburg et al., 2009). Both Akt and its downstream effector mammalian target of rapamycin (mTOR) share high percentage similarity at 88 % (Akt) and 99 % (mTOR), respectively (Akt *Homo sapiens* NP_001014432.1, *Mus musculus* NP_001103678; mTOR *Homo sapiens* NP_004949.1, *Mus musculus NP_064393.2).* Akt directly upregulates expression of GSK-3β, which shows 99 % identity between species (*Homo sapiens* NP_001139628, *Mus musculus* NP_062801). Downstream of

mTOR, both $p70^{S6k}$ and 4EBP-1 show 99 % and 91 % ($p70^{S6k}$ *Homo sapiens* NP_003152, *Mus musculus* NP_001107806; 4EBP-1 *Homo sapiens* NP_004086, *Mus musculus* NP_031944).

Activation of ActRIIB also induces activity of the 26-S proteasome via Forkhead box 1 (FoxO1) activation of atrogin and MuRF1, two muscle specific E3 ligases (McFarlane et al., 2006). FoxO1 shares 91 % (*Homo sapiens* NP_002006, *Mus musculus* NP_062713) while atrogin and MuRF1 record 95 % and 93 % respectively (atrogin *Homo sapiens* ABO37797, *Mus musculus* AAL49563: MuRF1 *Homo sapiens* NP_115977, *Mus musculus* CAM25927). Finally, the ubiquitin peptide itself it well conserved, showing 99 % similarity between species (*Homo sapiens* CAA28495, *Mus musculus* CAA35999).

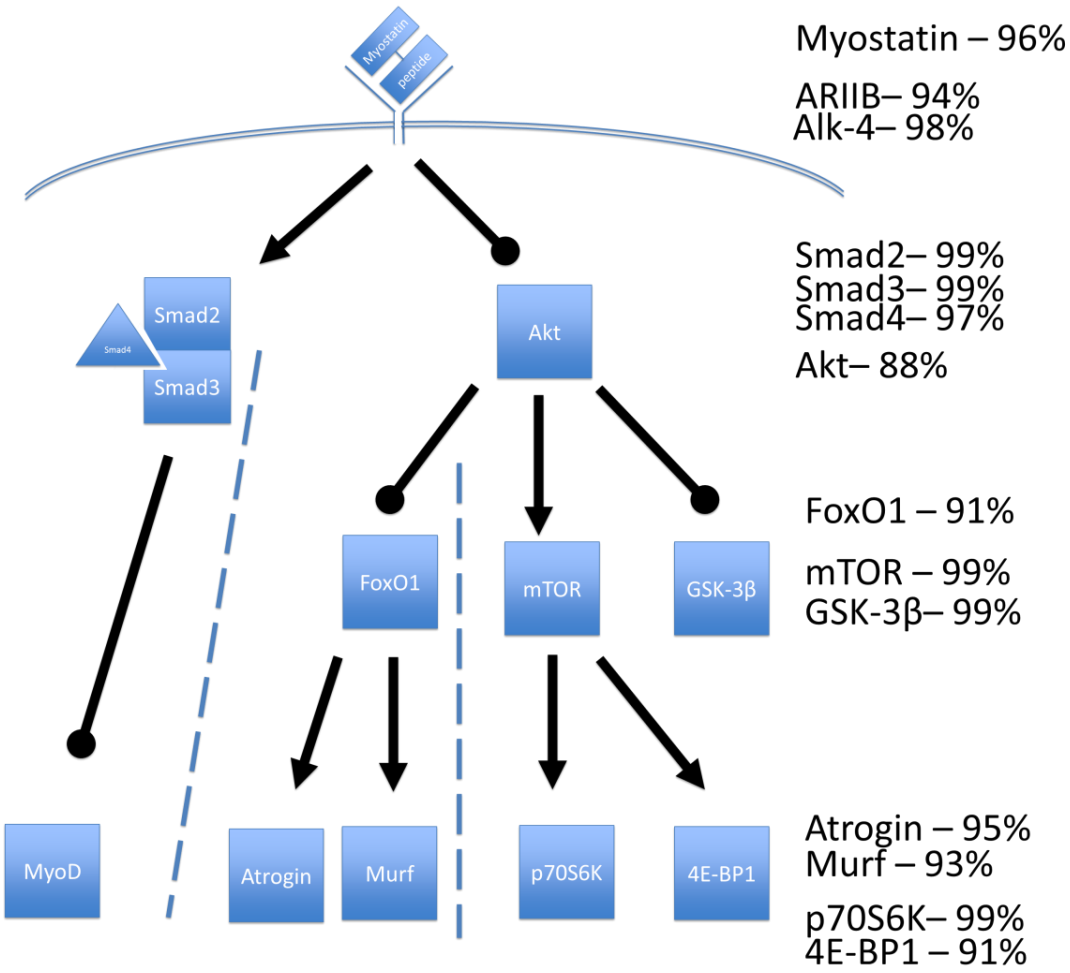

Figure 3.14: Myostatin and downstream intracellular signalling proteins and percentage identities between *Mus musculus* and *Homo sapiens* homologs. Protein accession numbers for both *Homo sapiens* and *Mus musculus* can be found in Table 3.2.

3.4 Discussion

It has been well described that chronic hypoxic exposure results in muscular atrophy i*n vitro* and *in vivo*. Here the mechanisms by which hypoxia has its atrophic effect on skeletal muscle have begun to be explored. *In vitro*, the novel demonstration that hypoxic exposure specifically slows chemotaxis in precursor myoblasts and directly induces cellular atrophy in mature myotubes is observed for the first time. Further, these effects are both partly dependent on NF-κB activation, as inhibition of NF-κB activity by the selective inhibitor PS1145 offset both the impaired chemotaxis and cellular atrophy seen post-hypoxic exposure. These witnessed effects may be in part via myostatin signalling, as alterations in cellular myostatin content was observed.

Counter to the hypothesis that an increase in myostatin expression would be observed following an acute hypoxic stimulus, here a decrease in myostatin peptide expression is seen. Therefore, the hypothesis as originally presented may be incorrect and myostatin increases do not drive hypoxic-induced atrophy. Conversely, myostatin may be acting in its endocrine manner (Gonzalez-Cadavid et al., 1998, Zimmers et al., 2002), and decreases in cellular myostatin peptide content may reflect secretion of myostatin into the extracellular media. Conformation or rejection of the role of myostatin could be performed in future work using a myostatin inhibitor in culture in combination with hypoxic exposure, or the use of myostatin detecting ELISA for the examination of myostatin concentration in the media of cultured myotubes +/- hypoxic exposure, thus demonstrating an increase (or not) of excreted myostatin by exposed myotubes.

Of interest is the intracellular signalling link between hypoxic stress and myostatin expression. The *in vitro* results presented here suggest an NF-κB dependent link, as inhibition of NF-κB activity offset atrophic effects in myotubes and cellular migration in myoblasts. It has previously been suggested that myostatin expression is linked to pro-inflammatory signalling, as stimulation of L6 myotubes

with LPS causes an increase in myostatin expression, and stimulation with the anti-inflammatory pharmaceutical Thalidomide prevented this in a concentration-dependent manner (Elliott et al., 2009). Increased myostatin expression is of interest to this study as myostatin activity inhibits myoblast proliferation and induces myotube atrophy via increases in ubiquitin and proteasomal activity (reviewed by Elliott et al., 2012). Under conditions of inadequate oxygen supply, stabilisation of HIF1α in myotubes induces a signalling cascade that activates NF-κB (Osorio-Fuentealba et al., 2009), separating it from its binding inhibitory protein Iκ-Bα and allowing translocation to the nucleus where it binds to promoter regions of multiple pro-inflammatory cytokines (Frost et al., 2002). The results presented here suggest that inhibition of NF-κB offsets both the atrophy of myotubes *in vitro* and chemotaxic migration of myoblasts *in vitro*. This suggests that the effect of hypoxia on muscle size may be in part dependent on inflammatory signalling.

The NF-κB dependent alterations in myotube size appear to be independent of any myostatin signalling, as addition of the NF-κB inhibitor PS1145 to cultures does not alter cellular myostatin content, yet does offset myotube atrophy under hypoxic conditions. These results suggest that the effect of hypoxia on myostatin expression may be independent of the effects of hypoxia on NF-κB and pro-inflammatory signalling.

If myostatin is acting in a bioactive manner, an increase in atrophic pathways downstream of myostatin should be seen. Whilst these results did not witness increases in bound ubiquitin, they did approach significance (Figure 3.8). Similarly, Caron and colleagues (2009) showed trends towards atrogin increases after only 4 hours of exposure to 1 % O_2, with further, significant increases after 24 hours in 1 % O_2. The role of these E3 ligases is to 'tag' proteins for destruction via ubiquitination & the 26S proteasome (Mitch and Goldberg, 1996). It may be that rate of ubiquitin binding is not the limiting step in hypoxic cellular atrophy, or the witnessed cell atrophy and loss of

cellular protein was via not via only ubiquitin / proteasomal pathways. Indeed, as Reid notes (2005), NF-κB activation can be used as a marker of ubiquitination. Thus, it is noteworthy that NF-κB inhibition induced as small, but significant protection against cellular atrophy and total protein loss (Figure 3.3Aand Figure 3.5A, respectively).

Other candidates for the rapid and significant cellular atrophy and loss of cellular protein seen here (Figure 3.2 and Figure 3.4, respectively) that future work could examine include lysosomal, autophagic and calcium-dependent (calpain) proteases, or the effect of cellular apoptosis on surviving myotubes. Severe hypoxia (7,620 m equivalent hypobaric hypoxia) in mice induces calpain activity 3 days after exposure that is further increased after 7 days exposure. No changes in activity of lysosomal activity was witnessed in the same group (Chaudhary et al., 2012). HIF-dependent autophagy is seen in multiple cell lines *in vitro* following 24 hours in 1 % O_2 (myogenic cells lines not reported; Bellot et al., 2009), and in human muscle in hypoxia, where it is increased relative to normoxic conditions both at rest and following moderate exercise (Deldicque et al., 2014).

Visual examination of the hypoxic myotubes used in here suggested elevated apoptosis, which has been previously reported in differentiated C2C12 myotubes in 1 % O_2, and also noted myotube atrophy and elevated LDH leakage (Joshi et al., 2011). Myotubes are noted to be more resistant to apoptosis than myoblasts (Xiao et al., 2011), potentially because they can regulate their metabolic demand and survival via degradation methods and loss of cytosolic structural proteins.

Conversely to the rapid induction of catabolic mechanisms, the effects of hypoxia on pro-synthesis pathway inhibition would appear to require greater time. Caron and colleagues (2009) note reductions in Akt phosphorylation at 48 hours, but not 24 hours. Unfortunately, protein phosphorylation of Akt pathway members was not able to be measured in the current study

The effect of time on these results is also of interest. Myotube atrophy was witnessed after only 2 hours, which is further increased after 24 hours (Figure 3.2), however measurable alterations in cellular protein content was not apparent until 48 hours of hypoxic exposure (Figure 3.4). The combination of these results suggests that the 2 hour alterations in myotube size are via a separate cause. The metabolic challenge of hypoxia decreases cellular ATP of C2C12 myotubes after 30 minutes (Matsuki et al., 2002), and in healthy humans, decreases muscle Na^+ / Ka^+ ATPase activity (Green et al., 1999). Subsequent changes in osmotic pressure may explain the rapid changes in cellular size seen here in the 2 hour time frame, while the longer term changes in size seen at 24 and 48 hours reflective of catabolic processes. Separation of the effects of each (osmosis vs. catabolism) would be possible with the addition of protease inhibitors in the presence of hypoxia, and could form part of future work.

One critique of the translation of the above findings from a mouse-derived cell lines into human models *in vivo* is the potential differences in mouse and human physiology, and specifically maintenance of intracellular signalling pathways, both in form and function. To help address this, a novel bioinformatics comparison was conducted *in silico*. This demonstrated the high percentage similarity between mouse and human myostatin protein, as well as its downstream signalling proteins. Markedly, this analysis revealed 100 % amino acid sequence agreement between the myostatin signalling peptide in mice and Humans. These results are in line with physiological observations, the phenotypic effect of myostatin deletion appears well maintained across mammalian species, including mouse (McPherron et al., 1997), dog (Mosher et al., 2007), cow (Grobet et al., 1997, Kambadur et al., 1997, McPherron and Lee, 1997) and human (Schuelke et al., 2004), suggesting a maintenance of function that is evolutionally conserved amongst Mammalia. These findings add weight to extrapolation of findings in small animal, and small animal derived cell lines, into human models, as are used in later chapters of this thesis.

The relevance of incubation of myocytes in 1 % O_2 as a model of intramuscular hypoxia does have limitations. This value was chosen based on previous reports (Caron et al., 2009, Li et al., 2013), and is based on the modelling of Flueck (2009) who suggests PO_2 of at least 8 mmHg is required for HIF-1α stabilisation and subsequent increase in activity of HIF-1α dependent pathways. A PO_2 of 8 mmHg gives an approximate equivalent of 1 % O_2 if normobaric hypoxic conditions are used (Appendix Thirteen). Similarly, where cell culture as used here is a model of muscle tissue in isolation, *in vivo* results may vary, as systemic endocrine responses from different tissues, combined with the ability of cardiovascular components to adapt to hypoxic stimuli, could alter the atrophic response seen here.

In conclusion, this Chapter demonstrates that hypoxia results in a rapid decrease in myoblast migration and myotube size *in vitro*. This decrease appears to be at least partly NF-κB dependent, and may also involve activity of myostatin and its downstream effects on the proteasomal activity during the later phases of this acute stimuli. While results should be considered in context of the restrictions of an *in vitro* model, if these results can be translated into an *in vivo* research model, they may help explain the underlying link between hypoxia and muscle atrophy witnessed in chronic cardiorespiratory disorders.

Chapter Four – The Effect of Acute Ambient Hypoxia on Myostatin Signalling and Protein Balance

4.1 Introduction

Loss of peripheral muscle mass is seen during hypoxia in humans. Hypobaric hypoxia during mountaineering in healthy individuals induces muscle atrophy greater than that expected due to increased energy expenditure and reduced diet alone (Boyer and Blume, 1984, Hoppeler et al., 1990, Cruz-Jentoft et al., 2010), while approximately 25 % of COPD patients show significant muscle atrophy relative to BMI matched healthy controls (Bernard et al., 1998). Hypoxia is one hypothesised cause underling the poorly understood muscle atrophy seen in conditions such as cachexia (reviewed by Wagner, 2008). During cachexia in COPD, muscle atrophy alone is a predictor of mortality (hazard ratio of 3.68), independent of disease severity (Marquis et al., 2002). A greater understanding of the mechanisms underlying hypoxic induced muscle atrophy is therefore clearly necessary.

The ability of hypoxia to reduce muscle mass *in vivo* in the adult human must either be via a reduction in protein synthesis, an increase in degradation, or some combination of the two. Indeed, hypoxic emphysemic patients demonstrate decreased global protein synthesis, with no alteration in local (muscle) degradation when compared with healthy, age-matched controls (Morrison et al., 1988). Exposure to a hypoxic stimulus (1 % O_2) significantly reduces phosphorylation of Akt in differentiating myotubes at 48 – 72 hours post exposure, but not 24 hours post exposure (Ren et al., 2010). Myotubes exposed to 1 % O_2 for 48 hours hypoxia show reduced protein synthesis, while those exposed for 24 hours do not (Caron et al., 2009). Similarly, rats exposed to 11 % O_2 for six hours do not show a reduction in protein synthesis (Preedy et al., 1985), and humans exposed to 12 % O_2 for two hours do not show altered rates of Akt phosphorylation or fractional synthesis rates (FSR; Etheridge et al., 2011). Combined, this data suggests hypoxia is capable of supressing protein synthesis, but only if the length of exposure is sufficient.

The activity of proteasomal mechanisms appear to increase rapidly after hypoxic exposure. Elevated actin breakdown is apparent after 12 hours in 1 % O_2, and elevated atrogin expression is seen after 24 hours, with trends towards increases after only 8 hours (Caron et al., 2009). These results are consistent with those of Chapter Three of this thesis, where trends towards elevated bound ubiquitin was seen at 2 hours and 24 hours post-hypoxic exposure, but not at 48 hours post hypoxia. Combined, these results suggest that while chronic hypoxia both suppresses synthesis pathways and increases activity of the proteasome, acutely proteasomal activity dominates in the initial 24 hours while protein synthesis pathways become involved after 48 hours. This hypothesis holds intrinsic logic; rapid loss of myocyte size (i.e. atrophy) decreases necessary O_2 diffusion distance from supplying capillaries, and the increase in rate of catabolism would result in a more rapid change in cellular atrophy relative to impairment of anabolism.

Limited investigations of the effects of hypoxia on organ level protein synthesis have taken place, using rate of enrichment of labelled protein isotope methods as originally described by Wolfe (1984). Etheridge and colleagues (Etheridge et al., 2011) note no alteration in rate of protein synthesis in healthy males exposed to 2 hours of hypoxia at 12 % O2, but on introduction of an exercise stimulus with hypoxia, note a blunting of post-exercise protein synthesis, relative to normoxic exercise. A longer exposure in a similar population (male, healthy, young) after 7 – 9 days at 4,559 m altitude results in elevated rates of muscle protein synthesis (Holm et al., 2010). Care must be taken with interpretation of data from alpine climbing cohorts, Imoberdorf and colleagues (2006) demonstrated no change in muscle protein synthesis rate following passive assent to 4,559 m (by helicopter) whilst the summiting group showed increases similar to those of Holm and colleagues (2010), suggesting the addition of the exercise stimulus may be key. *In vitro*, suppressed rates of protein synthesis are seen in myotubes cultured at 1 % O_2 for 24 hours (Caron et al., 2009), suggesting either a time-dependent response of muscle cells to hypoxia, or an intrinsic difference

between *in vitro* and *in vivo* responses. It would seem therefore that *in vitro* observations should be paralleled *in vivo* where possible.

With regards to measurement of muscle protein degradation by isotope tracer, as first described by Zhang and colleagues (1996), no direct measures have taken place in hypoxia. Holm and colleagues (2010) did estimated whole-body protein degradation by the method of leucine rate of appearance (unlabelled) and noted this estimate of degradation appeared to be elevated at 4,559 m.

Myostatin has well recognised effects on major protein synthesis and degradation pathways in skeletal muscle (Amirouche et al., 2009, McFarlane et al., 2006, Trendelenburg et al., 2009). Both rats exposed to 10 % O_2 for 6 weeks and hypoxemic COPD patients (> 6 months post diagnosis) show elevated myostatin peptide expression at the muscle level (Hayot et al., 2011). Two possible hypotheses emerge from this finding. It could be proposed that hypoxia directly increases myostatin expression. Alternatively, as plasma myostatin concentration is noted to correlate with muscle mass across both healthy and cachexic individuals (Gonzalez-Cadavid et al., 1998), this alteration in myostatin expression could be an indirect change, whereby hypoxia results in a reduction in skeletal muscle mass thereby reducing myostatin expression.

The two most commonly used research models for *in vivo* human hypoxic research are mountaineering, where healthy humans are exposed to hypobaric hypoxia, and chronic disorders such as COPD, where emphysema and / or pulmonary fibrosis result in hypoxemia. Both groups present as limited research models with numerous confounding factors. COPD patients present with elevated systemic inflammation (which may or may not be related to the disease-induced hypoxia), reduced physical activity, altered anabolic hormonal expression patterns and altered

energy input (reviewed by Wagner, 2008). Mountaineering involves chronic disruptions to sleep patterns, cold exposure, reduced satiety, increased physical activity and takes place in a difficult research environment (Wagner, 2010). Further, both occur over chronic timeframes of weeks – months. Therefore, these can be difficult research models, with several confounding factors besides the hypoxic stimuli and questions of causality. Healthy humans can be placed into normobaric hypoxic environments to induce hypoxemia and subsequently peripheral tissue hypoxia (Heyes et al., 1982). It should be recognised that the use of normobaric hypoxia does differ in physiological effect to hypobaric hypoxia, with a larger increase in V_E and decrease in arterial pH seen in normobaric hypoxia over hypobaric hypoxia (Faiss et al., 2013). Alternatively, normobaric hypoxia chambers represent practical advantages over hypobaric chambers, with greater safety, increased flexibility and reduced cost of usage.

4.1.1 Aims & Hypothesis

The aim of this Chapter was therefore to establish what effect acute normobaric hypoxia would have on plasma and muscle myostatin, fractional breakdown rate (FBR), and FSR. Specifically, the aims of this Chapter were;

1) determine the acute effect of hypoxia on myostatin signalling in both muscle and plasma *in vivo* in healthy humans *and*
2) establish the acute effect of hypoxia on FSR and FBR in *vivo* in healthy humans.

The hypothesis for this Chapter was that hypoxia would increase plasma myostatin concentration and muscle myostatin expression, and increase FBR without altering FSR. Specifically, this Chapter hypothesizes that;

1) plasma and muscle myostatin will be elevated following acute hypoxia exposure *and*
2) FBR will be elevated following acute hypoxic exposure but no alteration in FSR will be witnessed.

4.2 Methods

4.2.1 Ethical Approval

Ethical approval for the work described in this Chapter was provided by the University of Westminster Research Ethics Sub-committee (10/11/24) and the University of Brighton Faculty Research and Governance Committee (FREGH/29/09). Written informed consent was obtained from all participants prior to participation. All work described within this Chapter was completed within the Physiology Lab of Dr Peter Watt, University of Brighton, whom also collected the muscle biopsies described below.

4.2.2 Participant Recruitment

A cohort of healthy male participants was recruited for this study. Inclusion criteria for participation was male, 18 – 40 years of age with no exposure to altitude or hypoxic environments exceeding 3000 m within 3 months of participation, a body mass index (BMI) of 20 – 30 $kg.m^{-2}$. Exclusion criteria was presence of any cardiovascular, respiratory, metabolic or coagulation disorders, regular smoker (as defined by the World Health Organisation as daily usage of a tobacco product), or currently taking prescription medication. Participants were also excluded if they had a known allergy to lidocaine. Participants were asked to abstain from strenuous exercise for 48 hours prior to attending the laboratory, and abstain from caffeine for 24 hours prior to attending. A group of 9 participants were recruited who both met the above criteria and were able to comply with experiment protocols. One participants withdrew during the course of the investigation due to non-specified personal reasons; N = 8 participants completed this experiment (characterized in Table 4.1).

Table 4.1: Participant characteristics. N = 8.

Age (years)	Height (cm)	Weight (kg)	BMI ($kg.m^{-1}$)	Fasting Glucose ($mM.L^{-1}$)	Resting SpO_2 (%)
26 (2.0)	178 (0.50)	72.37 (0.67)	22.81 (1.92)	4.29 (0.51)	98 (0.54)

Expressed as mean (standard deviation). Body mass index (BMI). Oxygen saturation (SpO_2).

4.2.3 Experimental Design

After initial screening and consent was obtained, participants attended twice, with each session separated by at least 14 days. On presentation to the laboratory, a muscle biopsy was taken utilizing the conchotome technique (Dietrichson et al., 1987). Biopsies were taken from the belly of vastus lateralis, approximately halfway between the palpable greater trochanter of the femur and the lateral epicondyle of the femur. After site sterilization (chlorhexidine gluconate 0.5 %) and subcutaneous lidocaine injection (100 mg), a 10 mm incision through skin and underlying facia of the lateral mid-thigh was made (Figure 4.1). All biopsies in this chapter were taken by Professor Peter Watt (University of Brighton).

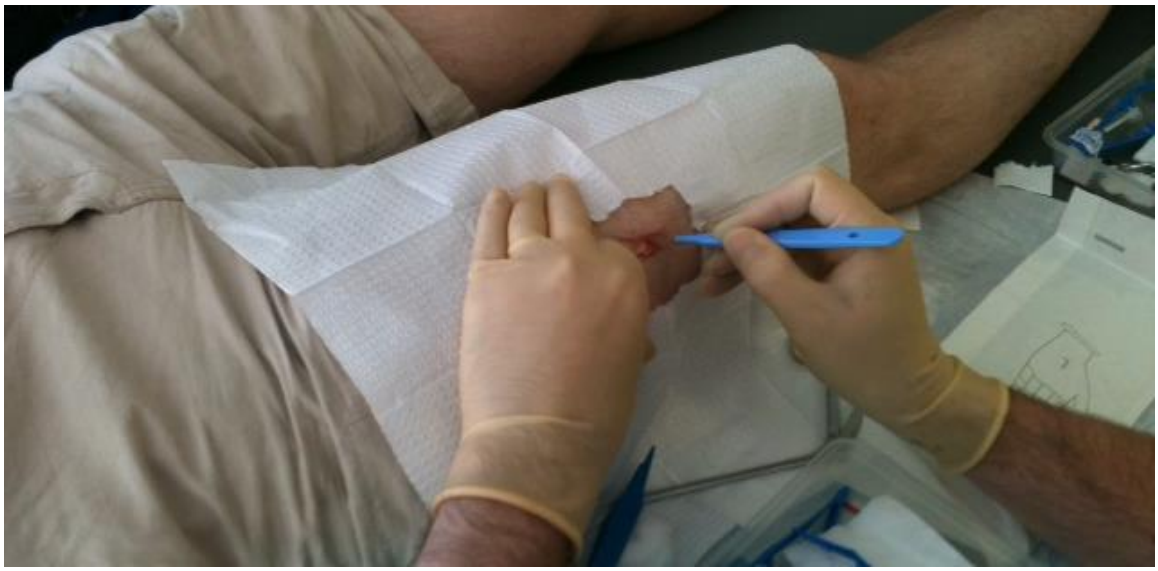

Figure 4.1: Incision prior to vastus lateralis muscle biopsy. Photo showing biopsy site, mid-thigh, lateral.

A 4 mm conchotome (Tilley Henckel) needle with jaws closed was advanced 4 – 6 cm, opened and advanced a further 1 cm before jaws were closed and sample removed. If necessary, this process was repeated to ensure total sample size collected was ~ 100 mg. Collected muscle tissue was immediately rinsed in ice-cold saline, trimmed of visible fat and frozen in liquid nitrogen before being stored at -80 °C for future analysis.

One cannula was placed into an antecubital vein of the non-dominant arm for the administration of primed constant infusion of isotopes phenyl-D_5-alanine (D_5-Phe; 615870, Sercon) to allow for the determination of protein synthesis, and L-phenylalanine-^{15}N (^{15}N-Phe; 490105, Sercon) for the determination of protein degradation. Isotopes were dissolved on the morning of experiments into 10 mL of 0.9 % NaCl sterile saline under sterile conditions, and twice filtered through 0.22 µm syringe filters before use. A second cannula was placed in an retrograde manner into a dorsal hand vein of the same arm, with the hand heated to 60 °C to allow mixed arterialised blood samples in the method of Sonnenberg and Keller (1982). While traditionally isotope calculations require arterial blood collection, heating of the hand to 60 - 70 °C has been demonstrated to induce venous shunting and allow less-invasive collection of blood closely replicating that seen from arterial cannulation, with no reported differences in concentration of glucose, lactate, PCO_2, or labelled tracer enrichment (McGuire et al., 1976, Sonnenberg and Keller, 1982).

Immediately following the baseline blood sample and muscle biopsy (time = -30 minutes) the labelled isotope tracer D_5-Phe (priming dose 2 µmol.kg^{-1}, constant infusion rate 0.05 µmol.kg^{-1}.min^{-1}) in 0.9 % saline was started. After three more blood samples (-20, -10 and 0 minute mark) to achieve a steady state enrichment of D_5-Phe, participants were introduced to the experimental chamber (11.9 % or 20.9 % O_2, indicating hypoxic or control, respectively) for 120 minutes. This concentration of O_2 was chosen based on previous similar reports (Etheridge et al., 2011). Order of

exposure (control or hypoxic) was randomised. While attempts to blind participants to control or hypoxic condition were made, this proved unsuccessful due to the perceivable effect of hypoxia and so blinding attempts were discontinued.

Arterialised blood, heart rate (HR), SpO_2 (Nonin, palmSAT 2500) and modified Lake Louise acute mountain sickness (mLLAMS) was obtained every 30 minutes during the hypoxic exposure. LLASM questionnaire was modified for acute usage by removal of the sleep question as described by Richard and colleagues (2014; Appendix Four). For the measurement of SpO_2, the index finger of the dominant hand was used, as recommended by O'Connor and colleagues (2004).

At the conclusion of the 2 hour experimental stimulus (time point 120 minutes) participants were removed from the chamber environment, the second biopsy was immediately taken and a 2 hours primed constant infusion of ^{15}N-Phe was commenced (prime 2 $\mu mol.kg^{-1}$, 0.05 $\mu mol.kg^{-1}.min^{-1}$ infusion rate) for 2 hours (ending at time point 240 minutes). At the 300 minutes and 320 minute time point, biopsies 3 and 4 were taken (as described above) for the calculation of decay of ^{15}N-Phe and calculation of protein degradation. After the 4th biopsy, all infusions were stopped; the participant was fed and left the laboratory. This experimental protocol is summarized in Figure 4.2.

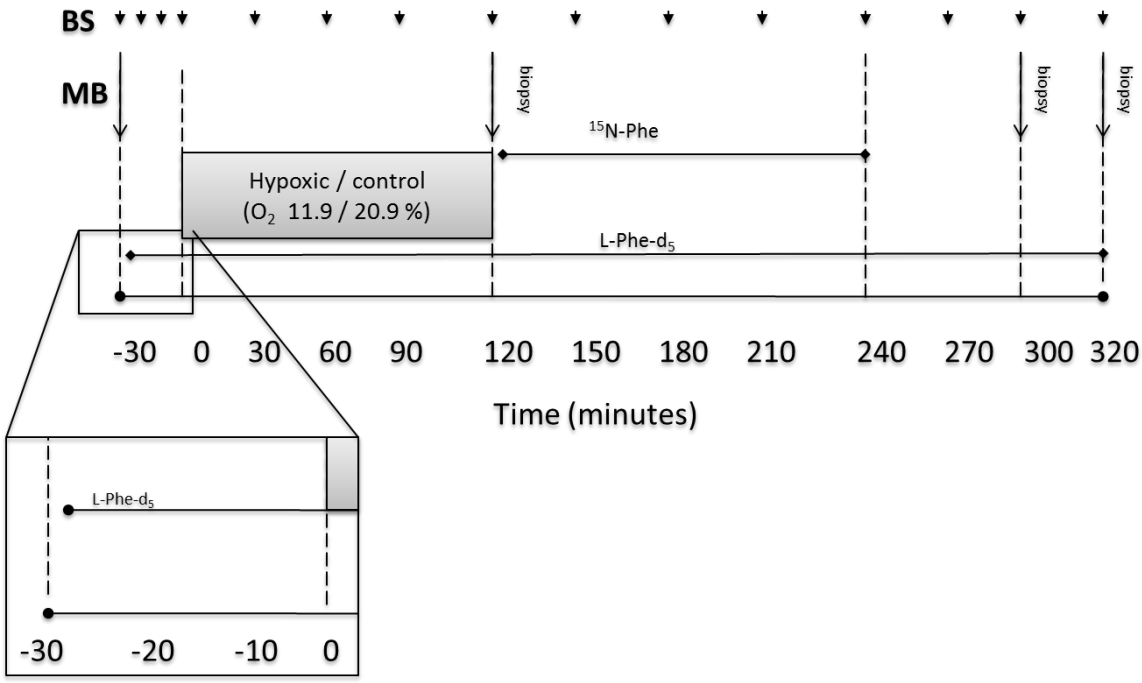

Figure 4.2: Schematic diagram of the experimental protocol, Chapter Four. Isotope infusions (^{15}N-Phe and D_5-Phe) start and finish times as shown. Hypoxic (~ 11.9 % O_2) or control (20.9 % O_2) between time point 0 – 120 minutes. Arrows indicate biopsy (MB) time points; arrow heads indicate blood sample (BS) time points. Time given in minutes.

4.2.4 Isotope Tracers

For calculation of FSR and FBR 500 µL of plasma was brought to room temperature, briefly vortexed and incubated with 10 µL urease (10 mg.mL^{-1}; U1500-20KU, Sigma) for 5 minutes. Plasma proteins were precipitated in 10 µL of 12 mol perchloric acid, vortexed and incubated with gentle agitation for 10 minutes at room temperature. Samples were then spun (6000 rpm, 10 minutes, 4 °C) and 400 µL supernatant extracted. Supernatant was incubated with 100 µL 1 mol potassium bicarbonate on ice for 20 minutes. Samples were then spun again (6000 rpm, 10 minutes, 4 °C), to remove excess potassium crystals, and 400 µL supernatant removed and neutralized with 10 µL concentrated (~11.5 mol) hydrochloric acid. Resultant samples were dried overnight at 50 °C in a rotary evaporator. Dried samples were derivatized with 50 µL pyridine (1 mol and 50 µL N-tert-Butyldimethysilyl-N-methyltrifluoro-acetamide (NTBSTFA; Sigma, 3948820) at 70 °C for 60 minutes.

Muscle samples from time points -30, 120, 300 and 320 minutes were used for calculation of both FSR and FBR post hypoxic exposure. An aliquot of each biopsy (~ 60 mg) were powered by mortar and pestle in liquid nitrogen, then resuspended in 0.5 mL ice cold perchloric acid (0.2 mol) and centrifuged (6000 rpm, 10 minutes). Resultant pellet was washed in 0.2 mol perchloric acid, spun and subsequent pellet run as above. First supernatant was incubated with 100 µL 1 mol ice cold potassium bicarbonate and incubated on ice (15 minutes), after which incubated with 10 µL urease (10 $mg.mL^{-1}$), as above and treated in the same manner as plasma samples.

Derivatized samples were analysed by gas chromatography mass spectrometer (GC-MS; Delta Plus XP, Perkin Elmer). Amino acid derivatives were measured for mass fragment peaks of the tracee (234 mHz, unlabelled phe) and two tracers (235 mHz, ^{15}N-Phe) and 239 (239 mHz, D_5-Phe; Figure 4.3).

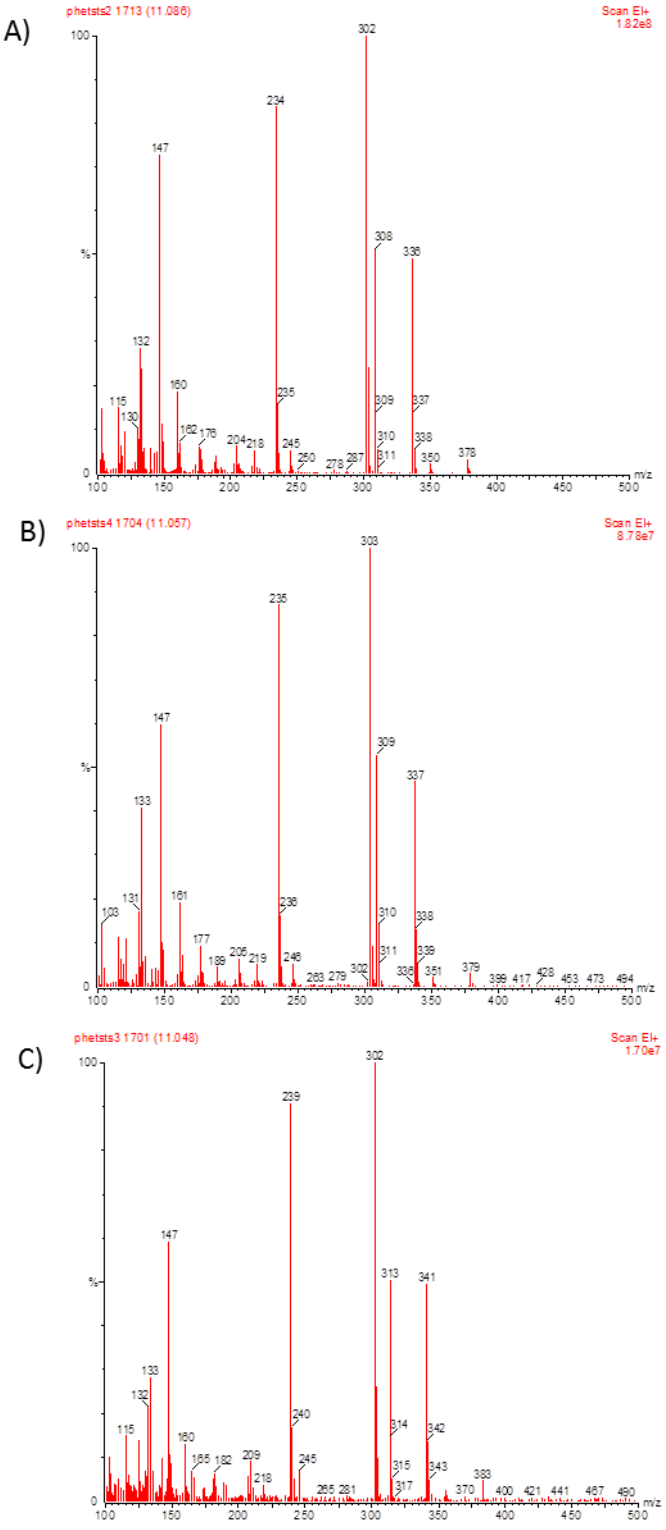

Figure 4.3: Peaks of tracer (t) and tracee (T). Isotope peak examples from with **A)** human muscle extract (234 mHz) **B)** ^{15}N-Phe (235 mHz; 490150, Sercon) and **C)** D_5-Phe (239 mHz; 615870, Sercon).

Calculations for Q, FSR and FBR were used as outlined previously, and are given below (Fearon et al., 1988, Phillips et al., 1996, Zhang et al., 1996). Net protein balance (%.hr^{-1}) is given by FSR – FBR, with positive values indicating positive balance. A more complete description of both methodology and formula can be found in Appendix Six.

$$Q.kg^{-1} = \dot{v} \times ({}^{d}/_{E})$$

Q.kg^{-1}, whole body turnover per kilogram body mass; v̇, rate of flow (µmol.min^{-1}); d, enrichment; E, enrichment at plateau).

$$FSR\ (\%.Hr^{-1}) = \left(\frac{\Delta Et}{[Ep \times (\Delta t)]}\right) \times 100$$

FSR, Fractional synthesis rate (in percent per hour); Δ*Et*, change in tissue enrichment; E*p* mean plasma enrichment; t, time (hours).

(Phillips et al., 1997)

$$FBR = \frac{E_M(t_2) - E_M(t_1)}{P\int_{t_1}^{t_2} E_A\,(t)dt - (1+P)\int_{t_1}^{t_2} E_M\,(t)dt} \times (\frac{Q_M}{T})$$

FBR, fractional breakdown rate; EM, enrichment muscle; EA, enrichment arterial; t, time; $\int_{t_1}^{t_2} E_X\,(t)dt$ gives area of decay curve of x (muscle or arterial); QM/T, ratio of intracellular free trace verses protein-bound trace content in the sample.

(Zhang et al., 1996)

$$Net\ balance(\%.hour) = FSR\ (\%.hour) - FBR\ (\%.hour)$$

FSR, Fractional synthesis rate; FBR, fractional breakdown rate

4.2.5 Protein Quantification

Approximately half of each biopsy (~ 40 mg) was powered by mortar and pestle in liquid nitrogen before being resuspended in 125 µL lysis buffer (10 mmol Tris-HCl, 150 mmol NaCl, 2 mmol EDTA, 2 % Triton X-100, protease & phosphatase inhibitor cocktail [Sigma, P8340], Appendix One), and shaken for 30 minutes at 4 °C. Samples were then spun (6000 rpm, 6 minutes, 4 °C) to fractionate total soluble protein from insoluble debris.

An aliquot of lysed muscle tissue extract were further diluted 1:10 in ice-cooled lysis buffer (Appendix One), before 5 µL of each sample and standards were loaded into U-bottomed clear 96-well plates in triplicate. Total protein content was measured in the method of Lowry (Appendix Five; 500-0116, BioRad). Bovine serum albumin (BSA) was used as a protein standard. Coefficient of variability of standards and samples was 0.13 and 0.08, respectively.

4.2.6 Western Blot

Western blots were run as described in the Chapter Three. Briefly, 40 µg total protein was run per lane on precast 10 % polyacrylamide gels (Invitrogen, NP0301), and transferred for 3 hours on ice to nitrocellulose membrane. Primary antibody conditions are given in Table 4.2. Primary antibodies were used 1:1000, secondary antibodies 1:10,000. Secondary antibody was anti-rabbit, and membranes were developed by hand onto film before being digitized and analysed with ImageJ open source software (ImageJ, version 1.45s). Blots were normalized to total protein stained for by ponceau rouge, using the method of Romero-Calvo and colleagues (2010).

Table 4.2: Western blot characteristics by target protein. Blocking, primary and secondary conditions are diluted into tris-buffered saline with tween (TBS-T).

Target	Supplier (Code)	Blocking	Primary antibody	Secondary antibody
Myostatin	Millipore (ab3239)	5 % BSA, 1 hour, RT	5 % BSA o/n, 4 °C	0.5 % BSA, 1 hour, RT
Ubiquitin	Cell Signalling (3933)	5 % BSA, 1 hour, RT	0.5 % BSA o/n, 4 °C	0.5 % BSA, 1 hour, RT
IκBα	Cell Signalling (9242)	5 % BSA, 1 hour, RT	5 % BSA o/n, 4 °C	0.5 % BSA, 1 hour, RT

Bovine serum albumin (BSA). Room temperature (RT). Overnight (o/n).

4.2.7 ELISA

ELISA for plasma myostatin was performed according to manufacturer's instructions (DGDF80, R&D Systems). Aliquoted plasma samples were defrosted from – 80 °C to room temperature before 100 µL plasma was activated for the removal of myostatin binding proteins (60 µL HCl, 6 M, 10 minutes at room temperature), then neutralized (40 µL NaOH + 1.2 mol HEPES), and finally diluted into 200 µL calibrator diluent (R&D, 895525) to give a prepared sample at a 1:4 dilution. Prepared samples were loaded in duplicate into pre-coated 96 well plates. Recombinant myostatin was used as a standard (range 31.3 – 2,000 pg.mL^{-1}), and calibrator dilutant used as a blank control. Plates were incubated at 37 °C with gentle agitation for 2 hours, washed 4 times (R&D, 895003) before myostatin conjugate (R&D, 894409) was added (200 µL) and plates incubates for 2 hours at room temperature. Wells were washed again (4 times) before 200 µL substrate solution was added and plates incubated (30 minutes, room temperature, protected from light). Colorimetric reaction was stopped with 50 µL 2 N sulphuric acid. Samples were read spectrophotometrically at 450 nm and blanked to 570 nm using a microplate reader (VersaMax, Molecular Devices, USA). Coefficient of variability of standards and samples were 0.03 and 0.13, respectively.

4.2.8 Statistical Analysis

Results are presented in figures as individuals data points, as outlined by Drummond and Vowler (2012) and written in text as 'mean (SD) units'. Repeated measures analysis of variance (ANOVA) or paired sample t-tests were used as appropriate. Friedman's ANOVA was utilized for mLLAMS data. P*ost hoc* analysis performed where needed in the method of Bonferroni, utilizing SPSS (IBM, version 20.0). Where a deviation from sphericity of groups was noted in repeated measures ANOVA, this was corrected for in the method of Greenhouse and Geisser. Linear correlations were determined in the method of Pearson. Significance was set at $p < 0.05$ throughout.

4.3 Results

4.3.1 Effect of Hypoxia on Homeostatic Measures

The effect of hypoxia on SpO_2 was examined by two-way (condition [control, hypoxic] × time [-10, 0, 30, 60, 90, 120, 130 minutes]) repeated measure ANOVA. A significant condition × time interaction was noted for the effect of hypoxia on SpO_2 ($p < 0.001$). Subsequent *post hoc* analysis reveals hypoxia significantly reduces SpO_2 at every time point during hypoxic exposure (Figure 4.4A). Mean SpO_2 during hypoxia was 77.7 (0.7) %, while control values remained unperturbed at 97.8 (0.4) %. Independent of time this effect is maintained, with paired sample t-test showing area under the curve of hypoxia being significantly reduced relative to control values ($p < 0.001$; Figure 4.4B).

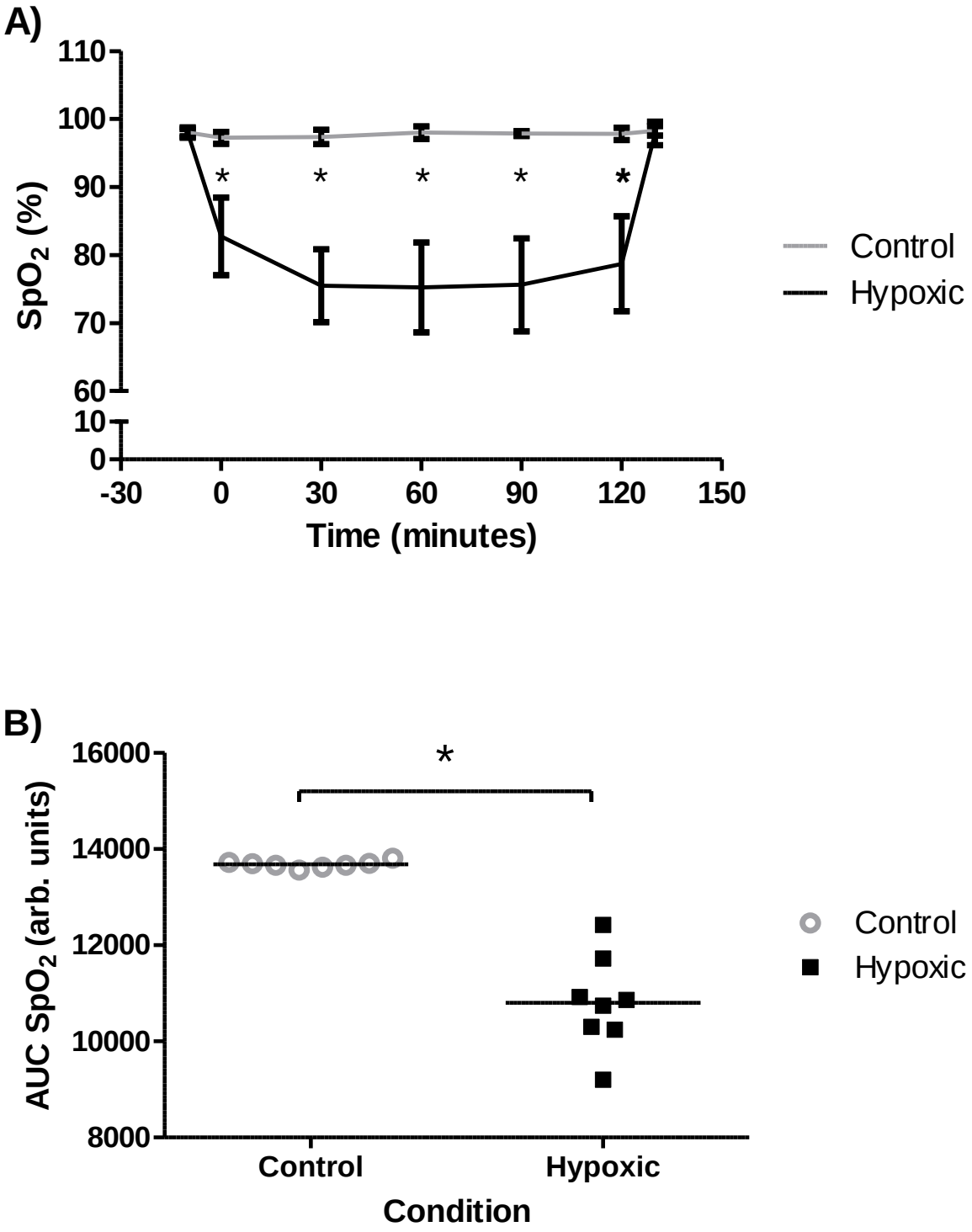

Figure 4.4: Effect of hypoxia on fingertip capillary haemoglobin oxygen saturation. A) Fingertip capillary haemoglobin oxygen saturation (%) as a function of time (minutes). Hypoxic exposure (11.9 % O_2) from time point 0 to 120 minutes, control condition in ambient air (20.9 % O_2). ✱ indicate significant difference between conditions at given time point ($p < 0.05$). N = 8 males per condition. Error bars represent SD. Grey line indicates control contidion, black hypoxic**. B)** Area under curve of SpO_2 by condition in hypoxia (black square) and control (open grey circle). ✱ indicate significant difference between groups ($p < 0.05$). Mean of individual groups given by horizontal black line. N = 8 individuals.

The effect of hypoxia on heart rate was examined by two-way (condition [control, hypoxic] × time [-10, 0, 30, 60, 90, 120, 130 minutes]) repeated measure ANOVA. A significant condition × time interaction was noted for the effect of hypoxia on heart rate ($p = 0.021$). Subsequent *post hoc* analysis shows hypoxia significantly increased heart rate at 60 minutes relative to the control values (122 [17.6] vs 97.8 [12.1] % in hypoxic and control respectively; $p = 0.03$, Figure 4.5A), but not at other time points during hypoxia. Independent of time, this effect is maintained, with area under the curve heart rate showing trends towards an increase relative to control values ($p = 0.053$, Figure 4.5B).

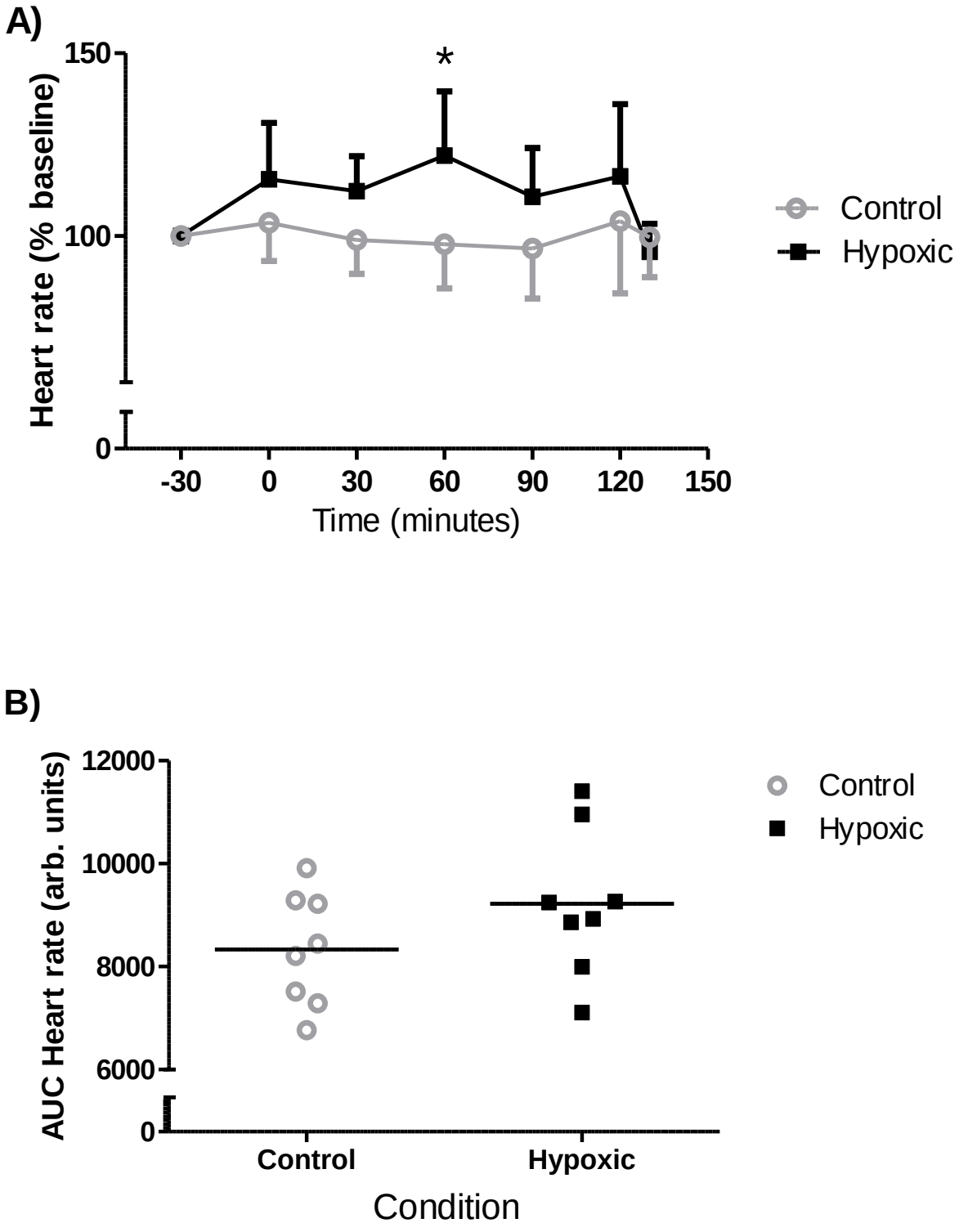

Figure 4.5: Effect of hypoxia on resting heart rate. A) HR (bpm) as a function of time (minutes). Hypoxic exposure (11.9 % O_2) from time point 0 to 120 minutes, control condition in ambient air (20.9% O_2). Hypoxic condition shown as closed black squares, control as open circles. Error bars represent SD. ∗ indicate significant difference between group at indicated time point ($p < 0.05$). Error bars represent SD. **B)** Area under curve of hearte rate (black square) and control (open grey circle).Mean of individual groups given by horizontal black line. N = 8 individuals.

Friedman's ANOVA suggests a significant difference in mLLAMS occurred in the participant population ($p < 0.00105$). *Post hoc* analysis with Wilcoxon signed-rank test corrected in the method of Bonferroni revealed hypoxia significantly reduced mLLAMS symptoms at the 90 minute time point, relative to control conditions ($p =< 0.03105$) but not at 0 ($p = 0.500$) or 60 minutes ($p = 0.063$; Figure 4.6(Figure 4.6).

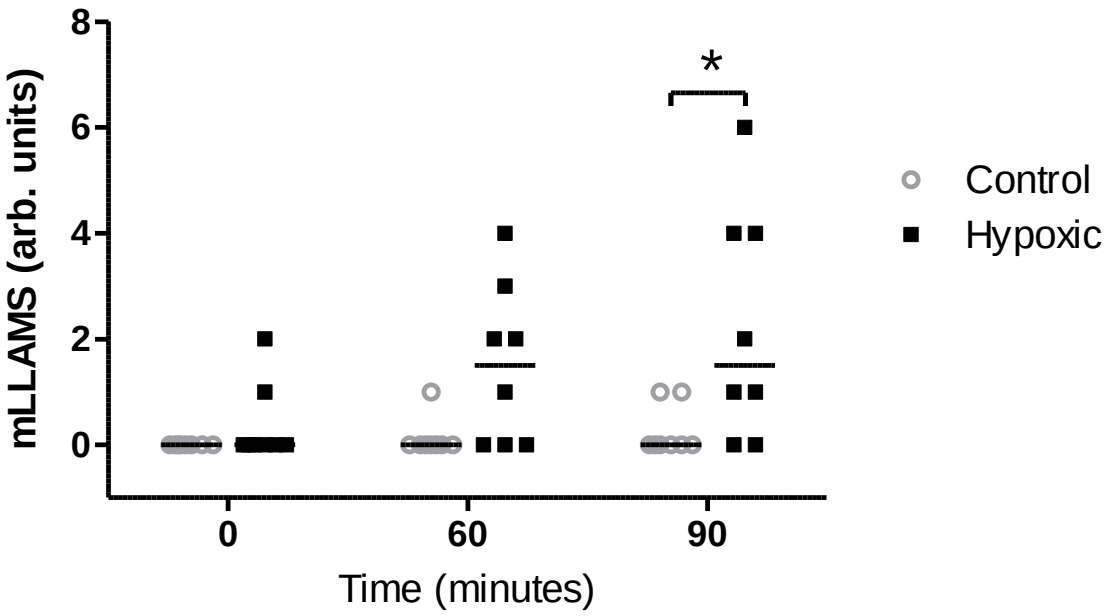

Figure 4.6: Effect of hypoxia on symptoms of acute mountain sickness. Modified Lake Louise Acute Mountain Sickness questionnaire (mLLAMS) score (arb. unit) as a function of time (minutes).LLAMS questionnaire modified for acute usage by removal of sleep specific questions. Hypoxic exposure (11.9 % O_2) from time point 0 to 90 minutes, control condition in ambient air (20.9 % O_2). Median of individual groups given by horizontal black line. N = 8 males per condition per time point. Open grey circles represent control condition, black squares hypoxic condition.

4.3.2 Effect of Hypoxia on Muscle and Plasma Myostatin

The effect of hypoxia on muscle myostatin was examined by two-way (condition [control, hypoxic] × time [-30, 120, 300, 320 minutes]) repeated measures ANOVA, with treatment order considered as a between-participant effect. No treatment order × group × time interaction was noted ($p = 0.126$). A significant condition × time interaction was noted for the effect of hypoxia on muscle myostatin peptide ($p = 0.005$) when results are expressed as a percentage change from baseline (-30 minutes). Subsequent *post hoc* analysis reveals hypoxia significantly decreased myostatin peptide at the 320 minute time point relative to the control condition ($p = 0.047$), but not at other time points during hypoxia (Figure 4.7A). When data is expressed as a function of control time points, this effect is maintained with a similar condition × time interaction ($p =< 0.035$), and *post hoc* effect of hypoxia noted at the 320 minute mark ($p = 0.002$), but no other time point (Figure 4.7B).

The effect of hypoxia on muscle myostatin LAP was examined by two-way (condition [control, hypoxic] × time [-30, 120, 300, 320 minutes]) repeated measures ANOVA. No condition × time interaction was noted ($p = 0.647$). No main effect of either group ($p = 0.854$) or time was noted ($p = 0.647$; Figure 4.7C). The effect of hypoxia on the ratio of LAP to myostatin was examined by two-way (condition [control, hypoxic] × time [-30, 120, 300, 320 minutes]) repeated measures ANOVA. No condition × time interaction was noted ($p = 0.212$). No main effect of either group ($p = 0.868$) or time was noted ($p = 0.102$; Figure 4.7D).

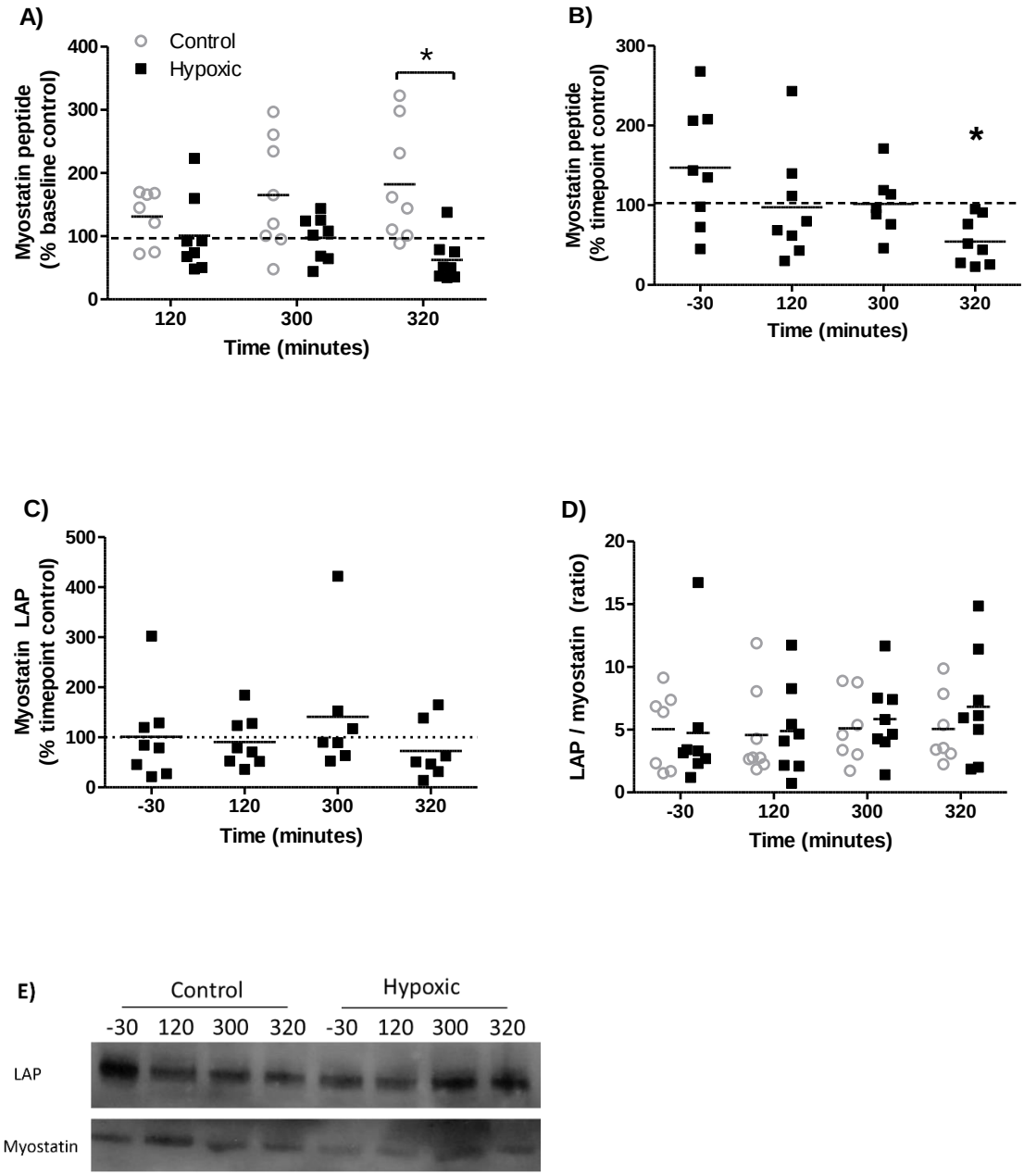

Figure 4.7: Effect of hypoxic treatment on myostatin expression. Western blot of myostatin peptide (ab3239, Millipore) at 26 kDa from vastus lateralis muscle biopsy prior and post 2 hours control (ambient) or hypoxic (11.9 % O_2) exposure. **A)** Individuals normalized to baseline values (-30 minutes). ✱ indicate significant difference between groups ($p < 0.05$). **B)** normalized to matching timepoint control. **C)** Myostatin latancy associated peptide normalized to matching timepoint control. **D)** LAP / myostatin ratio. N = 8 males per condition. 40 µg total protein loaded per well. Normalized to total protein per lane by ponceau rouge. Open circles represent control condition, black squares hypoxic condition. **E)** Representative image.

The effect of hypoxia on plasma myostatin was examined by two-way (condition [control, hypoxic] × time [-30, 120, 240, 320 minutes]) repeated measures ANOVA, with treatment order considered as a between-participant effect. No treatment order × group × time interaction was noted ($p = 0.064$). No effect of acute hypoxia was noted on plasma myostatin, with no condition × time interaction ($p = 0.69$), nor a main effect of group ($p = 0.11$) or time ($p = 0.28$) observed (Figure 4.8A). This effect is maintained if plasma myostatin during hypoxia is expressed as a function of matching time point control (Figure 4.8B), with no effect of group ($p = 0.09$) or time witnessed ($p = 0.95$).

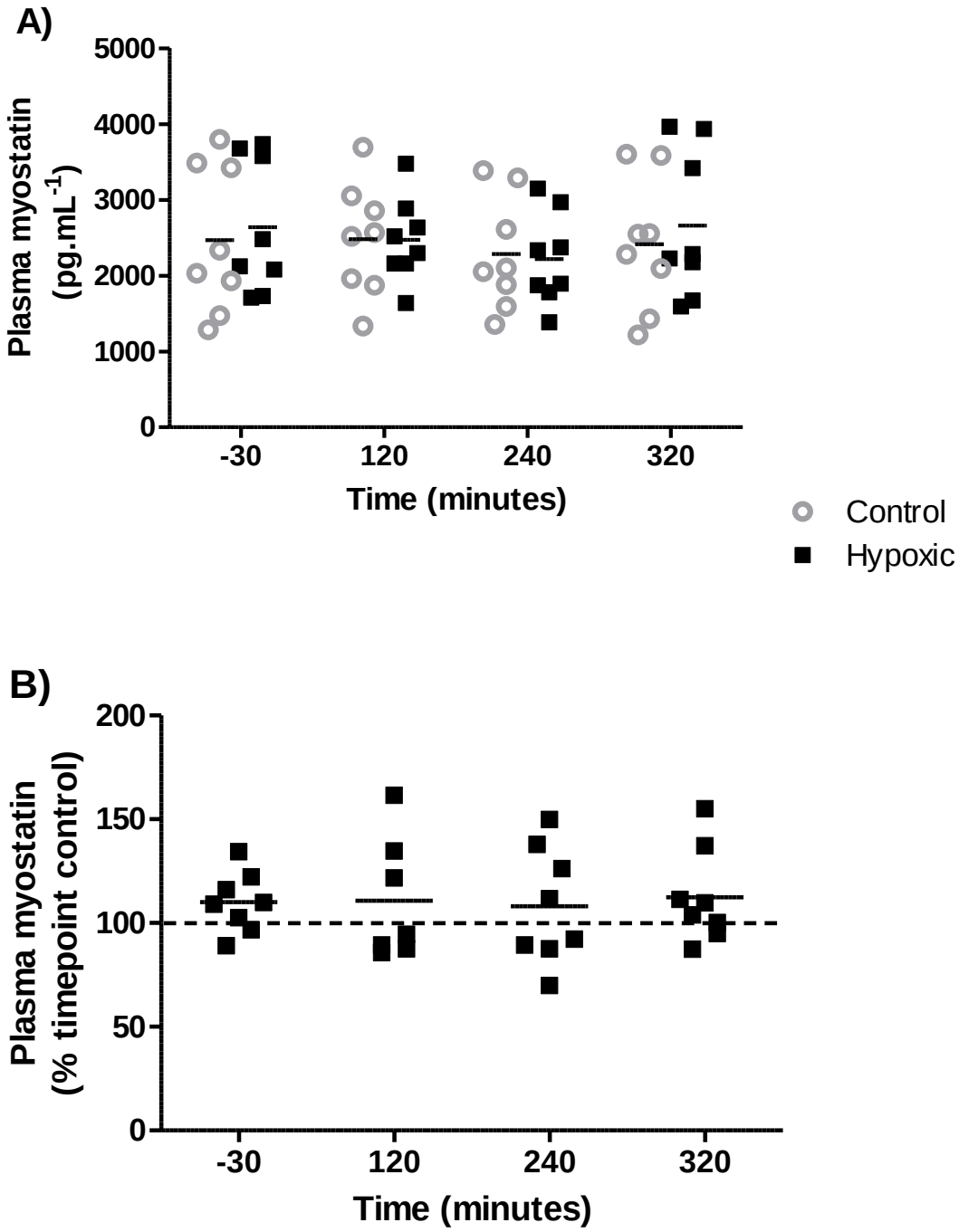

Figure 4.8: Effect of hypoxic exposure on plasma myostatin. ELISA for plasma myostatin (DGDF80, R&D Systems) concentration from venous plasma prior (-30 minutes), or following (120 minutes, 240 minutes or 320 minutes) a 11.9 % O_2 hypoxic stimulus administrated between time points 0 to 120 minutes**. A)** Absolute myostatin concentration ($pg.mL^{-1}$) in control (grey open circles) or hypoxic (black squares) conditions. **B)** Relative myostatin concentration in hypoxic conditions, expressed as a function of matching control time point (%). Black line indicates mean. N = 8.

4.3.3 Effect of Hypoxia on Proteasomal Activity

The effect of ubiquitin (both free and bound) was examined by two-way (condition [control, hypoxic] × time [-30, 120, 300, 320 minutes]) repeated measures ANOVA. No condition × time interaction was noted for the effect of hypoxia on muscle free ubiquitin (6 kDa), when results are expressed as a percentage change from baseline (-30 minutes; $p = 0.875$), nor is a main effect of group ($p = 0.846$) or time ($p = 0.345$) noted (Figure 4.9A). This effect is maintained if hypoxic results are expressed relative to matching time point control, with no effect of time on free ubiquitin expression ($p = 0.212$, Figure 4.9B).

In a similar manner, no condition × time interaction was noted for the effect of hypoxia on muscle bound ubiquitin, when results are expressed as a percentage change from baseline (-30 minutes; $p = 0.356$), nor is a main effect of group ($p = 0.25$) or time noted ($p = 0.99$, Figure 4.10A). No effect of time is noted if hypoxic results are expressed relative to matching time point controls ($p = 0.274$, Figure 4.10B), however a clear outlier can be seen at the -30 time point (517 % increase at baseline above control condition, greater than 3 SD from the mean). Removal of this outlier alters the result of statistical analysis, with a significant effect of time ($p = 0.002$). Subsequent *post hoc* analysis with this outlier removed suggests bound ubiquitin is increased following hypoxia, with bound ubiquitin at 320 minutes 198.5 % higher than matching time point controls ($p = 0.006$, $d = 1.95$; Figure 4.10B).

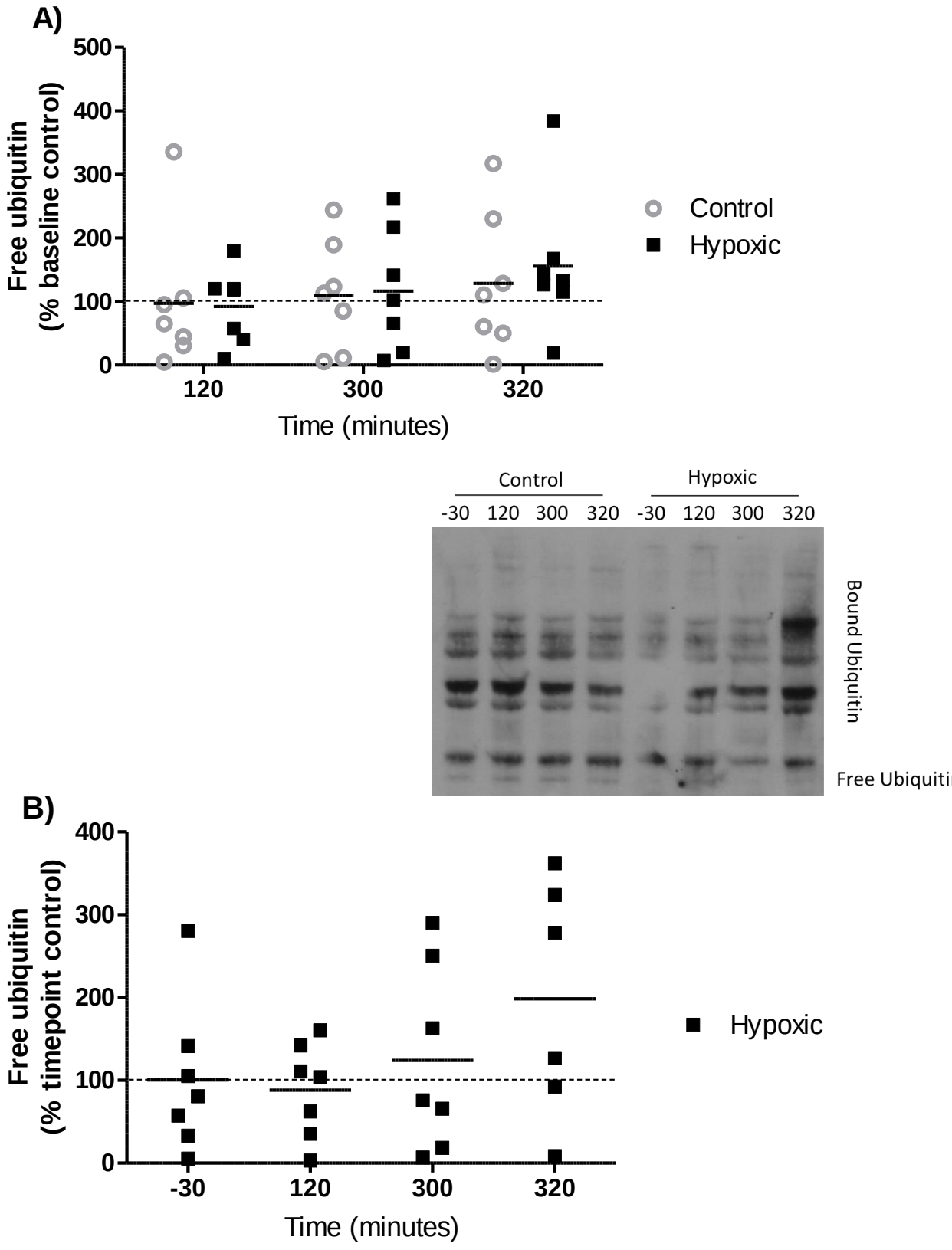

Figure 4.9: Effect of hypoxia on free ubiquitin. Western blot of free ubiquitin (3933, Cell Signalling) at 6 kDa from vastus lateralis muscle biopsy prior and post 2 hours control (ambient) or hypoxic (11.9 % O_2) exposure. **A)** Individuals normalized to baseline values (-30 minutes; dashed line). **B)** Hypoxic condition normalized to matching control time point value. N = 8 per condition. 40 µg total protein loaded per well. Normalized to total protein per lane by ponceau rouge. Open grey circles represent control condition, black squares hypoxic condition**. Insert** – representative image of ubiquitin blot show ubiquitin binding across proteins.

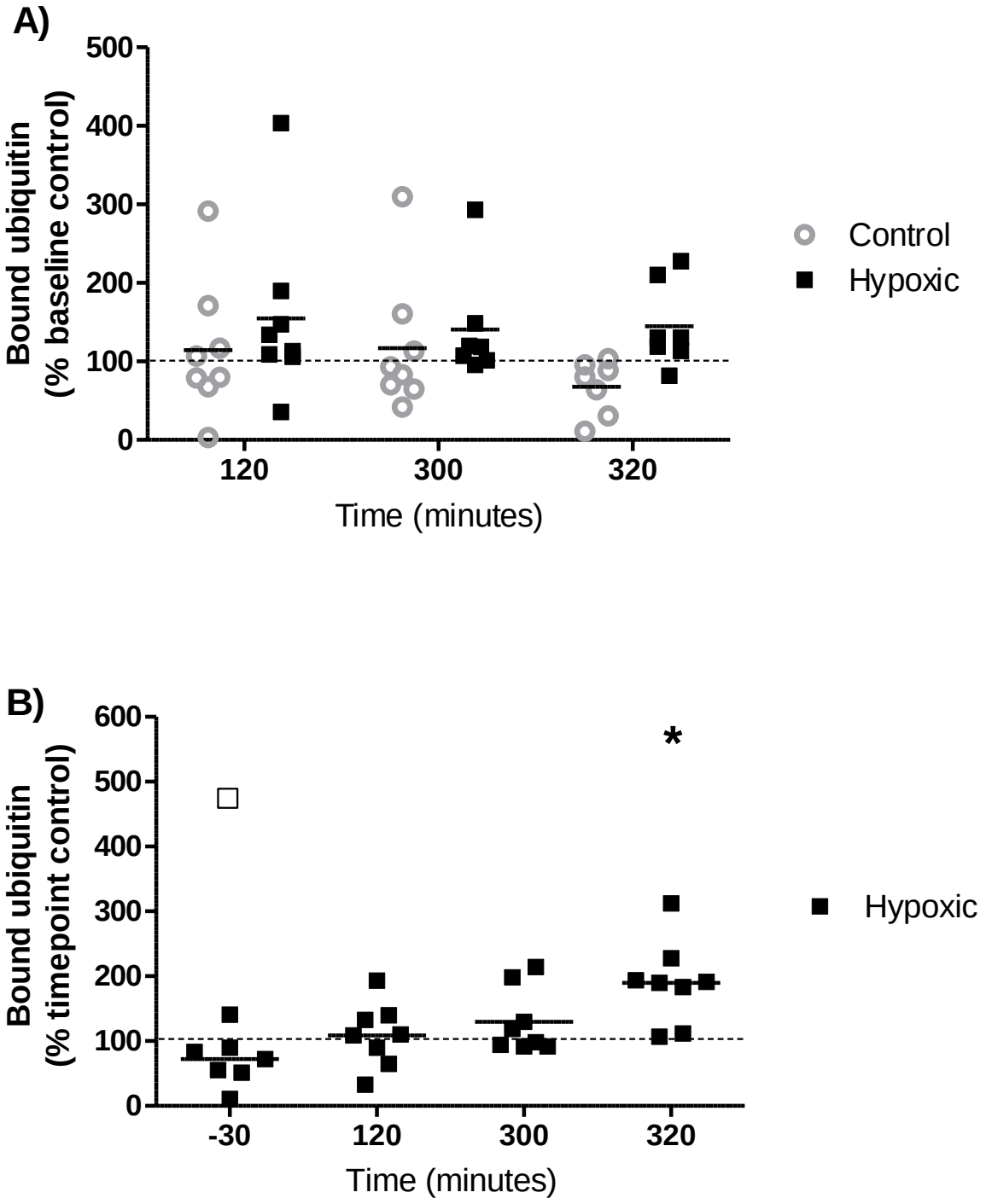

Figure 4.10: Effect of hypoxia on bound ubiquitin. Western blot of bound ubiquitin (3933, Cell Signalling) at from vastus lateralis muscle biopsy prior and post 2 hours control (ambient) or hypoxic (11.9 % O_2) exposure. **A)** Individuals normalized to baseline values (-30 minutes). **B)** Hypoxic condition normalized to matching control time point value. N = 8 per condition. 40 µg total protein loaded per well. Normalized to total protein per lane by ponceau rouge. Open grey circles represent control condition, black squares hypoxic condition (open black square indicates removed outlier). A representative image can be seen in Figure 4.9.

The effect of hypoxia on IκBα was examined by two-way (condition [control, hypoxic] × time [-30, 120, 300, 320 minutes]) repeated measures ANOVA. No condition × time interaction was noted for the effect of hypoxia on muscle IκBα, when results are expressed as a percentage change from baseline (-30 minutes, $p = 0.27$), nor is a main effect of group ($p = 0.58$) or time ($p = 0.76$) noted (Figure 4.11A). No effect of time was noted if hypoxic results are expressed relative to matching time point controls ($p = 0.98$, Figure 4.11B).

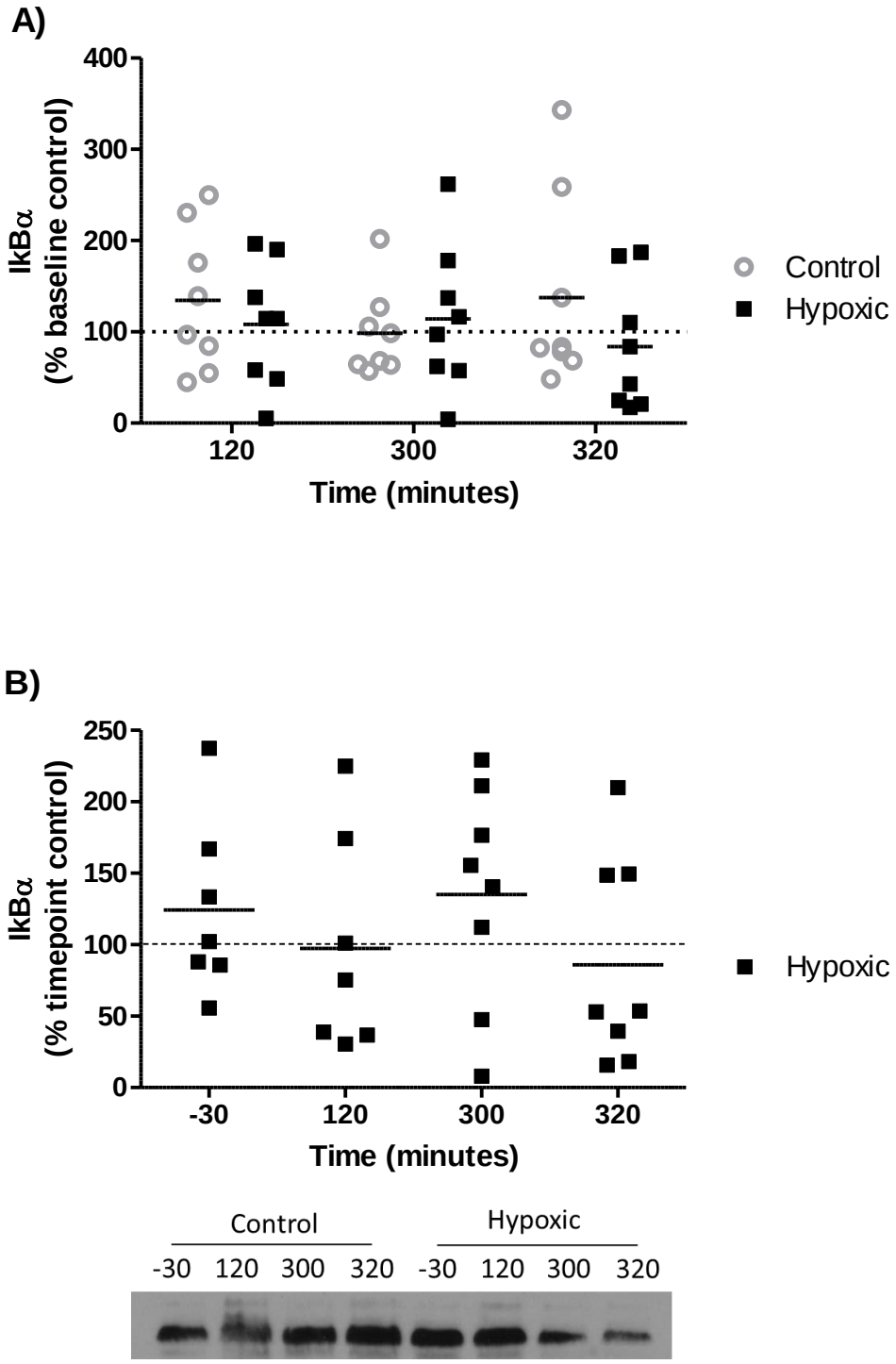

Figure 4.11: Effect of hypoxia on IκBα expression. Western blot of IκBα (9242, Cell Signalling) at from vastus lateralis muscle biopsy prior and post 2 hours control (ambient) or hypoxic (11.9 % O_2) exposure. **A)** Individuals normalized to baseline values (-30 minutes; dashed line). **B)** Hypoxic condition normalized to matching control time point value. N = 8 per condition. 40 µg total protein loaded per well. Normalized to total protein per lane by ponceau rouge. Open grey circles represent control condition, black squares hypoxic condition. **Insert** – representative image.

4.3.4 Correlations between Oxygen Delivery and Myostatin

A weak linear relationship is seen between the change in plasma myostatin concentration ($pg.mL^{-1}$) from baseline to 120 minutes (Δ plasma myostatin) and the change in SpO_2 (%) from baseline to 120 minutes (Δ SpO_2; $r^2 = 0.34$). Person's correlation suggests this relationship is not significant ($p = 0.13$ Figure 4.12).

As a proxy of total oxygen delivery (DO_2), the correlation between HR × SpO_2 during hypoxia and Δ plasma myostatin was examined. No relationship was noted between these variables ($r^2 = 0.07$; data not shown).

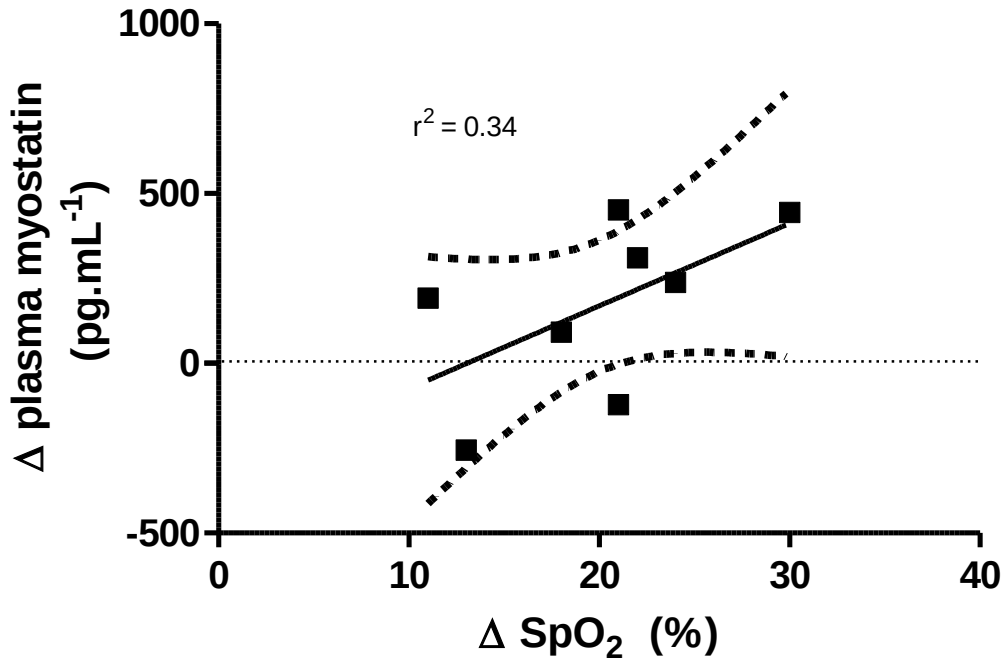

Figure 4.12: Correlation between Δ SpO_2 and Δ plasma myostatin. Δ SpO_2 calculated from difference between baseline and 120 minutes. Δ plasma myostatin calculated from difference between baseline and 120 minutes. Plasma myostatin concentration value ($ng.mL^{-1}$) from pooled baseline values between conditions, as measured by ELISA (DGDF80, R&D Systems). N = 8 individuals. Dashed lines indicate 95 % confidence limits.

No correlation is seen between the change in SpO_2 (%) from baseline to 120 minutes (Δ SpO_2) and the change in muscle myostatin peptide (%) either from baseline to 120 minutes (p = 0.70, Figure 4.13A) or from baseline to 320 minutes (p = 0.98, Figure 4.13B).

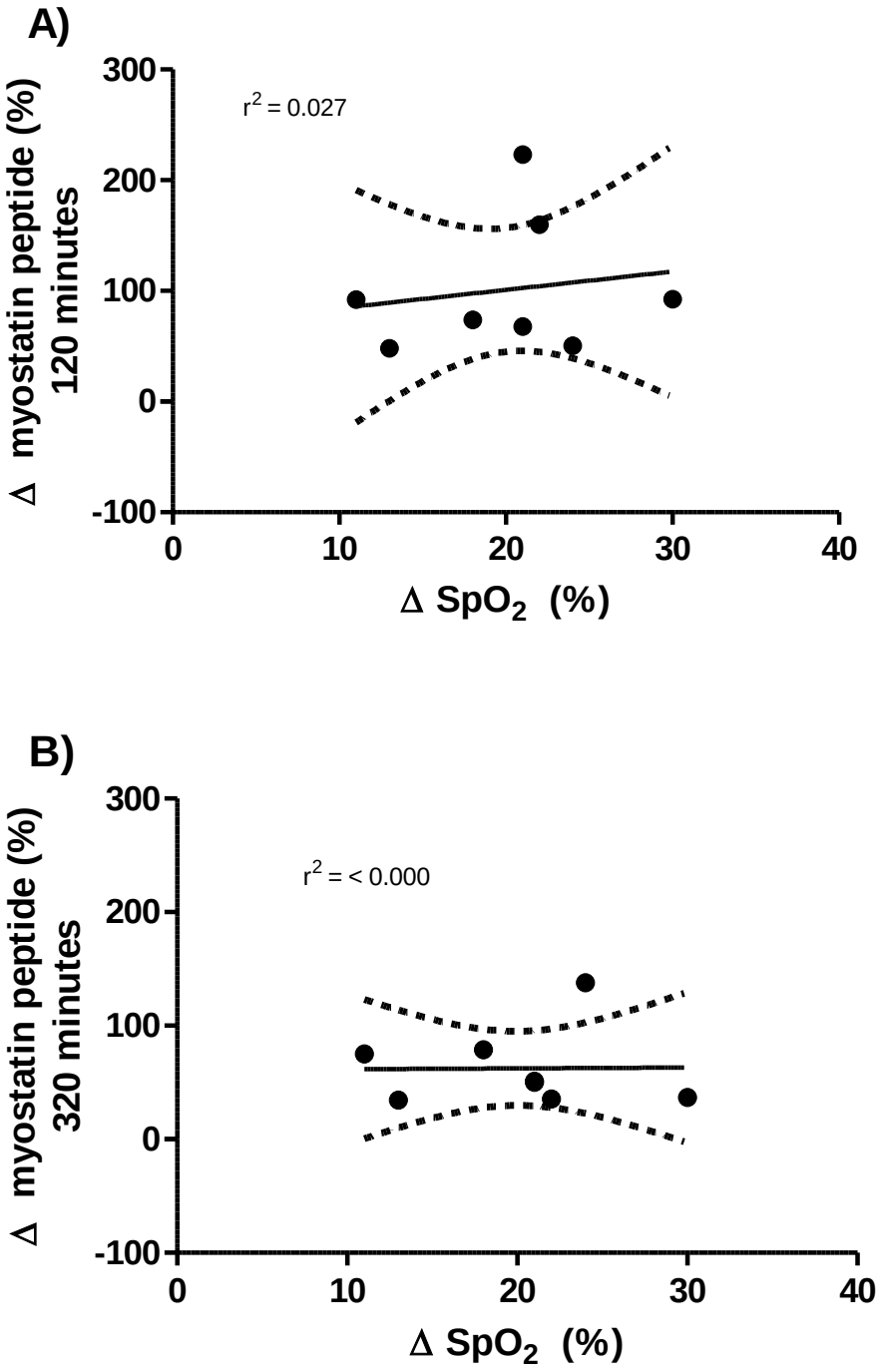

Figure 4.13: Correlation between Δ SpO_2 and Δ muscle myostatin. Change in muscle myostatin (%) measured by Western blot **A)** from baseline to immediately following hypoxic exposure or **B)** from baseline to 320 minutes (200 minutes following hypoxic exposure). Results expressed as a percentage change from control values. Average of SpO_2 during 120 minutes at 11.9 % O_2. N = 8 individuals. Dashed lines indicate 95 % confidence limits.

4.3.5 Effect of Hypoxia on Global and Muscle Protein Turnover

Whole body protein turnover (Q) was examined by two-way (condition [control, hypoxic] × time [-30, 120, 300 minutes) repeated measures ANOVA. No condition × time interaction is noted ($p = 0.227$), nor is an effect of time ($p = 0.306$) or condition ($p = 0.1$; Figure 4.14), suggesting protein turnover was not altered by acute hypoxic exposure (Figure 4.14).

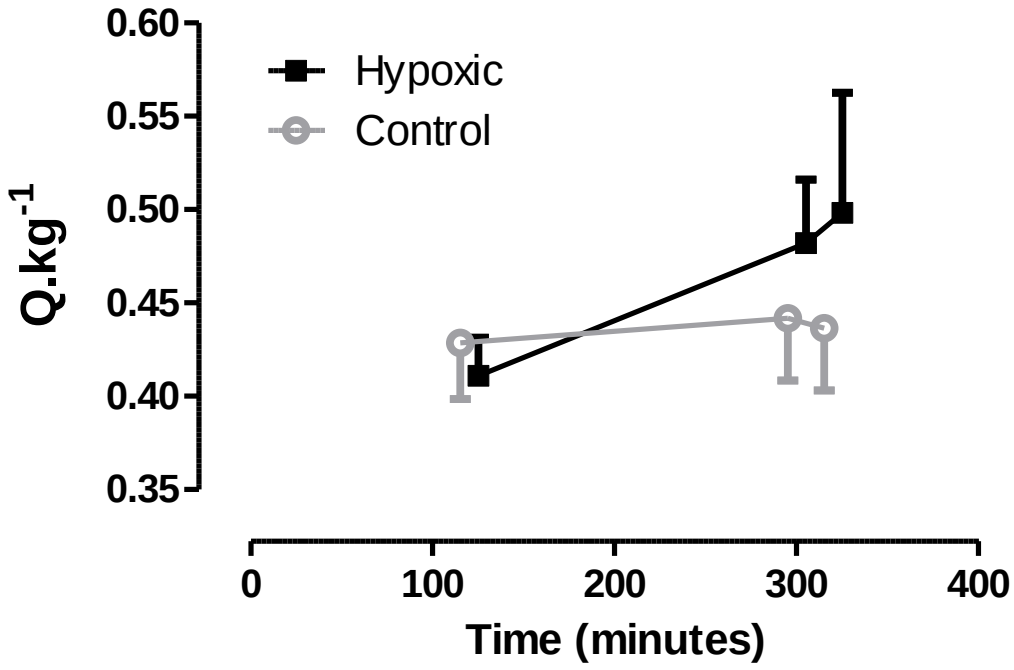

Figure 4.14: Whole body protein turnover per kilogram ($Q.kg^{-1}$) as a function of time (minutes). D_5-phenylalanine infusion (prime 2 $\mu mol.kg^{-1}$, rate 0.05 $\mu mol.kg^{-1}$) started at 0 minutes for 320 minutes. Tracer (*t*) D5-Phe, tracee (T) phenylalanine. Control (20.9 % O_2) indicated by open grey circles, hypoxic (11.9 % O_2). Hypoxic stimulus delivered between 0 – 120 minutes. N = 8.

FSR was directly quantified in a limited sub-group (n = 5) of the experimental cohort. The effect of hypoxia on FSR was examined by two-way (condition [control, hypoxic] × time [-30, 120, 300 minutes) repeated measures ANOVA. No condition × time interaction is noted ($p = 0.327$), nor is an effect of time ($p = 0.0.981$) or condition ($p = 101$; Figure 4.15), suggesting FSR was not altered by hypoxic exposure.

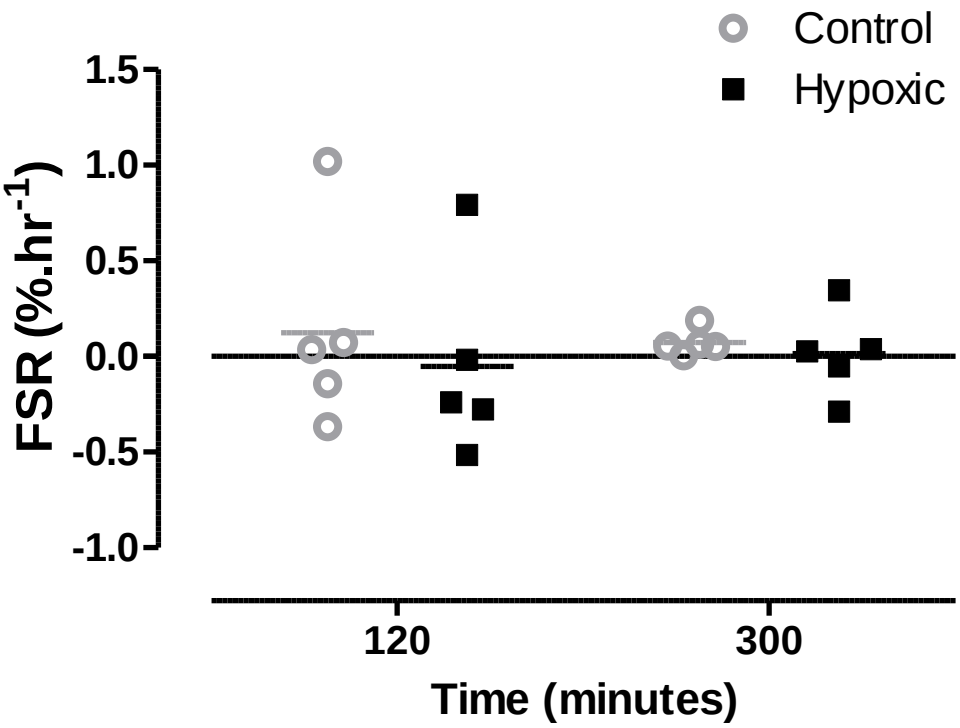

Figure 4.15: FSR (%.hr^{-1}) as a function of time (minutes). D_5-phenylalanine infusion (prime 2 µmol.kg^{-1}, rate 0.05 µmol.kg^{-1}) started at 0 minutes for 320 minutes. Tracer (*t*) D5-Phe, tracee (T) phenylalanine. Control (20.9 % O_2) indicated by open grey circles, hypoxic (11.9 % O_2). Hypoxic stimulus delivered between 0 – 120 minutes. N = 5.

Quantification of FBR requires the quantification of isotope tracer within three compartments, protein bound, unbound (free) and plasma, for subsequent quantification of dilution of free tracer (*t*) from protein and plasma tracee (T) (section 4.2.4). Repeated attempts to quantify ^{15}N-Phe *t* in plasma have been unsuccessful to date, precluding calculation and reporting of FBR results here.

4.4 Discussion

When humans are exposed chronically to a hypoxic environment, losses of muscle mass are often witnessed. The results demonstrated here show that 2 hours of hypoxia is sufficient to reduce the expression of the myostatin peptide within muscle *in vivo* in healthy males, and further, this is coupled with evidence for increased ubiquitin activity but no apparent alteration in pro-synthesis events.

These results represent the first report of changes in muscle myostatin peptide expression in any *in vivo* model in an acute timeframe. The acute alteration in myostatin signalling following 2 hours of hypoxic exposure in healthy humans suggests that hypoxic exposure alone may be sufficient to induce muscle atrophy, independent of the cause of hypoxia. Counter to the initial hypothesis, here a decrease in muscle myostatin expression following hypoxic exposure is seen. One interpretation of this result is that myostatin is acting in its endocrine manner, as first suggested by Gonzalez-Cadavid and colleagues (1998), and this decrease represents secretion of the myostatin peptide. An alternative hypothesis is that myostatin cellular content may be being degraded in an attempt to save muscle mass, potentially via the ubiquitin proteasomal pathway, the activity of which was shown here to be increased. This effect would be similar in nature to that shown by Doucet and colleagues (2007), who showed significantly increased expression in downstream members of the pro-synthesis Akt pathway, albeit in a different model of hypoxia (chronically hypoxic COPD patients).

If myostatin is acting in an endocrine manner, then it would be expected that an increase in plasma myostatin concentration would be seen. The results presented here do not support this, with no increase in plasma myostatin seen at any time point measured. However, it should be noted that the decrease in muscle myostatin was seen at the final measured time point (t = 320 minutes). It

may be physiologically unreasonable to expect any movement of an endocrine hormone out of muscle to appear immediately in plasma, although this has not been examined by published literature to date. The delay between leaving the intracellular space and appearing systemically at a measurable concentration may have resulted in the missing of an increase in the model studied here, suggesting examination of longer timeframes may be of interest.

Increased activity of the proteasomal pathway fits with the preceding Chapters *in vitro* results and with those of Caron and colleagues (2009). It therefore seems that in acute timeframes, the effect of hypoxia on muscle size is regulated primarily via degradative pathways, not inhibition of pro-synthesis activity. Unfortunately, methodological constraints prevented the measurement of phosphorylated proteins, therefore this Chapter was unable to quantify changes in Akt signalling. The results of Etheridge and colleagues (2011) provide support for a lack of change in pro-Akt signalling, with no change in Akt pathway members ($p70^{s6k}$, pAkt [Ser473] or mTOR [S448]).

Supporting these results, acute hypoxic does not appear to alter FSR, as shown by Etheridge and colleagues (2011) immediately after 2 hours normobaric hypoxia (12 % O_2), by Imoberdorf and colleagues after 24 hour at 4,559 m altitude (Imoberdorf et al., 2006), and by the FSR results presented in this Chapter (2 hours normobaric hypoxia, 11.9 % O_2). These findings both confirm previous results (Etheridge et al., 2011), and extended this finding up to 3 hours following hypoxic exposure. It is tempting to speculate changes in FBR may have occurred in this acute time frame, and indeed, whole body protein turnover trended towards an increase in the hypoxic group. Such a finding would be consistent with the results of Caron and colleagues (2009) *in vitro* and also the proposed initiation of atrophic processes due to the hypoxic stimulus used here, explaining the method of atrophy of muscle during severe hypoxic stimulation. It should be noted that whole body turnover is not representative of muscle atrophy, but all tissues' protein turnover systemically.

Confirmation by successful measurement of FBR, to balance the lack of response on FSR, is needed to confirm this hypothesis.

The results presented here suggest no link between acute hypoxic exposure and increased inflammatory signalling, indicated by no decrease in IκBα expression. Similar findings were found Koong and colleagues (1994b) *in vitro*, who showed decreased IκBα in the acute phases (30 minutes – 4 hours) of the hypoxic response in NIH3T3 (fibroblast cell line). Conversely, Burki and Tetenta (2014) showed no change in interleukin (IL) 1 and 6, or C-reactive protein following either 30 or 60 minutes of normobaric hypoxia (11 % O_2) in a similar population examined here. Chronic disorders such as COPD are associated with body mass loss and increased pro-inflammatory cytokine expression (Eid et al., 2001), however a number of confounding factors associated with the disease mean causality cannot be attributed to hypoxia alone. Further, Chapter Three of this work showed increased TNFα expression following 24 and 48 hours of hypoxic exposure *in vitro*, but not 2 hours, suggesting time of exposure used in this Chapter, and by Burki and Tetenta (2014), may be insufficient to induce a pro-inflammatory reaction *in vivo*.

Finally, the weaknesses associated with such an acute study in a healthy model should be noted. This Chapter attempted to model the initial changes in myostatin in response to a hypoxic stimulation in an attempt to model the changes seen in chronic disorders such as COPD, CHF and mountaineering in healthy individuals. Future work should extend either the duration of time in hypoxia, or the magnitude of hypoxia delivered, to examine what effect concentration of oxygen and time in a hypoxic state have on the response to hypoxia. One downside of specifically choosing an acute model of hypoxia is no direct measure of phenotypic muscle atrophy is possible as the timeframes are too rapid to induce measurable losses in muscle size.

In conclusion, this Chapter demonstrates that a 2 hour hypoxic exposure is sufficient to reduce the expression of muscle myostatin peptide, but not alter plasma myostatin concentration. Further, rate of phenylalanine uptake into muscle cells is not altered by acute hypoxic exposure. These results suggest hypoxia alone is sufficient to alter myostatin signalling, but not acutely alter protein synthesis. Alteration in myostatin signalling may in part underlie the atrophy seen in hypoxic disorders such as COPD and CHF, as well as environmental conditions such as mountaineering.

Chapter Five – The Effect of Time in Acute Hypoxia on Plasma Myostatin

5.1 Introduction

Homo sapiens are obligate aerobes, and as such a reduction or impairment of oxygen supply results in a number of physiological adaptations. These adaptations are dependent on the magnitude of the hypoxic stimulus. One phenotypical example of hypoxic adaptation is a loss of muscle mass. These effects are seen in healthy individuals during mountaineering, where a greater degree of muscle mass is lost than would be expected due to alterations in diet and energy expenditure alone (Hoppeler et al., 1990, Wagner, 2010) or in approximately 25 % of patients with chronic disorders such as COPD and CHF, where cachexic loss of muscle mass co-presents with systemic hypoxemia (Baarends et al., 1997, Bernard et al., 1998).

A time-dependent adaptive effect of hypobaric hypoxia is seen across physiological systems. Acute exposure to hypobaric hypoxia of ~ 4,000 m in healthy adults increases ventilatory frequency to approximately 200 % of sea level values, over the course of 100 hours exposure. The morphology of this shift is approximately exponential, with greater increases seen at later stages (Lenfant and Sullivan, 1971). Carotid body chemoreceptor sensitivity is increased following 28 days of hypobaric hypoxia, but not 3 hours (Barnard et al., 1987), while HR increases and mean arterial pressure (MAP) decreases in a time dependent manner following chronic intermittent hypoxia (1 minute of 10 % O_2 : 3 minutes of 21 % O_2) over 14 days (Marcus et al., 2009). Finally, and importantly for this work, a proteomic investigation of trout (*Oncorhynchus mykiss*) exposed to hypoxia show time dependent decreases in a number of muscle structural proteins including Myosin and Tubulin, and increases in proteasomal proteins, including ubiquitin and proteasomal subunits, at 1, 2 and 24 hours (Wulff et al., 2012). While caution should be made in the extrapolation of results from fish, if these results are maintained in humans, then a similar time-dependent effect may be seen in regulatory mechanisms of muscle size.

The role of myostatin as a negative regulator of muscle mass is also well described. First identified by McPherron and colleagues (1997), myostatin directly alters myocyte size by inhibiting the actions of the Akt-mTOR signalling pathway (Trendelenburg et al., 2009) and thus preventing Akt-dependent protein synthesis, as well as increasing activity of the ubiquitin-proteasomal system (McFarlane et al., 2006), a regulator of the rate of protease activity and protein degradation within cells (Mitch and Goldberg, 1996). Myostatin is known to respond to various atrophic and hypertrophic stimuli, as discussed in Chapter Two. Further, interactions between proteasomal activity, canonical pro-inflammatory cytokines and hypoxia have previously been reported (Murphy et al., 2011, Reardon et al., 2001), suggesting examinations of hypoxia and atrophy of muscle should consider cytokine responses. The concentration of plasma myostatin is reduced in response to resistance training (Walker et al., 2004) and increased in response to starvation (Jeanplong et al., 2003) and disuse (Murphy et al., 2011, Reardon et al., 2001). As such, myostatin is thought to play a central role in the regulation of muscle size in Mammalia (Lee, 2004, Rodriguez et al., 2014).

It was recently noted that both rats exposed to 10 % O_2 for 6 weeks and human COPD patients who are chronically hypoxemic show increased muscle myostatin expression (Hayot et al., 2011), suggesting hypoxia may induce increased myostatin expression. It is difficult to directly compare severity of hypoxic insult between models. Desaturation in severe COPD (FEV_1 < 50 %) is reported to be ~90 %, however (relatively) moderate activity can reduce this to 70 – 80 % (Phillips, 2004). Further, causality can be questioned with regards to chronic changes in myostatin in COPD patients. It could be hypothesized that hypoxia has induced a loss of muscle mass, which has therefore resulted in a reduction in myostatin, as myostatin negatively correlates with muscle mass across both healthy and cachexic patients (Gonzalez-Cadavid et al., 1998). Further, COPD presents a difficult research model, with altered nutritional intake, systemic inflammation and altered levels of physical activity (Wagner, 2008), all of which could conceivably alter myostatin.

Chapter Three of this thesis therefore examined the muscle and plasma myostatin response to 2 hours of hypoxia in healthy humans, hypothesizing an increase in myostatin would be seen. Counter to this hypothesis, myostatin expression within muscle decreased following acute hypoxic exposure. If the myostatin response to acute hypoxia is to decrease expression, while chronic hypoxia increases expression, this suggests a time-dependent effect is present. One hypothesis explaining these results seen in Chapter Four is the decrease in myostatin peptide expression represents myostatin leaving the muscle to act in its endocrine manner before increases in myostatin peptide production can compensate for this endocrine loss. If healthy individuals spend a longer period in hypoxic conditions, they thus may show the originally hypothesized increase in myostatin concentration at the plasma and increased expression at the muscle cellular level.

5.1.1 Aims and Hypothesis

The aim of this Chapter was therefore to examine what effect time of hypoxic exposure has on myostatin expression in muscle and concentration in plasma. Specifically, this Chapter aimed to;

1. demonstrate the presence or absence of a time dependent effect of hypoxia on myostatin signalling *in vivo* in healthy humans.

The hypothesis for this Chapter was that myostatin would increase at both the muscle and plasma level after 10 hours of 12 % O_2. Specifically, it is hypothesized that;

1. the effect of hypoxia on myostatin *in vivo* will be time dependent, with increased myostatin both within muscle and in plasma following 10 hours, but not 2 hours, of hypoxic exposure.

5.2 Methods

5.2.1 Ethical Approval

Ethical approval for the work described in this Chapter was provided by the University of Westminster Research Ethics Sub-committee (12/13/46) and conformed to the guidelines laid out by the Declaration of Helsinki. Written informed consent was obtained from all participants prior to participation. All work described within this chapter took place within the physiology labs of Dr Richard Mackenzie at the University of Westminster, London. Muscle Biopsies were collected by Dr David Howard, University College London.

5.2.2 Participant Description

A cohort of healthy male participants was recruited for this study. Inclusion criteria for participation was male, 18 – 40 years of age with no exposure to altitude or hypoxic environments exceeding 3000 m (or equivalent) within 3 months, with a body mass index (BMI) of 20 – 30 $kg.m^{-2}$. Exclusion criteria used was the presence of any cardiovascular, respiratory, metabolic or coagulation disorder, regular smoker, or currently on prescription medication. Participants were also excluded if they had a known allergy to lidocaine. Participants were asked to abstain from strenuous exercise for 48 hours prior to attending the laboratory, and abstain from caffeine for 24 hours prior to attending.

Screening of participants took place after a 12 hour fast, and involved measurement of resting metabolic rate by indirect calorimetry (Cortex, metalyser II) followed by body composition by air displacement plethysmography (BodPod, A/T2002A). Participants spent 40 minutes in a darkened room in a supine position during which expired gas fractions and volumes were measured. The initial 10 minutes of resting data was discarded, giving a 30 minute average for calculation of resting metabolic rate (Haugen et al., 2007), a complete protocol of which is given in Appendix Eleven. For

body composition measurement, participants wore minimal, tight-fitting clothing and a standard latex swim cap. After initial screening of 14 individuals, eight participants who met all criteria and were able to comply with study requirements were invited to participate in this study and are characterized in Table 5.1 and Table 5.2.

Table 5.1: Participant characteristics. N = 8.

Age (years)	Height (cm)	Weight (kg)	BMI ($kg.m^{-1}$)	FFM (%)	FFM (kg)	Resting SpO_2 (%)
29.8 (4.7)	180 (0.70)	78.99 (9.83)	24.22 (1.79)	85.1 (7.19)	66.85 (6.53)	97.9 (1.1)

Expressed as mean (standard deviation). Body mass index (BMI). Fat free mass (FFM).

Table 5.2: Participant indirect calorimetry data. N = 8.

VO_2 ($L.min^{-1}$)	VCO_2 ($L.min^{-1}$)	RER	EE ($kj.h^{-1}$)
0.29 (0.02)	0.24 (0.02)	0.81 (0.05)	346.66 (19.20)

Expressed as mean (standard deviation). Volume of oxygen consumed (VO_2) and Volume of carbon dioxide (VCO_2). Respiratory exchange ratio (RER). Energy Expenditure (EE).

5.2.3 Experimental Design

Normobaric hypoxia was delivered inside of a commercial hypoxic chamber (Figure 5.1). Two hypoxic generator pumps (Hypoxico, Summit II) utilizing activated carbon molecular sieves were used to reduce the percentage of oxygen from ambient 20.9 % towards a target of 12 % O_2. The average concentration across individuals was 12.5 (0.3) % O_2. Participants were exposed to this hypoxic stimulus for 10 hours. Physical activity was restricted to habitual activities within the chamber environment (standing and sitting).

Figure 5.1: Commercial hypoxic chamber utilized and hypoxic gas generators. Hypoxic gas generators seen to left of image.

All but one participant left the chamber environment once per 10 hour stay to use the bathroom. During this time hypoxia was maintained utilizing a modified reverse Douglas bag system for breathing of hypoxic air at a matching O_2 % to that of the chamber environment. A total of four bags were connected in circuit, each filled to ~ 1/4 capacity to maintain ambient pressure. This system was connected via a ~ 1 m flexible hose to a non-rebreathing, nose-mouth covering facemask (Figure 5.3).

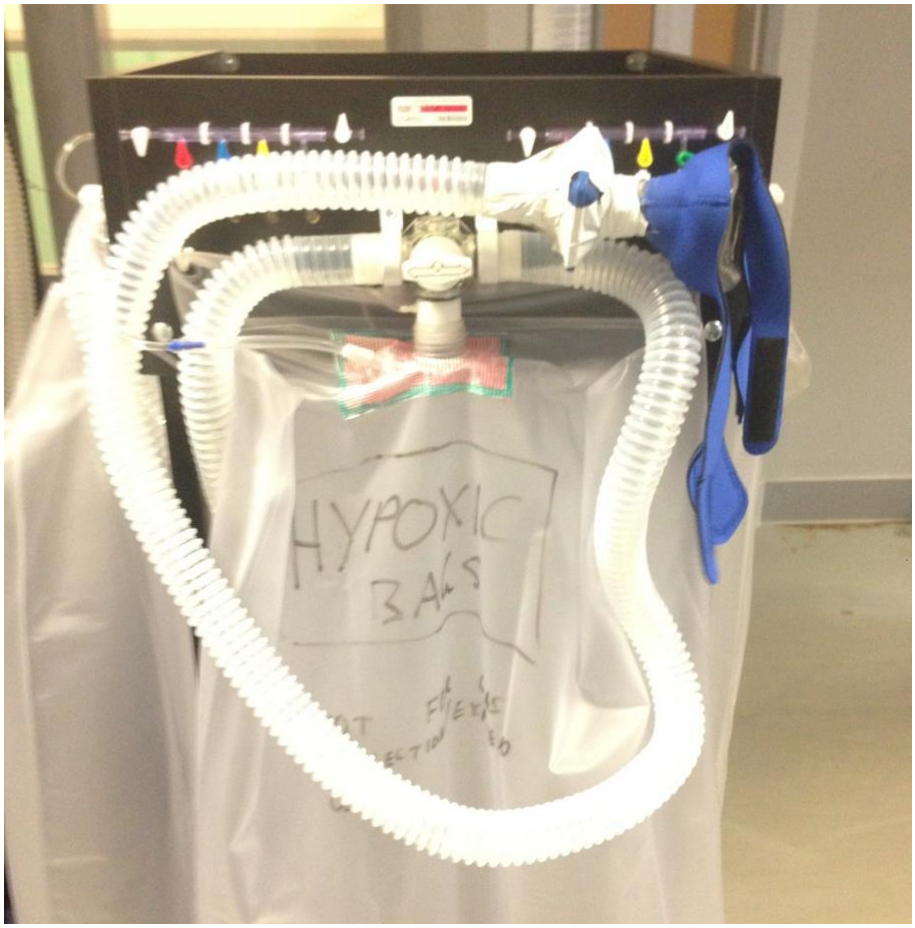

Figure 5.2: Modified Douglas bag system. Four 100 L bags are interconnected and partially filled to provide a large reservoir of hypoxic gas at atmospheric pressure. A non-rebreathing, nose-and-mouth mask is attached to allow inspiration of hypoxic gas and expiration into atmosphere.

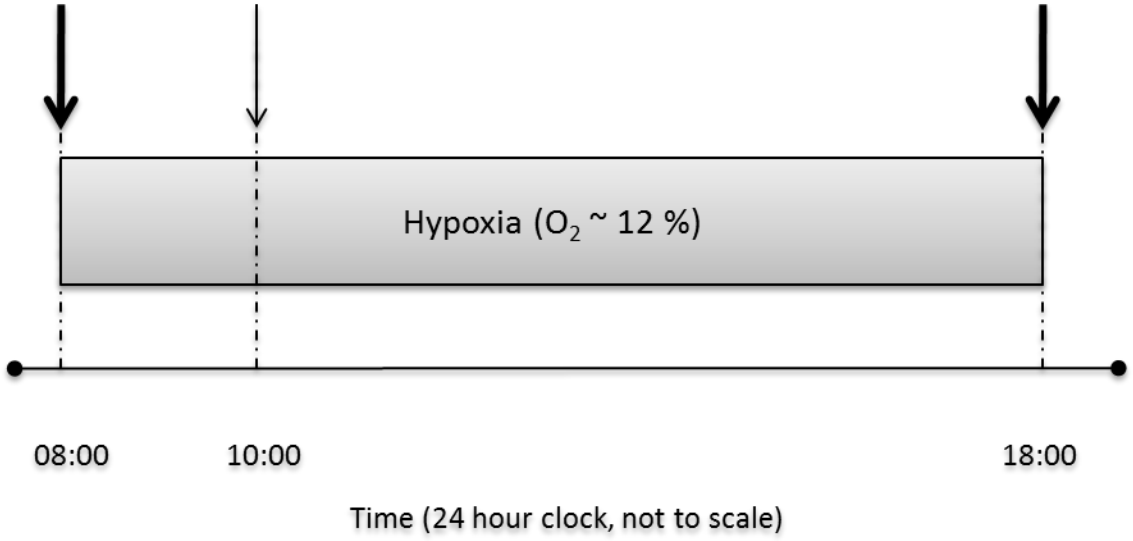

Figure 5.3: Schematic representation of experimental protocol.. Thick arrows indicate timing of blood sample and muscle biopsy, thin arrow blood sample only. Time (24 hour clock, not to scale) indicated in the horizontal axis.

Measurement of SpO_2 and HR was carried out using a pulse oxymeter (Pulsox-3iA, Konica) attached to the left index finger. SpO_2 and HR were recorded every 30 minutes for the first 120 minutes, then every 60 minutes for the remainder of the hypoxic exposure. The participant's response to mLLAMS was recorded at matching time points (Figure 5.3). In an identical manner as described in Chapter Three, a conchotome biopsy was taken from all participants just prior to (0 hours) and within 10 minutes of exiting the hypoxic environment (10 hours). Biopsies were taken by Professor David Howard (University College London). Biopsies were rapidly rinsed in ice-cold saline, separated from any visible fat and immediately frozen in liquid nitrogen for future analysis. Venous blood samples were taken immediately prior to (0 hours), 2 hours into (2 hours), and within 10 minutes of exiting the hypoxic environment (10 hours). Whole blood was drawn from a convenient antecubital vein into 10 mL lithium heparin tubes and spun (10,000 rpm, 10 minutes, 4 °C) to separate plasma from cellular material. Collected plasma was stored at -80 °C for future analysis.

Water was provided *ad libitum* throughout the exposure. Participants were fed once during their stay in the hypoxic environment, immediately post the 2 hour blood sample. Participants' meal contained a macronutrient distribution of ~ 55 % carbohydrate, ~ 30 % fat and ~ 15 % protein, with an energy content of 1 / 3rd of their predicted daily energy requirement, as established from the following equation. A physical activity level factor (PAL) of 1.4 was selected, as participants would remain sedentary during the trial (Bonetto et al., 2011).

$$Daily\ Energy\ requirement\ (kj) = \frac{[(RMR\ (kj.hour) \times 24\ hours) \times \mathrm{PAL}]}{3}$$

RMR, Resting metabolic rate; PAL, physical activity level factor.

5.2.4 Protein Quantification

Biopsies from 0 and 10 hours (~ 100 mg) were powered by mortar and pestle in liquid nitrogen before being resuspended in 125 µL lysis buffer (10 mmol Tris-HCl, 150 mmol NaCl, 2 mmol EDTA, 2 % Triton X-100, protease inhibitor [Sigma, P8340] and phosphatase inhibitor [Sigma, P6624], Appendix One), and shaken for 30 minutes at 4 °C. Samples were then spun (6000 rpm, 6 minutes, 4 °C) to fractionate total protein supernatant from insoluble debris.

An aliquot of lysed muscle tissue extract was further diluted 1:10 in ice-cooled lysis buffer (Appendix One), before 5 µL of each sample and standards were loaded into flat-bottomed clear 96-well plates in triplicate. Total protein content was measured in the method of Lowry (BioRad, 500-0116; Appendix Five). Bovine serum albumin (BSA) was used as a protein standard. Coefficient of variability of standards and samples was 0.13 and 0.078, respectively. Aliquots of lysed supernatant were diluted to 2 $mg.mL^{-1}$ into Laemmli's loading buffer (Appendix One). Subsequent samples were frozen and stored at -80 °C for later analysis by Western blot.

5.2.5 Western Blot

Western blots were run as described in Chapter Three. Briefly, 40 µg of total protein was run per lane on precast 10 % polyacrylamide gels (Invitrogen, NP0301), and transferred for 3 hours on ice to nitrocellulose membrane (GE, RPD30320). Blocking and primary antibody conditions are given in Table 5.3. All primary antibodies were used 1:1000. Secondary antibody was anti-rabbit, used 1:10,000. Membranes were developed by hand onto film (Appendix Seven) before being digitized and analysed with ImageJ open source software (ImageJ, version 1.45s). Blots were normalized to total protein stained for by ponceau rouge, using the method of Romero-Calvo and colleagues (2010).

Table 5.3: Western blot characteristics by target protein. Blocking, primary and secondary conditions are diluted into tris-buffered saline with tween (TBS-T).

Target	Supplier (code)	Blocking	Primary antibody	secondary antibody
Myostatin	BIOSS antibodies (2227G)	5 % BSA, 1 hour, RT	0.5 % BSA o/n, 4 °C	0.5 % BSA, 1 hour, RT
Ubiquitin	Cell Signalling (3933)	5 % BSA, 1 hour, RT	0.5 % BSA o/n, 4 °C	0.5 % BSA, 1 hour, RT
pAkt (Ser473)	Cell Signalling (9271)	5 % BSA, O/N, RT	0.5 % BSA, 1 hour, 4 °C	0.5 % BSA, 1 hour, RT
TNFα	Sigma (WH0007124M2)	5 % BSA, 1 hour, RT	5 % BSA o/n, 4 °C	0.5 % BSA, 1 hour, RT

Bovine serum albumin (BSA). Room temperature (RT). Overnight (o/n).

5.2.6 ELISA

ELISA for plasma myostatin was performed according to manufacturer's instructions (DGDF80, R&D Systems). Aliquoted plasma samples were defrosted from – 80 °C to room temperature before 100 µL plasma was activated for the removal of myostatin binding proteins (60 µL HCl, 6 M, 10 minutes at room temperature), then neutralized (40 µL NaOH + 1.2 mol HEPES), and finally diluted into 200 µL calibrator diluent (R&D, 895525) to give a prepared sample at a 1:4 dilution. Recombinant myostatin was used as a standard (range 31.3 – 2,000 $pg.mL^{-1}$; R&D, 894410), and calibrator diluent used as a blank control. Plates were incubated at 37 °C with gentle agitation for 2 hours, washed 4 times (R&D, 895003) before myostatin conjugate (R&D, 894409) was added (200 µL) and plates incubates for 2 hours at room temperature. Wells were washed again (4 times) before 200 µL substrate solution was added and plates incubated at room temperature, protected from light. Colorimetric reaction was stopped with 50 µL 2 N sulphuric acid. Samples were read spectrophotometrically at 450 nm and blanked to 570 nm using a microplate reader (VersaMax, Molecular Devices, USA). Coefficient of variability of standards and samples were 0.09 and 0.05, respectively.

5.2.7 Statistical Analysis

Results are presented in figures as individual data points, as outlined by Drummond and Vowler (2012) and written in text as 'mean (standard deviation) units'. Repeated measures analysis of variance (ANOVA), Friedman's or single-sample t-tests were used as appropriate, with *post hoc* analysis performed where needed in the method of Bonferroni, using SPSS (IBM, version 20.0). Where a deviation from sphericity of groups was noted, this was corrected for in the method of Greenhouse and Geisser (1959). Linear correlations were determined in the method of Pearson. Significance was set at $p < 0.05$ throughout.

5.3 Results

5.3.1 Effect of Hypoxia on Homeostatic Measures

The effect of hypoxia on SpO_2 was examined by repeated measures (0, 30, 60, 90, 120, 300, 360, 420, 480, 540, 600, 610 minutes) ANOVA. A significant effect of time on SpO_2 ($p < 0.001$) was noted. *Post hoc* analysis shows SpO_2 is significantly reduced at every time point except at 240 ($p = 0.052$) and 610 minutes ($p = 1.0$; Figure 5.4). Mean SpO_2 immediately prior to hypoxic exposure was 97.9 % (1.1 %), decreasing to mean of 84.4 % (1.2 %) during hypoxia and returning rapidly to baseline values following hypoxic exposure.

One participant recorded a notably higher value at time point 240 minutes of 96 % SpO_2 (where mean results is 87 (5.0) %) giving $p = 0.052$ at this time point. This data point was not removed as it did not meet this dissertations definition of an outlier (> 3 SD from the sample mean) (Hopkins et al., 2011).

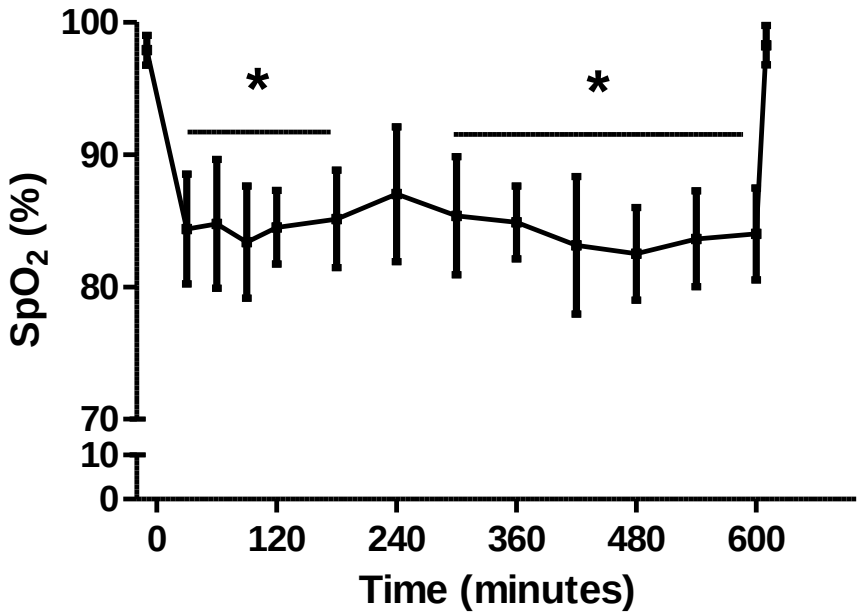

Figure 5.4: Effect of hypoxia on fingertip capillary haemoglobin oxygen saturation. Fingertip capillary haemoglobin oxygen saturation (%) as a function of time (minutes). Hypoxic exposure (12.5 % O_2) from time point 0 to 600 minutes. ∗ indicate significant difference from baseline with bonferroni correction (-10 minutes, $p < 0.05$). N = 8 males. Error bars indicate SD.

The effect of time in hypoxia on HR was examined by repeated measures ANOVA (0, 30, 60, 90, 120, 300, 360, 420, 480, 540, 600, 610 minutes). A significant effect of time on HR was noted ($p < 0.001$). *Post hoc* analysis reveals heart rate increased from baseline (- 10 minutes) at the 180 ($p = 0.003$) and 240 minute ($p = 0.012$) time points (Figure 5.5A). When heart rate results are expressed as a percentage change from baseline, similar effects are seen, with a significant effect of time on HR ($p < 0.001$), and *post hoc* analysis revealing hypoxia increases HR at the 180 minute time point ($p = 0.002$, Figure 5.5B).

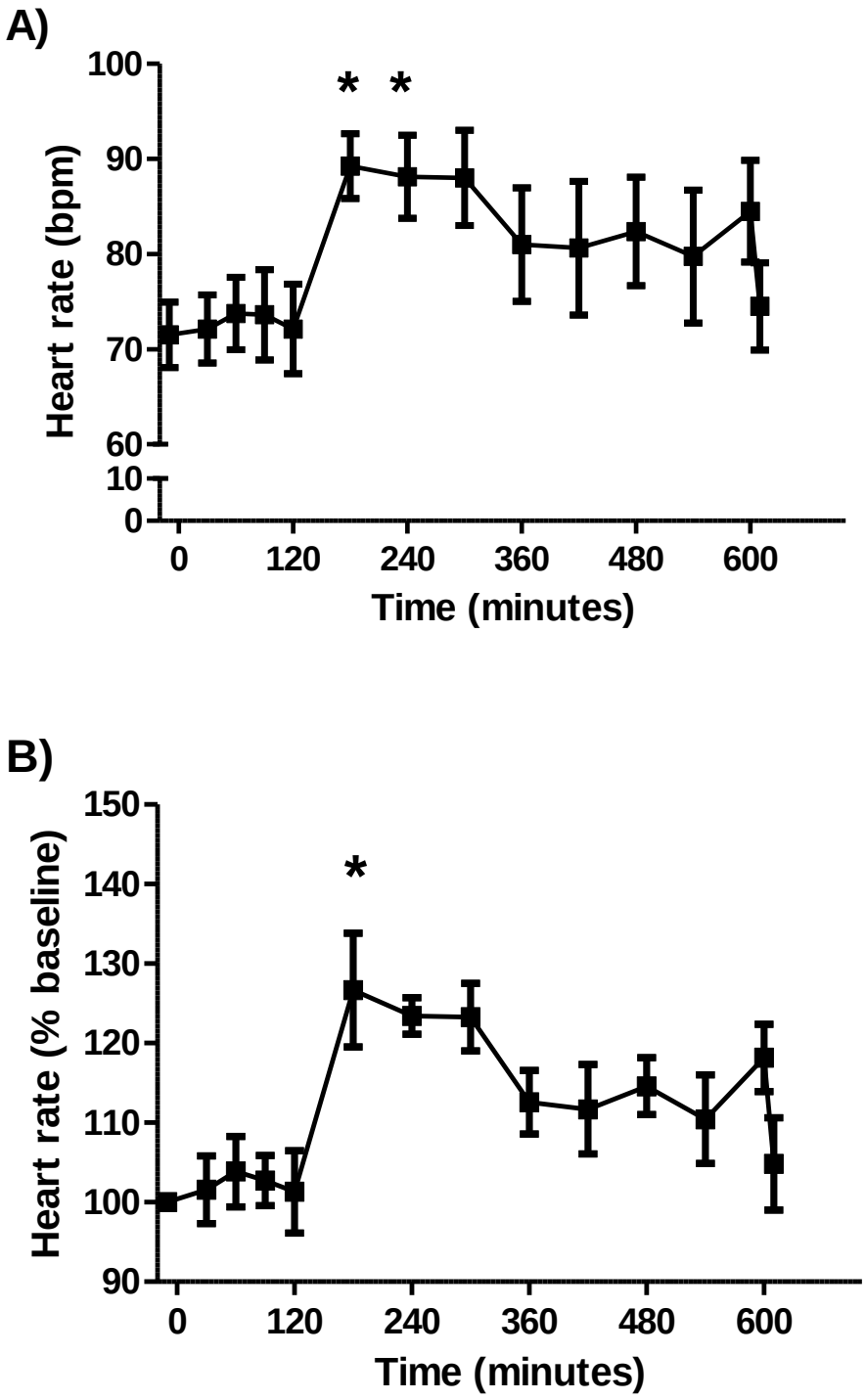

Figure 5.5: Effect of hypoxia on resting heart rate. A) Absolute HR (bpm) **B)** Relative to baseline (%). Hypoxic exposure (12.5 % O_2) from time point 0 to 600 minutes. * indicates significant difference from baseline at indicated time point ($p < 0.05$). Error bars represent SD. N = 8 males.

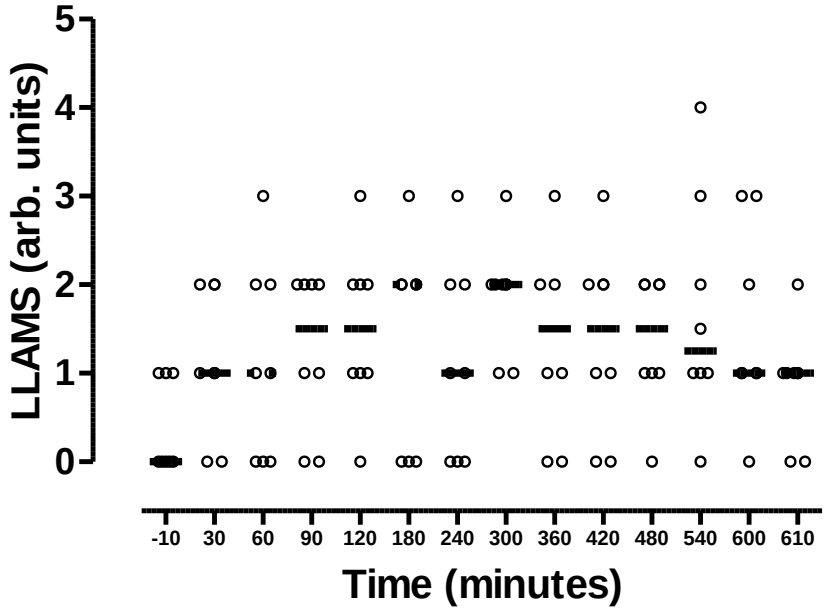

Figure 5.6: Effect of hypoxia on acute mountain sickness symptoms. Median of mLLAMS score (arb. units, thick line) as a function of time (minutes). Open circles indicates individuals data points, horizontal lanes indicate time point median. Hypoxic exposure (12.5 % O_2) from time point 0 to 600 minutes. N = 8 males.

Friedman's test suggests there is an effect of time in hypoxia on the occurrence of acute mountain symptoms, as measured by the mLLAMS questionnaire (p = 0.045, Figure 5.6). Significant variability of responses is noted, with one individual indicating a score of 0 arb. unit at every hypoxic time point except one, which scored 1 arb. unit (Table 5.4).

Table 5.4: Lake Louse acute mountain sickness questionnaire score (arb. units) by participants (A – H) during (time = 30 minutes – 600 minutes) hypoxic exposure (12.5 % O_2).

Participant	A	B	C	D	E	F	G	H
median	2	2	2.5	1	0	2	1	1
maximum	4	3	3	2	1	2	2	2
minimum	1	0	1	1	0	0	0	0

5.3.2 Effect of Hypoxia on Plasma Myostatin

The effect of 10 hours hypoxia on plasma myostatin was examined by repeated measures (0, 2, 10 hours) ANOVA. A significant effect of time was noted on plasma myostatin ($p < 0.001$). Subsequent *post hoc* analysis shows plasma myostatin concentration is maintained from 0 hours to 2 hours, with a concentration of 2.96 (1.12) $ng.mL^{-1}$ and 2.91 (1.14) $ng.mL^{-1}$, respectively ($p = 1.0$, $d = 0.04$), but decreased following 10 hours of hypoxic exposure to 2.45 (1.03) $ng.mL^{-1}$ ($p = 0.022$, $d = 0.48$; Figure 5.7A). One data point for plasma myostatin concentration is noticeably higher at every time point (0 hours = 5.42 $ng.mL^{-1}$, 2 hours = 5.56 $ng.mL^{-1}$, 10 hours 4.92 $ng.mL^{-1}$, (Figure 5.7A). These values are from the same individual and removal does not alter the results shown here.

The effect of hypoxia on plasma myostatin is maintained if data is expressed relative to individual baseline values (time = 0 hours). A repeated measure ANOVA suggests time in hypoxia alters plasma myostatin ($p = 0.004$). *Post hoc* analysis suggests no effect of hypoxia after 2 hours, with mean plasma myostatin 99.2 (9.9) % of baseline ($p = 1.0$, $d = 0.11$). Following 10 hours of hypoxia, plasma myostatin is decreased to 83.9 (12.6) % of control values ($p = 0.026$, $d = 1.28$, Figure 5.7B).

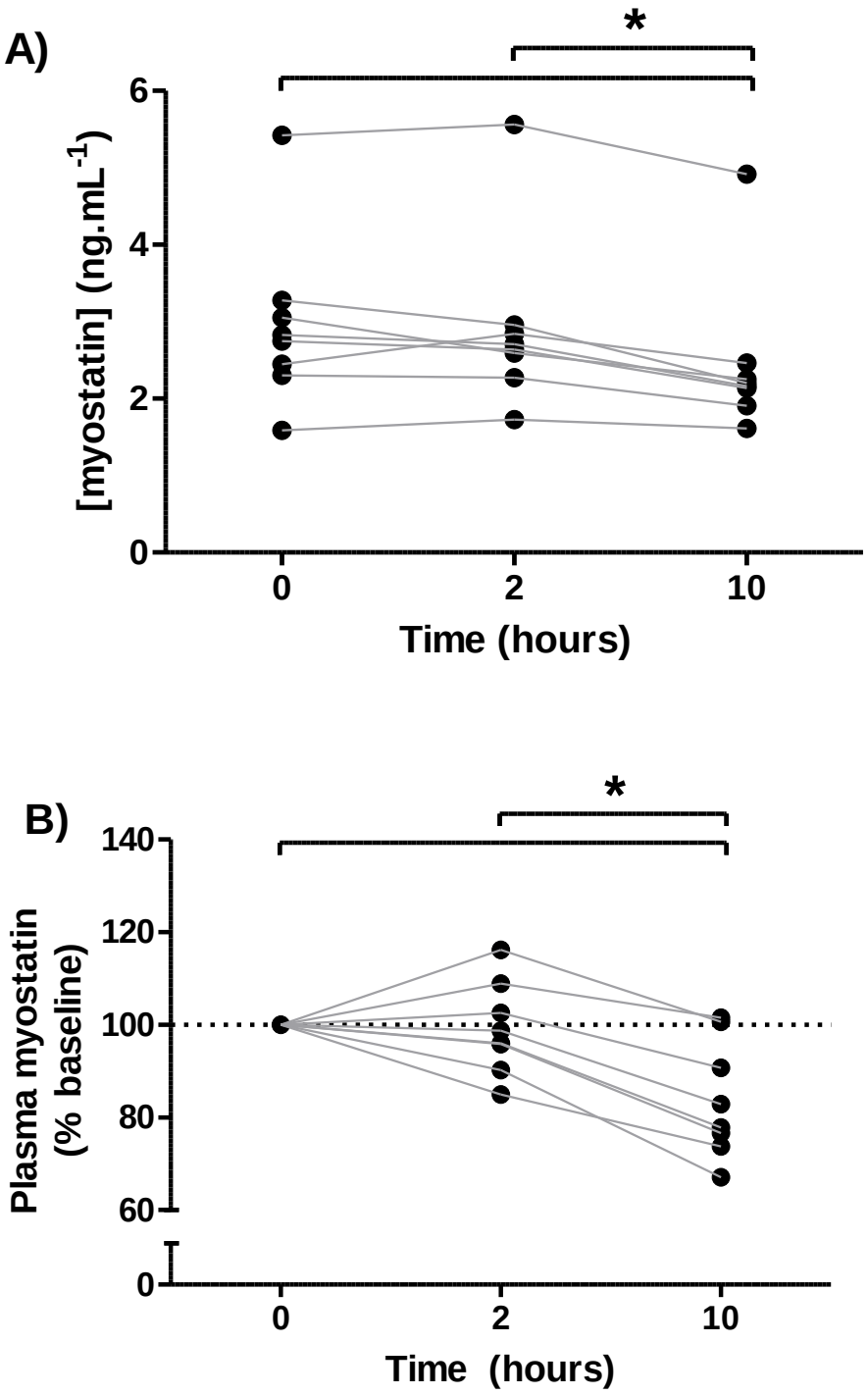

Figure 5.7: Effect of hypoxia on plasma myostatin concentration. ELISA for plasma myostatin from venous plasma prior (0 hours), during (2 hours), or following (10 hours) 12.5 % O_2 hypoxic stimulus. **A)** Absolute concentration ($pg.mL^{-1}$) **B)** Relative to individual 0 hour concentration (%).* indicates differences between times as marked. Closed circles indicate 0 hours, squares indicate 2 hours and triangles indicate 10 hours. Black line indicates mean. N = 8.

5.3.3 Correlations between Desaturation and the Plasma Myostatin Response

No correlation is seen between the desaturation of SpO_2 during 2 hours of hypoxia (ΔSpO_2) and the change in plasma myostatin from baseline to 2 hours (Δ plasma myostatin; Figure 5.8A; $r^2 = 0.038$), with Pearson's correlation suggesting no significant relationship between the two variables ($p = 0.65$). In a similar manner, no correlation is seen between the desaturation of SpO_2 during 10 hours of hypoxia (ΔSpO_2) and the change in plasma myostatin from baseline to 10 hours (Δ plasma myostatin; Figure 5.8B; $r^2 = 0.062$). Again, Pearson's correlation suggests no significant relationship between the two variables ($p = 0.55$).

As a proxy of DO_2, the correlation between HR × SpO_2 during hypoxia and Δ plasma myostatin was examined. A strong correlation is noted between HR × SpO_2 during hypoxia and Δ plasma myostatin ($r^2 = 0.677$), with Pearson's correlation suggesting a significant relationship between these two variables ($p = 0.0121$; Figure 5.8C).

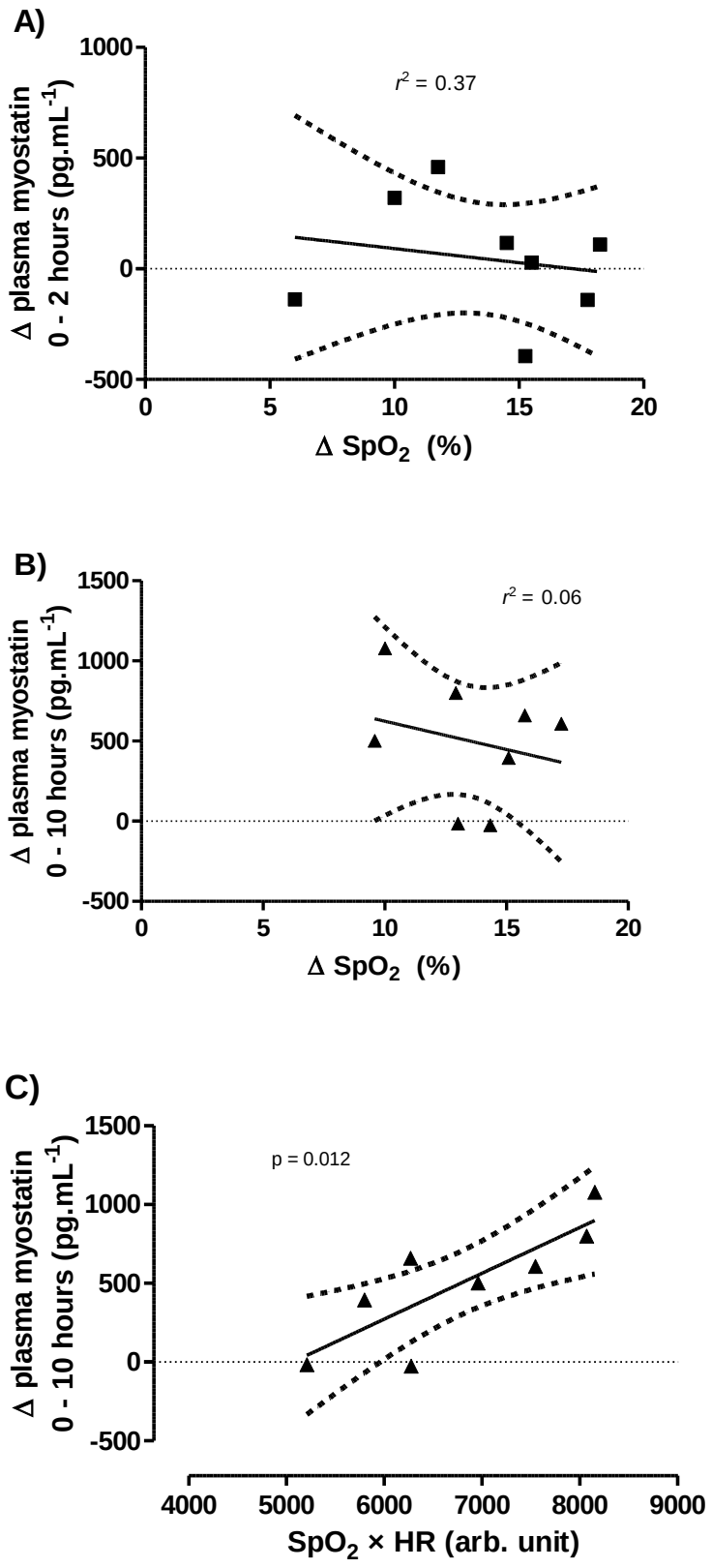

Figure 5.8: Correlation between Δ SpO_2 and Δ plasma myostatin during hypoxia. Myostatin (pg.mL^{-1}) from venous plasma pre and post hypoxia (Δ plasma myostatin) as a function of decrease in average SpO_2 during hypoxic stimulus relative to baseline (ΔSpO_2). **A)** Δ plasma myostatin over 2 hours as a function of ΔSpO_2 over 2 hours (squares) **B)** Δ plasma myostatin over 10 hours as a function of ΔSpO_2 over 10 hours (triangles). **C)** Δ plasma myostatin over 10 hours as a function of SpO_2 × HR. Hypoxic stimulus of 12.5 % O_2. N = 8 males.

5.3.4 Effect of Hypoxia on Muscle Myostatin Expression

Single sample t-test suggests a trend towards increased myostatin peptide expression following 10 hours of hypoxic exposure, with a mean result of 144 (71) % of baseline values and a large effect size seen ($p = 0.06$, $d = 0.62$; Figure 5.9A). No effect of hypoxic exposure is seen on myostatin LAP expression ($p = 0.34$, $d = 0.42$; Figure 5.9B). No effect of hypoxic exposure is seen on the ratio of LAP to myostatin peptide ($p = 0.40$, $d = 0.31$, Figure 5.9C).

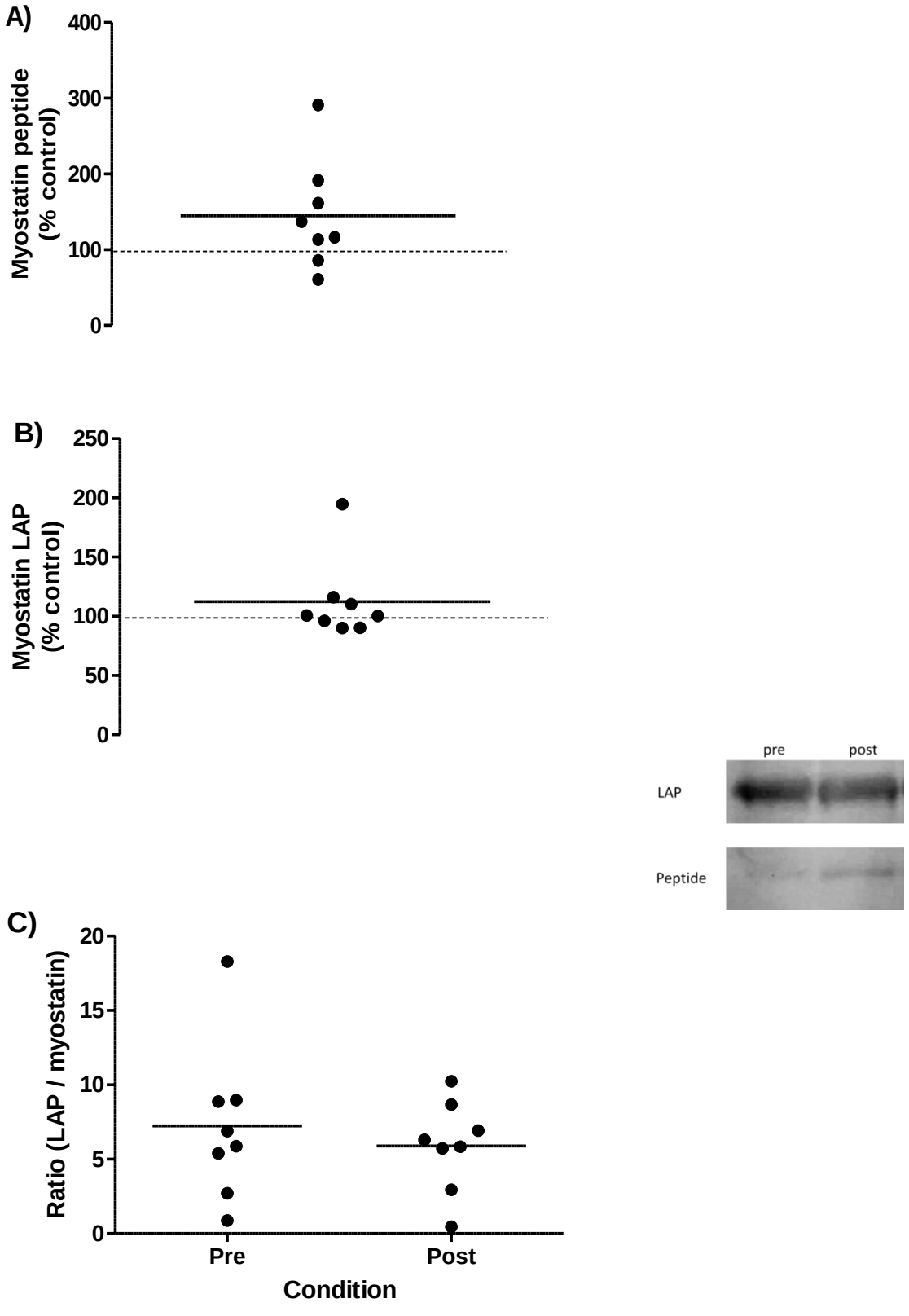

Figure 5.9: Effect of 10 hours of hypoxic exposure on myostatin expression. Western blot of myostatin (Bioss, 1288R **A)** peptide (26 kDa), **B)** latency associated propeptide (LAP; 45 kDa) and **C)** ratio of LAP to myostatin peptide from vastus lateralis muscle biopsy prior (baseline) and post 10 hours hypoxic (12 % O_2) exposure. Results are expressed as individual percentage change from baseline. N = 8 males. 40 µg total protein loaded per well. Blot density normalized to total protein per lane by ponceau rouge. **Insert)** Representative image.

Single sample t-test shows no change in free ubiquitin at 10 hours post hypoxic exposure, with a mean post hypoxia of 98.8 (33.8) % of baseline ($p = 0.93$, $d = 0.03$; Figure 5.10A). Single sample t-test show a trend towards a change in bound ubiquitin, with a mean post hypoxia of 147.4 (90.7) %, relative to baseline ($p = 0.09$, $d = 0.52$; Figure 5.10B). A single visually high value for bound ubiquitin can be seen (Figure 5.10B) which does not meet this works requirement as an outlier, therefore this value was not removed from analysis.

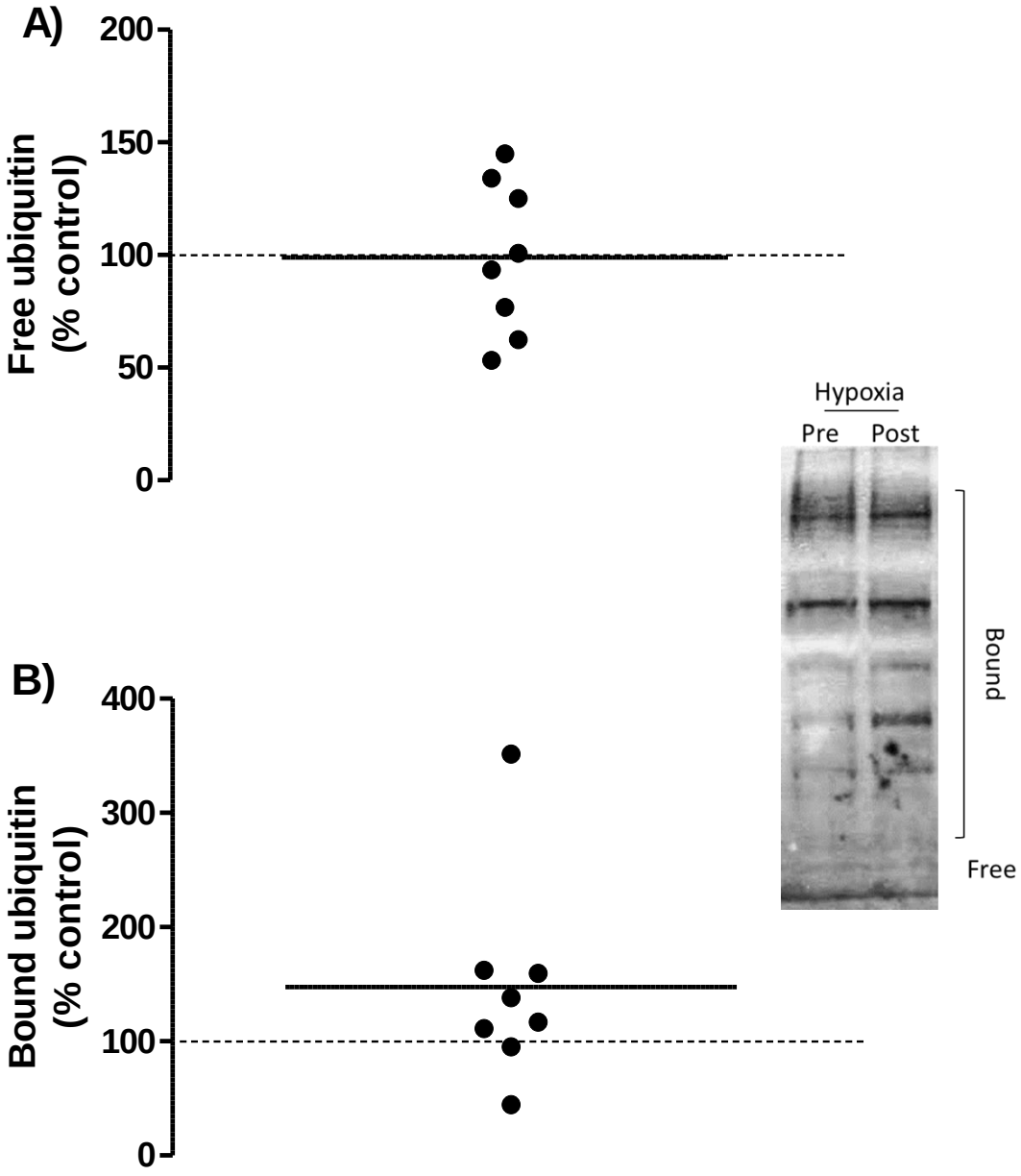

Figure 5.10: Effect of 10 hours hypoxic exposure on ubiquitin (bound and free) expression. Western blot of ubiquitin (Cell Signalling, 3933) **A)** Free peptide **(**6 kDa) **B)** protein bound (all other weights) from vastus lateralis muscle biopsy prior (baseline) and post 10 hours hypoxic (12.5 % O_2) exposure. Results are expressed as individual percentage change from baseline. N = 8 males per condition. 40 µg total protein loaded per well. Blot density normalized to total protein per lane by ponceau rouge. **Insert)** Representative image.

A single sample t-test shows no change in phosphorylation of Akt at serine 473 (pAkt [Ser473]). Following 10 hours hypoxia, mean pAkt (Ser473) is 95.2 (37.9) % of baseline values ($p = 0.73$, $d = 0.13$; Figure 5.11).

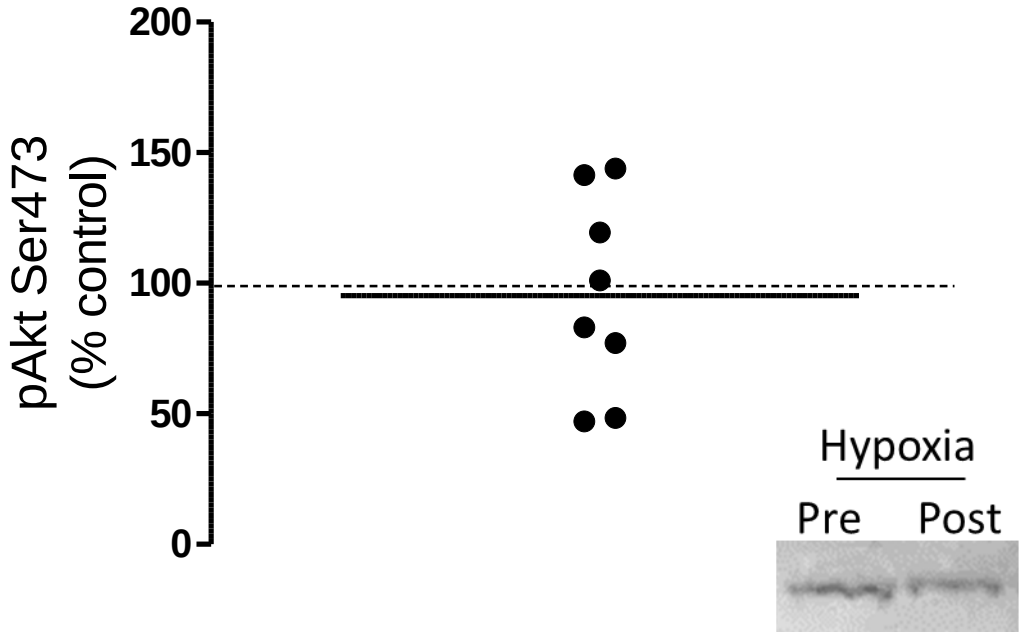

Figure 5.11: Effect of 10 hours hypoxia on phosphorylation of Akt (Ser473). Western blot of pAkt Ser473 (Cell Signalling, 9271) from vastus lateralis muscle biopsy prior (baseline) and post 10 hours hypoxic (12.5 % O_2) exposure. Results are expressed as individual percentage change from baseline. N = 8 males per condition. 40 µg total protein loaded per well. Blot density normalized to total protein per lane by ponceau rouge. **Insert)** Representative image.

Single sample t-test shows no change in TNFα expression following hypoxic exposure. TNFα expression was 121.2 (115) % of baseline expression, with a small effect size noted (p = 0.62, *d* = 0.18; Figure 5.12). A notably exceptional data point occurs (382 % increase above control) that meets this works definition of an outlier (> 3 SD from group mean). Removal of this data point reduces mean increase to 89.4 (50.6) % of baseline, does not change the statistical outcome (p = 0.43), but increases the effect size magnitude from small to moderate (*d* = 0.31).

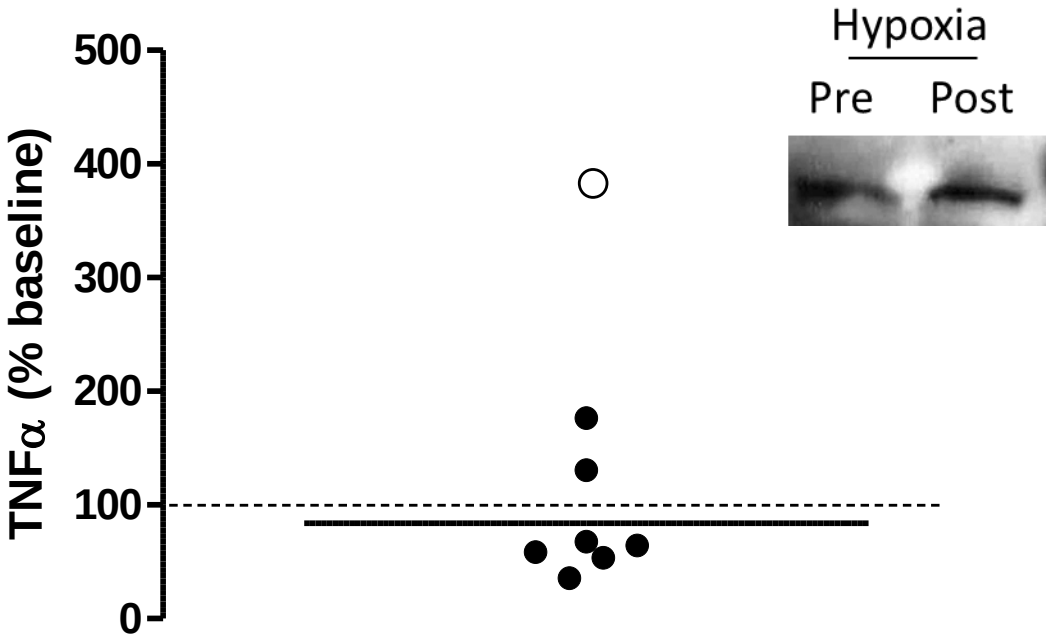

Figure 5.12: Effect of 10 hours of hypoxia on TNFα expression. Western blot of TNFα (Sigma, T83000) from vastus lateralis muscle biopsy prior (baseline) and post 10 hours hypoxic (12.5 % O_2) exposure. Results are expressed as individual percentage change from baseline. N = 8 males per condition. 40 µg total protein loaded per well. Blot density normalized to total protein per lane by ponceau rouge. Open circle, removed outlier data point. Horizontal line represents mean (excluding outlier). **Insert)** Representative image.

5.4 Discussion

The induction of peripheral tissue hypoxia, either by reductions in atmospheric pressure (such as during mountaineering sojourns) or pathological impairment of systemic oxygen supply (hypoxemia), results in atrophy of muscle. This Chapter aimed to examine the effect of 10 hours of hypoxia on plasma and muscle myostatin. The primary finding presented here is a trend towards an increase in muscle myostatin and significant decrease in plasma myostatin concentration in response to 10 hours hypoxia.

While caution should be applied in interpretation of results across Chapters, with differing methodologies and participant populations, broad comparisons can be made. Chapter Four and this Chapter used similar population groups (healthy young males). Further, hypoxia was delivered in the same mechanism, by a molecular sieve pump into an enclosed chamber space to reduce the ambient percentage of oxygen. The most striking finding when comparing between Chapters was the differing effect of time in hypoxia on muscle myostatin expression. Whereas Chapter Three showed a decrease in muscle myostatin peptide following 2 hours of hypoxia, the current study utilising a 10 hour exposure showed a trend towards an increase in muscle myostatin. Furthermore, where no effect of 2 hours hypoxia on plasma myostatin is seen in Chapter Four, the current work suggests that 10 hours of hypoxic exposure results in a decrease in plasma myostatin.

Alterations in plasma volume have been reported in the literature following acute hypoxic exposures of similar magnitudes and participants populations as reported here. Healthy male participants show a decrease in plasma volume of 10.3 % (3.39 L to 3.04 L) following passive assent to 4,350 m by helicopter (Poulsen et al., 1998), whilst an exposure of 1 hour in a similar population to 12.6 % O_2 results in a 2.7 % decrease in plasma volume (Miles et al., 1981). Thus, any effect of hypoxia on plasma volume would likely have been to decrease volume, artificially inflating

concentration measures of circulating hormones. In context of the decreases reported here of plasma myostatin (Figure 5.7) it would appear likely that this results may have been conservative, and correction for changes in plasma volume could increase the magnitude of this reduction.

The physiological meaning of the muscle myostatin finding is difficult to interpret, but of interest here. The concentration of a given endocrine peptide within a cell is a function of both the secretory loss and production gain of that peptide by the cell(s) sampled. It is proposed here that the initial decrease in cellular myostatin content following 2 hours of hypoxia (as seen in Chapter Three) represents the secretion of the basal myostatin peptide with a temporal delay before replacement peptide can be synthesized. The result of this Chapter following 10 hours of hypoxia then represents the increased production of myostatin peptide over the secretory loss.

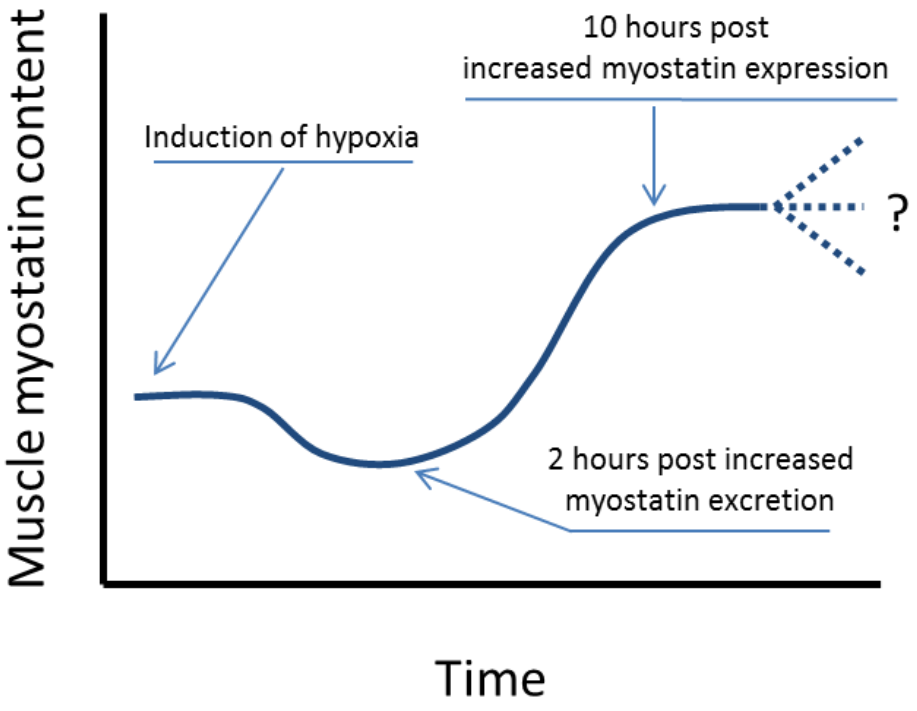

Figure 5.13: Proposed temporal muscle myostatin peptide response acute hypoxia. Myostatin peptide concentration as a function of time. Arrows indicate significant events; dotted line indicates unknown response of myostatin peptide.

The loss of muscle mass is seen both in response to chronic hypoxia (Bernard et al., 1998, Hoppeler et al., 1990) and starvation (Medina et al., 1995). No alteration is seen in plasma myostatin, nor muscle myostatin RNA expression, after 15 or 40 hours of fasting in otherwise healthy individuals (Larsen et al., 2006). Similarly, no significant alterations in muscle myostatin peptide expression are seen in response to 5 - 20 weeks underfeeding in sheep (Jeanplong et al., 2003). It is noted that starvation and hypoxia appear to regulate muscle size via different signalling pathways. Chronic severe hypoxia (8 % O_2 for 2 – 21 days) in mice activates several steps in the ubiquitin proteasomal pathway but not in a model of semi-starvation (de Theije et al., 2013). Importantly, in the work of de Theije and colleagues (2013) the semi-starvation model used was a pair-feed group to the hypoxic group. This pair feed-group, while demonstrating significant atrophy, showed lesser atrophy than the hypoxic group, suggesting a cumulative effect of both starvation and hypoxia. Therefore, the rational in the current study was to feed participants after 2 hours to dissect the effects of hypoxia in the absence of any effects of starvation. This feeding time point allowed the 0 hour biopsy and plasma sample, and the 2 hour plasma sample, to be taken in a fasted state to maintain consistency with Chapter Four.

Besides the work of the previous Chapter, there are no reports in the literature examining myostatin protein changes over the course of hours. For this reason, Chapter Three included a control visit, whereby participants visited on two separate occasions and repeated the experiment without the hypoxia stimulus. The control group results of Chapter Three suggest that myostatin expression within muscle, and concentration within plasma, does not vary in healthy male individuals, at least during the 6 hours of the study interval (08:00 to 14:00). Indeed, no change in muscle myostatin protein expression is seen in the control group of a human disuse study (Dirks et al., 2014), suggesting that myostatin peptide expression is relatively stable. These results, combined with the inherent difficulty involved in including a control group for the 10 hour exposure period, lead to the exclusion of a control session from the experimental design.

One limitation of this Chapter was the inability to take a muscle biopsy at the 2 hour time point, when the participant was within the chamber environment. This biopsy time point would have allowed us to directly compare results from this Chapter with the preceding Chapter's results. Further, a decision was made to not include a control group, whereby individuals would return to the lab with a biopsy pre- and post-10 hours following exposure to normal environmental conditions. This was justified in part due to the results of Chapter three, showing no change in muscle or plasma myostatin in the control group between baseline (time = -30 minutes) and the final biopsy (time = 320 minutes), a period of almost 6 hours. Furthermore, no alteration is seen in serum myostatin in healthy individuals over 4 or 8 weeks (Saremi et al., 2010), however no measure of muscle myostatin was performed. These results combined suggest resting myostatin is stable in the absence of external factors.

It is of interest to note that there was no difference in ubiquitin binding after 10 hours of hypoxic exposure. During preceding Chapters, an increase was noted following 2 hours of hypoxia in healthy individuals *in vivo*, and a trend towards an increase was seen at 2 hours *in vitro* that appears to disappear at longer timeframes (24 and 48 hours). Caron and colleagues (2009) noted a time dependent effect of hypoxia on atrophic pathway members, with elevated activity in the initial 24 hours. Rats exposed to chronic hypoxia for 3 weeks show depressed mTOR protein activity, as do chronically hypoxemic COPD patients, yet neither group shows elevation in ubiquitin binding (Favier et al., 2010). Thus, it would appear that the atrophic effects of hypoxia are time-dependent, with the acute actions occurring via activation of degradative mechanisms, while the longer-term remodelling is via a reduction in activation of pro-synthesis mechanisms.

No change in pAkt (Ser473) protein expression was seen following experimental hypoxia. This finding is in line with previous reports, Etheridge and colleagues (2011) noted no change in pAkt

(Ser473) or several other Akt-mTOR family members, including phosphorylation of mTOR and 4E-BP1 after 2 hours of hypoxia at a matching concentration to that used here. Similarly, rats exposed to 10 % O_2 for 6 hours show no change in muscle protein synthesis (Preedy et al., 1985). Finally, Caron and colleagues (2009) showed changes in pAkt (Ser473) at 24 hours, but not earlier time points. Thus, it would appear that acute hypoxic stimuli, extended to the 10 hours utilized here and possibly as far as 24 hours, does not impair markers of protein synthesis.

It is surprising to note a lack of immediate response to heart rate following hypoxia exposure, with elevations in heart rate only becoming apparent after 120 minutes exposure (Figure 5.5). It has long been recognised that acute hypoxic exposures tends to increases HR at rest, but substantial individual variation in response exists as to the magnitude of this response (Jennett, 1969). The results reported here recorded HR by SpO_2, whilst SpO_2 and ECG have been reported to have a high level of agreement with regards to HR (Dawson et al., 2013), these results may have been improved by directly measuring HR by ECG. Indeed, it is noteworthy that SpO_2 variability can be increased by variables such as skin colour, blood temperature and gender (Feiner et al., 2007, Ralston et al., 1991). Participants were fed immediately post the 120 minute blood sample, and 7 of 8 participants left the chamber (whilst remaining in a hypoxic environment with a portable reservoir of hypoxic gas), in the hour post feeding to use a bathroom. This feeding and activity stimulus, in the presence of hypoxia, may have resulted in the witnessed HR spike at the 200 minute mark.

In conclusion, this Chapter notes a significant decrease in plasma myostatin concentration and a trend towards increases in muscle myostatin peptide expression after 10 hours of hypoxic exposure. This decrease in plasma myostatin appears time-dependent, with no change seen following 2 hours of hypoxia. These acute changes in the temporal profile of myostatin are intriguing and may influence future experimental design. Finally, such alterations in myostatin

expression may in part explain the losses of muscle mass seen during longer hypoxic exposures, such as those seen in hypoxemic COPD patients and healthy individuals during mountaineering expeditions.

Chapter Six – The Effect of Two Different Oxygen Concentrations on Plasma Myostatin

6.1 Introduction

It is well recognised that a chronic reduction in the supply of oxygen to peripheral muscle mass results in muscular atrophy, as has been discussed in previous Chapters. This atrophy can result from either a pathological reduction of oxygen uptake, as seen during COPD (Bernard et al., 1998) or during exposure to high altitude, where hypobaric hypoxia occurs (Hoppeler et al., 1990, Rose et al., 1988). While this atrophy occurs across hypoxic conditions by varying causes, the mechanism inducing muscle atrophy is uncertain.

Myostatin is a significant and powerful negative regulator of muscle mass (Lee, 2004), and so forms an excellent candidate for the causative inductor of muscle atrophy during hypoxic exposure. Indeed, myostatin peptide is elevated in the muscle of chronically hypoxemic (greater than 6 months post diagnosis) COPD patients relative to healthy control individuals (Hayot et al., 2011). A similar result is also shown in rats exposed to 5 weeks of severe hypoxia (10 % O_2), with significant loss of muscle mass and elevated myostatin peptide expression (Hayot et al., 2011).

The effect of hypoxia on a biological system is dependent on the magnitude of hypoxic stimulus delivered. With regards to hypoxia, magnitude is formed by a combination of duration in hypoxia and the ambient PO_2, as either reduced due to a reduction of ambient pressure or concertation of O_2. The effect of hypobaric hypoxia is known to have an altitude-dependent effect on aerobic metabolism in the healthy human. Above 1500 m (~17.5 % O_2 equivalency) a non-linear decrease in maximal aerobic metabolism is noted, and the rate of decrease is greater as altitude increases (Brooks et al., 2005). Acute exposure (The exact length of time not given by authors, but an acclimatisation trial is repeated after 4 days, suggesting 'acute' in this context is less than 4 days) in unacclimatized individuals results in altitude-dependent ventilatory equivalent (V_E / VO_2) changes, with no effect seen up to 3,000 m, but an exponential increase in ventilatory equivalent between

3,000 and 6,000 m (Lenfant and Sullivan, 1971). If the effect of hypoxia on cardiovascular and respiratory factors is altitude-dependent, then it would be logical to hypothesize that the hypoxic-induced changes to myostatin and other endocrine mechanisms would also be affected in a similar manner.

No rigorous attempt has been made to examine the effect of the magnitude of hypoxia (either normobaric or hypobaric) in healthy individuals on body composition changes. Hoppeler and colleagues (1990) showed a 10 % loss in thigh muscle cross sectional area following a climb to >5,000 m. A simulated ascent of Everest (5,000 to 8,800 m over 40 days) within a hypobaric chamber induces significant muscular atrophy (Rose et al., 1988). Conversely, high performance swimmers at a high altitude training camp (3,000 m, 3 weeks) do not show losses in muscle mass (Chia et al., 2013). Furthermore, healthy individuals trekking to 3,255 m also show no loss of lean body mass (Schena et al., 1992). While one report (Cruz-Jentoft et al., 2010) does note loss of muscle mass during a summit attempt of Denali / Mt McKinley which reached 4,300 m, it should be noted that the authors note the climb to be difficult with weather and food shortages preventing a successful summit, potentially confounding results.

Thus, it would seem that a threshold may occur for hypoxic-induced atrophy in the healthy individual during hypobaric hypoxic exposure. If exposure to differing altitudes differentially alters muscle mass, it is reasonable to hypothesize that the response of mediators of atrophy, such as myostatin, would be affected in a PO_2 dependent-manner *in vivo*.

6.1.1 Chronic Adaptation to Altitude

The most chronic example of adaptation to a hypoxic environment in *Homo sapiens* is in Tibetan and Sherpa individuals, who are thought to have lived at altitudes of 3,000 - 4,500 m for 7,000 to 20,000 years (Su et al., 2000, Zhao et al., 2009). These individuals show several genetic variations that are thought have arisen through positive selection pressures, such as *EPAS1* (coding for HIF2) (Yi et al., 2010), *EGLN1* and *PPARA* (coding for hypoxia-inducible factor prolyl hydroxylase 2 [HIF-PH2] and peroxisome proliferator-activated receptor alpha [PPARα], respectively (Simonson et al., 2010). Sherpa maintain excellent metabolic function at high altitude relative to lowlander populations (Beall, 2007), and do not demonstrate decreased muscle mass relative to lowlander populations (Sloan and Masali, 1978). Further, when challenged with an acute extreme hypoxia stimulus (hypobaric hypoxia ~ 10,000 m), high altitude Peruvian natives show an increased time to loss of consciousness than unacclimatized lowlanders (Velasquez, 1959). Thus, if the acute response of atrophy inducing mediators, such as myostatin, is dependent on the magnitude of the hypoxic stimuli received, then it could be hypothesized that such adapted individuals would show an altered response to acute hypoxic-induced alterations in atrophy mediators.

6.1.2 Aims and Hypotheses

The aim of this Chapter was therefore to examine the effect of O_2 concentration on plasma myostatin concentration. Further, due to the unexpected availability of a participant of Sherpa origin, a second *post hoc* aim and hypothesis was added (herein aim and hypothesis 2). Specifically, the aims of this Chapter were to;

1) determine if the effect of hypoxia on myostatin is O_2 concentration-dependent *in vivo* in healthy lowlander humans *and*
2) examine any difference in the response of myostatin between a Sherpa case study participant to that of lowlander controls.

The hypothesis for this Chapter was that myostatin would be increased in an O_2 concentration--dependent manner. Specifically, it is hypothesized that;

1) the effect of hypoxia on plasma myostatin concentration *in vivo* will be O_2 concentration-dependent, with increased myostatin concentration seen following 10 %, but not 12 % O_2 for 2 hours *and*
2) the effect of hypoxia on plasma myostatin will be reduced in an individual of a Sherpa origin.

6.2 Methods

6.2.1 Ethical Approval

Ethical approval for the work described in this Chapter was provided by the University of Westminster Research Ethics Sub-committee (12-13-46) and the University of California, San Diego Institutional Review Board (131521). Written informed consent was obtained from all participants prior to participation. The work described in this Chapter took place in the physiology laboratory of Professor Peter Wagner, University of California, San Diego.

6.2.2 Participant Descriptors

A cohort of healthy male participants was recruited for this study. Inclusion criteria for participation was male, 18 – 40 years of age with no exposure to altitude or hypoxic environments exceeding 3,000 m (or equivalent) within 3 months, with a BMI of 20 – 30 $kg.m^{-2}$. Further exclusion criteria included known history of cardiovascular, respiratory, metabolic or coagulation disorder, regular smoker, or currently on prescription medication. To maintain continuity with previous experimental Chapters, participants were also excluded if they had a known allergy to lidocaine. Participants were asked to abstain from strenuous exercise for 24 hours prior to attending the laboratory, and abstain from caffeine on the day of the experimental protocol. Screening of participants involved a questions regarding health and physical performance and brief examination administrated by a registered medical doctor of the State of California. A total of 11 participants were recruited for this study, 9 of whom were able to comply with the study requirements were screened and participated in this study (Table 6.1).

6.2.3 Case Study Descriptors

Of the 9 participants, one is herein further described individually. Whilst meeting all criteria for participation, this participant was noteworthy due to his ethnic heritage. This case study was a Sherpa individual, born in Nepal, and lived at an altitude of ~ 3,000 m, until migrating to a sea-level location on the West Coast of the United States of America 8 years prior to participation in this study. During this time, he has not ascended to any altitudes > 1,000 m nor has he returned to Nepal. This case study was shorter than the participant group, with a height 2 SD below the participant mean, and also had a notably low resting blood pressure of 99 / 58 mmHg (5.1 and 2.4 SD below participant group), but did not demonstrate any symptoms of hypotension. All other baseline characteristics were non-remarkable. These characteristics are summarized in Table 6.1.

Table 6.1: Participant characteristics (N = 9).

	Lowlander Characteristics (n = 8)	Sherpa case study (n = 1)
Age	27.5 (8.1)	26
height (cm)	174.6 (7.7)	160.0
Weight (kg)	76.9 (12.9)	70.3
BMI ($kg.m^{-2}$)	22.3 (8.7)	27.5
BP S / D (mmHg)	130.8 / 75.1 (6.2 / 7.2)	99 / 58
Resting SpO_2	98.8 (1.0)	98.5

Expressed as mean (SD). Body mass index (BMI). Blood pressure (BP) expressed as systole (S) over diastole (D).

6.2.4 Experimental Design

Whole body normobaric hypoxia was delivered via a non-rebreathing facemask connected to a pressurised bottle supply of 12.3 (0.1) % or 10.7 (0.2) % O_2, which was generated from atmospheric air diluted with 100 % N_2. A 100 L latex balloon was used to dissipate the bottled gas pressure before participants inhaled from this balloon via a standard mask set-up, to ensure inspired gas was at a normobaric pressure.

A venous blood sample was drawn from all participants immediately prior to, immediately post- and 2 hours-post exposure to the hypoxic stimulus. A venous cannula was placed into an antecubital or forearm vein and kept patent by flow of 0.9 % sterile saline with 2,000 $U.L^{-1}$ heparin throughout the experiment. Whole blood was collected into lithium heparin tubes and spun (10,000 rpm, 10 minutes, 4 °C) to separate plasma. Collected plasma was aliquoted (100 µL) and stored at -80 °C for future analysis. SpO_2, HR and mLLAMS was recorded immediately prior to, every 15 minutes during and 10 minutes post hypoxic exposure. Participant's order of exposure was randomised and participants were blinded to hypoxic condition received. A schematic of this experimental design can be seen in Figure 6.1.

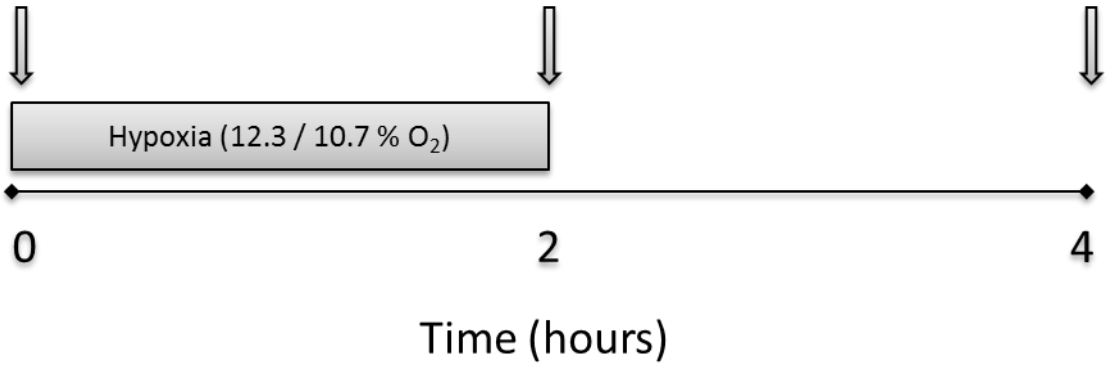

Figure 6.1: Schematic representation of experimental protocol. Arrows indicate timing of blood samples. Time (hours) indicated on the horizontal axis.

6.2.5 ELISA

ELISA for plasma myostatin was performed according to manufacturer's instructions (DGDF80, R&D Systems). Aliquoted plasma samples were defrosted from – 80 °C to room temperature before 100 µL plasma was activated for the removal of myostatin binding proteins (60 µL HCl, 6 M, 10 minutes at room temperature), then neutralized (40 µL NaOH + 1.2 mol HEPES), and finally diluted into 200 µL calibrator diluent (R&D, 895525) to give a prepared sample at a 1:4 dilution. Recombinant myostatin was used as a standard (range 31.3 – 2,000 $pg.mL^{-1}$; R&D, 894410), and calibrator diluent used as a blank control. Plates were incubated at 37 °C with gentle agitation for 2 hours, washed 4 times (R&D, 895003) before myostatin conjugate (R&D, 894409) was added (200 µL) and plates incubated for 2 hours at room temperature. Wells were washed again (4 times) before 200 µL substrate solution was added and plates incubated at room temperature, protected from light. Colorimetric reaction was stopped with 50 µL 2 N sulphuric acid. Coefficient of variability of standards and samples was 0.067 and 0.057, respectively.

6.2.6 Statistical Analysis

Results are presented in figures as individual data points, as outlined by Drummond and Vowler (2012) and written in text as 'mean (SD) units'. Two-way repeated measure analysis of variance (ANOVA) or paired-sample t-tests were used as appropriate, with Friedman's ANOVA used for non-parametric mLLAMS data. Where a deviation from sphericity was noted for repeated measures ANOVA, this was corrected for in the method of Greenhouse and Geisser. *Post hoc* analysis was performed where needed in the method of Bonferroni, using SPSS (IBM, version 20.0). Linear correlations were determined in the method of Pearson. Significance was set at $p < 0.05$ throughout.

6.3 Results

6.3.1 Effect of Hypoxia on Homeostatic Measures

The effect of hypoxic condition on SpO_2 was examined by two-way (condition [10.7, 12.3 % O_2] × time [0, 2, 4 hours]) repeated measures ANOVA. A significant condition × time interaction was noted with respect to the effect of hypoxia on SpO_2 ($p < 0.001$). Subsequent *post hoc* analysis suggested that hypoxia was reduced in both conditions from baseline (time = -10 minutes). Further, the 10.7 % O_2 condition showed a reduction in SpO_2 that was greater than the 12.3 % O_2 condition at every time point except 15 minutes, during hypoxic exposure (Figure 6.2A). Paired sample t-test on AUC SpO_2 noted no difference between these two variables ($p = 0.079$; Figure 6.2B). The response to 10.7 % O_2 is noted to appear more variable, with two sub-groups spread either side of the mean response (Figure 6.2B).

The Sherpa case study participant showed a variable response to desaturation, with a near-lack of desaturation response during the 12.3 % O_2 condition (mean SpO_2 of 94.3 %). Conversely, during the 10.7 % O_2 condition, where the lowlander participant population showed variation in response (Figure 6.2B, black triangles), this participants results were within the larger magnitude response group, with a mean SpO_2 desaturation of 62.6 % (open triangles, Figure 6.2A and B).

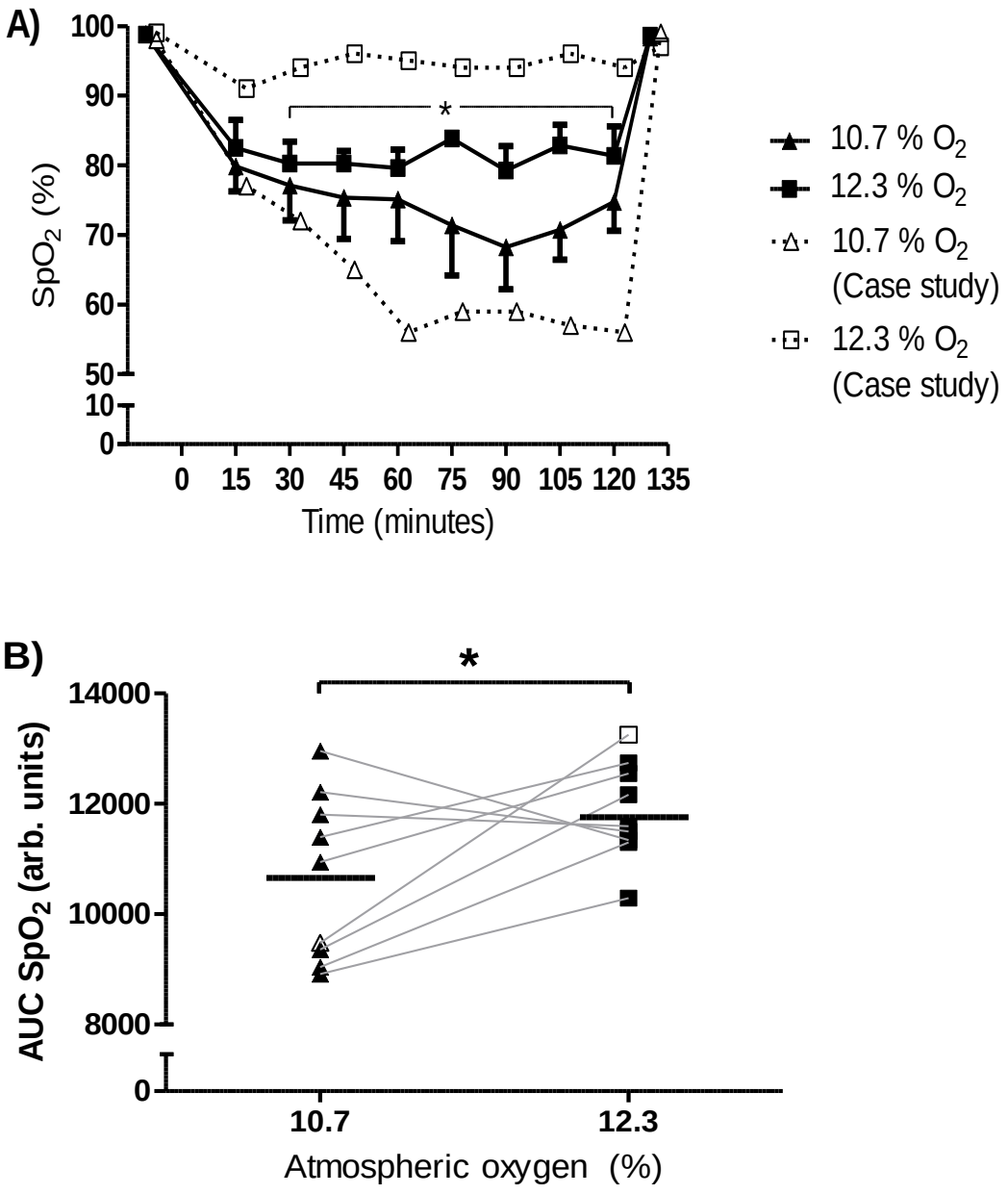

Figure 6.2: Comparison of effect of two different O_2 concentrations on SpO_2 in lowlanders and a case study individual. A) SpO_2 (%) as a function of time (minutes). Hypoxic exposure of either 10.7 % O_2 (tirangle) or 12.3 % O_2 (square) from time point 0 to 120 minutes. N = 8. Error bars represent SE. Case study (n = 1) shown by open symbols and dashed lines, with data points offset by 3 minutes for clarity. * indicates difference between lowlander group at given timepont. **B)** Area under curve of SpO_2 in 10.7 % O_2 (triagle) and 12.3 % O_2 (square) with paired samples linkd by gray line. Mean indicated by black horizontal lines. N = 8. Case study (n = 1) indicatd by open symbols. * indicates difference between lowlander group.

Friedman's test suggests a trend towards altered mLLAMS occurred in the lowlander population (p = 0.053, Figure 6.3). Noticeably more variability is noted in the 10.7 % O_2 condition, with occurrence of symptoms first occurring at the 30 minute mark (median = 0.75), while the 12.3 % O_2 shows occurrence of symptoms first occurring by the 60 minute mark (median = 0). Of interest, the case study individual showed no response of mLLAMS, indicating 0 throughout each hypoxic condition (data not shown).

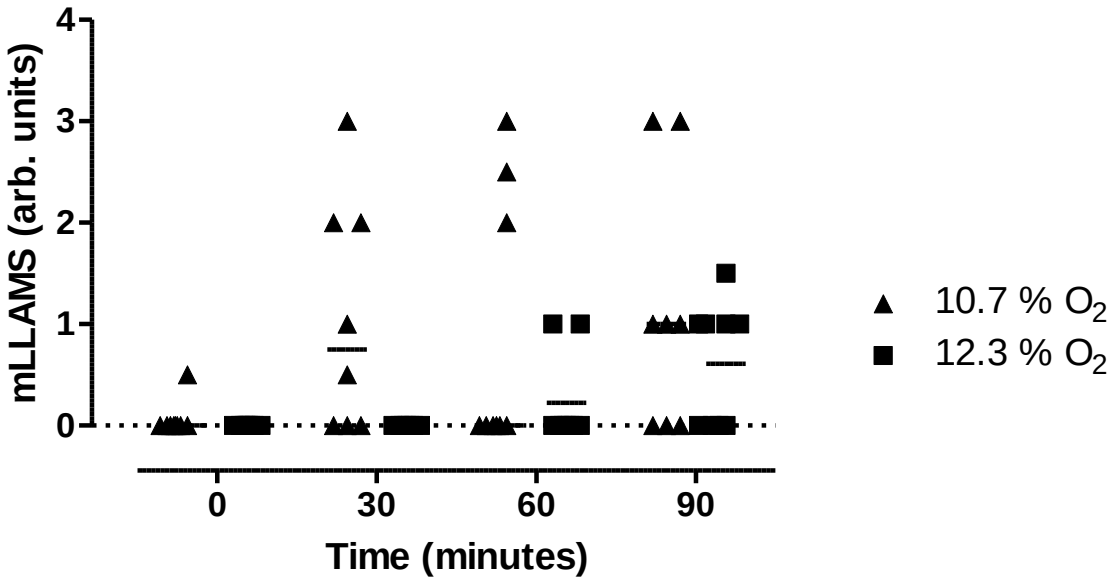

Figure 6.3: Effect of two different O_2 concentrations on mLLAMS symptoms. mLLAMS as a function of time in hypoxia at either 10.7 % O_2 (triangle) or 12.3 % O_2 (square). Horizontal line indicates median. N = 8.

The effect of O_2 concentration on HR was examined by two-way (condition [10.7, 12.3 % O_2] × time (0, 2, 4 hours) repeated measures ANOVA. No significant condition × time interaction was noted with respect the effect of hypoxia on HR ($p = 0.63$). A main effect of time was noted ($p = 0.001$), but no effect of condition was noted ($p = 0.71$; Figure 6.4A). This result is mirrored by paired sample t-test on AUC HR, with no difference noted between condition ($p = 0.62$, $d = 0.13$; Figure 6.4B). No alteration in the HR response of the case study individual relative to the control group response is seen (Figure 6.4A and B)

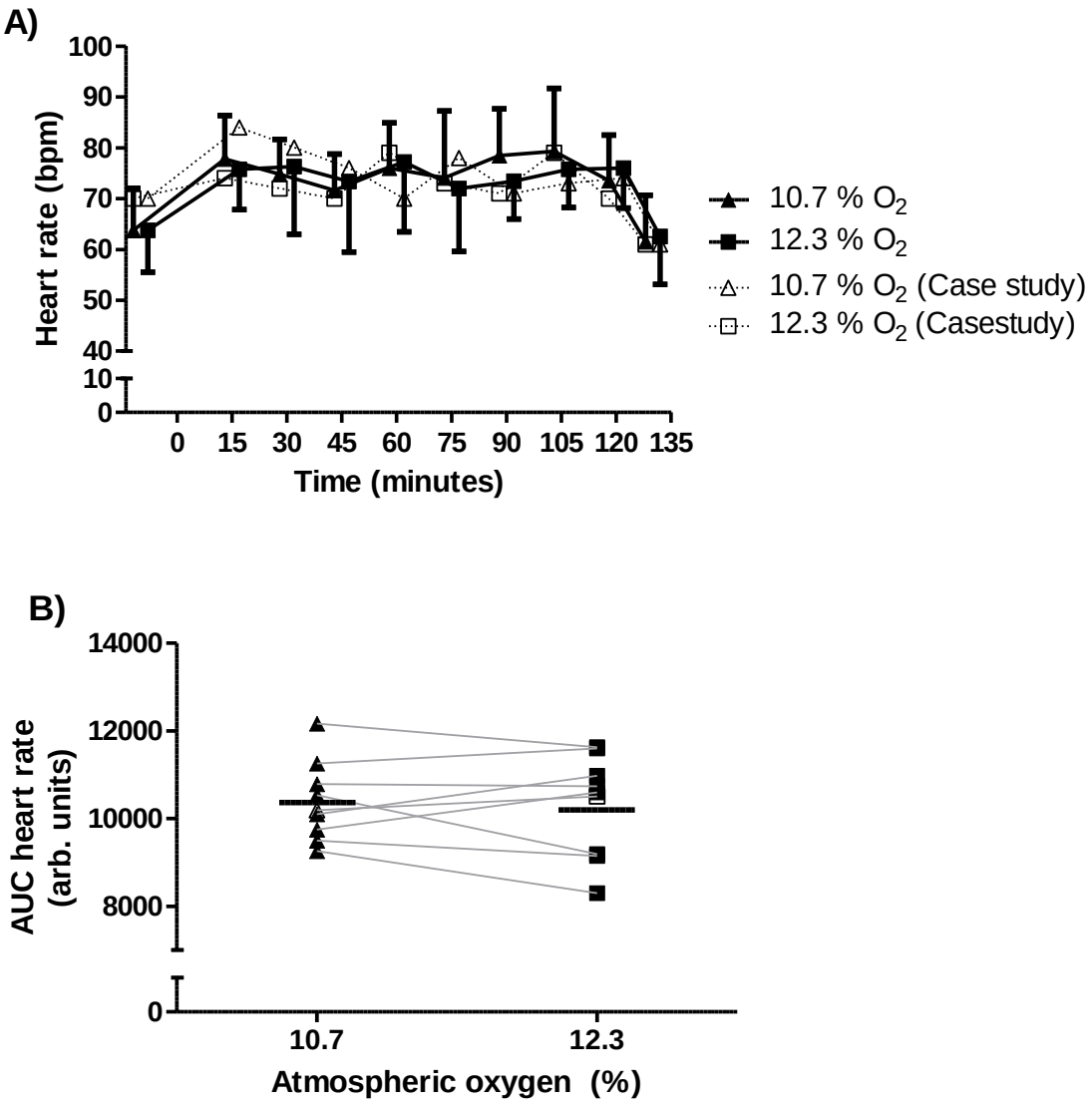

Figure 6.4: Comparison of the effect of two different O_2 concentrations on HR between lowlanders and a case study individual. A) HR (bpm) as a function of time (minutes). Hypoxic exposure of either 10.7 % O_2 (tirangle) or 12.3 % O_2 (square) from time point 0 to 120 minutes. Control participants (n = 8) with closed symbols, case study (n = 1) with open symbols. Error bars represent SD. **B)** Area under curve of hearte rate in 10.7 % O_2 (triagle) and 12.3 % O_2 (square). Control participants (n = 8) with closed symbols, case study (n = 1) with open symbols. Mean of lowlander responses given by horizontal black lines.

6.3.2 Effect of Two Different O_2 Concentrations on Plasma Myostatin

The effect of O_2 concentration on plasma myostatin was examined by two-way (condition [10.7, 12.3 % O_2] × time [0, 2, 4 hours]) repeated measures ANOVA, with treatment order considered as a between participant effect. No treatment order × group × time interaction was noted ($p = 0.704$). No effect of hypoxic condition is seen on plasma myostatin, with no condition × time interaction ($p = 0.73$), nor a main effect of condition ($p = 0.28$). A main effect of time was seen ($p = 0.02$), therefore individual's values across conditions were averaged for *post hoc* analysis. Subsequent *post hoc* analysis showed plasma myostatin values unchanged between 0 and 2 hours ($p = 0.17$, $d = 0.28$), but significantly reduced at 4 hours, relative to 0 hours ($p = 0.004$, $d = 1.21$) and 2 hours ($p = 0.005$, $d = 2.94$; Figure 6.5A).

This result is maintained if plasma myostatin concentration is expressed relative to baseline (time = 0 hours), with no interaction ($p = 0.80$), nor a main effect of condition ($p = 0.74$), but an effect of time ($p = 0.002$). Subsequent *post hoc* testing (pooled values) showed plasma myostatin is unchanged between 0 and 2 hours ($p = 0.017$, $d = 0.49$), but significantly reduced at 4 hours, relative to 0 hours ($p = 0.017$, $d = 5.62$) and 2 hours ($p = 0.002$, $d = 1.81$; Figure 6.5B).

The case study participant's plasma myostatin response to hypoxia does not appear to be grossly different to that of the lowlander population group presented here. Baseline (time = 0 hours) plasma myostatin was 3423.6 and 4103.0 $pg.mL^{-1}$ at 10.7 % and 12.3 % O_2, respectively, which falls 0.15 and 0.67 of a SD away from the mean response, respectively. Following the 10.7 % condition, this case study gives plasma myostatin concentrations that are 0.16 and 0.08 of a SD from the mean at 2 and 4 hours, respectively (Figure 6.5A). Following the 12.3 % O_2 condition, the case study plasma myostatin response is 0.93 and 1.25 of a SD above the group mean. However, when expressed relative to baseline, no significant alteration of myostatin at the 4 hour time in the 12.3 % O_2 condition is noted for the case study (Figure 6.5B).

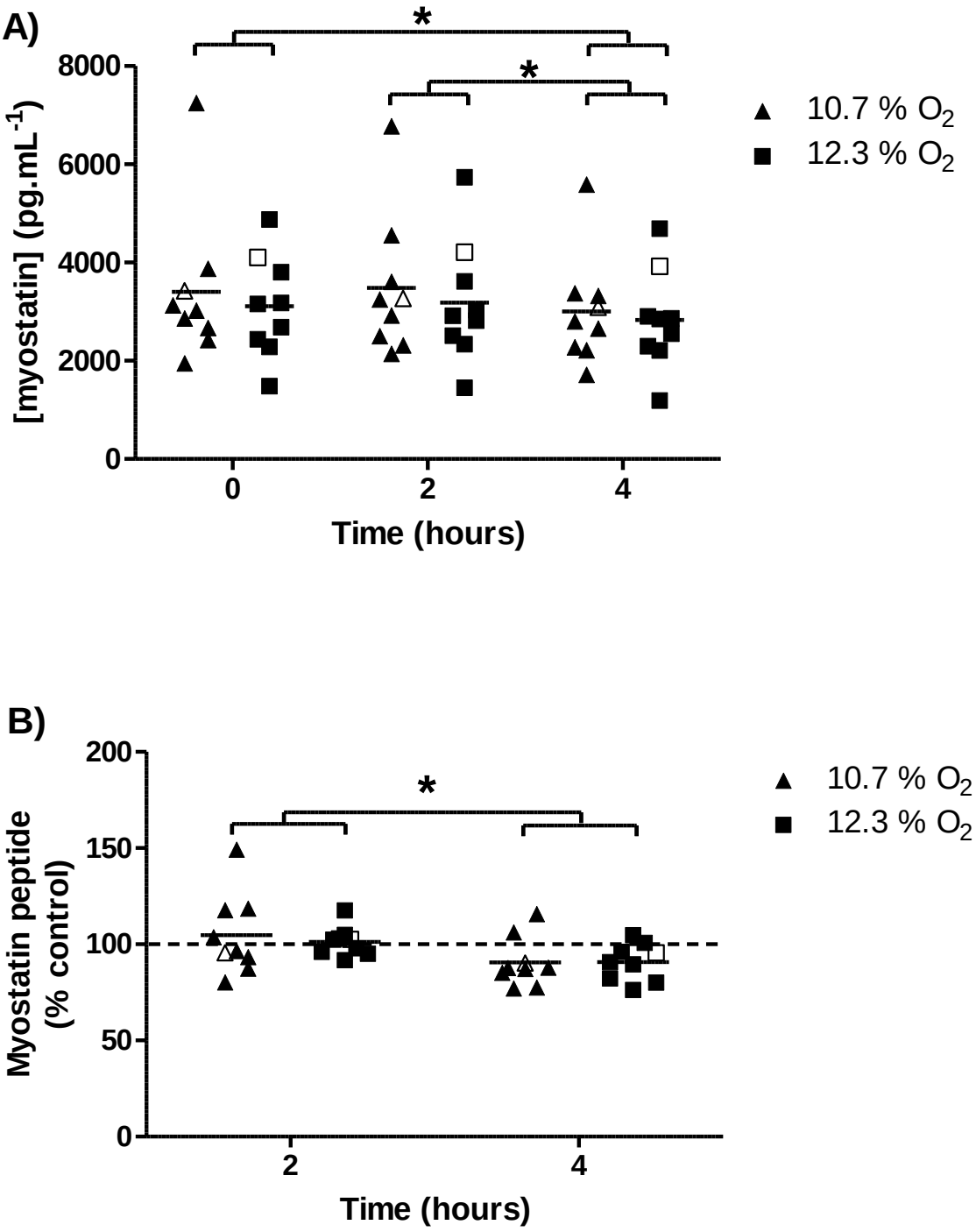

Figure 6.5: Effect of differing O_2 concentration on plasma myostatin. ELISA for plasma myostatin from venous plasma prior (time = 0 hours), immediately post (time = 2 hours) or 2 hours following (time = 4 hours hours) either 10.7 % O_2 (triangles) or 12.3 % O_2 (squares) hypoxic stimulus. **A)** Absolute concentration ($pg.mL^{-1}$) **B)** Relative to individual 0 hour concentration (%). Black horizontal line indicates mean. Dashed line indicates 100 %. Lowlander individuals (n = 8) closed symbols, case study (n = 1) open symbols. * indicates significance ($p < 0.05$) between lowlander groups as marked.

6.3.3 Correlations between Desaturation and Plasma Myostatin

A weak positive linear relationship is noted between the mean desaturation in SpO_2 during hypoxic stimulus from baseline (Δ SpO_2) and the subsequent decrease in plasma myostatin between 0 and 4 hours (Δ plasma myostatin; Figure 6.6; r^2 = 0.083). Pearson's correlation suggests no significant relationship between the two variables (p = 0.25).

As a proxy of DO_2, the correlation between HR × SpO_2 during hypoxia and Δ plasma myostatin was examined. No relationship was noted between these variables (r^2 = 0.03; data not shown).

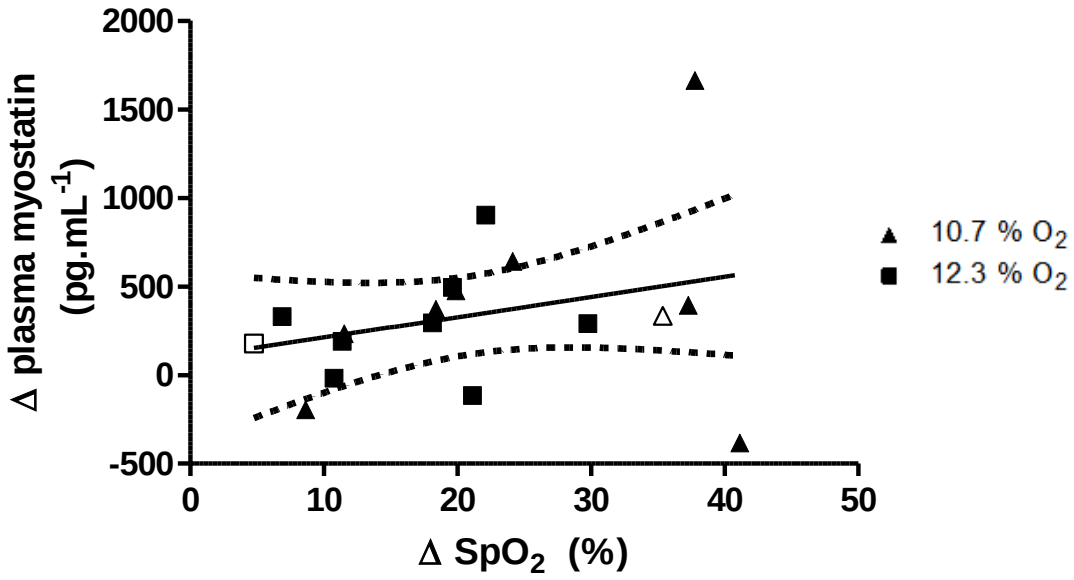

Figure 6.6: Correlation between Δ SpO_2 and Δ plasma myostatin in both lowlanders and a case study individual. SpO_2 desaturation during hypoxia from baseline (Δ SpO_2) as a function of change in plasma myostatin between 0 and 4 hours (Δ plasma myostatin). Plasma myostatin measured by ELISA with recombinant myostatin used for generation of standard curve. Average of SpO_2 from 0 – 2 hours at either 10.7 % (triangles) or 12.3 % O_2 (squares), with open triangle and square indicates case study at 10.7 % or 12.3 %, respectively. Dashed lines indicate 95 % confidence limits.

6.4 Discussion

The primary novel result of this Chapter is the lack of an O_2 concentration-dependent effect on plasma myostatin concentration in healthy lowlander males, within the range of O_2 concentrations examined here. Further, it appears that the plasma myostatin response of a case study Sherpa individual does not differ to that seen in lowlanders, despite inherent genetic adaptation to hypoxia.

Human physiological adaption to high altitude is altitude-dependent between 0 – 6000 m. Respiratory, cardiovascular and plasma volume changes during mountaineering occur as a function of altitude (Brooks et al., 2005, Lenfant and Sullivan, 1971). No rigorous attempt has been made to examine the effect of magnitude of hypoxic stimulus on loss of muscle mass. Individuals up to ~ 4,500 m above sea level tend to not show atrophy of muscle (Chia et al., 2013, Holm et al., 2010), while those at 5,000 m and higher lose significant muscle mass (Hoppeler et al., 1990, Rose et al., 1988). These results are confounded by experimental group differences. Where the population examined by Chia and colleagues (2013) were elite swimmers participating in a training camp, Hoppeler and colleagues (1990) examined mountaineers during technically challenging summit attempts. Both groups participated in large volumes of aerobic exercise, but the nature of the exercise performed (swimming vs. climbing) is fundamentally different as a mechanical and metabolic stimulus. Further, environmental differences such as nutrition and sleep cannot be ruled out. Finally, these studies have examined changes in response to chronic exposure. This Chapter examined two concentrations of O_2 (10.7 % and 12.3 % O_2) with an approximate equivalent of 5,500 and 4,500 m, respectively, hypothesizing a concentration-dependent effect of hypoxia on plasma myostatin. By inducing hypoxia in the manner reported in this chapter, the effect of these confounding factors has been removed.

One critique of this work could be the concentrations used were too similar to distinguish a noticeable difference. Indeed, those studies showing a lack of atrophic effect were at ~ 3,000 m (Chia et al., 2013, Schena et al., 1992), whilst those showing atrophic effects were completed at > 5,000 m (Hoppeler et al., 1990, Rose et al., 1988). This Chapter used 12.3 % and 10.7 % O_2 as the 12 % condition was used throughout previous Chapters and the 10.7 % was considered the lowest ambient O_2 individuals could be safely introduced to without acclimatisation. While humans are capable of withstanding greater altitudes for acute timeframes following adaptation, acute exposure to equivalent altitudes of 7000 meters or higher produce rapid loss of cognitive function and conscious (McFarland, 1971), whilst prolonged exposure to altitudes greater than 6,000 m results in death, even in altitude adapted individuals (Gleason et al., 2011). While a significant difference in SpO_2, and trends towards difference in mLLAMS were seen in the O_2 concentrations examined, a further intervention group at a lower (3,000 m equivalent, ~ 14.5 % O_2) or higher (6000 m equivalent, ~ 9.5 % O_2) may have been a useful addition to this work.

The results of Chapter's Three, Four and Five of this thesis showed similar results to those found here. Chapter Five showed no change in plasma myostatin following 2 hours of hypoxic exposure, but a decrease in plasma myostatin after 10 hours hypoxic exposure at 12 % O_2 in a similar population group to that examined in this Chapter (Appendix Fourteen). Thus, it would appear that in response to acute hypoxic stimulus plasma myostatin begins to be sequestered from plasma. Detection of this effect takes more than 2 hours, but is present by at least 4 hours, and maintained for up to 10 hours. Presumably, the movement of plasma myostatin is into muscle tissue, its primary site of action. Indeed, the results of Chapter Five suggest this, with a trend towards increased muscle myostatin peptide. Finally, Chapter Three also showed a time dependent effect of hypoxia on myotube size, with 2 hours showing a decrease in myostatin peptide expression. These contrasting results could arise due to differences between *in vitro* and *in vivo* models, an *in vitro*

model is less able to respond to significant homeostatic challenges with the systemic metabolic resources available *in vivo*.

Unfortunately, the work performed within this Chapter had practical limitations preventing the collection of muscle biopsies. Had muscle biopsies been collected, it is tempting to speculate matching findings with respect to those seen in Chapter Four would be seen, with a maintained reduction at the two hour time point. This work also make the decision not to include a third control group in a blinded ambient conditions. This decision was based on findings of Chapter Four, showing no alteration in plasma myostatin in resting males under ambient conditions over a 6 hour time period. Further, myostatin does not vary in healthy young males at rest, when examined hourly over 24 hours with no administrated stimulus (Vamvini et al., 2011).

It is of interest to note the variation in SpO_2 response to hypoxic exposure witnessed, both within individuals, and between stimulus conditions. It seems apparent that variation of the SpO_2 desaturation response was greater in the 10.7 % O_2 than the 12.3 % O_2 condition (Figure 6.2B). Due to nonlinearity of the haemoglobin dissociation curve at a lower PO_2, small changes in in PaO_2 can result in large changes in SpO_2 (Miller, 2010), as does individual variation within individual's *in vivo* haemoglobin dissociation curve. In N = 10,079 independent arterial samples at a similar PaO_2 (60 [+/- 4] mmHg), significant individual variation in SaO_2 (as directly measured) was noted, with values between 69.7 and 99.4 % reported (Gothgen et al., 1990). Further, increased error of SpO_2 values is noted as arterial saturation approaches 70 % (Feiner et al., 2007).

The availability of a Sherpa case study was an unexpected addition to this work. Positive genetic selection, especially with regards to metabolic and hypoxic sensing processes (Huerta-Sanchez et al., 2014, Simonson et al., 2010) may underlie the ability of Sherpa and Tibetan populations to

maintain aerobic metabolism during high altitude exposures, despite reduced mitochondrial and haemoglobin mass (Hoppeler et al., 2003). It was hypothesized that the Sherpa would be relatively protected against hypoxia, and thus would not show hypoxia-induced changes in plasma myostatin. The results presented here do not suggest this to be the case, with results typically within one SD of the lowlander group. The only exception to this was during the 12.3 % O_2 condition at the 4 hour time point, where the case study individual showed a 1.25 SD increase in plasma myostatin concentration relative to the lowlander group. However, any potential effect is not maintained when plasma myostatin data is examined as a relative change from baseline. The SpO_2 response of the Sherpa individual is notable, a mean desaturation of 94.3 % at 12.3 % O_2 is similar in nature to the hypoxic response seen in native Sherpa at 4,000 m (Beall, 2007). Indeed, Sherpa showing preserved SpO_2 (relative to lowlanders) at moderate altitudes (similar to the 12 % condition) both at rest and during exercise have been reported by others (Hackett et al., 1980, Park et al., 2014). One case study reports a similarly severe SaO_2 desaturation response to acute exposure to 5,500 meters hypobaric hypoxic in a Sherpa case study relative to a case study lowlander, with the Sherpa showing approximately 50 % desaturation, whilst the lowlander SaO_2 was approximately 70 % (exact values not given; West et al., 1984), very similar to the values reported here.

However, despite this blunted response relative to the lowlander cohort, his plasma myostatin matched that of the lowlanders. The mechanistic effect underlying decreased in plasma myostatin in healthy males may be separate to the adaptations highlanders show. Due to the inherent caution required in interpretation from n = 1, larger cohorts are needed to examine this hypothesis.

In conclusion, here this Chapter show no difference in the plasma myostatin response to two different concentrations of O_2. The response in both hypoxic conditions examined here is a decrease in plasma myostatin concentration, suggesting myostatin is leaving the plasma. While it is

tempting to speculate this movement is towards peripheral muscle to begin the hypoxia-induced atrophy seen in chronic models of hypoxia, further work is needed to establish this. Finally, intergeneration adaptation to hypoxic environments does not appear to alter this response, as the case study Sherpa individual presented here does not notably vary in his response to acute hypoxic stimuli.

Chapter Seven – General Discussion

This thesis aimed to examine the acute effects of hypoxia on myostatin *in vitro* and in healthy male adults. It was hypothesized that myostatin peptide would increase in response to acute hypoxic stimuli, both intracellular myostatin in the C2C12 cell line *in vitro*, and in muscle and plasma *in vivo*. The primary finding from this thesis is the consistent response of myostatin to an acute hypoxic stimulus across models, and in the absence of other confounding factors. Counter to the above hypothesis, decreased intracellular myostatin peptide expression was noted in C2C12 myotubes following 2 – 48 hours hypoxic exposure. This decrease in muscle myostatin peptide was maintained in healthy males following 2 hours of hypoxic exposure in Chapter Four, but not following 10 hours of hypoxia in chapter Five. Concentration of plasma myostatin was reduced following 10 hours of hypoxic exposure (Chapter Five), and 2 hours hypoxia (Chapter Six), each time by ~ 20 % of baseline. It is well described in the literature that chronic tissue hypoxia, by either environmental or pathological cause, results in the atrophy of muscle. As myostatin is a significant regulator of muscle mass, alterations in myostatin expression following hypoxia are likely to be involved in this atrophy. It is therefore proposed that this acute myostatin response to hypoxia contributes as an early regulator of the atrophic response, the effect of which is capable of being induced by hypoxia alone, independent of confounding factors.

Previous work on hypoxia-induced atrophy has taken place over chronic time frames of weeks or months, and has typically used clinical models such as COPD or CHF, or hypobaric environments such as the mountaineering sojourn by unacclimatized lowlanders. Patients with COPD typically present with increased systemic inflammation, inactivity, malnutrition, and frequently smoking behaviour (Debigare et al., 2001). Mountaineering individuals typically undergo strenuous exercise, cold exposure, reduced food intake and a reduction in sleep duration and quality (Wagner, 2010). Thus, the models used (*in vitro* culture and the healthy individual) were explicitly chosen as research models, as they present with the minimum of confounding factors.

Chapter Three of this thesis examined the effects of varying times in hypoxia on myostatin expression in both myoblasts and myotubes. Atrophy of muscle *in vivo* is a function of both protein balance within mature myocytes and renewal (or lack thereof) of myonuclei from precursor satellite cells. This work therefore examined both the chemotaxic response of myoblasts *in vitro* to damage and showed an impairment of this response in a hypoxic environment compared with a normoxic environment. Further, myotubes showed significant atrophy in response to a matching hypoxic stimulus in a time-dependent manner. Thus, a mechanism for the regulation of muscle mass in mammalian cells that both regulated satellite cell activity and myotube size was sought. Myostatin, with its well defined roles in the regulation of both myotube size and satellite cell activity, was hypothesized to underlie these witnessed effects, and indeed, myostatin peptide was suppressed at every time point studied during the *in vitro* work in Chapter Three.

Chapter Four, Five and Six exposed healthy, unacclimatized young males to hypoxic environments for varying acute times and O_2 concentrations. Each Chapter was completed within different physiology laboratories, with Chapter Four completed in the laboratory of Dr Peter Watt, University of Brighton, Chapter Five completed at the University of Westminster in the laboratory of Dr Richard Mackenzie, while Chapter Six was completed in the laboratory of Dr Peter Wagner, University of California, San Diego, USA. As such, differences in experimental design exist, which are described below. Despite the variation of time and the concentrations used, consistent trends in results occurred, both in relation to other *in vivo* Chapters, the *in vitro* work of Chapter Three, and in similar work found in the existing literature.

7.1 Between Chapter Comparison

The populations used in each Chapter were homogenous in terms of their demographics (age, height, weight, BMI, HR, resting SpO_2 and SpO_2 desaturation response; Appendix Fourteen) which increase confidence in the comparison of results between experimental Chapters. In all Chapters, hypoxia was induced via a normobaric method, whereby ambient O_2 availability was reduced, by replacement with alternative gas(es).The work of Chapters Four and Five utilized hypoxic chambers, with hypoxic air provided via a molecular sieve pump. Oxygen concentration of the chamber space was controlled via a constant feedback mechanism, thereby maintaining the ambient concentration of O_2 at ~ 12 %. The delivery of hypoxic gas in Chapter Six differed; atmospheric air was bottled under pressure and diluted with 100 % nitrogen to give a pressurised bottled supply of hypoxic gases. Thus, while every participant in Chapter Six received an identical O_2 concentration, this differed slightly from the targeted 10 % or 12 % for each condition.

The molecular sieve approach preferentially filters and removes oxygen, due to its larger molecular mass, leading to a slightly hypercapnic environment. The bottled gases model results in slight hypocapnea, due to the dilution of ambient atmospheric CO_2 with 100 % N_2. An elevation in F_iCO_2 results in hypercapnia, leading to an increased respiratory rate and depth (Schaefer, 1958), while hypocapnea reduces respiratory rate (Corne et al., 2003). Hypercapnia, as induced by increasing ambient CO_2 from normal (0.03 %) to 12 %, results in decreased protein synthesis (Caso et al., 2005). However, the increase in CO_2 is significantly higher than anything seen in this work, and the authors do not report changes in protein synthesis with 4 % or 8 % CO_2.

The respiratory response of participants (while not measured) may therefore have differed between Chapters Four and Five (chamber-induced hypoxia) and Chapter Six (mask-induced hypoxia). As identified in Appendix Fourteen, the mean desaturation response between Chapters

does not differ, as identified by the SpO_2 decrease over 2 hours (initial 2 hours in Chapter Five) in each studies equivalent 12 % O_2 condition. Thus, while the method of inducing hypoxia between chapters does differ, the end hypoxemic result was similar.

Whilst mean SpO_2 was noted to be reduced under hypoxic conditions to a similar magnitude between Chapters (Appendix Fourteen), intra-individual variation in the magnitude of this response is noted to occur, especially within the lower O_2 % condition of Chapter Six. Individuals response to hypoxic exposure is known to vary significantly (Martin et al., 2010), with some speculating to a 'responder / non-responder' effect based on retrospective analyses of training data from 'live-high-train—low' models of adaptation to low-moderate hypoxia (for example Chapman et al., 1998). Monozygotic twins are noted to have more similar hypoxic ventilatory responses than dizygotic twins (reviewed by MacLeod et al., 2013), suggesting this variance is responses may have a genetic aspect. Indeed, Ogata et al (2011) noted 12 hours exposure to 15.4 % O_2 results in alterations in the plasma EPO, and the magnitude of this response between individuals was linked to a common HIF1-α polymorphism. Whilst this same cohort also showed significant variation in their SpO_2 desaturation response (80 % - 97 %) this response was not a polar responder / non-responder grouping, instead being evenly spread within the reported range (Ogata et al., 2011). Further, whilst annual 19 day visits to a 2100 m training camp by an elite Australian-Rules Football team show responder / non-responder responses with increases in EPO and haemoglobin concentrations, the individuals who 'responded' differed with each years visit (McLean et al., 2013), suggesting the this response factor is not simply genetic alone.

With regards to the findings of this thesis, it is however worth considering the range of variation of hypoxic responses that can occur within individuals, and what effect this may have on this works primary measures. Indeed, Etheridge and colleagues (2011) noted a moderate correlation between SpO_2 desaturation and suppression of FSR following an exercise stimulus. This work noted no

correlation between SpO_2 desaturation and changes in myostatin expression, nor did it not a difference in myostatin response to the two differing O_2 % of Chapter Six, suggesting, at least within the range examined here, the magnitude of the desaturation response does not affect the magnitude of the myostatin response.

This significant intra-individual variation in the hypoxic ventilatory response, which while primarily driven by P_aCO_2, is also influenced by magnitude of hypoxia, prior adaptation and neuro-endocrine factors (Powell et al., 1998). As such it was recently proposed that the use of isocapnic hypoxic models, inducing a drop in atmospheric PO_2 while holding end-tidal partial pressure CO_2 constant (end-tidal PCO_2), may provide a better research model. Such a model removes the intra-individual hypoxic ventilatory response by removing the variation in respiratory alkalosis (Howard et al., 1995), and may be applicable for future work, as the argument could be presented that the changes witnessed were due to respiratory alkalosis, not hypoxia *per se*. Such a research model, while useful for removing individual variation in the hypoxic response, does result in a stimulus that is a step further removed from the physiological effects of hypoxic via pathophysiological or hypobaric stimuli. Alternatively, a SpO_2 clamp approach could be used in future work, varying environmental oxygen to produce a matching SpO_2 desaturation between individuals, to ensure the oxygen desaturation received was identical. This research model, done in parallel with a control group of hypoxic exposure only (no clamp) would be of interest, establishing the role of desaturation alone.

7.1.1 Consistent Trends

The primary hypothesis presented for this work was that an increase in myostatin (at both the muscle and plasma level) would be seen following an acute hypoxic exposure. One of the most consistent findings here was counter to this hypothesis, with a decrease in plasma myostatin seen following 10 hours of hypoxia in Chapter Five, and 2 hours following a 2 hour hypoxic exposure in Chapter Six, with no change seen in Chapter Four.

The underlying biological process regulating this decrease in plasma myostatin peptide concentration is of interest to the interpretation of these results. A decrease could represent either a) an increase in myostatin removal from plasma, b) a decrease in production of myostatin or c) some combination of the two. It is unlikely that this process represents an increase in plasma myostatin binding proteins, such as follistatin and FLRG, as the plasma myostatin ELISA used here involved a binding protein removal step (Appendix Ten). Thus, it would appear that either removal of myostatin from the plasma is increased, or production is decreased. Myostatin acts in an endocrine manner, an increase in exogenous myostatin induces atrophy, both in terms of muscle weight across multiple muscles (35 – 50 % wet weight loss) and cellular diameter within gastrocnemius (25 % reduction; Zimmers et al., 2002). Therefore, the hypothesis presented here is this decrease in myostatin in the plasma represents the movement of myostatin from the plasma into the peripheral muscle where it can instigate its classic atrophic pathways. The alternative hypothesis, that plasma myostatin is being degraded and then excreted cannot be ruled out; as yet there is no published research on the degradation or filtration of plasma myostatin for removal of function.

At the muscular level, Chapter Four showed a decrease in myostatin peptide in the hours following 2 hours hypoxic exposure, where a trend towards increased muscle myostatin peptide immediately following 10 hours hypoxic exposure was seen in Chapter Five. Similarly, the *in vitro* results of Chapter Three show a decrease in intracellular myostatin peptide following 2 hours hypoxic exposure (1 % O_2); however this decrease was maintained at during 24 and 48 hours of hypoxic exposure. This difference could arise due to differences in the model studied. Myotubes *in vitro* do not have the integrative or protective physiological feedback mechanisms against hypoxia that humans can utilize *in vivo*, such as alterations in metabolism, respiratory rate, CO_2 buffering and endocrine responses. In response to a hypoxic stimulus, humans increase breath frequency and depth, engage in significant fluid shifts to increase plasma volume and systemically alter cytokine

production in tissues that are not muscle (Corne et al., 2003, Eltzschig and Carmeliet, 2011, Poulsen et al., 1998). If myostatin-induced atrophy occurs to reduce metabolic cost then cross tissue metabolic mechanisms may be involved. The lack of a intercellular lactate shuttle mechanism or Cori cycle, (Brooks, 1986), whereby excess glycolytically produced lactate can be transported to distant tissues and metabolically utilized, may also alter the response of myotubes *in vitro*.

The results of Chapter Five could be interpreted to support a net flux of myostatin from plasma to muscle, with a decrease at the plasma level and trends towards an increase at the muscular level following a 10 hour hypoxic exposure. While possible, this interpretation should be viewed with caution. Myostatin acts as an intercellular signalling peptide (Figure 7.1), thus this witnessed trend towards an intracellular increase may represent either a) an increase in myostatin production by muscle cells in response to the hypoxic stimulus or b) decreased myostatin secretion from the muscle cells as a protective response (e.g. increased cytoplasmic sequestration of myostatin).

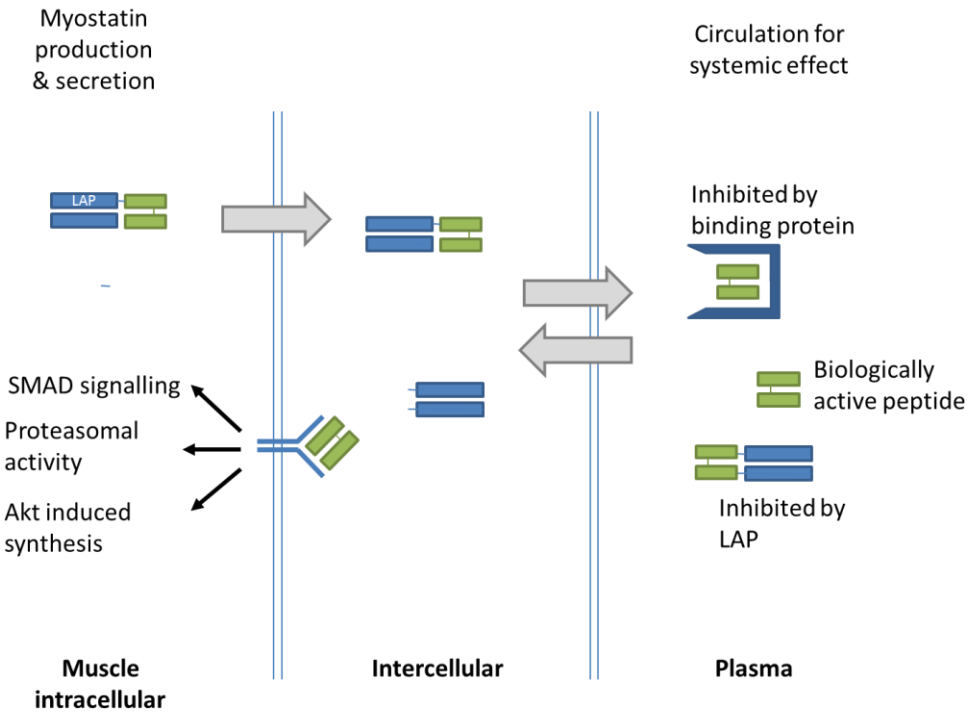

Figure 7.1: Myostatin protein by compartment. Myostatin transcription in the myofibril space (left) and can be found either bound to its latency associated peptide (LAP, blue) bound to the bioactive peptide (green). Secretion of myostatin into the intercellular space (middle) where myostatin can then act in an autocrine or paracrine manner, or further secreted into the plasma (right) where myostatin can be found biologically active (unbound) or inactive (bound to either its LAP or various binding proteins). Intercellular myostatin demonstrated by Anderson and colleagues (2008).

7.1.2 Inconsistencies between Studies

Chapter Four (2 hours of hypoxia or control) notes no change in plasma myostatin peptide immediately post or in the in the hours following 2 hours of hypoxic exposure at 12 % O_2, while Chapters Five (10 hour hypoxic exposure) and Six (2 hour hypoxic exposure at 2 difference concentrations) showed a decrease in plasma myostatin at similar O_2 concentrations and times in hypoxia. It is unclear as to why this difference occurs, plasma samples were taken from similar populations and participants showed a similar desaturation response to similar hypoxic stimuli (Appendix Fourteen). The measures of plasma myostatin across Chapters were performed using matching commercial ELISA kits and production lots (R&D, DGDF80, lot #318772). Budgetary constraints required plasma samples from Chapter Four to be run in duplicate, whilst results from Chapters Five and Six were run in triplicate. Relative power of each measure may influence results obtains, this consideration is discussed below.

The differing response of muscle myostatin peptide following hypoxia is also of interest, with a decrease seen following 2 hours of hypoxia and a trend towards increased expression following 10 hours of hypoxic. This differing response, and suggestions regarding physiological meaning, are discussed below (7.1.3 Modelling of the Temporal Effect of Acute Hypoxia on Myostatin).

7.1.3 Modelling of the Temporal Effect of Acute Hypoxia on Myostatin

As previously mentioned, the experiments described within this thesis are the first to describe changes in plasma and muscle myostatin in response to an acute hypoxic stimulus. Hayot and colleagues (2011) showed increases in muscle myostatin peptide expression in COPD patients with chronic hypoxemia (P_aO_2 64 [2] mmHg), suggesting this hypoxemia may result in elevated myostatin and the subsequent loss in lean muscle mass seen in approximately 25 % of COPD patients. These authors also found elevated muscle myostatin peptide in rats exposed to 5 weeks hypobaric hypoxia (equivalent to ~ 4500 m), and in human primary cell culture exposed to cobalt chloride

(HIF-1α stabilizer) for 24 hours. Counter to these findings, this thesis shows myostatin decreases across times and concentrations examined. Differences *in vitro* could arise due to the research model used as Hayot and colleagues (2011) used cobalt chloride to model a hypoxic stimuli *in vitro*, whereas this thesis utilized normobaric hypoxia within the incubator environment. Cobalt chloride mimics a hypoxic stimuli via stabilisation of the HIF-1α protein (Goldberg et al., 1988). However, HIF-independent regulation of VEGF in response to hypoxic stimulation has been seen in C2C12 myotubes and in rat neurons (Arany et al., 2008, Ndubuizu et al., 2010), thus cobalt chloride forms a HIF activator, but not necessarily a hypoxic mimic. Further, a question of hypoxic equivalency arises, as a cross comparison between the relative hypoxia stimulus induced by cobalt chloride by Hayot and colleagues (2011) and the 1 % ambient O_2 used in this work is difficult to quantify. Finally, when directly examining the effect of cobalt chloride versus hypoxia in yeast, hypoxia (0 % O_2) was noted to differentially affect a number of cell signalling process relative cobalt chloride treatment, including protein degradation (Gleason et al., 2011). Thus, where possible, investigation of the effects of hypoxia *in vitro* should attempt to use hypoxia where possible.

An attempt to model the acute changes in myostatin in both muscle and plasma based on the results of this thesis is presented in Figure 7.2A. The results of Chapter Six show a decrease in plasma myostatin following 2 hours of hypoxia at both 10.7 % and 12.3 % O_2, which Chapter Five suggests is maintained following 10 hours of hypoxia (12.5 % O_2). Conversely, the decrease in muscle myostatin following 2 hours of hypoxia in Chapter Four is not maintained in Chapter Five, where following 10 hours of hypoxia, trends towards increased muscle myostatin peptide are seen. The integration of these results suggests that an acute (2 hour) hypoxic stimuli induces a decrease in muscle myostatin and may induce a matching decrease in plasma myostatin. In response to this acute atrophic stimulus, myostatin's flux is thought to be from the plasma into peripheral tissues (LeBrasseur et al., 2009, Zimmers et al., 2002). However, as outlined in Figure 7.1, a third compartment of biological relevance exists that was not measured here, the intercellular space.

Anderson and colleagues (2008) suggested, at least in mice, that this compartment represent the major storage site of myostatin in its biologically active form, however this work has yet to be repeated in humans. Similar work to those presented within this thesis, with the addition of microdialysis for collection of intercellular samples as well as plasma and muscle samples at matching time-points, are needed. In light of the results reported here, and the work of Anderson and colleagues (2008), it is hypothesised that the reduction of myostatin concentration in plasma represents the movement of myostatin into this space for myostatin to have its biological effect (Figure 7.2B). It should however be noted that the degradation or removal of plasma myostatin by some inactivating mechanism cannot be ruled out.

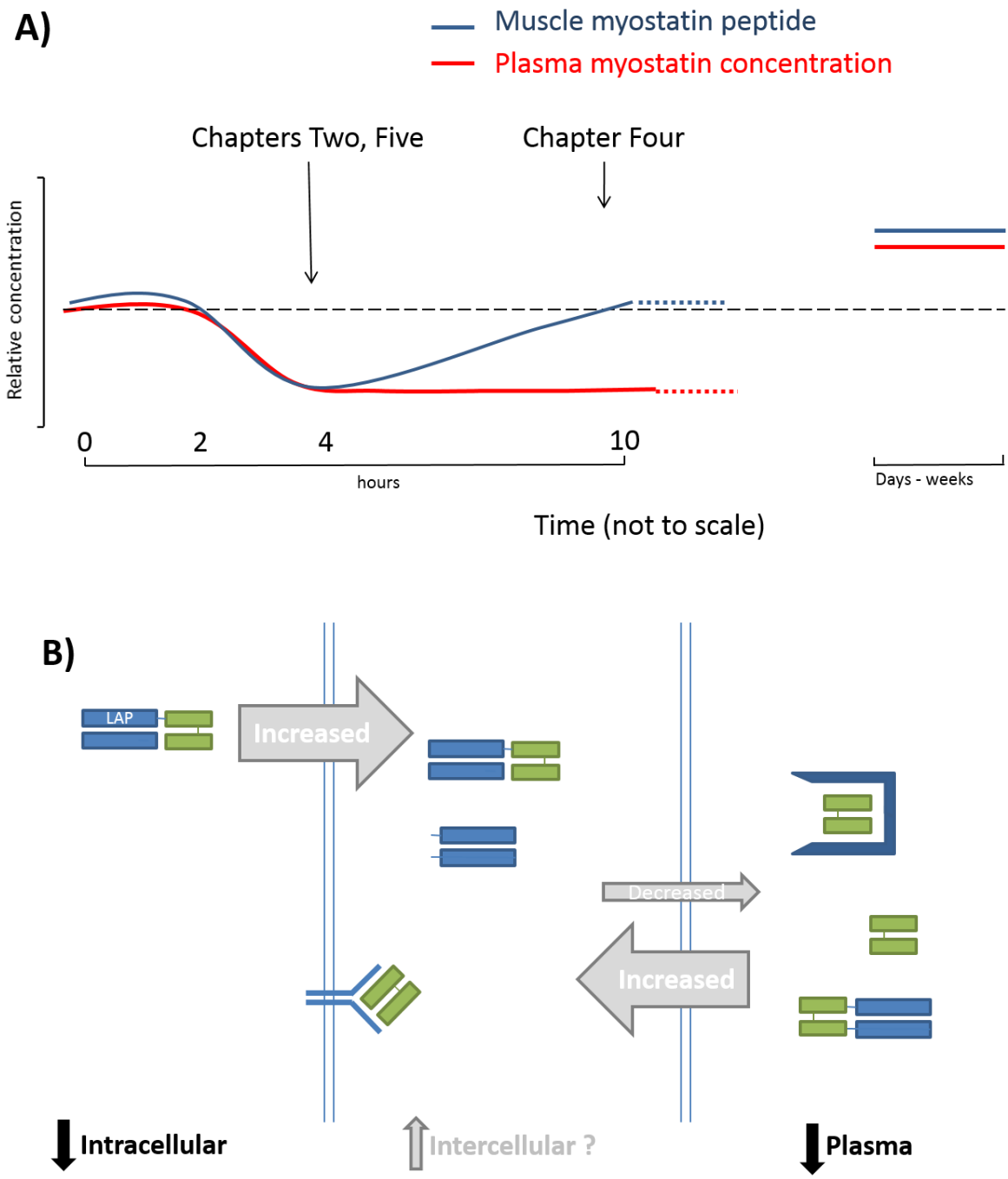

Figure 7.2: Hypothesized responses of plasma and muscle myostatin to acute and chronic hypoxic stimulus. A) Plasma myostatin indicated in red, muscle myostatin peptide in blue. Dashed black line indicates baseline without external stimulus. Labels indicate experimental evidence and associated Chapters. **B)** Intracellular, intercellular and endocrine movement in response to acute hypoxic stimuli. Black arrows and labels refer to findings of this thesis, grey indicates hypothesized responses.

The relative change in muscle myostatin peptide is to decrease following 2 hours of hypoxia and trend towards an increase following 10 hours. The original hypothesis was for an increase following 2 hours; however an expectation for a detectable increase in myostatin transcription and translation within 2 hours of an atrophic stimulus may have been ambitious. Conversely, a 10 hour period may allow sufficient time for an increase in myostatin translation to occur, hence the relative increase in muscle myostatin expression seen in Chapter Five.

7.2 Findings in Relation to the Literature

No reports of acute changes in myostatin peptide in either muscle or plasma have been reported in published literature. The range of plasma results compared here are in line with those of others, where plasma myostatin concentrations from healthy humans are reported between 1,000 to 5,000 $pg.mL^{-1}$ (Kim et al., 2007, Szulc et al., 2012), with one report (Kim et al., 2007) noting a range of serum myostatin peptide from a large cohort of healthy adults ranging between < 1000 pg.mL to > 100 ng.mL.

One report examined the effect of an acute exercise stimulus (N = 6, 3 × 10 bilateral knee extensions at 70 % of one-repetition maximum) on catabolic signalling pathways and showed a reduction in myostatin mRNA 1 – 24 hours following training which peaked at 8 hours post exercise (Louis et al., 2007). If an acute anabolic stimulus decreases myostatin mRNA, then it could be speculated that an acute catabolic stimulus would increase it, however measurement of this is required to confirm any increase in protein translation. While an increase in transcription would be reasonably expected to result in increased translation, the work of McMahon and colleagues (Oldham et al., 2009) should be noted, where a lack of association between myostatin mRNA and protein was shown.

Published literature has examined the effect of acute hypoxic stimuli on markers of protein synthesis and degradation. Rats show decreases in various body tissues protein synthesis rates (heart, bone, skin, brain kidney) following 6 hours hypoxia (10 % O_2), but no change in synthesis rate of muscle in this time frame (Preedy et al., 1985). Humans exposed to 12 % O_2 for 2 hours show no change in FSR or phosphorylation of pAkt (Ser473) while at rest (Etheridge et al., 2011). This lack of effect of 12 % O_2 on pAkt (Ser473) is in agreement with the results of Chapter Five. Furthermore, humans flown from an altitude of 550 m to 4,559 m above sea level by helicopter (to remove the exercise stimulus of climbing) show no alteration in FSR of muscle after a 24 hour period

(Imoberdorf et al., 2006). These results suggest, at least in the acute timeframes of 2 – 24 hours, that hypoxia alone (within the range examined here) is insufficient to impair protein synthesis at the muscular level, and are in agreement with the findings presented within Chapter Four of this work, with no alteration in Q or FSR of muscle.

Counter to the acute effects of hypoxia on protein synthesis, cellular markers of protein degradation are elevated in acute hypoxia (Caron et al., 2009). Both protein synthesis and degradation are elevated in an exposure time-dependent manner in response to chronic hypobaric hypoxia in rats, but the increase in degradation outweighs that of synthesis (Chaudhary et al., 2012). Rate of ubiquitination binding is elevated as is calpain and chymotrypsin-like enzyme activities (Chaudhary et al., 2012). The E3 ligase atrogin, but not MuRF1, is elevated in response to 12 hours hypoxia in L6 myotubes (Caron et al., 2009) while rats exposed to 5 days of hypobaric hypoxia (~ 5,500 m) show increases in atrogin and MuRF (Chaillou et al., 2012), in agreement with the consistent increases in bound ubiquitin seen throughout Chapters Three – Five of this thesis. Furthermore, while Etheridge and colleagues (2011) examined the effect of acute hypoxia on protein synthesis, this work expanded from these findings by examining both the synthesis and degradative response to acute hypoxia. As muscle atrophy can result from either an increase in degradation, or a decrease in synthesis, it is important to examine both aspects where possible. Whilst it is tempting to speculate that FBR would have been increased, a lack of a clear ^{15}N-Phe signal from plasma collected in this work has precluded quantification FBR.

Gender specific effects of hypoxia exist, but this has yet to be fully examined in the human. Retrospective data suggests males and females have similar success rates when summiting Mt Everest (Huey et al., 2007). Female rats survive up to 30 minutes of 2 % O_2, where male rats have a reduced survival time (Wood and Stabenau, 1998). Female rats exposed to hypoxia (equivalent to

5,500 m) may be resistant to atrophy, with no loss of body mass after 3 days in hypoxia, and non-significant trends towards loss of muscle mass of plantaris after 56 days in hypoxia (Chaillou et al., 2012). However, no male comparison group was included in the work of Chaillou and colleagues (2012). Female rats show a larger increase in respiratory rate in response to hypxioa than male rats, and these gender differences are maintained following ovariectomy (Phillips et al., 1997). Thus, this work chose to examine male participants only, an attempt to minimise potential confounding factors. However, future work needs to be performed examining both males and females; if the protection against hypoxic stimuli observed in female rats extends to humans may protect against hypoxic-induced myostatin alterations.

7.2.1 Results with Respect to Chronic Disease States

Chronic cardiorespiratory disorders often present with atrophy of muscle. Loss of muscle mass is seen in approximately 25 % of COPD (Bernard et al., 1998) and CHF (Libera and Vescovo, 2004) patients. Such disorders present with a number of confounding factors besides peripheral tissue hypoxia, including a reduction in energy input, reduced physical activity, and increased systemic inflammation (Wagner, 2008). Myostatin was noted recently to be elevated in the muscle of chronically hypoxemic COPD patients (Hayot et al., 2011), suggesting myostatin increases may in part underlie the observed atrophy. Thus, this thesis attempted to apply a hypoxic stimulus in a model of healthy individuals, in the absence of these confounding factors.

While the results of this thesis suggest hypoxia alone is sufficient to induce alterations in myostatin peptide that may be partially causative of atrophy, it is recognised that myostatin signalling is unlikely to act in isolation. Chronic inflammation is noted across chronic hypoxic disorders (Di Francia et al., 1994, Zhao and Zeng, 1997), and pro-inflammatory cytokines (TNF-α, IL-1β, IL-6 and IFN-γ) directly induce muscle atrophy (Guttridge et al., 2000, Lang and Frost, 2007, Langen et al., 2001) and may regulate myostatin peptide expression (Elliott et al., 2009). Physical activity is noted

to be reduced in COPD as a function of disease severity (Ferrando et al., 1996), while chronic disuse is associated with increased muscle myostatin expression and losses of muscle mass (Bunn et al., 2011, Murphy et al., 2011). Therefore, any hypoxic-induced changes in myostatin are likely to act in parallel with a number of other atrophic mechanisms.

7.2.2 Results with Respect to the Mountaineering Environment

As with the chronic hypoxic disorders discussed above, chronic exposure to a hypobaric hypoxic environment is also associated with loss of muscle mass (Hoppeler et al., 1990). This environmental stimulus is required to be of a sufficient magnitude, studies examining altitudes below 5,000 m tend not to show changes in muscle mass (Chia et al., 2013, Schena et al., 1992), while those climbing above this altitude do exhibit muscle atrophy (Hoppeler et al., 1990, Rose et al., 1988). As with chronic disease states, this altitude-induced atrophy of skeletal muscle occurs in the presence of a number of confounding factors. High-altitude sojourns involve reductions in food intake, a reduction in the amount and quality of sleep, increased physical exercise, and elevations in cosmic radiation exposure (George et al., 2010, Wagner, 2010). These effects increase with altitude gain, and as such any confounding factors are likely to be magnified as the climber increases in altitude.

Indeed, in mountaineering models where passive and active ascents to altitudes similar to those examined here are compared, differences in adaptive responses are noted. Reductions in PO_2 with increasing altitude results in reductions in absolute workload, and thus physical performance (Fagraeus et al., 1973, Wehrlin and Hallen, 2006). Mirroring this, fractional protein synthesis is not altered 24 hours following passive ascent to 4,559 m by helicopter, but it is increased in a matching group following active ascent (Imoberdorf et al., 2006). In an acute model, 2 hours at 12 % O_2 does not alter fractional protein synthesis, but 12 % O_2 with the addition of moderate intensity exercise suppresses the (normoxic) exercise-induced increase in protein synthesis (Etheridge et al., 2011).

Finally, it should be noted that positive adaptations to acute hypoxic exposure in endurance athlete models, such as the live-high-train-low models, all occur at equivalent altitudes of 2500 – 3000 m (Gore et al., 2001, Wehrlin et al., 2006). Atrophic effects of moderate – severe hypoxia, as described in this work, should not be extrapolated into training models conducted at these lower altitudes.

This atrophic response is traditionally seen as a maladaptive response to a reduction in oxygen supply, but may confer several physiological advantages. A reduction in size of muscle both reduces metabolic cost to the individual when the energy input from oxidative metabolism is limited and reduces oxygen diffusion distance from supplying capillaries parallel to individual myofibers. Furthermore, myofiber breakdown releases essential amino-acids that are metabolically functional for rapid energy provision and modulation of oxidation metabolism (Murray and Montgomery, 2014). Thus, while inhibition of myostatin signalling may be proposed for minimization of hypoxic-induced muscle loss, caution should be applied, as this atrophy may represent a necessary functional adaption in such physiologically challenging situations

7.2.3 Results with Respect to Wider Physiology

Loss of muscle mass in response to hypoxia is maintained across species, with few exceptions (Hopkins and Powell, 2001). A well maintained response suggests a selective advantage. Loss of muscle size in humans *in vivo* is paired with no change in capillary density, at least in a timeframe of weeks (Hoppeler et al., 1990), resulting in a relative increase in capillary density and a decreased capillary diffusion ratio and diffusion distance at the muscle level. Furthermore, as would be expected in a hypoxic environment, a shift towards non-oxidative metabolism rapidly occurs (Mackenzie et al., 2012a), at the cost of decreased energy efficiency. In such a condition, a minimization of basal metabolic demand would be advantageous, and so loss of metabolically demanding (muscular) tissue takes place.

Links between hypoxia and altered myostatin may involve HIF-1 dependent signalling. Studies on HIF-1α deficient cells and or *in vivo* models may be useful in determining this. Indeed, Chuvash Polycythaemic individuals show a homozygous mutation in exon 3 of the *VHL* gene, impairing VHL – HIF biding, reducing the rate of HIF breakdown under normoxic conditions (Ang et al., 2002, Bushuev et al., 2006). Whilst no published examination of body composition appears to have been conducted in these individuals, Chuvash Polycythaemic individuals show a reduced maximal work rate relative to control individuals when matched to body weight, as well as an earlier onset of lactate threshold, but no change in muscle fibre type proportion, suggesting a reduced lean mass content relative to total body mass (Formenti et al., 2010). Conversely, adult-onset muscle specific HIF-1α knock-down mice show a fast – to – slow fibre type switch and an increase in endurance during swimming and uphill running (Mason et al., 2004). The maintenance of HIF signalling is clearly important in the regulation of muscle homeostasis.

7.3 Limitations

7.3.1 *In vitro* Model

One potential critique of the *in vitro* work is the question of relevance of 1 % O_2 to *in vivo* conditions. PO_2 at the myofibril level is 2 – 3 mmHg, and at the mitochondrial level is essentially zero (Hoppeler et al., 2003). This value of 1 % ambient O_2 is widely used when examining the hypoxic response of myotubes *in vitro* (examples include Caron et al., 2009, Joshi et al., 2011, Li et al., 1998, Pescador et al., 2010, Wang and Semenza, 1993a), and indeed is more likely to be physiologically relevant than the use of 20.9 % O_2 for control conditions throughout the field. Intramuscular oxygen concentration is a dynamic value that is affected by blood flow, pH, 2,3-disphosphoglyceric acid, haemoglobin and myoglobin mass, and local PO_2 and PCO_2 pressures, thus the use of a single constant value may not represent physiological conditions and is a recognised weakness of an *in vitro* model.

7.3.2 Comparison between Normobaric and Hypobaric Hypoxia

A normobaric hypoxic model was chosen for this work as the capacity for hypobaric hypoxia was not available. Similarities and differences exist in the response to these two models of hypoxia, and it is important to be aware of these when examining changes in response to hypoxic stimuli. Faiss and colleagues (2013) examined normobaric or hypobaric hypoxia for 24 hours in a similar cohort of healthy young men as used here and showed no differences in SpO_2, blood pressure (systolic or diastolic), heart rate, breath frequency, RER, or partial pressure of end tidal O_2. V_E was not altered in hypobaric hypoxia compared to normobaric hypoxic before 8 hours, but was reduced in hypobaric hypoxia between 8 and 24 hours. End tidal partial pressure CO_2, while lowered relative to a control baseline condition, is elevated at every time point examined (1, 8, 16, 24 hours) in hypobaric hypoxia, when compared to normobaric hypoxia (Faiss et al., 2013). Similar results were shown by Richard and colleagues (2014) who showed no difference in V_E, heart rate or SpO_2 between hypobaric and normobaric hypoxia. The Lake Louise acute mountain sickness

questionnaire is recognized to under-report scores in normobaric hypoxia relative to real altitude exposure by ~ 1 arb. unit (at 432 mmHg, ~ 4,500 m vs 11.5 % O_2) but no difference between normobaric and hypobaric hypoxia (within a chamber) is noted (Roach et al., 1996). Thus, while hypobaric hypoxia and normobaric hypoxic models do show respiratory differences, these tend to become apparent after longer time frames (> 8 hours), which supports comparison of the findings of this thesis with those during hypobaric exposures.

Heyes and colleagues (1982) compared changes in plasma arginine vasopressin and cortisol and showed similar responses between individuals exposed to a matching PO_2 stimulus, but delivered under normobaric or hypobaric conditions. This finding is of interest as no difference was seen in response of two endocrine hormones in either model of hypoxia. With specific reference to the experiments presented in this thesis, where the primary measure in the three *in vivo* results Chapters was plasma myostatin, this provides some support for cross comparison with hypobaric hypoxic environments. Further work directly comparing normobaric with hypobaric hypoxia may be necessary to confirm this.

7.3.3 Extrapolation of Findings into Chronic Models

This thesis was in part driven by the inherent confounding factors found in the two major occurrences of hypoxia in *Homo sapiens*, namely disease models such as COPD and mountaineering models in healthy lowlanders, and driven by the common observation that both groups show muscle atrophy and hypoxia. However, by choosing such an acute research model to study this phenomenon, this work has run the risk of removing itself from applied conditions where hypoxia occurs. Thus, it would be of interest to examine further models where those factors that have been considered here as confounding are reintroduced. Such an example could be a small animal models +/- hypoxia, LPS (or other pro-inflammatory stimuli) and dietary restriction, all in isolation, and combined together, to begin to build research models of chronic clinical disorders, and the

combined effects of these factors. Furthermore, an examination of acute-to-chronic timeframes in an animal model to bridge the results presented in this thesis with those reported in the literature may be called for.

7.3.4 Absolute Oxygen Delivery

Whilst no correlations were noted between the SpO_2 desaturation response to hypoxia and changes in muscle or endocrine myostatin (Chapters Four, Five & Six), it should be noted that SpO_2 does not directly measure the amount of oxygen delivered to peripheral tissues. Oxygen delivery (DO_2) can be calculated by the following formulae (McLellan and Walsh, 2004).

$$DO_2 = \dot{Q} \times CaO_2 \times 10$$

DO_2, delivery of oxygen ($mL.min^{-1}$); Q, cardiac output ($L.min^{-1}$); CaO_2, arterial oxygen content (%).

Where CaO_2 is given by

$$CaO_2 = (Hb \times 1.35 \times SaO_2) + (PaO_2 \times 0.003)$$

CaO_2, arterial oxygen content (%); Hb, haemoglobin ($g.dL^{-1}$), SaO_2, arterial oxygen saturation (%); PaO_2, partial pressure oxygen (mmHg).

In the absence of measurement of haemoglobin, arterial oxygen tension and cardiac output (Q), a simple estimation of DO_2 can were made by HR × SpO_2. No relationship was noted in Chapter Four between this proxy of DO_2 and Δ plasma myostatin at 2 hours, nor was any relationship between this measure and Δ plasma myostatin in Chapter Six. However a positive, linear trend is noted

between SpO_2 × HR and Δ plasma myostatin following 10 hours of hypoxia in Chapter Five. This relationship suggests that the ability to maintain absolute peripheral oxygen delivery is associated with greater decreases in plasma myostatin in hypoxia. What physiological meaning can be prescribed to this is unclear, future work should directly measure DO_2 and associate this against both acute changes in myostatin and chronic changes in muscle mass.

7.3.5 Statistical Considerations

Financial and practical limitations restricted the size and therefore subsequent statistical power of *in vivo* work presented in this thesis. With a lack of any published work examining acute changes in myostatin *in vivo* in any model, *a priori* power calculations in the manner of Cohen (1988), were not possible. *Post hoc* calculations of observed power of plasma myostatin across Chapters Four, Five and Six give observed power of 0.061, 0.99 and 0.76 respectively (condition × time for Chapters Four and Six, time for Chapter Five). While observed power should be interpreted cautiously, and should not be used for *post hoc* calculation of sample size suitability (O'Keefe, 2007), a valid use of observed power is for comparison between experiments (Erturk, 2005). Thus, it is of note that there is substantially decreased observed power in Chapter Four.

Power is a function of 1) sample population size 2) magnitude of effect size and 3) precisions of the measure used (Jones et al., 2003). Sample size was consistent between experiments, and effect size would be expected to be reasonably consistent given the hypoxic stimulus was maintained between Chapters, therefore precision is the most likely variable giving this low power score. More confidence should therefore be placed in the findings of Chapters Five and Six. Furthermore, as is stated by the (anonymous) statistics editor in commentary to the work of Erturk (2005), the likelihood of any type one error is substantially reduced (but not removed) in the case of statistically significant results, giving further support to the findings of Chapters Five and Six.

7.4 Recommendations for Future Work

Based on the outcomes of the studies described herein, and in light of the discussion points raised within this Chapter, the following recommendations for future research are made;

1) Confirmation of a role of myostatin in the hypoxic induced atrophy seen in myotubes *in vitro* by **a**) examination of any increase in plasma myostatin in the media of cells exposed to hypoxia and **b**) exposure of myotubes to hypoxia or control environment before exchanging media between models as well as **c**) co-incubation of cells in hypoxia with myostatin inhibitors and / or HIF-1α destabilisers and **d)** exposure of myostatin knock down cells to hypoxia.
2) An examination of the intercellular space within muscle by microdialysis in parallel with muscle biopsies and plasma collection in healthy humans.
3) An examination of the **a**) strength, **b**) muscle atrophy and **c**) mortality of an *in vivo* model when exposed to decreasing concentrations of O_2 with / without a systemic myostatin inhibitor (or wild type and myostatin -/- mice).
4) A comparison of the effect of gender, age, fibre type variation and chronic or evolutionary adaptation on the effects seen here.
5) An examination of hypoxic participants or patients over longer timeframes, bridging the gap between acute time frames examined here and chronic models discussed in the literature.

7.5 Conclusions

Here the effect of acute hypoxia on muscle *in vitro* and *in vivo* is examined in isolation of peripheral confounding factors. The novel findings of this work are;

- Acute hypoxia reduces myoblast migration *in vitro*, and this effect is partially dependent on NF-κB signalling.
- Acute hypoxia reduces myotube size *in vitro* in a time dependent manner, the effect of which may be partially dependent on NF-κB signalling.
- Two hours of hypoxia (11.9 % O_2) decreases muscle myostatin expression following the termination of the hypoxic stimulus, while trends towards increases muscle myostatin expression immediately following 10 hours of hypoxic exposure are seen.
- Plasma myostatin concentration is reduced after 10 hours hypoxia (12.5 % O_2), and also 2 hours following a 2 hours exposure to hypoxia.
- The reduction in plasma myostatin 2 hours after a 2 hour hypoxic stimulation does not appear to be O_2 concentration-dependent within the range of hypoxia measured here (10.7 % or 12.3 % O_2).
- The response of plasma myostatin in a case-study of a high-altitude native Sherpa individual in response to acute hypoxic stimuli is not different from that of unacclimatized lowlander individuals.

In conclusion, it would seem that plasma myostatin concentration is decreased in response to an acute hypoxic exposure in the healthy human. The response of muscle myostatin appears to be time-dependent, with a decrease following 2 hours and a trend towards an increase following 10 hours of hypoxia. These findings suggest hypoxia alone is sufficient to alter myostatin peptide expression; these changes could in part underlie hypoxic-induced atrophy. While future work could examine the role of myostatin inhibition in the prevention of hypoxic-induced atrophy, caution should be applied as this atrophy may be a protective adaption to a limited supply of oxygen.

References

ALCHIN, D. R. 2014. Sarcopenia: describing rather than defining a condition. *J Cachexia Sarcopenia Muscle,* 5**,** 265-8.

ALESSI, D. R. 2001. Discovery of PDK1, one of the missing links in insulin signal transduction. Colworth Medal Lecture. *Biochem Soc Trans,* 29**,** 1-14.

ALESSI, D. R., JAMES, S. R., DOWNES, C. P., HOLMES, A. B., GAFFNEY, P. R., REESE, C. B. & COHEN, P. 1997. Characterization of a 3-phosphoinositide-dependent protein kinase which phosphorylates and activates protein kinase Balpha. *Curr Biol,* 7**,** 261-9.

ALLEN, D. L., HITTEL, D. S. & MCPHERRON, A. C. 2011. Expression and function of myostatin in obesity, diabetes, and exercise adaptation. *Med Sci Sports Exerc,* 43**,** 1828-35.

ALLEN, D. L. & UNTERMAN, T. G. 2007. Regulation of myostatin expression and myoblast differentiation by FoxO and SMAD transcription factors. *Am J Physiol Cell Physiol,* 292**,** C188-99.

ALTSCHUL, S. F., MADDEN, T. L., SCHAFFER, A. A., ZHANG, J., ZHANG, Z., MILLER, W. & LIPMAN, D. J. 1997. Gapped BLAST and PSI-BLAST: a new generation of protein database search programs. *Nucleic acids research,* 25**,** 3389-402.

AMELN, H., GUSTAFSSON, T., SUNDBERG, C. J., OKAMOTO, K., JANSSON, E., POELLINGER, L. & MAKINO, Y. 2005. Physiological activation of hypoxia inducible factor-1 in human skeletal muscle. *Faseb J,* 19**,** 1009-11.

AMIROUCHE, A., DURIEUX, A. C., BANZET, S., KOULMANN, N., BONNEFOY, R., MOURET, C., BIGARD, X., PEINNEQUIN, A. & FREYSSENET, D. 2009. Down-regulation of Akt/mammalian target of rapamycin signaling pathway in response to myostatin overexpression in skeletal muscle. *Endocrinology,* 150**,** 286-94.

AMTHOR, H., OTTO, A., VULIN, A., ROCHAT, A., DUMONCEAUX, J., GARCIA, L., MOUISEL, E., HOURDÉ, C., MACHARIA, R., FRIEDRICHS, M., RELAIX, F., ZAMMIT, P. S., MATSAKAS, A., PATEL, K. & PARTRIDGE, T. 2009. Muscle hypertrophy driven by myostatin blockade does not require stem/precursor-cell activity. *Proc Natl Acad Sci U S A,* 106**,** 7479-7484.

ANDERSEN, P. & SALTIN, B. 1985. Maximal perfusion of skeletal muscle in man. *J Physiol,* 366**,** 233-49.

ANDERSON, S. B., GOLDBERG, A. L. & WHITMAN, M. 2008. Identification of a novel pool of extracellular pro-myostatin in skeletal muscle. *J Biol Chem,* 283**,** 7027-35.

ANG, S. O., CHEN, H., HIROTA, K., GORDEUK, V. R., JELINEK, J., GUAN, Y., LIU, E., SERGUEEVA, A. I., MIASNIKOVA, G. Y., MOLE, D., MAXWELL, P. H., STOCKTON, D. W., SEMENZA, G. L. & PRCHAL, J. T. 2002. Disruption of oxygen homeostasis underlies congenital Chuvash polycythemia. *Nat Genet,* 32**,** 614-21.

ANKER, S. D., NEGASSA, A., COATS, A. J., AFZAL, R., POOLE-WILSON, P. A., COHN, J. N. & YUSUF, S. 2003. Prognostic importance of weight loss in chronic heart failure and the effect of treatment with angiotensin-converting-enzyme inhibitors: an observational study. *Lancet,* 361**,** 1077-83.

APPELHOFF, R. J., TIAN, Y. M., RAVAL, R. R., TURLEY, H., HARRIS, A. L., PUGH, C. W., RATCLIFFE, P. J. & GLEADLE, J. M. 2004. Differential function of the prolyl hydroxylases PHD1, PHD2, and PHD3 in the regulation of hypoxia-inducible factor. *J Biol Chem,* 279**,** 38458-65.

ARANY, Z., FOO, S. Y., MA, Y., RUAS, J. L., BOMMI-REDDY, A., GIRNUN, G., COOPER, M., LAZNIK, D., CHINSOMBOON, J., RANGWALA, S. M., BAEK, K. H., ROSENZWEIG, A. & SPIEGELMAN, B. M. 2008. HIF-independent regulation of VEGF and angiogenesis by the transcriptional coactivator PGC-1alpha. *Nature,* 451**,** 1008-12.

ARTAZA, J. N., BHASIN, S., MALLIDIS, C., TAYLOR, W., MA, K. & GONZALEZ-CADAVID, N. F. 2002. Endogenous expression and localization of myostatin and its relation to myosin heavy chain distribution in C2C12 skeletal muscle cells. *J Cell Physiol,* 190**,** 170-9.

AUGSTEIN, A., POITZ, D. M., BRAUN-DULLAEUS, R. C., STRASSER, R. H. & SCHMEISSER, A. 2011. Cell-specific and hypoxia-dependent regulation of human HIF-3alpha: inhibition of the expression of HIF target genes in vascular cells. *Cell Mol Life Sci,* 68**,** 2627-42.

BAARENDS, E. M., SCHOLS, A. M., MOSTERT, R. & WOUTERS, E. F. 1997. Peak exercise response in relation to tissue depletion in patients with chronic obstructive pulmonary disease. *Eur Respir J,* 10**,** 2807-13.

BARANANO, K. W. & HARTMAN, A. L. 2008. The ketogenic diet: uses in epilepsy and other neurologic illnesses. *Curr Treat Options Neurol,* 10**,** 410-9.

BARNARD, P., ANDRONIKOU, S., POKORSKI, M., SMATRESK, N., MOKASHI, A. & LAHIRI, S. 1987. Time-dependent effect of hypoxia on carotid body chemosensory function. *J Appl Physiol (1985),* 63**,** 685-91.

BEALL, C. M. 2006. Andean, Tibetan, and Ethiopian patterns of adaptation to high-altitude hypoxia. *Integr Comp Biol,* 46**,** 18-24.

BEALL, C. M. 2007. Two routes to functional adaptation: Tibetan and Andean high-altitude natives. *Proc Natl Acad Sci U S A,* 104 Suppl 1**,** 8655-60.

BEAUCHAMP, J. R., HESLOP, L., YU, D. S., TAJBAKHSH, S., KELLY, R. G., WERNIG, A., BUCKINGHAM, M. E., PARTRIDGE, T. A. & ZAMMIT, P. S. 2000. Expression of CD34 and Myf5 defines the majority of quiescent adult skeletal muscle satellite cells. *J Cell Biol,* 151**,** 1221-34.

BELLOT, G., GARCIA-MEDINA, R., GOUNON, P., CHICHE, J., ROUX, D., POUYSSEGUR, J. & MAZURE, N. M. 2009. Hypoxia-induced autophagy is mediated through hypoxia-inducible factor induction of BNIP3 and BNIP3L via their BH3 domains. *Mol Cell Biol,* 29**,** 2570-81.

BERNARD, S., LEBLANC, P., WHITTOM, F., CARRIER, G., JOBIN, J., BELLEAU, R. & MALTAIS, F. 1998. Peripheral muscle weakness in patients with chronic obstructive pulmonary disease. *Am J Respir Crit Care Med,* 158**,** 629-34.

BLOEMBERG, D. & QUADRILATERO, J. 2012. Rapid determination of myosin heavy chain expression in rat, mouse, and human skeletal muscle using multicolor immunofluorescence analysis. *PLoS One,* 7**,** e35273.

BODINE, S. C., LATRES, E., BAUMHUETER, S., LAI, V. K., NUNEZ, L., CLARKE, B. A., POUEYMIROU, W. T., PANARO, F. J., NA, E., DHARMARAJAN, K., PAN, Z. Q., VALENZUELA, D. M., DECHIARA, T. M., STITT, T. N., YANCOPOULOS, G. D. & GLASS, D. J. 2001a. Identification of ubiquitin ligases required for skeletal muscle atrophy. *Science,* 294**,** 1704-8.

BODINE, S. C., STITT, T. N., GONZALEZ, M., KLINE, W. O., STOVER, G. L., BAUERLEIN, R., ZLOTCHENKO, E., SCRIMGEOUR, A., LAWRENCE, J. C., GLASS, D. J. & YANCOPOULOS, G. D. 2001b. Akt/mTOR pathway is a crucial regulator of skeletal muscle hypertrophy and can prevent muscle atrophy in vivo. *Nat Cell Biol,* 3**,** 1014-9.

BONETTO, A., AYDOGDU, T., KUNZEVITZKY, N., GUTTRIDGE, D. C., KHURI, S., KONIARIS, L. G. & ZIMMERS, T. A. 2011. STAT3 activation in skeletal muscle links muscle wasting and the acute phase response in cancer cachexia. *PLoS One,* 6**,** e22538.

BORSI, E., TERRAGNA, C., BRIOLI, A., TACCHETTI, P., MARTELLO, M. & CAVO, M. 2015. Therapeutic targeting of hypoxia and hypoxia-inducible factor 1 alpha in multiple myeloma. *Transl Res,* 165**,** 641-50.

BOTTINELLI, R., BETTO, R., SCHIAFFINO, S. & REGGIANI, C. 1994a. Maximum shortening velocity and coexistence of myosin heavy chain isoforms in single skinned fast fibres of rat skeletal muscle. *J Muscle Res Cell Motil,* 15**,** 413-9.

BOTTINELLI, R., CANEPARI, M., REGGIANI, C. & STIENEN, G. J. 1994b. Myofibrillar ATPase activity during isometric contraction and isomyosin composition in rat single skinned muscle fibres. *J Physiol,* 481 (Pt 3)**,** 663-75.

BOYER, S. J. & BLUME, F. D. 1984. Weight loss and changes in body composition at high altitude. *J Appl Physiol Respir Environ Exerc Physiol,* 57**,** 1580-5.

BOYLE, R. 1660. *New Experiments Physico-Mechanical, Touching the Air,* Oxford: H. Hall, .

BREITBART, A., AUGER-MESSIER, M., MOLKENTIN, J. D. & HEINEKE, J. 2011. Myostatin from the heart: local and systemic actions in cardiac failure and muscle wasting. *Am J Physiol Heart Circ Physiol,* 300**,** H1973-82.

BROOKS, G., RAHEY, T. & BALDWIN, K. 2005. *Exercise physiology: human bioenergetics and its applications,* New York, New York, USA, McGraw-Hill.

BROOKS, G. A. 1986. The lactate shuttle during exercise and recovery. *Med Sci Sports Exerc,* 18**,** 360-8.

BROOKS, G. A., BUTTERFIELD, G. E., WOLFE, R. R., GROVES, B. M., MAZZEO, R. S., SUTTON, J. R., WOLFEL, E. E. & REEVES, J. T. 1991. Increased dependence on blood glucose after acclimatization to 4,300 m. *J Appl Physiol,* 70**,** 919-27.

BUNN, J. A., BUFORD, T. W., SERRA, M. C., KREIDER, R. B. & WILLOUGHBY, D. S. 2011. Protein and Amino Acid Supplementation Does Not Alter Proteolytic Gene Expression following Immobilization. *J Nutr Metab,* 2011**,** 539690.

BURKI, N. K. & TETENTA, S. U. 2014. Inflammatory response to acute hypoxia in humans. *Pulm Pharmacol Ther,* 27**,** 208-11.

BUSHUEV, V. I., MIASNIKOVA, G. Y., SERGUEEVA, A. I., POLYAKOVA, L. A., OKHOTIN, D., GASKIN, P. R., DEBEBE, Z., NEKHAI, S., CASTRO, O. L., PRCHAL, J. T. & GORDEUK, V. R. 2006. Endothelin-1, vascular endothelial growth factor and systolic pulmonary artery pressure in patients with Chuvash polycythemia. *Haematologica,* 91**,** 744-9.

CAI, D., FRANTZ, J. D., TAWA, N. E., JR., MELENDEZ, P. A., OH, B. C., LIDOV, H. G., HASSELGREN, P. O., FRONTERA, W. R., LEE, J., GLASS, D. J. & SHOELSON, S. E. 2004. IKKbeta/NF-kappaB activation causes severe muscle wasting in mice. *Cell,* 119**,** 285-98.

CARON, M. A., THERIAULT, M. E., PARE, M. E., MALTAIS, F. & DEBIGARE, R. 2009. Hypoxia alters contractile protein homeostasis in L6 myotubes. *FEBS Lett*.

CASH, J. N., ANGERMAN, E. B., KATTAMURI, C., NOLAN, K., ZHAO, H., SIDIS, Y., KEUTMANN, H. T. & THOMPSON, T. B. 2012. Structure of myostatin.follistatin-like 3: N-terminal domains of follistatin-type molecules exhibit alternate modes of binding. *J Biol Chem,* 287**,** 1043-53.

CASO, G., GARLICK, B. A., CASELLA, G. A., SASVARY, D. & GARLICK, P. J. 2005. Response of protein synthesis to hypercapnia in rats: independent effects of acidosis and hypothermia. *Metabolism,* 54**,** 841-7.

CASSENS, R. G. & COOPER, C. C. 1971. Red and white muscle. *Adv Food Res,* 19**,** 1-74.

CHAILLOU, T., KOULMANN, N., MEUNIER, A., PUGNIERE, P., MCCARTHY, J. J., BEAUDRY, M. & BIGARD, X. 2014. Ambient hypoxia enhances the loss of muscle mass after extensive injury. *Pflugers Arch,* 466**,** 587-98.

CHAILLOU, T., KOULMANN, N., SIMLER, N., MEUNIER, A., SERRURIER, B., CHAPOT, R., PEINNEQUIN, A., BEAUDRY, M. & BIGARD, X. 2012. Hypoxia transiently affects skeletal muscle hypertrophy in a functional overload model. *Am J Physiol Regul Integr Comp Physiol,* 302**,** R643-54.

CHAMBERS, R. L. & MCDERMOTT, J. C. 1996. Molecular basis of skeletal muscle regeneration. *Can J Appl Physiol,* 21**,** 155-84.

CHAPMAN, R. F., STRAY-GUNDERSEN, J. & LEVINE, B. D. 1998. Individual variation in response to altitude training. *J Appl Physiol (1985),* 85**,** 1448-56.

CHAUDHARY, P., SURYAKUMAR, G., PRASAD, R., SINGH, S. N., ALI, S. & ILAVAZHAGAN, G. 2012. Chronic hypobaric hypoxia mediated skeletal muscle atrophy: role of ubiquitin-proteasome pathway and calpains. *Mol Cell Biochem,* 364**,** 101-13.

CHEN, Y., YE, J., CAO, L., ZHANG, Y., XIA, W. & ZHU, D. 2010. Myostatin regulates glucose metabolism via the AMP-activated protein kinase pathway in skeletal muscle cells. *Int J Biochem Cell Biol,* 42**,** 2072-81.

CHEN, Y. W., GREGORY, C. M., SCARBOROUGH, M. T., SHI, R., WALTER, G. A. & VANDENBORNE, K. 2007. Transcriptional pathways associated with skeletal muscle disuse atrophy in humans. *Physiol Genomics,* 31**,** 510-20.

CHENG, Z. Q., ADI, S., WU, N. Y., HSIAO, D., WOO, E. J., FILVAROFF, E. H., GUSTAFSON, T. A. & ROSENTHAL, S. M. 2000. Functional inactivation of the IGF-I receptor delays differentiation of skeletal muscle cells. *J Endocrinol,* 167**,** 175-82.

CHIA, M., LIAO, C. A., HUANG, C. Y., LEE, W. C., HOU, C. W., YU, S. H., HARRIS, M. B., HSU, T. S., LEE, S. D. & KUO, C. H. 2013. Reducing body fat with altitude hypoxia training in swimmers: role of blood perfusion to skeletal muscles. *Chin J Physiol,* 56**,** 18-25.

CLOSE, R. 1965. The relation between intrinsic speed of shortening and duration of the active state of muscle. *J Physiol,* 180**,** 542-59.

COHEN, J. 1988. *Statistical power analysis for the behavioral sciences,* Hillsdale, N.J., L. Erlbaum Associates.

COONEY, R., KIMBALL, S. R., ECKMAN, R., MAISH, G., 3RD, SHUMATE, M. & VARY, T. C. 1999. TNF-binding protein ameliorates inhibition of skeletal muscle protein synthesis during sepsis. *Am J Physiol,* 276**,** E611-9.

CORNE, S., WEBSTER, K. & YOUNES, M. 2003. Hypoxic respiratory response during acute stable hypocapnia. *Am J Respir Crit Care Med,* 167**,** 1193-9.

CORRICK, K. L., STEC, M. J., MERRITT, E. K., WINDHAM, S. T., THOMAS, S. J., CROSS, J. M. & BAMMAN, M. M. 2015. Serum from human burn victims impairs myogenesis and protein synthesis in primary myoblasts. *Front Physiol,* 6**,** 184.

COSTELLI, P., MUSCARITOLI, M., BONETTO, A., PENNA, F., REFFO, P., BOSSOLA, M., BONELLI, G., DOGLIETTO, G. B., BACCINO, F. M. & FANELLI, F. R. 2008. Muscle myostatin signalling is enhanced in experimental cancer cachexia. *Eur J Clin Invest,* 38**,** 531-8.

COTE, T. R., STROUP, D. F., DWYER, D. M., HORAN, J. M. & PETERSON, D. E. 1993. Chronic obstructive pulmonary disease mortality. A role for altitude. *Chest,* 103**,** 1194-7.

COUX, O., TANAKA, K. & GOLDBERG, A. L. 1996. Structure and functions of the 20S and 26S proteasomes. *Annu Rev Biochem,* 65**,** 801-47.

COX, P. J. & CLARKE, K. 2014. Acute nutritional ketosis: implications for exercise performance and metabolism. *Extrem Physiol Med,* 3**,** 17.

COYLE, E. F. 2005. Improved muscular efficiency displayed as Tour de France champion matures. *J Appl Physiol (1985),* 98**,** 2191-6.

CROSS, D. A., ALESSI, D. R., COHEN, P., ANDJELKOVICH, M. & HEMMINGS, B. A. 1995. Inhibition of glycogen synthase kinase-3 by insulin mediated by protein kinase B. *Nature,* 378**,** 785-9.

CRUZ-JENTOFT, A. J., BAEYENS, J. P., BAUER, J. M., BOIRIE, Y., CEDERHOLM, T., LANDI, F., MARTIN, F. C., MICHEL, J. P., ROLLAND, Y., SCHNEIDER, S. M., TOPINKOVA, E., VANDEWOUDE, M. & ZAMBONI, M. 2010. Sarcopenia: European consensus on definition and diagnosis: Report of the European Working Group on Sarcopenia in Older People. *Age Ageing,* 39**,** 412-23.

D'HULST, G., JAMART, C., VAN THIENEN, R., HESPEL, P., FRANCAUX, M. & DELDICQUE, L. 2013. Effect of acute environmental hypoxia on protein metabolism in human skeletal muscle. *Acta Physiol (Oxf)*.

DARMAUN, D., MATTHEWS, D. E. & BIER, D. M. 1988. Physiological Hypercortisolemia Increases Proteolysis, Glutamine, and Alanine Production. *American Journal of Physiology,* 255**,** E366-E373.

DAWSON, J. A., SARASWAT, A., SIMIONATO, L., THIO, M., KAMLIN, C. O., OWEN, L. S., SCHMOLZER, G. M. & DAVIS, P. G. 2013. Comparison of heart rate and oxygen saturation measurements from Masimo and Nellcor pulse oximeters in newly born term infants. *Acta Paediatr,* 102**,** 955-60.

DE BOER, M. D., SELBY, A., ATHERTON, P., SMITH, K., SEYNNES, O. R., MAGANARIS, C. N., MAFFULLI, N., MOVIN, T., NARICI, M. V. & RENNIE, M. J. 2007. The temporal responses of protein synthesis, gene expression and cell signalling in human quadriceps muscle and patellar tendon to disuse. *J Physiol,* 585**,** 241-51.

DE THEIJE, C. C., LANGEN, R. C., LAMERS, W. H., SCHOLS, A. M. & KOHLER, S. E. 2013. Distinct responses of protein turnover regulatory pathways in hypoxia- and semistarvation-induced muscle atrophy. *Am J Physiol Lung Cell Mol Physiol,* 305**,** L82-91.

DEBIGARE, R., COTE, C. H. & MALTAIS, F. 2001. Peripheral muscle wasting in chronic obstructive pulmonary disease. Clinical relevance and mechanisms. *Am J Respir Crit Care Med,* 164**,** 1712-7.

DELDICQUE, L., MASSCHELEIN, E., VAN THIENEN, R., D'HULST, G., HESPEL, P. & THOMIS, M. 2014. Acute environmental hypoxia activates autophagy in human skeletal muscle. *FASEB,* 28.

DENT, P., LAVOINNE, A., NAKIELNY, S., CAUDWELL, F. B., WATT, P. & COHEN, P. 1990. The molecular mechanism by which insulin stimulates glycogen synthesis in mammalian skeletal muscle. *Nature,* 348**,** 302-8.

DI FRANCIA, M., BARBIER, D., MEGE, J. L. & OREHEK, J. 1994. Tumor necrosis factor-alpha levels and weight loss in chronic obstructive pulmonary disease. *Am J Respir Crit Care Med,* 150**,** 1453-5.

DIETRICHSON, P., COAKLEY, J., SMITH, P. E., GRIFFITHS, R. D., HELLIWELL, T. R. & EDWARDS, R. H. 1987. Conchotome and needle percutaneous biopsy of skeletal muscle. *J Neurol Neurosur Ps,* 50**,** 1461-7.

DIRKS, M. L., WALL, B. T., SNIJDERS, T., OTTENBROS, C. L., VERDIJK, L. B. & VAN LOON, L. J. 2014. Neuromuscular electrical stimulation prevents muscle disuse atrophy during leg immobilization in humans. *Acta Physiol (Oxf),* 210**,** 628-41.

DOUCET, M., RUSSELL, A. P., LEGER, B., DEBIGARE, R., JOANISSE, D. R., CARON, M. A., LEBLANC, P. & MALTAIS, F. 2007. Muscle atrophy and hypertrophy signaling in patients with chronic obstructive pulmonary disease. *Am J Respir Crit Care Med,* 176**,** 261-9.

DRUMMOND, G. B. & VOWLER, S. L. 2012. Do as you would be done by: write as you would wish to read. *J Physiol,* 590**,** 6251-4.

DRUMMOND, M. J., FUJITA, S., ABE, T., DREYER, H. C., VOLPI, E. & RASMUSSEN, B. B. 2008. Human muscle gene expression following resistance exercise and blood flow restriction. *Med Sci Sports Exerc,* 40**,** 691-8.

DUPLAIN, H., VOLLENWEIDER, L., DELABAYS, A., NICOD, P., BARTSCH, P. & SCHERRER, U. 1999. Augmented sympathetic activation during short-term hypoxia and high-altitude exposure in subjects susceptible to high-altitude pulmonary edema. *Circulation,* 99**,** 1713-8.

EASTON, P. A., SLYKERMAN, L. J. & ANTHONISEN, N. R. 1986. Ventilatory response to sustained hypoxia in normal adults. *J Appl Physiol (1985),* 61**,** 906-11.

ECKARDT, K. U., BOUTELLIER, U., KURTZ, A., SCHOPEN, M., KOLLER, E. A. & BAUER, C. 1989. Rate of erythropoietin formation in humans in response to acute hypobaric hypoxia. *J Appl Physiol (1985),* 66**,** 1785-8.

EDVARDSEN, A., AKERO, A., CHRISTENSEN, C. C., RYG, M. & SKJONSBERG, O. H. 2012. Air travel and chronic obstructive pulmonary disease: a new algorithm for pre-flight evaluation. *Thorax,* 67**,** 964-9.

EDWARDS, C., CANFIELD, J., COPES, N., REHAN, M., LIPPS, D. & BRADSHAW, P. C. 2014. D-beta-hydroxybutyrate extends lifespan in C. elegans. *Aging (Albany NY),* 6**,** 621-44.

EID, A. A., IONESCU, A. A., NIXON, L. S., LEWIS-JENKINS, V., MATTHEWS, S. B., GRIFFITHS, T. L. & SHALE, D. J. 2001. Inflammatory response and body composition in chronic obstructive pulmonary disease. *Am J Respir Crit Care Med,* 164**,** 1414-8.

EL-KHOURY, R., BRADFORD, A. & O'HALLORAN, K. D. 2012. Chronic hypobaric hypoxia increases isolated rat fast-twitch and slow-twitch limb muscle force and fatigue. *Physiol Res,* 61**,** 195-201.

ELLIOTT, B., RENSHAW, D., GETTING, S. & MACKENZIE, R. 2012. The central role of myostatin in skeletal muscle and whole body homeostasis. *Acta Physiol (Oxf),* 205**,** 324-40.

ELLIOTT, B. T., PARE, M., DEBIGARE, R. & MALTAIS, F. LPS-Induced Inflammation Regulates Myostatin and Myotube Homeostasis In Vitro. Am J Respir Crit Care Med, April 1, 2009 2009. A4195-.

ELTZSCHIG, H. K. & CARMELIET, P. 2011. Hypoxia and inflammation. *N Engl J Med,* 364**,** 656-65.

ENNION, S., SANT'ANA PEREIRA, J., SARGEANT, A. J., YOUNG, A. & GOLDSPINK, G. 1995. Characterization of human skeletal muscle fibres according to the myosin heavy chains they express. *J Muscle Res Cell Motil,* 16**,** 35-43.

EPSTEIN, A. C., GLEADLE, J. M., MCNEILL, L. A., HEWITSON, K. S., O'ROURKE, J., MOLE, D. R., MUKHERJI, M., METZEN, E., WILSON, M. I., DHANDA, A., TIAN, Y. M., MASSON, N., HAMILTON, D. L., JAAKKOLA, P., BARSTEAD, R., HODGKIN, J., MAXWELL, P. H., PUGH, C. W., SCHOFIELD, C. J. & RATCLIFFE, P. J. 2001. C. elegans EGL-9 and mammalian homologs define a family of dioxygenases that regulate HIF by prolyl hydroxylation. *Cell,* 107**,** 43-54.

ERTURK, S. M. 2005. Retrospective power analysis: when? *Radiology,* 237**,** 743; author reply 743; discussion 743-4.

ETHERIDGE, T., ATHERTON, P. J., WILKINSON, D., SELBY, A., RANKIN, D., WEBBORN, N., SMITH, K. & WATT, P. W. 2011. Effects of hypoxia on muscle protein synthesis (MPS) and anabolic signaling at rest and in response to acute resistance exercise. *Am J Physiol Endocrinol Metab*.

FAGRAEUS, L., KARLSSON, J., LINNARSSON, D. & SALTIN, B. 1973. Oxygen uptake during maximal work at lowered and raised ambient air pressures. *Acta Physiol Scand,* 87**,** 411-21.

FAISS, R., PIALOUX, V., SARTORI, C., FAES, C., DERIAZ, O. & MILLET, G. P. 2013. Ventilation, oxidative stress, and nitric oxide in hypobaric versus normobaric hypoxia. *Med Sci Sports Exerc,* 45**,** 253-60.

FANDREY, J., GORR, T. A. & GASSMANN, M. 2006. Regulating cellular oxygen sensing by hydroxylation. *Cardiovasc Res,* 71**,** 642-51.

FAVIER, F. B., COSTES, F., DEFOUR, A., BONNEFOY, R., LEFAI, E., BAUGE, S., PEINNEQUIN, A., BENOIT, H. & FREYSSENET, D. 2010. Downregulation of Akt/mammalian target of rapamycin pathway in skeletal muscle is associated with increased REDD1 expression in response to chronic hypoxia. *Am J Physiol Regul Integr Comp Physiol,* 298**,** R1659-66.

FEARON, K. C., HANSELL, D. T., PRESTON, T., PLUMB, J. A., DAVIES, J., SHAPIRO, D., SHENKIN, A., CALMAN, K. C. & BURNS, H. J. 1988. Influence of whole body protein turnover rate on resting energy expenditure in patients with cancer. *Cancer Res,* 48**,** 2590-5.

FEINER, J. R., SEVERINGHAUS, J. W. & BICKLER, P. E. 2007. Dark skin decreases the accuracy of pulse oximeters at low oxygen saturation: the effects of oximeter probe type and gender. *Anesth Analg,* 105**,** S18-23, tables of contents.

FERRANDO, A. A., LANE, H. W., STUART, C. A., DAVIS-STREET, J. & WOLFE, R. R. 1996. Prolonged bed rest decreases skeletal muscle and whole body protein synthesis. *Am J Physiol,* 270**,** E627-33.

FLUECK, M. 2009. Plasticity of the muscle proteome to exercise at altitude. *High Alt Med Biol,* 10**,** 183-93.

FORMENTI, F., CONSTANTIN-TEODOSIU, D., EMMANUEL, Y., CHEESEMAN, J., DORRINGTON, K. L., EDWARDS, L. M., HUMPHREYS, S. M., LAPPIN, T. R., MCMULLIN, M. F., MCNAMARA, C. J., MILLS, W., MURPHY, J. A., O'CONNOR, D. F., PERCY, M. J., RATCLIFFE, P. J., SMITH, T. G., TREACY, M., FRAYN, K. N., GREENHAFF, P. L., KARPE, F., CLARKE, K. & ROBBINS, P. A. 2010. Regulation of human metabolism by hypoxia-inducible factor. *Proc Natl Acad Sci U S A,* 107**,** 12722-7.

FRAYSER, R., RENNIE, I. D., GRAY, G. W. & HOUSTON, C. S. 1975. Hormonal and electrolyte response to exposure to 17,500 ft. *J Appl Physiol,* 38**,** 636-42.

FRIEDMANN, B., FRESE, F., MENOLD, E., KAUPER, F., JOST, J. & BARTSCH, P. 2005. Individual variation in the erythropoietic response to altitude training in elite junior swimmers. *Br J Sports Med,* 39**,** 148-53.

FROST, R. A., NYSTROM, G. J., JEFFERSON, L. S. & LANG, C. H. 2007. Hormone, cytokine, and nutritional regulation of sepsis-induced increases in atrogin-1 and MuRF1 in skeletal muscle. *Am J Physiol Endocrinol Metab,* 292**,** E501-12.

FROST, R. A., NYSTROM, G. J. & LANG, C. H. 2002. Lipopolysaccharide regulates proinflammatory cytokine expression in mouse myoblasts and skeletal muscle. *Am J Physiol Regul Integr Comp Physiol,* 283**,** R698-709.

FRYBURG, D. A. & BARRETT, E. J. 1993. Growth hormone acutely stimulates skeletal muscle but not whole-body protein synthesis in humans. *Metabolism,* 42**,** 1223-7.

GABBASOV, R. T., ARKHIPOVA, A. A., BORISOVA, A. V., HAKIMULLINA, A. M., KUZNETSOVA, A. V., WILLIAMS, A. G., DAY, S. H. & AHMETOV, II 2013. The HIF1A gene Pro582Ser polymorphism in Russian strength athletes. *J Strength Cond Res,* 27**,** 2055-8.

GARATACHEA, N., PINOS, T., CAMARA, Y., RODRIGUEZ-ROMO, G., EMANUELE, E., RICEVUTI, G., VENTURINI, L., SANTOS-LOZANO, A., SANTIAGO-DORREGO, C., FIUZA-LUCES, C., YVERT, T., ANDREU, A. L. & LUCIA, A. 2013. Association of the K153R polymorphism in the myostatin gene and extreme longevity. *Age (Dordr),* 35**,** 2445-54.

GE, R. L., WITKOWSKI, S., ZHANG, Y., ALFREY, C., SIVIERI, M., KARLSEN, T., RESALAND, G. K., HARBER, M., STRAY-GUNDERSEN, J. & LEVINE, B. D. 2002. Determinants of erythropoietin release in response to short-term hypobaric hypoxia. *J Appl Physiol (1985),* 92**,** 2361-7.

GENTRY, B. A., FERREIRA, J. A., PHILLIPS, C. L. & BROWN, M. 2010. Hindlimb skeletal muscle function in myostatin-deficient mice. *Muscle Nerve,* 43**,** 49-57.

GEORGE, T., VELLOSO, C. P., ALSHARIDAH, M., LAZARUS, N. R. & HARRIDGE, S. D. 2010. Sera from young and older humans equally sustain proliferation and differentiation of human myoblasts. *Exp Gerontol,* 45**,** 875-81.

GIATROMANOLAKI, A., KOUKOURAKIS, M. I., SIVRIDIS, E., TURLEY, H., TALKS, K., PEZZELLA, F., GATTER, K. C. & HARRIS, A. L. 2001. Relation of hypoxia inducible factor 1 alpha and 2 alpha in operable non-small cell lung cancer to angiogenic/molecular profile of tumours and survival. *Br J Cancer,* 85**,** 881-90.

GILSON, H., SCHAKMAN, O., COMBARET, L., LAUSE, P., GROBET, L., ATTAIX, D., KETELSLEGERS, J. M. & THISSEN, J. P. 2007. Myostatin gene deletion prevents glucocorticoid-induced muscle atrophy. *Endocrinology,* 148**,** 452-60.

GLEASON, J. E., CORRIGAN, D. J., COX, J. E., REDDI, A. R., MCGINNIS, L. A. & CULOTTA, V. C. 2011. Analysis of hypoxia and hypoxia-like states through metabolite profiling. *PLoS One,* 6**,** e24741.

GOLDBERG, M. A., DUNNING, S. P. & BUNN, H. F. 1988. Regulation of the erythropoietin gene: evidence that the oxygen sensor is a heme protein. *Science,* 242**,** 1412-5.

GOLDSPINK, D. F. 1986. Muscle proteinase activities during compensatory growth and atrophy. *Experientia,* 42**,** 133-4.

GOLDSPINK, D. F., GARLICK, P. J. & MCNURLAN, M. A. 1983. Protein turnover measured in vivo and in vitro in muscles undergoing compensatory growth and subsequent denervation atrophy. *Biochem J,* 210**,** 89-98.

GOLDSTEIN, G., SCHEID, M., HAMMERLING, U., SCHLESINGER, D. H., NIALL, H. D. & BOYSE, E. A. 1975. Isolation of a polypeptide that has lymphocyte-differentiating properties and is probably represented universally in living cells. *Proc Natl Acad Sci U S A,* 72**,** 11-5.

GOLLNICK, P. D., ARMSTRONG, R. B., SALTIN, B., SAUBERT, C. W. T., SEMBROWICH, W. L. & SHEPHERD, R. E. 1973. Effect of training on enzyme activity and fiber composition of human skeletal muscle. *J Appl Physiol,* 34**,** 107-11.

GOMES, M. D., LECKER, S. H., JAGOE, R. T., NAVON, A. & GOLDBERG, A. L. 2001. Atrogin-1, a muscle-specific F-box protein highly expressed during muscle atrophy. *Proc Natl Acad Sci U S A,* 98**,** 14440-5.

GONCALVES, M. D., PISTILLI, E. E., BALDUZZI, A., BIRNBAUM, M. J., LACHEY, J., KHURANA, T. S. & AHIMA, R. S. 2010. Akt deficiency attenuates muscle size and function but not the response to ActRIIB inhibition. *PLoS One,* 5**,** e12707.

GONZALEZ-CADAVID, N. F., TAYLOR, W. E., YARASHESKI, K., SINHA-HIKIM, I., MA, K., EZZAT, S., SHEN, R., LALANI, R., ASA, S., MAMITA, M., NAIR, G., ARVER, S. & BHASIN, S. 1998. Organization of the human myostatin gene and expression in healthy men and HIV-infected men with muscle wasting. *Proc Natl Acad Sci U S A,* 95**,** 14938-43.

GORDON, A. M., HOMSHER, E. & REGNIER, M. 2000. Regulation of contraction in striated muscle. *Physiol Rev,* 80**,** 853-924.

GORE, C. J., HAHN, A. G., AUGHEY, R. J., MARTIN, D. T., ASHENDEN, M. J., CLARK, S. A., GARNHAM, A. P., ROBERTS, A. D., SLATER, G. J. & MCKENNA, M. J. 2001. Live high:train low increases muscle buffer capacity and submaximal cycling efficiency. *Acta Physiol Scand,* 173**,** 275-86.

GOTHGEN, I. H., SIGGAARD-ANDERSEN, O. & KOKHOLM, G. 1990. Variations in the hemoglobin-oxygen dissociation curve in 10079 arterial blood samples. *Scand J Clin Lab Invest Suppl,* 203**,** 87-90.

GREEN, H., MACDOUGALL, J., TARNOPOLSKY, M. & MELISSA, N. L. 1999. Downregulation of Na+-K+-ATPase pumps in skeletal muscle with training in normobaric hypoxia. *J Appl Physiol (1985),* 86**,** 1745-8.

GREEN, H. J., SUTTON, J. R., CYMERMAN, A., YOUNG, P. M. & HOUSTON, C. S. 1989. Operation Everest II: adaptations in human skeletal muscle. *J Appl Physiol (1985),* 66**,** 2454-61.

GREENHOUSE, S. & GEISSER, S. 1959. On methods in the analysis of profile data. *Psychometrika,* 24**,** 95-112.

GRIMSHAW, M. J. & MASON, R. M. 2000. Bovine articular chondrocyte function in vitro depends upon oxygen tension. *Osteoarthritis Cartilage,* 8**,** 386-92.

GROBET, L., MARTIN, L. J., PONCELET, D., PIROTTIN, D., BROUWERS, B., RIQUET, J., SCHOEBERLEIN, A., DUNNER, S., MENISSIER, F., MASSABANDA, J., FRIES, R., HANSET, R. & GEORGES, M. 1997. A deletion in the bovine myostatin gene causes the double-muscled phenotype in cattle. *Nat Genet,* 17**,** 71-4.

GROCOTT, M. P., MARTIN, D. S., LEVETT, D. Z., MCMORROW, R., WINDSOR, J. & MONTGOMERY, H. E. 2009. Arterial blood gases and oxygen content in climbers on Mount Everest. *N Engl J Med,* 360**,** 140-9.

GRUSON, D., AHN, S. A., KETELSLEGERS, J. M. & ROUSSEAU, M. F. 2011. Increased plasma myostatin in heart failure. *Eur J Heart Fail*.

GUO, J., TIAN, T., LU, D., XIA, G., WANG, H. & DONG, M. 2012. Alterations of maternal serum and placental follistatin-like 3 and myostatin in pre-eclampsia. *J Obstet Gynaecol Res,* 38**,** 988-96.

GUTTRIDGE, D. C., MAYO, M. W., MADRID, L. V., WANG, C. Y. & BALDWIN, A. S., JR. 2000. NF-kappaB-induced loss of MyoD messenger RNA: possible role in muscle decay and cachexia. *Science,* 289**,** 2363-6.

HACKETT, P. H., REEVES, J. T., REEVES, C. D., GROVER, R. F. & RENNIE, D. 1980. Control of breathing in Sherpas at low and high altitude. *J Appl Physiol Respir Environ Exerc Physiol,* 49**,** 374-9.

HANNON, J. P., SHIELDS, J. L. & HARRIS, C. W. 1969. Effects of altitude acclimatization on blood composition of women. *J Appl Physiol,* 26**,** 540-7.

HANSEN, J. M., KANSTRUP, I. L., RICHALET, J. P. & OLSEN, N. V. 1996. High altitude-induced albuminuria in normal man is enhanced by infusion of low-dose dopamine. *Scand J Clin Lab Invest,* 56**,** 367-72.

HARA, S., HAMADA, J., KOBAYASHI, C., KONDO, Y. & IMURA, N. 2001. Expression and characterization of hypoxia-inducible factor (HIF)-3alpha in human kidney: suppression of HIF-mediated gene expression by HIF-3alpha. *Biochem Biophys Res Commun,* 287**,** 808-13.

HARRIDGE, S. D., KRYGER, A. & STENSGAARD, A. 1999. Knee extensor strength, activation, and size in very elderly people following strength training. *Muscle Nerve,* 22**,** 831-9.

HARVEY, E. N. 1928. The Oxygen Consumption of Luminous Bacteria. *J Gen Physiol,* 11**,** 469-75.

HAUERSLEV, S., VISSING, J. & KRAG, T. O. 2014. Muscle atrophy reversed by growth factor activation of satellite cells in a mouse muscle atrophy model. *PLoS One,* 9**,** e100594.

HAUGEN, H. A., CHAN, L. N. & LI, F. 2007. Indirect calorimetry: a practical guide for clinicians. *Nutr Clin Pract,* 22**,** 377-88.

HAWKE, T. J. & GARRY, D. J. 2001. Myogenic satellite cells: physiology to molecular biology. *J Appl Physiol,* 91**,** 534-51.

HAYOT, M., RODRIGUEZ, J., VERNUS, B., CARNAC, G., JEAN, E., ALLEN, D., GORET, L., OBERT, P., CANDAU, R. & BONNIEU, A. 2011. Myostatin up-regulation is associated with the skeletal muscle response to hypoxic stimuli. *Mol Cell Endocrinol,* 332**,** 38-47.

HERSHKO, A., CIECHANOVER, A., HELLER, H., HAAS, A. L. & ROSE, I. A. 1980. Proposed role of ATP in protein breakdown: conjugation of protein with multiple chains of the polypeptide of ATP-dependent proteolysis. *Proc Natl Acad Sci U S A,* 77**,** 1783-6.

HEYES, M. P., FARBER, M. O., MANFREDI, F., ROBERTSHAW, D., WEINBERGER, M., FINEBERG, N. & ROBERTSON, G. 1982. Acute effects of hypoxia on renal and endocrine function in normal humans. *Am J Physiol,* 243**,** R265-70.

HILL, J. J., DAVIES, M. V., PEARSON, A. A., WANG, J. H., HEWICK, R. M., WOLFMAN, N. M. & QIU, Y. 2002. The myostatin propeptide and the follistatin-related gene are inhibitory binding proteins of myostatin in normal serum. *J Biol Chem,* 277**,** 40735-41.

HILL, J. J., QIU, Y., HEWICK, R. M. & WOLFMAN, N. M. 2003. Regulation of myostatin in vivo by growth and differentiation factor-associated serum protein-1: a novel protein with protease inhibitor and follistatin domains. *Mol Endocrinol,* 17**,** 1144-54.

HIROFUJI, C., ISHIHARA, A., ITOH, K., ITOH, M., TAGUCHI, S. & TAKEUCHI-HAYASHI, H. 1992. Fibre type composition of the soleus muscle in hypoxia-acclimatised rats. *J Anat,* 181 (Pt 2)**,** 327-33.

HOFFMAN, C. E., CLARK, R. T., JR. & BROWN, E. B., JR. 1946. Blood oxygen saturations and duration of consciousness in anoxia at high altitudes. *Am J Physiol,* 145**,** 685-92.

HOFFMAN, E. P., KNUDSON, C. M., CAMPBELL, K. P. & KUNKEL, L. M. 1987. Subcellular fractionation of dystrophin to the triads of skeletal muscle. *Nature,* 330**,** 754-8.

HOLLOWAY, C. J., MONTGOMERY, H. E., MURRAY, A. J., COCHLIN, L. E., CODREANU, I., HOPWOOD, N., JOHNSON, A. W., RIDER, O. J., LEVETT, D. Z., TYLER, D. J., FRANCIS, J. M., NEUBAUER, S., GROCOTT, M. P. & CLARKE, K. 2011. Cardiac response to hypobaric hypoxia: persistent changes in cardiac mass, function, and energy metabolism after a trek to Mt. Everest Base Camp. *Faseb J,* 25**,** 792-6.

HOLM, L., HASLUND, M. L., ROBACH, P., VAN HALL, G., CALBET, J. A., SALTIN, B. & LUNDBY, C. 2010. Skeletal muscle myofibrillar and sarcoplasmic protein synthesis rates are affected differently by altitude-induced hypoxia in native lowlanders. *PLoS One,* 5**,** e15606.

HOPKINS, S. R. & POWELL, F. L. 2001. Common themes of adaptation to hypoxia. Insights from comparative physiology. *Adv Exp Med Biol,* 502**,** 153-67.

HOPKINS, W. G., BATTERHAM, A. M., IMPELLIZZERI, F. M., PYNE, D. B. & ROWLANDS, D. S. 2011. Statistical perspectives: all together NOT. *J Physiol,* 589**,** 5327-9; author reply 5331-2.

HOPPELER, H., KLEINERT, E., SCHLEGEL, C., CLAASSEN, H., HOWALD, H., KAYAR, S. R. & CERRETELLI, P. 1990. Morphological adaptations of human skeletal muscle to chronic hypoxia. *Int J Sports Med,* 11 Suppl 1**,** S3-9.

HOPPELER, H., VOGT, M., WEIBEL, E. R. & FLUCK, M. 2003. Response of skeletal muscle mitochondria to hypoxia. *Exp Physiol,* 88**,** 109-19.

HORSCROFT, J. A. & MURRAY, A. J. 2014. Skeletal muscle energy metabolism in environmental hypoxia: climbing towards consensus. *Extrem Physiol Med,* 3**,** 19.

HOUSH, D. J., HOUSH, T. J., JOHNSON, G. O. & CHU, W. K. 1992. Hypertrophic response to unilateral concentric isokinetic resistance training. *J Appl Physiol (1985),* 73**,** 65-70.

HOWARD, L. S., BARSON, R. A., HOWSE, B. P., MCGILL, T. R., MCINTYRE, M. E., O'CONNOR, D. F. & ROBBINS, P. A. 1995. Chamber for controlling end-tidal gas tensions over sustained periods in humans. *J Appl Physiol (1985),* 78**,** 1088-91.

HUERTA-SANCHEZ, E., JIN, X., ASAN, BIANBA, Z., PETER, B. M., VINCKENBOSCH, N., LIANG, Y., YI, X., HE, M., SOMEL, M., NI, P., WANG, B., OU, X., HUASANG, LUOSANG, J., CUO, Z. X., LI, K., GAO, G., YIN, Y., WANG, W., ZHANG, X., XU, X., YANG, H., LI, Y., WANG, J. & NIELSEN, R. 2014. Altitude adaptation in Tibetans caused by introgression of Denisovan-like DNA. *Nature,* 512**,** 194-7.

HUET, C., LI, Z. F., LIU, H. Z., BLACK, R. A., GALLIANO, M. F. & ENGVALL, E. 2001. Skeletal muscle cell hypertrophy induced by inhibitors of metalloproteases; myostatin as a potential mediator. *Am J Physiol Cell Physiol,* 281**,** C1624-34.

HUEY, R. B., SALISBURY, R., WANG, J. L. & MAO, M. 2007. Effects of age and gender on success and death of mountaineers on Mount Everest. *Biol Lett,* 3**,** 498-500.

HULMI, J. J., KOVANEN, V., LISKO, I., SELANNE, H. & MERO, A. A. 2008. The effects of whey protein on myostatin and cell cycle-related gene expression responses to a single heavy resistance exercise bout in trained older men. *Eur J Appl Physiol,* 102**,** 205-13.

IMOBERDORF, R., GARLICK, P. J., MCNURLAN, M. A., CASELLA, G. A., MARINI, J. C., TURGAY, M., BARTSCH, P. & BALLMER, P. E. 2006. Skeletal muscle protein synthesis after active or passive ascent to high altitude. *Med Sci Sports Exerc,* 38**,** 1082-7.

IYER, N. V., KOTCH, L. E., AGANI, F., LEUNG, S. W., LAUGHNER, E., WENGER, R. H., GASSMANN, M., GEARHART, J. D., LAWLER, A. M., YU, A. Y. & SEMENZA, G. L. 1998. Cellular and developmental control of O2 homeostasis by hypoxia-inducible factor 1 alpha. *Genes Dev,* 12**,** 149-62.

JACKMAN, R. W. & KANDARIAN, S. C. 2004. The molecular basis of skeletal muscle atrophy. *Am J Physiol Cell Physiol,* 287**,** C834-43.

JACOBS, R. A., BOUSHEL, R., WRIGHT-PARADIS, C., CALBET, J. A., ROBACH, P., GNAIGER, E. & LUNDBY, C. 2013. Mitochondrial function in human skeletal muscle following high-altitude exposure. *Exp Physiol,* 98**,** 245-55.

JANSSEN, I., HEYMSFIELD, S. B., WANG, Z. M. & ROSS, R. 2000. Skeletal muscle mass and distribution in 468 men and women aged 18-88 yr. *J Appl Physiol (1985),* 89**,** 81-8.

JEANPLONG, F., BASS, J. J., SMITH, H. K., KIRK, S. P., KAMBADUR, R., SHARMA, M. & OLDHAM, J. M. 2003. Prolonged underfeeding of sheep increases myostatin and myogenic regulatory factor Myf-5 in skeletal muscle while IGF-I and myogenin are repressed. *J Endocrinol,* 176**,** 425-37.

JENNETT, S. 1969. Changes in ventilation and heart rate during and after brief moderate hypoxia in resting man. *J Physiol,* 200**,** 106P-107P.

JESPERSEN, J. G., NEDERGAARD, A., ANDERSEN, L. L., SCHJERLING, P. & ANDERSEN, J. L. 2011. Myostatin expression during human muscle hypertrophy and subsequent atrophy: increased myostatin with detraining. *Scand J Med Sci Sports,* 21**,** 215-23.

JI, M., ZHANG, Q., YE, J., WANG, X., YANG, W. & ZHU, D. 2008. Myostatin induces p300 degradation to silence cyclin D1 expression through the PI3K/PTEN/Akt pathway. *Cell Signal,* 20**,** 1452-8.

JIANG, M. S., LIANG, L. F., WANG, S., RATOVITSKI, T., HOLMSTROM, J., BARKER, C. & STOTISH, R. 2004. Characterization and identification of the inhibitory domain of GDF-8 propeptide. *Biochem Biophys Res Commun,* 315**,** 525-31.

JOBIN, J., MALTAIS, F., DOYON, J. F., LEBLANC, P., SIMARD, P. M., SIMARD, A. A. & SIMARD, C. 1998. Chronic obstructive pulmonary disease: capillarity and fiber-type characteristics of skeletal muscle. *J Cardiopulm Rehabil,* 18**,** 432-7.

JONES, S. R., CARLEY, S. & HARRISON, M. 2003. An introduction to power and sample size estimation. *Emerg Med J,* 20**,** 453-8.

JOSEPHSON, R. K. 1993. Contraction dynamics and power output of skeletal muscle. *Annu Rev Physiol,* 55**,** 527-46.

JOSHI, D., PATEL, H., BAKER, D. M., SHIWEN, X., ABRAHAM, D. J. & TSUI, J. C. 2011. Development of an in vitro model of myotube ischemia. *Lab Invest,* 91**,** 1241-52.

JUNG, R. C., DILL, D. B., HORTON, R. & HORVATH, S. M. 1971. Effects of age on plasma aldosterone levels and hemoconcentration at altitude. *J Appl Physiol,* 31**,** 593-7.

KADI, F., ERIKSSON, A., HOLMNER, S., BUTLER-BROWNE, G. S. & THORNELL, L. E. 1999. Cellular adaptation of the trapezius muscle in strength-trained athletes. *Histochem Cell Biol,* 111**,** 189-95.

KADI, F., SCHJERLING, P., ANDERSEN, L. L., CHARIFI, N., MADSEN, J. L., CHRISTENSEN, L. R. & ANDERSEN, J. L. 2004. The effects of heavy resistance training and detraining on satellite cells in human skeletal muscles. *J Physiol,* 558**,** 1005-12.

KALCKAR, H. M. 1991. 50 years of biological research--from oxidative phosphorylation to energy requiring transport regulation. *Annu Rev Biochem,* 60**,** 1-37.

KALLMAN, D. A., PLATO, C. C. & TOBIN, J. D. 1990. The role of muscle loss in the age-related decline of grip strength: cross-sectional and longitudinal perspectives. *J Gerontol,* 45**,** M82-8.

KAMBADUR, R., SHARMA, M., SMITH, T. P. & BASS, J. J. 1997. Mutations in myostatin (GDF8) in double-muscled Belgian Blue and Piedmontese cattle. *Genome Res,* 7**,** 910-6.

KELLY, K. R., WILLIAMSON, D. L., FEALY, C. E., KRIZ, D. A., KRISHNAN, R. K., HUANG, H., AHN, J., LOOMIS, J. L. & KIRWAN, J. P. 2010. Acute altitude-induced hypoxia suppresses plasma glucose and leptin in healthy humans. *Metabolism,* 59**,** 200-5.

KIM, J. S., PETRELLA, J. K., CROSS, J. M. & BAMMAN, M. M. 2007. Load-mediated downregulation of myostatin mRNA is not sufficient to promote myofiber hypertrophy in humans: a cluster analysis. *J Appl Physiol (1985),* 103**,** 1488-95.

KIRK, S., OLDHAM, J., KAMBADUR, R., SHARMA, M., DOBBIE, P. & BASS, J. 2000. Myostatin regulation during skeletal muscle regeneration. *J Cell Physiol,* 184**,** 356-63.

KON, M., IKEDA, T., HOMMA, T., AKIMOTO, T., SUZUKI, Y. & KAWAHARA, T. 2010. Effects of acute hypoxia on metabolic and hormonal responses to resistance exercise. *Med Sci Sports Exerc,* 42**,** 1279-85.

KOONG, A. C., CHEN, E. Y. & GIACCIA, A. J. 1994a. Hypoxia causes the activation of nuclear factor kappa B through the phosphorylation of I kappa B alpha on tyrosine residues. *Cancer Res,* 54**,** 1425-30.

KOONG, A. C., CHEN, E. Y., MIVECHI, N. F., DENKO, N. C., STAMBROOK, P. & GIACCIA, A. J. 1994b. Hypoxic activation of nuclear factor-kappa B is mediated by a Ras and Raf signaling pathway and does not involve MAP kinase (ERK1 or ERK2). *Cancer Res,* 54**,** 5273-9.

KRANTZ, S. B. 1991. Erythropoietin. *Blood,* 77**,** 419-34.

KRIEGENBURG, F., SEEGER, M., SAEKI, Y., TANAKA, K., LAURIDSEN, A. M., HARTMANN-PETERSEN, R. & HENDIL, K. B. 2008. Mammalian 26S proteasomes remain intact during protein degradation. *Cell,* 135**,** 355-65.

KRIVICKAS, L. S., DORER, D. J., OCHALA, J. & FRONTERA, W. R. 2011. Relationship between force and size in human single muscle fibres. *Exp Physiol,* 96**,** 539-47.

KUNG, T., SZABO, T., SPRINGER, J., DOEHNER, W., ANKER, S. D. & VON HAEHLING, S. 2011. Cachexia in heart disease: highlights from the ESC 2010. *J Cachexia Sarcopenia Muscle,* 2**,** 63-69.

LANDGRAF, H., SCHULTE-HUERMANN, D., VALLBRACHT, C. & EHRLY, A. M. 1994. Muscle tissue PO2 during moderate altitude exposure in patients with peripheral arterial occlusive disease. *Presse Med,* 23**,** 164-8.

LANG, C. H. & FROST, R. A. 2007. Sepsis-induced suppression of skeletal muscle translation initiation mediated by tumor necrosis factor alpha. *Metabolism,* 56**,** 49-57.

LANG, C. H., KRAWIEC, B. J., HUBER, D., MCCOY, J. M. & FROST, R. A. 2006. Sepsis and inflammatory insults downregulate IGFBP-5, but not IGFBP-4, in skeletal muscle via a TNF-dependent mechanism. *Am J Physiol Regul Integr Comp Physiol,* 290**,** R963-72.

LANGEN, R. C., SCHOLS, A. M., KELDERS, M. C., WOUTERS, E. F. & JANSSEN-HEININGER, Y. M. 2001. Inflammatory cytokines inhibit myogenic differentiation through activation of nuclear factor-kappaB. *Faseb J,* 15**,** 1169-80.

LANGLEY, B., THOMAS, M., BISHOP, A., SHARMA, M., GILMOUR, S. & KAMBADUR, R. 2002. Myostatin inhibits myoblast differentiation by down-regulating MyoD expression. *J Biol Chem,* 277**,** 49831-40.

LARSEN, A. E., TUNSTALL, R. J., CAREY, K. A., NICHOLAS, G., KAMBADUR, R., CROWE, T. C. & CAMERON-SMITH, D. 2006. Actions of short-term fasting on human skeletal muscle myogenic and atrogenic gene expression. *Ann Nutr Metab,* 50**,** 476-81.

LAWLOR, M. A. & ROTWEIN, P. 2000. Coordinate control of muscle cell survival by distinct insulin-like growth factor activated signaling pathways. *J Cell Biol,* 151**,** 1131-40.

LE ROITH, D., BONDY, C., YAKAR, S., LIU, J. L. & BUTLER, A. 2001. The somatomedin hypothesis: 2001. *Endocr Rev,* 22**,** 53-74.

LEBRASSEUR, N. K., SCHELHORN, T. M., BERNARDO, B. L., COSGROVE, P. G., LORIA, P. M. & BROWN, T. A. 2009. Myostatin inhibition enhances the effects of exercise on performance and metabolic outcomes in aged mice. *J Gerontol A Biol Sci Med Sci,* 64**,** 940-8.

LEE, S. J. 2004. Regulation of muscle mass by myostatin. *Annu Rev Cell Dev Biol,* 20**,** 61-86.

LEE, S. J. 2007. Quadrupling muscle mass in mice by targeting TGF-beta signaling pathways. *PLoS One,* 2**,** e789.

LEE, S. J. & MCPHERRON, A. C. 2001. Regulation of myostatin activity and muscle growth. *Proc Natl Acad Sci U S A,* 98**,** 9306-11.

LEEPER-WOODFORD, S. K. & DETMER, K. 1999. Acute hypoxia increases alveolar macrophage tumor necrosis factor activity and alters NF-kappaB expression. *Am J Physiol,* 276**,** L909-16.

LEGER, B., DERAVE, W., DE BOCK, K., HESPEL, P. & RUSSELL, A. P. 2008. Human sarcopenia reveals an increase in SOCS-3 and myostatin and a reduced efficiency of Akt phosphorylation. *Rejuvenation Res,* 11**,** 163-175B.

LENFANT, C. & SULLIVAN, K. 1971. Adaptation to high altitude. *N Engl J Med,* 284**,** 1298-309.

LENK, K., ERBS, S., HOLLRIEGEL, R., BECK, E., LINKE, A., GIELEN, S., WINKLER, S. M., SANDRI, M., HAMBRECHT, R., SCHULER, G. & ADAMS, V. 2012. Exercise training leads to a reduction of elevated myostatin levels in patients with chronic heart failure. *Eur J Prev Cardiol,* 19**,** 404-11.

LEVETT, D. Z., RADFORD, E. J., MENASSA, D. A., GRABER, E. F., MORASH, A. J., HOPPELER, H., CLARKE, K., MARTIN, D. S., FERGUSON-SMITH, A. C., MONTGOMERY, H. E., GROCOTT, M. P. & MURRAY, A. J. 2012. Acclimatization of skeletal muscle mitochondria to high-altitude hypoxia during an ascent of Everest. *Faseb J,* 26**,** 1431-41.

LEVINE, B. D. & STRAY-GUNDERSEN, J. 2006. Dose-response of altitude training: how much altitude is enough? *Adv Exp Med Biol,* 588**,** 233-47.

LEXELL, J., HENRIKSSON-LARSEN, K., WINBLAD, B. & SJOSTROM, M. 1983. Distribution of different fiber types in human skeletal muscles: effects of aging studied in whole muscle cross sections. *Muscle Nerve,* 6**,** 588-95.

LEXELL, J., TAYLOR, C. C. & SJOSTROM, M. 1988. What is the cause of the ageing atrophy? Total number, size and proportion of different fiber types studied in whole vastus lateralis muscle from 15- to 83-year-old men. *J Neurol Sci,* 84**,** 275-94.

LEYVA, F., ANKER, S., SWAN, J. W., GODSLAND, I. F., WINGROVE, C. S., CHUA, T. P., STEVENSON, J. C. & COATS, A. J. 1997. Serum uric acid as an index of impaired oxidative metabolism in chronic heart failure. *Eur Heart J,* 18**,** 858-65.

LI, W., HU, Z. F., CHEN, B. & NI, G. X. 2013. Response of C2C12 myoblasts to hypoxia: the relative roles of glucose and oxygen in adaptive cellular metabolism. *Biomed Res Int,* 2013**,** 326346.

LI, X., LU, Y., JIN, W., LIANG, K., MILLS, G. B. & FAN, Z. 2006. Autophosphorylation of Akt at threonine 72 and serine 246. A potential mechanism of regulation of Akt kinase activity. *J Biol Chem,* 281**,** 13837-43.

LI, X., WANG, S. J., TAN, S. C., CHEW, P. L., LIU, L., WANG, L., WEN, L. & MA, L. 2014. The A55T and K153R polymorphisms of MSTN gene are associated with the strength training-induced muscle hypertrophy among Han Chinese men. *J Sports Sci,* 32**,** 883-91.

LI, Y. P. & REID, M. B. 2000. NF-kappaB mediates the protein loss induced by TNF-alpha in differentiated skeletal muscle myotubes. *Am J Physiol Regul Integr Comp Physiol,* 279**,** R1165-70.

LI, Y. P., SCHWARTZ, R. J., WADDELL, I. D., HOLLOWAY, B. R. & REID, M. B. 1998. Skeletal muscle myocytes undergo protein loss and reactive oxygen-mediated NF-kappaB activation in response to tumor necrosis factor alpha. *Faseb J,* 12**,** 871-80.

LIANG, C. C., PARK, A. Y. & GUAN, J. L. 2007. In vitro scratch assay: a convenient and inexpensive method for analysis of cell migration in vitro. *Nature protocols,* 2**,** 329-33.

LIBERA, L. D. & VESCOVO, G. 2004. Muscle wastage in chronic heart failure, between apoptosis, catabolism and altered anabolism: a chimaeric view of inflammation? *Curr Opin Clin Nutr Metab Care,* 7**,** 435-41.

LIU, A. G., MATTHEWS, J. J., MENON, L. R., MCILROY, D. & BRASIER, M. D. 2014. Haootia quadriformis n. gen., n. sp., interpreted as a muscular cnidarian impression from the Late Ediacaran period (approx. 560 Ma). *Proc Biol Sci,* 281.

LIU, C., LI, W., ZHANG, X., ZHANG, N., HE, S., HUANG, J., GE, Y. & LIU, M. 2012. The critical role of myostatin in differentiation of sheep myoblasts. *Biochem Biophys Res Commun,* 422**,** 381-6.

LIU, W., THOMAS, S. G., ASA, S. L., GONZALEZ-CADAVID, N., BHASIN, S. & EZZAT, S. 2003. Myostatin is a skeletal muscle target of growth hormone anabolic action. *J Clin Endocrinol Metab,* 88**,** 5490-6.

LOKIREDDY, S., WIJESOMA, I. W., BONALA, S., WEI, M., SZE, S. K., MCFARLANE, C., KAMBADUR, R. & SHARMA, M. 2012. Myostatin is a novel tumoral factor that induces cancer cachexia. *Biochem J,* 446**,** 23-36.

LOUIS, E., RAUE, U., YANG, Y., JEMIOLO, B. & TRAPPE, S. 2007. Time course of proteolytic, cytokine, and myostatin gene expression after acute exercise in human skeletal muscle. *J Appl Physiol,* 103**,** 1744-51.

LUNDBY, C., CALBET, J. A. & ROBACH, P. 2009. The response of human skeletal muscle tissue to hypoxia. *Cell Mol Life Sci,* 66**,** 3615-23.

LUNDBY, C., GASSMANN, M. & PILEGAARD, H. 2006. Regular endurance training reduces the exercise induced HIF-1alpha and HIF-2alpha mRNA expression in human skeletal muscle in normoxic conditions. *Eur J Appl Physiol,* 96**,** 363-9.

LUSK, G. 1924. Analysis of the Oxidation of Mixtures of Carbohydrate and Fat. *J Biol Chem,* 59**,** 41-42.

MACDOUGALL, J. D., GREEN, H. J., SUTTON, J. R., COATES, G., CYMERMAN, A., YOUNG, P. & HOUSTON, C. S. 1991. Operation Everest II: structural adaptations in skeletal muscle in response to extreme simulated altitude. *Acta Physiol Scand,* 142**,** 421-7.

MACKENZIE, R., ELLIOTT, B., MAXWELL, N., BRICKLEY, G. & WATT, P. 2012a. The effect of hypoxia and work intensity on insulin resistance in type 2 diabetes. *J Clin Endocrinol Metab,* 97**,** 155-62.

MACKENZIE, R., MAXWELL, N., CASTLE, P., BRICKLEY, G. & WATT, P. 2011. Acute hypoxia and exercise improve insulin sensitivity (S(I) (2) *) in individuals with type 2 diabetes. *Diabetes Metab Res Rev,* 27**,** 94-101.

MACKENZIE, R., MAXWELL, N., CASTLE, P., ELLIOTT, B., BRICKLEY, G. & WATT, P. 2012b. Intermittent exercise with and without hypoxia improves insulin sensitivity in individuals with type 2 diabetes. *J Clin Endocrinol Metab,* 97**,** E546-55.

MACKENZIE, R. W., WATT, P. W. & MAXWELL, N. S. 2008. Acute normobaric hypoxia stimulates erythropoietin release. *High Alt Med Biol,* 9**,** 28-37.

MACLEOD, K. E., MACINNIS, M. J., MANOKHINA, I. & RUPERT, J. L. 2013. Twin studies in altitude and hypoxia research. *Aviat Space Environ Med,* 84**,** 613-9.

MAGALHAES, J., ASCENSAO, A., SOARES, J. M., FERREIRA, R., NEUPARTH, M. J., OLIVEIRA, J., AMADO, F., MARQUES, F. & DUARTE, J. A. 2005. Acute and chronic exposition of mice

to severe hypoxia: the role of acclimatization against skeletal muscle oxidative stress. *Int J Sports Med,* 26**,** 102-9.

MAINARDI, F., MAGGIONI, F., LISOTTO, C. & ZANCHIN, G. 2013. Diagnosis and management of headache attributed to airplane travel. *Curr Neurol Neurosci Rep,* 13**,** 335.

MALHOTRA, A. & WHITE, D. P. 2002. Obstructive sleep apnoea. *Lancet,* 360**,** 237-45.

MALTAIS, F., DECRAMER, M., CASABURI, R., BARREIRO, E., BURELLE, Y., DEBIGARE, R., DEKHUIJZEN, P. N., FRANSSEN, F., GAYAN-RAMIREZ, G., GEA, J., GOSKER, H. R., GOSSELINK, R., HAYOT, M., HUSSAIN, S. N., JANSSENS, W., POLKEY, M. I., ROCA, J., SAEY, D., SCHOLS, A. M., SPRUIT, M. A., STEINER, M., TAIVASSALO, T., TROOSTERS, T., VOGIATZIS, I. & WAGNER, P. D. 2014. An official American Thoracic Society/European Respiratory Society statement: update on limb muscle dysfunction in chronic obstructive pulmonary disease. *Am J Respir Crit Care Med,* 189**,** e15-62.

MANTYSAARI, M., JOUTSI-KORHONEN, L., SIIMES, M. A., SIITONEN, S., PARKKOLA, K., LEMPONEN, M. & LASSILA, R. 2011. Unaltered blood coagulation and platelet function in healthy subjects exposed to acute hypoxia. *Aviat Space Environ Med,* 82**,** 699-703.

MARCELL, T. J., HARMAN, S. M., URBAN, R. J., METZ, D. D., RODGERS, B. D. & BLACKMAN, M. R. 2001. Comparison of GH, IGF-I, and testosterone with mRNA of receptors and myostatin in skeletal muscle in older men. *Am J Physiol Endocrinol Metab,* 281**,** E1159-64.

MARCUS, N. J., OLSON, E. B., JR., BIRD, C. E., PHILIPPI, N. R. & MORGAN, B. J. 2009. Time-dependent adaptation in the hemodynamic response to hypoxia. *Respir Physiol Neurobiol,* 165**,** 90-6.

MARQUIS, K., DEBIGARE, R., LACASSE, Y., LEBLANC, P., JOBIN, J., CARRIER, G. & MALTAIS, F. 2002. Midthigh muscle cross-sectional area is a better predictor of mortality than body mass index in patients with chronic obstructive pulmonary disease. *Am J Respir Crit Care Med,* 166**,** 809-13.

MARSHAK, M. E. & MAEVA, T. A. 1956. [Hypoxic phenomena in muscular activity]. *Biull Eksp Biol Med,* 41**,** 13-5.

MARTIN, D. S., LEVETT, D. Z., GROCOTT, M. P. & MONTGOMERY, H. E. 2010. Variation in human performance in the hypoxic mountain environment. *Exp Physiol,* 95**,** 463-70.

MASON, S. D., HOWLETT, R. A., KIM, M. J., OLFERT, I. M., HOGAN, M. C., MCNULTY, W., HICKEY, R. P., WAGNER, P. D., KAHN, C. R., GIORDANO, F. J. & JOHNSON, R. S. 2004. Loss of skeletal muscle HIF-1alpha results in altered exercise endurance. *PLoS Biol,* 2**,** e288.

MASON, S. D., RUNDQVIST, H., PAPANDREOU, I., DUH, R., MCNULTY, W. J., HOWLETT, R. A., OLFERT, I. M., SUNDBERG, C. J., DENKO, N. C., POELLINGER, L. & JOHNSON, R. S. 2007. HIF-1alpha in endurance training: suppression of oxidative metabolism. *Am J Physiol Regul Integr Comp Physiol,* 293**,** R2059-69.

MATSAKAS, A., BOZZO, C., CACCIANI, N., CALIARO, F., REGGIANI, C., MASCARELLO, F. & PATRUNO, M. 2006. Effect of swimming on myostatin expression in white and red gastrocnemius muscle and in cardiac muscle of rats. *Exp Physiol,* 91**,** 983-94.

MATSAKAS, A., MOUISEL, E., AMTHOR, H. & PATEL, K. 2010. Myostatin knockout mice increase oxidative muscle phenotype as an adaptive response to exercise. *J Muscle Res Cell Motil,* 31**,** 111-25.

MATSUKI, N., INABA, M. & ONO, K. 2002. Catabolism of cytoplasmic and intramitochondrial adenine nucleotides in C2C12 skeletal myotube under chemical hypoxia. *J Vet Med Sci,* 64**,** 341-7.

MAURO, A. 1961. Satellite cell of skeletal muscle fibers. *J Biophys Biochem Cytol,* 9**,** 493-5.

MCCARTHY, J. J., MULA, J., MIYAZAKI, M., ERFANI, R., GARRISON, K., FAROOQUI, A. B., SRIKUEA, R., LAWSON, B. A., GRIMES, B., KELLER, C., VAN ZANT, G., CAMPBELL, K. S., ESSER, K. A., DUPONT-VERSTEEGDEN, E. E. & PETERSON, C. A. 2011. Effective fiber hypertrophy in satellite cell-depleted skeletal muscle. *Development,* 138**,** 3657-66.

MCCROSKERY, S., THOMAS, M., MAXWELL, L., SHARMA, M. & KAMBADUR, R. 2003. Myostatin negatively regulates satellite cell activation and self-renewal. *J Cell Biol,* 162**,** 1135-47.

MCFARLAND, R. A. 1971. Human factors in relation to the development of pressurized cabins. *Aerosp Med,* 42**,** 1303-18.

MCFARLANE, C., HENNEBRY, A., THOMAS, M., PLUMMER, E., LING, N., SHARMA, M. & KAMBADUR, R. 2008. Myostatin signals through Pax7 to regulate satellite cell self-renewal. *Exp Cell Res,* 314**,** 317-29.

MCFARLANE, C., LANGLEY, B., THOMAS, M., HENNEBRY, A., PLUMMER, E., NICHOLAS, G., MCMAHON, C., SHARMA, M. & KAMBADUR, R. 2005. Proteolytic processing of myostatin is auto-regulated during myogenesis. *Dev Biol,* 283**,** 58-69.

MCFARLANE, C., PLUMMER, E., THOMAS, M., HENNEBRY, A., ASHBY, M., LING, N., SMITH, H., SHARMA, M. & KAMBADUR, R. 2006. Myostatin induces cachexia by activating the ubiquitin proteolytic system through an NF-kappaB-independent, FoxO1-dependent mechanism. *J Cell Physiol,* 209**,** 501-14.

MCFARLANE, C., VAJJALA, A., ARIGELA, H., LOKIREDDY, S., GE, X., BONALA, S., MANICKAM, R., KAMBADUR, R. & SHARMA, M. 2014. Negative auto-regulation of myostatin expression is mediated by Smad3 and microRNA-27. *PLoS One,* 9**,** e87687.

MCGUIRE, E. A., HELDERMAN, J. H., TOBIN, J. D., ANDRES, R. & BERMAN, M. 1976. Effects of arterial versus venous sampling on analysis of glucose kinetics in man. *J Appl Physiol,* 41**,** 565-73.

MCLEAN, B. D., BUTTIFANT, D., GORE, C. J., WHITE, K. & KEMP, J. 2013. Year-to-year variability in haemoglobin mass response to two altitude training camps. *Br J Sports Med,* 47 Suppl 1**,** i51-8.

MCLELLAN, S. A. & WALSH, T. S. 2004. Oxygen delivery and haemoglobin. *Contin Educ Anaesth Crit Care Pain,* 4**,** 123-126.

MCMAHON, C. D., POPOVIC, L., JEANPLONG, F., OLDHAM, J. M., KIRK, S. P., OSEPCHOOK, C. C., WONG, K. W., SHARMA, M., KAMBADUR, R. & BASS, J. J. 2003a. Sexual dimorphism is associated with decreased expression of processed myostatin in males. *Am J Physiol Endocrinol Metab,* 284**,** E377-81.

MCMAHON, C. D., POPOVIC, L., OLDHAM, J. M., JEANPLONG, F., SMITH, H. K., KAMBADUR, R., SHARMA, M., MAXWELL, L. & BASS, J. J. 2003b. Myostatin-deficient mice lose more

skeletal muscle mass than wild-type controls during hindlimb suspension. *Am J Physiol Endocrinol Metab,* 285**,** E82-7.

MCPHERRON, A. C., LAWLER, A. M. & LEE, S. J. 1997. Regulation of skeletal muscle mass in mice by a new TGF-beta superfamily member. *Nature,* 387**,** 83-90.

MCPHERRON, A. C. & LEE, S. J. 1997. Double muscling in cattle due to mutations in the myostatin gene. *Proc Natl Acad Sci U S A,* 94**,** 12457-61.

MEDINA, R., WING, S. S. & GOLDBERG, A. L. 1995. Increase in levels of polyubiquitin and proteasome mRNA in skeletal muscle during starvation and denervation atrophy. *Biochem J,* 307 (Pt 3)**,** 631-7.

MILES, D. S., BRANSFORD, D. R. & HORVATH, S. M. 1981. Hypoxia effects on plasma volume shifts at rest, work, and recovery in supine posture. *J Appl Physiol Respir Environ Exerc Physiol,* 51**,** 148-53.

MILLER, R. D. 2010. *Miller's anesthesia,* Philadelphia, PA, Churchill Livingstone/Elsevier.

MILLMAN, A. L., PAYNE, B., QU, Z., DOUGLAS, M. J., HUTCHEON, J. A., LEE, T., MAGEE, L. A., WALLEY, K. R. & VON DADELSZEN, P. 2011. Oxygen saturation as a predictor of adverse maternal outcomes in women with preeclampsia. *J Obstet Gynaecol Can,* 33**,** 705-14.

MITCH, W. E. & GOLDBERG, A. L. 1996. Mechanisms of muscle wasting. The role of the ubiquitin-proteasome pathway. *N Engl J Med,* 335**,** 1897-905.

MOORE, L. G. & REGENSTEINER, J. G. 1983. Adaptation to High Altitude. *Annual Review of Anthropology,* 12**,** 285-304.

MOORE, L. G., ROHR, A. L., MAISENBACH, J. K. & REEVES, J. T. 1982. Emphysema mortality is increased in Colorado residents at high altitude. *Am Rev Respir Dis,* 126**,** 225-8.

MORITA, S., TSUJINAKA, T., YANO, M., EBISUI, C., MORIMOTO, T., FUJITA, J., OGAWA, A., TANIGUCHI, M., SHIOZAKI, H. & MONDEN, M. 1996. Temperature-dependent enhancement of proteolysis in C2C12 myotubes in association with the activation of 26S proteasome. *Biochem Biophys Res Commun,* 228**,** 813-8.

MORRISON, W. L., GIBSON, J. N., SCRIMGEOUR, C. & RENNIE, M. J. 1988. Muscle wasting in emphysema. *Clin Sci (Lond),* 75**,** 415-20.

MOSHER, D. S., QUIGNON, P., BUSTAMANTE, C. D., SUTTER, N. B., MELLERSH, C. S., PARKER, H. G. & OSTRANDER, E. A. 2007. A mutation in the myostatin gene increases muscle mass and enhances racing performance in heterozygote dogs. *PLoS Genet,* 3**,** e79.

MOTOHASHI, N. & ASAKURA, A. 2014. Muscle satellite cell heterogeneity and self-renewal. *Front Cell Dev Biol,* 2.

MOUNIER, R., PEDERSEN, B. K. & PLOMGAARD, P. 2010. Muscle-specific expression of hypoxia-inducible factor in human skeletal muscle. *Exp Physiol,* 95**,** 899-907.

MURPHY, K. T., COBANI, V., RYALL, J. G., IBEBUNJO, C. & LYNCH, G. S. 2011. Acute antibody-directed myostatin inhibition attenuates disuse muscle atrophy and weakness in mice. *J Appl Physiol*.

MURPHY, R. M. 2011. Enhanced technique to measure proteins in single segments of human skeletal muscle fibers: fiber-type dependence of AMPK-alpha1 and -beta1. *J Appl Physiol (1985),* 110**,** 820-5.

MURRAY, A. J. 2014. Mitochondria at the extremes: pioneers, protectorates, protagonists. *Extrem Physiol Med,* 3**,** 10.

MURRAY, A. J. & MONTGOMERY, H. E. 2014. How wasting is saving: Weight loss at altitude might result from an evolutionary adaptation. *Bioessays*.

NAKATANI, M., TAKEHARA, Y., SUGINO, H., MATSUMOTO, M., HASHIMOTO, O., HASEGAWA, Y., MURAKAMI, T., UEZUMI, A., TAKEDA, S., NOJI, S., SUNADA, Y. & TSUCHIDA, K. 2008. Transgenic expression of a myostatin inhibitor derived from follistatin increases skeletal muscle mass and ameliorates dystrophic pathology in mdx mice. *Faseb J,* 22**,** 477-87.

NDUBUIZU, O. I., TSIPIS, C. P., LI, A. & LAMANNA, J. C. 2010. Hypoxia-inducible factor-1 (HIF-1)-independent microvascular angiogenesis in the aged rat brain. *Brain Res,* 1366**,** 101-9.

NICHOLAS, G., THOMAS, M., LANGLEY, B., SOMERS, W., PATEL, K., KEMP, C. F., SHARMA, M. & KAMBADUR, R. 2002. Titin-cap associates with, and regulates secretion of, Myostatin. *J Cell Physiol,* 193**,** 120-31.

NISHIMURA, A., SUGITA, M., KATO, K., FUKUDA, A., SUDO, A. & UCHIDA, A. 2010. Hypoxia increases muscle hypertrophy induced by resistance training. *Int J Sports Physiol Perform,* 5**,** 497-508.

NOZAKI, M., LI, Y., ZHU, J., AMBROSIO, F., UEHARA, K., FU, F. H. & HUARD, J. 2008. Improved muscle healing after contusion injury by the inhibitory effect of suramin on myostatin, a negative regulator of muscle growth. *A J Sport Med,* 36**,** 2354-62.

O'CONNOR, T., DUBOWITZ, G. & BICKLER, P. E. 2004. Pulse oximetry in the diagnosis of acute mountain sickness. *High Alt Med Biol,* 5**,** 341-8.

O'KEEFE, D. J. 2007. Brief Report: Post Hoc Power, Observed Power, A Priori Power, Retrospective Power, Prospective Power, Achieved Power: Sorting Out Appropriate Uses of Statistical Power Analyses. *Com Meth Meas,* 1**,** 291-299.

OGATA, T., TOKIZAWA, K., KAJIKAWA, S. & MURAOKA, I. 2011. Effects of Genetic Variations in HIF-1α on Physiological Response to Hypoxia (低酸素に対する生理的応答における HIF-1α 遺伝子多型の影響). *Sports Sci. Res. (スポーツ科学研究),* 8**,** 296-305.

OGRYZKO, V. V., SCHILTZ, R. L., RUSSANOVA, V., HOWARD, B. H. & NAKATANI, Y. 1996. The transcriptional coactivators p300 and CBP are histone acetyltransferases. *Cell,* 87**,** 953-9.

OHANNA, M., SOBERING, A. K., LAPOINTE, T., LORENZO, L., PRAUD, C., PETROULAKIS, E., SONENBERG, N., KELLY, P. A., SOTIROPOULOS, A. & PENDE, M. 2005. Atrophy of S6K1(-/-) skeletal muscle cells reveals distinct mTOR effectors for cell cycle and size control. *Nat Cell Biol,* 7**,** 286-94.

OLDHAM, J. M., OSEPCHOOK, C. C., JEANPLONG, F., FALCONER, S. J., MATTHEWS, K. G., CONAGLEN, J. V., GERRARD, D. F., SMITH, H. K., WILKINS, R. J., BASS, J. J. & MCMAHON, C. D. 2009. The decrease in mature myostatin protein in male skeletal muscle is developmentally regulated by growth hormone. *J Physiol,* 587**,** 669-77.

OP DEN KAMP, C. M., LANGEN, R. C., SNEPVANGERS, F. J., DE THEIJE, C. C., SCHELLEKENS, J. M., LAUGS, F., DINGEMANS, A. M. & SCHOLS, A. M. 2013. Nuclear transcription factor

kappaB activation and protein turnover adaptations in skeletal muscle of patients with progressive stages of lung cancer cachexia. *Am J Clin Nutr*.

OSORIO-FUENTEALBA, C., VALDES, J. A., RIQUELME, D., HIDALGO, J., HIDALGO, C. & CARRASCO, M. A. 2009. Hypoxia stimulates via separate pathways ERK phosphorylation and NF-kappaB activation in skeletal muscle cells in primary culture. *J Appl Physiol,* 106**,** 1301-10.

OWEN, O. E., REICHARD, G. A., JR., BODEN, G. & SHUMAN, C. 1974. Comparative measurements of glucose, beta-hydroxybutyrate, acetoacetate, and insulin in blood and cerebrospinal fluid during starvation. *Metabolism,* 23**,** 7-14.

PALSTRA, A. P., TUDORACHE, C., ROVIRA, M., BRITTIJN, S. A., BURGERHOUT, E., VAN DEN THILLART, G. E., SPAINK, H. P. & PLANAS, J. V. 2010. Establishing zebrafish as a novel exercise model: swimming economy, swimming-enhanced growth and muscle growth marker gene expression. *PLoS One,* 5**,** e14483.

PANG, C. Y., YANG, R. Z., ZHONG, A., XU, N., BOYD, B. & FORREST, C. R. 1995. Acute ischaemic preconditioning protects against skeletal muscle infarction in the pig. *Cardiovasc Res,* 29**,** 782-8.

PARK, J. Y., HWANG, T. K., PARK, H. K. & AHN, R. S. 2014. Differences in cardiovascular and hypothalamic-pituitary-adrenal axis functions between high-altitude visitors and natives during a trek on the Annapurna circuit. *Neuroendocrinology,* 99**,** 130-8.

PARSLOW, G. R. 2014. Commentary: Google glass: a head-up display to facilitate teaching and learning. *Biochem Mol Biol Educ,* 42**,** 91-2.

PATEL, K. 1998. Follistatin. *Int J Biochem Cell Biol,* 30**,** 1087-93.

PEACOCK, A. J. 1998. ABC of oxygen: oxygen at high altitude. *BMJ,* 317**,** 1063-6.

PELED, Y., GRAMLICH, M., YOSKOVITZ, G., FEINBERG, M. S., AFEK, A., POLAK-CHARCON, S., PRAS, E., SELA, B. A., KONEN, E., WEISSBROD, O., GEIGER, D., GORDON, P. M., THIERFELDER, L., FREIMARK, D., GERULL, B. & ARAD, M. 2014. Titin mutation in familial restrictive cardiomyopathy. *Int J Cardiol,* 171**,** 24-30.

PESCADOR, N., VILLAR, D., CIFUENTES, D., GARCIA-ROCHA, M., ORTIZ-BARAHONA, A., VAZQUEZ, S., ORDONEZ, A., CUEVAS, Y., SAEZ-MORALES, D., GARCIA-BERMEJO, M. L., LANDAZURI, M. O., GUINOVART, J. & DEL PESO, L. 2010. Hypoxia promotes glycogen accumulation through hypoxia inducible factor (HIF)-mediated induction of glycogen synthase 1. *PLoS One,* 5**,** e9644.

PETERS, D., BARASH, I. A., BURDI, M., YUAN, P. S., MATHEW, L., FRIDEN, J. & LIEBER, R. L. 2003. Asynchronous functional, cellular and transcriptional changes after a bout of eccentric exercise in the rat. *J Physiol,* 553**,** 947-57.

PETERSEN, A. M., MAGKOS, F., ATHERTON, P., SELBY, A., SMITH, K., RENNIE, M. J., PEDERSEN, B. K. & MITTENDORFER, B. 2007. Smoking impairs muscle protein synthesis and increases the expression of myostatin and MAFbx in muscle. *Am J Physiol Endocrinol Metab,* 293**,** E843-8.

PETOUSI, N., CROFT, Q. P., CAVALLERI, G. L., CHENG, H. Y., FORMENTI, F., ISHIDA, K., LUNN, D., MCCORMACK, M., SHIANNA, K. V., TALBOT, N. P., RATCLIFFE, P. J. & ROBBINS, P. A. 2014. Tibetans living at sea level have a hyporesponsive hypoxia-inducible factor system and blunted physiological responses to hypoxia. *J Appl Physiol (1985),* 116**,** 893-904.

PHILLIPS, S. K., SANDERSON, A. G., BIRCH, K., BRUCE, S. A. & WOLEDGE, R. C. 1996. Changes in maximal voluntary force of human adductor pollicis muscle during the menstrual cycle. *J Physiol,* 496 (Pt 2)**,** 551-7.

PHILLIPS, S. M. 2004. Protein requirements and supplementation in strength sports. *Nutrition,* 20**,** 689-95.

PHILLIPS, S. M., TIPTON, K. D., AARSLAND, A., WOLF, S. E. & WOLFE, R. R. 1997. Mixed muscle protein synthesis and breakdown after resistance exercise in humans. *Am J Physiol,* 273**,** E99-107.

PLANT, P. J., BROOKS, D., FAUGHNAN, M., BAYLEY, T., BAIN, J., SINGER, L., CORREA, J., PEARCE, D., BINNIE, M. & BATT, J. 2010. Cellular markers of muscle atrophy in chronic obstructive pulmonary disease. *Am J Respir Cell Mol Biol,* 42**,** 461-71.

POLLOCK, R. D., CARTER, S., VELLOSO, C. P., DUGGAL, N. A., LORD, J. M., LAZARUS, N. R. & HARRIDGE, S. D. 2015. An investigation into the relationship between age and physiological function in highly active older adults. *J Physiol,* 593**,** 657-80; discussion 680.

POULSEN, T. D., KLAUSEN, T., RICHALET, J. P., KANSTRUP, I. L., FOGH-ANDERSEN, N. & OLSEN, N. V. 1998. Plasma volume in acute hypoxia: comparison of a carbon monoxide rebreathing method and dye dilution with Evans' blue. *Eur J Appl Physiol Occup Physiol,* 77**,** 457-61.

POUW, E. M., SCHOLS, A. M., DEUTZ, N. E. & WOUTERS, E. F. 1998. Plasma and muscle amino acid levels in relation to resting energy expenditure and inflammation in stable chronic obstructive pulmonary disease. *Am J Respir Crit Care Med,* 158**,** 797-801.

POWELL, F. L., MILSOM, W. K. & MITCHELL, G. S. 1998. Time domains of the hypoxic ventilatory response. *Respir Physiol,* 112**,** 123-34.

PREEDY, V. R., SMITH, D. M. & SUGDEN, P. H. 1985. The effects of 6 hours of hypoxia on protein synthesis in rat tissues in vivo and in vitro. *Biochem J,* 228**,** 179-85.

PROUDFOOT, C., CARLSON, D. F., HUDDART, R., LONG, C. R., PRYOR, J. H., KING, T. J., LILLICO, S. G., MILEHAM, A. J., MCLAREN, D. G., WHITELAW, C. B. & FAHRENKRUG, S. C. 2015. Genome edited sheep and cattle. *Transgenic Res,* 24**,** 147-53.

PRZYBYLSKI, R. J., BULLARO, J. C. & MACBRIDE, R. 1979. Reversible suppression of skeletal myotube formation in vitro obtained by varying [CO2]. *Am J Physiol,* 237**,** C166-76.

RALSTON, A. C., WEBB, R. K. & RUNCIMAN, W. B. 1991. Potential errors in pulse oximetry. I. Pulse oximeter evaluation. *Anaesthesia,* 46**,** 202-6.

RATKEVICIUS, A., JOYSON, A., SELMER, I., DHANANI, T., GRIERSON, C., TOMMASI, A. M., DEVRIES, A., RAUCHHAUS, P., CROWTHER, D., ALESCI, S., YAWORSKY, P., GILBERT, F., REDPATH, T. W., BRADY, J., FEARON, K. C., REID, D. M., GREIG, C. A. & WACKERHAGE, H. 2011. Serum concentrations of myostatin and myostatin-interacting proteins do not differ between young and sarcopenic elderly men. *J Gerontol A Biol Sci Med Sci,* 66**,** 620-6.

RAVAL, R. R., LAU, K. W., TRAN, M. G., SOWTER, H. M., MANDRIOTA, S. J., LI, J. L., PUGH, C. W., MAXWELL, P. H., HARRIS, A. L. & RATCLIFFE, P. J. 2005. Contrasting properties of hypoxia-inducible factor 1 (HIF-1) and HIF-2 in von Hippel-Lindau-associated renal cell carcinoma. *Mol Cell Biol,* 25**,** 5675-86.

REARDON, K. A., DAVIS, J., KAPSA, R. M., CHOONG, P. & BYRNE, E. 2001. Myostatin, insulin-like growth factor-1, and leukemia inhibitory factor mRNAs are upregulated in chronic human disuse muscle atrophy. *Muscle Nerve,* 24**,** 893-9.

REBBAPRAGADA, A., BENCHABANE, H., WRANA, J. L., CELESTE, A. J. & ATTISANO, L. 2003. Myostatin signals through a transforming growth factor beta-like signaling pathway to block adipogenesis. *Mol Cell Biol,* 23**,** 7230-42.

REED, S. A., SANDESARA, P. B., SENF, S. M. & JUDGE, A. R. 2012. Inhibition of FoxO transcriptional activity prevents muscle fiber atrophy during cachexia and induces hypertrophy. *Faseb J,* 26**,** 987-1000.

REID, M. B. 2005. Response of the ubiquitin-proteasome pathway to changes in muscle activity. *Am J Physiol Regul Integr Comp Physiol,* 288**,** R1423-31.

REN, H., ACCILI, D. & DUAN, C. 2010. Hypoxia converts the myogenic action of insulin-like growth factors into mitogenic action by differentially regulating multiple signaling pathways. *Proc Natl Acad Sci U S A,* 107**,** 5857-62.

RENNIE, M. J., WACKERHAGE, H., SPANGENBURG, E. E. & BOOTH, F. W. 2004. Control of the size of the human muscle mass. *Annu Rev Physiol,* 66**,** 799-828.

REYNAFARJE, C., LOZANO, R. & VALDIVIESO, J. 1959. The polycythemia of high altitudes: iron metabolism and related aspects. *Blood,* 14**,** 433-55.

RICHALET, J. P., SOUBERBIELLE, J. C., ANTEZANA, A. M., DECHAUX, M., LE TRONG, J. L., BIENVENU, A., DANIEL, F., BLANCHOT, C. & ZITTOUN, J. 1994. Control of erythropoiesis in humans during prolonged exposure to the altitude of 6,542 m. *Am J Physiol,* 266**,** R756-64.

RICHARD, N. A., SAHOTA, I. S., WIDMER, N., FERGUSON, S., SHEEL, A. W. & KOEHLE, M. S. 2014. Acute mountain sickness, chemosensitivity, and cardiorespiratory responses in

humans exposed to hypobaric and normobaric hypoxia. *J Appl Physiol (1985),* 116**,** 945-52.

RIOS, R., CARNEIRO, I., ARCE, V. M. & DEVESA, J. 2002. Myostatin is an inhibitor of myogenic differentiation. *Am J Physiol Cell Physiol,* 282**,** C993-9.

ROACH, R. C., LOEPPKY, J. A. & ICENOGLE, M. V. 1996. Acute mountain sickness: increased severity during simulated altitude compared with normobaric hypoxia. *J Appl Physiol,* 81**,** 1908-10.

RODRIGUEZ, J., VERNUS, B., CHELH, I., CASSAR-MALEK, I., GABILLARD, J. C., HADJ SASSI, A., SEILIEZ, I., PICARD, B. & BONNIEU, A. 2014. Myostatin and the skeletal muscle atrophy and hypertrophy signaling pathways. *Cell Mol Life Sci,* 71**,** 4361-71.

ROMERO-CALVO, I., OCON, B., MARTINEZ-MOYA, P., SUAREZ, M. D., ZARZUELO, A., MARTINEZ-AUGUSTIN, O. & DE MEDINA, F. S. 2010. Reversible Ponceau staining as a loading control alternative to actin in Western blots. *Anal Biochem,* 401**,** 318-20.

ROSE, M. S., HOUSTON, C. S., FULCO, C. S., COATES, G., SUTTON, J. R. & CYMERMAN, A. 1988. Operation Everest. II: Nutrition and body composition. *J Appl Physiol (1985),* 65**,** 2545-51.

ROSENBLATT, J. D. & PARRY, D. J. 1992. Gamma irradiation prevents compensatory hypertrophy of overloaded mouse extensor digitorum longus muscle. *J Appl Physiol,* 73**,** 2538-43.

ROSENBLATT, J. D., YONG, D. & PARRY, D. J. 1994. Satellite cell activity is required for hypertrophy of overloaded adult rat muscle. *Muscle Nerve,* 17**,** 608-13.

ROSENZWEIG, R. & GLICKMAN, M. H. 2008. Forging a proteasome alpha-ring with dedicated proteasome chaperones. *Nat Struct Mol Biol,* 15**,** 218-20.

ROTH, S. M., MARTEL, G. F., FERRELL, R. E., METTER, E. J., HURLEY, B. F. & ROGERS, M. A. 2003. Myostatin gene expression is reduced in humans with heavy-resistance strength training: a brief communication. *Exp Biol Med (Maywood),* 228**,** 706-9.

RUSKO, H. K., TIKKANEN, H. O. & PELTONEN, J. E. 2004. Altitude and endurance training. *J Sports Sci,* 22**,** 928-44; discussion 945.

SAEKI, Y. & TANAKA, K. 2008. Cell biology: two hands for degradation. *Nature,* 453**,** 460-1.

SAREMI, A., GHARAKHANLOO, R., SHARGHI, S., GHARAATI, M. R., LARIJANI, B. & OMIDFAR, K. 2010. Effects of oral creatine and resistance training on serum myostatin and GASP-1. *Mol Cell Endocrinol,* 317**,** 25-30.

SARTORI, R., SCHIRWIS, E., BLAAUW, B., BORTOLANZA, S., ZHAO, J., ENZO, E., STANTZOU, A., MOUISEL, E., TONIOLO, L., FERRY, A., STRICKER, S., GOLDBERG, A. L., DUPONT, S., PICCOLO, S., AMTHOR, H. & SANDRI, M. 2013. BMP signaling controls muscle mass. *Nat Genet,* 45**,** 1309-18.

SAUER, H. I. 1980. Geographic patterns in the risk of dying and associated factors ages 35-74 years: United States, 1968-72. *Vital Health Stat 3***,** 1-120.

SAVAGE, K. J. & MCPHERRON, A. C. 2010. Endurance exercise training in myostatin null mice. *Muscle Nerve,* 42**,** 355-62.

SCHAEFER, K. E. 1958. Respiratory pattern and respiratory response to CO2. *J Appl Physiol,* 13**,** 1-14.

SCHENA, F., GUERRINI, F., TREGNAGHI, P. & KAYSER, B. 1992. Branched-chain amino acid supplementation during trekking at high altitude. The effects on loss of body mass, body composition, and muscle power. *Eur J Appl Physiol Occup Physiol,* 65**,** 394-8.

SCHIAFFINO, S., GORZA, L., SARTORE, S., SAGGIN, L., AUSONI, S., VIANELLO, M., GUNDERSEN, K. & LOMO, T. 1989. Three myosin heavy chain isoforms in type 2 skeletal muscle fibres. *J Muscle Res Cell Motil,* 10**,** 197-205.

SCHREINER, P., CHEN, X., HUSNJAK, K., RANDLES, L., ZHANG, N., ELSASSER, S., FINLEY, D., DIKIC, I., WALTERS, K. J. & GROLL, M. 2008. Ubiquitin docking at the proteasome through a novel pleckstrin-homology domain interaction. *Nature,* 453**,** 548-52.

SCHUELKE, M., WAGNER, K. R., STOLZ, L. E., HUBNER, C., RIEBEL, T., KOMEN, W., BRAUN, T., TOBIN, J. F. & LEE, S. J. 2004. Myostatin mutation associated with gross muscle hypertrophy in a child. *N Engl J Med,* 350**,** 2682-8.

SCHWARTZ, J. S., BENCOWITZ, H. Z. & MOSER, K. M. 1984. Air travel hypoxemia with chronic obstructive pulmonary disease. *Ann Intern Med,* 100**,** 473-7.

SEALE, P., SABOURIN, L. A., GIRGIS-GABARDO, A., MANSOURI, A., GRUSS, P. & RUDNICKI, M. A. 2000. Pax7 is required for the specification of myogenic satellite cells. *Cell,* 102**,** 777-86.

SEIBERT, M. J., XUE, Q. L., FRIED, L. P. & WALSTON, J. D. 2001. Polymorphic variation in the human myostatin (GDF-8) gene and association with strength measures in the Women's Health and Aging Study II cohort. *J Am Geriatr Soc,* 49**,** 1093-6.

SEMENZA, G. L. 2003. Targeting HIF-1 for cancer therapy. *Nat Rev Cancer,* 3**,** 721-32.

SHARMA, M., KAMBADUR, R., MATTHEWS, K. G., SOMERS, W. G., DEVLIN, G. P., CONAGLEN, J. V., FOWKE, P. J. & BASS, J. J. 1999. Myostatin, a transforming growth factor-beta superfamily member, is expressed in heart muscle and is upregulated in cardiomyocytes after infarct. *J Cell Physiol,* 180**,** 1-9.

SHARPLES, A. P., PLAYER, D. J., MARTIN, N. R., MUDERA, V., STEWART, C. E. & LEWIS, M. P. 2012. Modelling in vivo skeletal muscle ageing in vitro using three-dimensional bioengineered constructs. *Aging Cell,* 11**,** 986-95.

SILLAU, A. H. & BANCHERO, N. 1977. Effects of hypoxia on capillary density and fiber composition in rat skeletal muscle. *Pflugers Arch,* 370**,** 227-32.

SIMONSON, T. S., WEI, G., WAGNER, H. E., WUREN, T., QIN, G., YAN, M., WAGNER, P. D. & GE, R. L. 2015. Low haemoglobin concentration in Tibetan males is associated with greater high-altitude exercise capacity. *J Physiol,* 593**,** 3207-18.

SIMONSON, T. S., YANG, Y., HUFF, C. D., YUN, H., QIN, G., WITHERSPOON, D. J., BAI, Z., LORENZO, F. R., XING, J., JORDE, L. B., PRCHAL, J. T. & GE, R. 2010. Genetic evidence for high-altitude adaptation in Tibet. *Science,* 329**,** 72-5.

SINGER, P. 1997. *Selected Works by Galen*, Oxford University Press.

SINGH, M. V., JAIN, S. C., RAWAL, S. B., DIVEKAR, H. M., PARSHAD, R., TYAGI, A. K. & SINHA, K. C. 1986. Comparative study of acetazolamide and spironolactone on body fluid compartments on induction to high altitude. *Int J Biometeorol,* 30**,** 33-41.

SLOAN, A. W. & MASALI, M. 1978. Anthropometry of Sherpa men. *Ann Hum Biol,* 5**,** 453-8.

SMITH, H. K., MATTHEWS, K. G., OLDHAM, J. M., JEANPLONG, F., FALCONER, S. J., BASS, J. J., SENNA-SALERNO, M., BRACEGIRDLE, J. W. & MCMAHON, C. D. 2014. Translational signalling, atrogenic and myogenic gene expression during unloading and reloading of skeletal muscle in myostatin-deficient mice. *PLoS One,* 9**,** e94356.

SMITH, H. K. & MERRY, T. L. 2012. Voluntary resistance wheel exercise during post-natal growth in rats enhances skeletal muscle satellite cell and myonuclear content at adulthood. *Acta Physiol (Oxf),* 204**,** 393-402.

SMITH, K., REYNOLDS, N., DOWNIE, S., PATEL, A. & RENNIE, M. J. 1998. Effects of flooding amino acids on incorporation of labeled amino acids into human muscle protein. *Am J Physiol,* 275**,** E73-8.

SONNENBERG, G. E. & KELLER, U. 1982. Sampling of arterialized heated-hand venous blood as a noninvasive technique for the study of ketone body kinetics in man. *Metabolism,* 31**,** 1-5.

SOUTHGATE, R. J., NEILL, B., PRELOVSEK, O., EL-OSTA, A., KAMEI, Y., MIURA, S., EZAKI, O., MCLOUGHLIN, T. J., ZHANG, W., UNTERMAN, T. G. & FEBBRAIO, M. A. 2007. FOXO1 regulates the expression of 4E-BP1 and inhibits mTOR signaling in mammalian skeletal muscle. *J Biol Chem,* 282**,** 21176-86.

SPANGENBURG, E. E., LE ROITH, D., WARD, C. W. & BODINE, S. C. 2008. A functional insulin-like growth factor receptor is not necessary for load-induced skeletal muscle hypertrophy. *J Physiol,* 586**,** 283-91.

SRIVASTAVA, S., KASHIWAYA, Y., KING, M. T., BAXA, U., TAM, J., NIU, G., CHEN, X., CLARKE, K. & VEECH, R. L. 2012. Mitochondrial biogenesis and increased uncoupling protein 1 in brown adipose tissue of mice fed a ketone ester diet. *FASEB J,* 26**,** 2351-62.

STEWART, C. C. 1898. Variations In daily activity production by alcohol and by chages in barometric pressure and diet, with a description of recording methods. *Am J Physiol,* 1**,** 40-56.

STITT, T. N., DRUJAN, D., CLARKE, B. A., PANARO, F., TIMOFEYVA, Y., KLINE, W. O., GONZALEZ, M., YANCOPOULOS, G. D. & GLASS, D. J. 2004. The IGF-1/PI3K/Akt pathway prevents

expression of muscle atrophy-induced ubiquitin ligases by inhibiting FOXO transcription factors. *Mol Cell,* 14**,** 395-403.

STOKKE, K. T., ROOTWELT, K., WERGELAND, R. & VALE, J. R. 1986. Changes in plasma and red cell volumes during exposure to high altitude. *Scand J Clin Lab Invest Suppl,* 184**,** 113-7.

STOLZ, L. E., LI, D., QADRI, A., JALENAK, M., KLAMAN, L. D. & TOBIN, J. F. 2008. Administration of myostatin does not alter fat mass in adult mice. *Diabetes Obes Metab,* 10**,** 135-42.

STROKA, D. M., BURKHARDT, T., DESBAILLETS, I., WENGER, R. H., NEIL, D. A., BAUER, C., GASSMANN, M. & CANDINAS, D. 2001. HIF-1 is expressed in normoxic tissue and displays an organ-specific regulation under systemic hypoxia. *Faseb J,* 15**,** 2445-53.

SU, B., XIAO, C., DEKA, R., SEIELSTAD, M. T., KANGWANPONG, D., XIAO, J., LU, D., UNDERHILL, P., CAVALLI-SFORZA, L., CHAKRABORTY, R. & JIN, L. 2000. Y chromosome haplotypes reveal prehistorical migrations to the Himalayas. *Hum Genet,* 107**,** 582-90.

SUGI, H., IWAMOTO, H., AKIMOTO, T. & USHITANI, H. 1998. Evidence for the load-dependent mechanical efficiency of individual myosin heads in skeletal muscle fibers activated by laser flash photolysis of caged calcium in the presence of a limited amount of ATP. *Proc Natl Acad Sci U S A,* 95**,** 2273-8.

SUGINO, H., SUGINO, K., HASHIMOTO, O., SHOJI, H. & NAKAMURA, T. 1997. Follistatin and its role as an activin-binding protein. *J Med Invest,* 44**,** 1-14.

SULLIVAN, M. J., DUSCHA, B. D., KLITGAARD, H., KRAUS, W. E., COBB, F. R. & SALTIN, B. 1997. Altered expression of myosin heavy chain in human skeletal muscle in chronic heart failure. *Med Sci Sports Exerc,* 29**,** 860-6.

SURKS, M. I. 1966. Elevated PBI, free thyroxine, and plasma protein concentration in man at high altitude. *J Appl Physiol,* 21**,** 1185-90.

SWALLOW, E. B., REYES, D., HOPKINSON, N. S., MAN, W. D., PORCHER, R., CETTI, E. J., MOORE, A. J., MOXHAM, J. & POLKEY, M. I. 2007. Quadriceps strength predicts mortality in patients with moderate to severe chronic obstructive pulmonary disease. *Thorax,* 62**,** 115-20.

SZULC, P., SCHOPPET, M., GOETTSCH, C., RAUNER, M., DSCHIETZIG, T., CHAPURLAT, R. & HOFBAUER, L. C. 2012. Endocrine and clinical correlates of myostatin serum concentration in men--the STRAMBO study. *J Clin Endocrinol Metab,* 97**,** 3700-8.

TAN, B. H. & FEARON, K. 2008. Cachexia: prevalence and impact in medicine. *Curr Opin Clin Nutr Metab Care,* 11**,** 400-7.

TAWA, N. E., JR., ODESSEY, R. & GOLDBERG, A. L. 1997. Inhibitors of the proteasome reduce the accelerated proteolysis in atrophying rat skeletal muscles. *J Clin Invest,* 100**,** 197-203.

TAYLOR, W. E., BHASIN, S., ARTAZA, J., BYHOWER, F., AZAM, M., WILLARD, D. H., JR., KULL, F. C., JR. & GONZALEZ-CADAVID, N. 2001. Myostatin inhibits cell proliferation and protein synthesis in C2C12 muscle cells. *Am J Physiol Endocrinol Metab,* 280**,** E221-8.

THIES, R. S., CHEN, T., DAVIES, M. V., TOMKINSON, K. N., PEARSON, A. A., SHAKEY, Q. A. & WOLFMAN, N. M. 2001. GDF-8 propeptide binds to GDF-8 and antagonizes biological activity by inhibiting GDF-8 receptor binding. *Growth Factors,* 18**,** 251-9.

THOMAS, M., LANGLEY, B., BERRY, C., SHARMA, M., KIRK, S., BASS, J. & KAMBADUR, R. 2000. Myostatin, a negative regulator of muscle growth, functions by inhibiting myoblast proliferation. *J Biol Chem,* 275**,** 40235-43.

TRAENCKNER, E. B., WILK, S. & BAEUERLE, P. A. 1994. A proteasome inhibitor prevents activation of NF-kappa B and stabilizes a newly phosphorylated form of I kappa B-alpha that is still bound to NF-kappa B. *Embo J,* 13**,** 5433-41.

TRENDELENBURG, A. U., MEYER, A., ROHNER, D., BOYLE, J., HATAKEYAMA, S. & GLASS, D. J. 2009. Myostatin reduces Akt/TORC1/p70S6K signaling, inhibiting myoblast differentiation and myotube size. *Am J Physiol Cell Physiol,* 296**,** C1258-70.

TUVDENDORJ, D., CHINKES, D. L., BAHADORANI, J., ZHANG, X. J., SHEFFIELD-MOORE, M., KILLEWICH, L. A. & WOLFE, R. R. 2014. Comparison of bolus injection and constant infusion methods for measuring muscle protein fractional synthesis rate in humans. *Metabolism,* 63**,** 1562-7.

VAMVINI, M. T., ARONIS, K. N., CHAMBERLAND, J. P. & MANTZOROS, C. S. 2011. Energy deprivation alters in a leptin- and cortisol-independent manner circulating levels of

activin A and follistatin but not myostatin in healthy males. *J Clin Endocrinol Metab,* 96**,** 3416-23.

VELASQUEZ, T. 1959. Tolerance to acute anoxia in high altitude natives. *J Appl Physiol,* 14**,** 357-62.

VIGANO, A., RIPAMONTI, M., DE PALMA, S., CAPITANIO, D., VASSO, M., WAIT, R., LUNDBY, C., CERRETELLI, P. & GELFI, C. 2008. Proteins modulation in human skeletal muscle in the early phase of adaptation to hypobaric hypoxia. *Proteomics,* 8**,** 4668-79.

VYAS, D. R., SPANGENBURG, E. E., ABRAHA, T. W., CHILDS, T. E. & BOOTH, F. W. 2002. GSK-3beta negatively regulates skeletal myotube hypertrophy. *Am J Physiol Cell Physiol,* 283**,** C545-51.

WADDELL, D. S., BAEHR, L. M., VAN DEN BRANDT, J., JOHNSEN, S. A., REICHARDT, H. M., FURLOW, J. D. & BODINE, S. C. 2008. The glucocorticoid receptor and FOXO1 synergistically activate the skeletal muscle atrophy-associated MuRF1 gene. *Am J Physiol Endocrinol Metab,* 295**,** E785-97.

WAGNER, P. D. 2008. Possible mechanisms underlying the development of cachexia in COPD. *Eur Respir J,* 31**,** 492-501.

WAGNER, P. D. 2010. Operation Everest II. *High Alt Med Biol,* 11**,** 111-9.

WALKER, K. S., KAMBADUR, R., SHARMA, M. & SMITH, H. K. 2004. Resistance training alters plasma myostatin but not IGF-1 in healthy men. *Med Sci Sports Exerc,* 36**,** 787-93.

WALTER, R. C., BUFFLER, R. T., BRUGGEMANN, J. H., GUILLAUME, M. M., BERHE, S. M., NEGASSI, B., LIBSEKAL, Y., CHENG, H., EDWARDS, R. L., VON COSEL, R., NERAUDEAU, D. & GAGNON, M. 2000. Early human occupation of the Red Sea coast of Eritrea during the last interglacial. *Nature,* 405**,** 65-9.

WANG, G. L. & SEMENZA, G. L. 1993a. Characterization of hypoxia-inducible factor 1 and regulation of DNA binding activity by hypoxia. *J Biol Chem,* 268**,** 21513-8.

WANG, G. L. & SEMENZA, G. L. 1993b. General involvement of hypoxia-inducible factor 1 in transcriptional response to hypoxia. *Proc Natl Acad Sci U S A,* 90**,** 4304-8.

WANG, K., LI, Z., LI, Y., ZENG, J., HE, C., YANG, J., LIU, D. & WU, Z. 2013. Muscle-specific transgenic expression of porcine myostatin propeptide enhances muscle growth in mice. *Transgenic Res,* 22**,** 1011-9.

WEHRLIN, J. P. & HALLEN, J. 2006. Linear decrease in .VO2max and performance with increasing altitude in endurance athletes. *Eur J Appl Physiol,* 96**,** 404-12.

WEHRLIN, J. P., ZUEST, P., HALLEN, J. & MARTI, B. 2006. Live high-train low for 24 days increases hemoglobin mass and red cell volume in elite endurance athletes. *J Appl Physiol (1985),* 100**,** 1938-45.

WELLE, S., TAWIL, R. & THORNTON, C. A. 2008. Sex-related differences in gene expression in human skeletal muscle. *PLoS One,* 3**,** e1385.

WEST, J. B. 2002. Highest permanent human habitation. *High Alt Med Biol,* 3**,** 401-7.

WEST, J. B., LAHIRI, S. & AMERICAN PHYSIOLOGICAL SOCIETY (1887-) 1984. *High altitude and man,* Bethesda, Md.

Baltimore, American Physiological Society ;

Distributed by Williams & Wilkins Co.

WEST, J. B. & WAGNER, P. D. 1980. Predicted gas exchange on the summit of Mt. Everest. *Respir Physiol,* 42**,** 1-16.

WHITTEMORE, L. A., SONG, K., LI, X., AGHAJANIAN, J., DAVIES, M., GIRGENRATH, S., HILL, J. J., JALENAK, M., KELLEY, P., KNIGHT, A., MAYLOR, R., O'HARA, D., PEARSON, A., QUAZI, A., RYERSON, S., TAN, X. Y., TOMKINSON, K. N., VELDMAN, G. M., WIDOM, A., WRIGHT, J. F., WUDYKA, S., ZHAO, L. & WOLFMAN, N. M. 2003. Inhibition of myostatin in adult mice increases skeletal muscle mass and strength. *Biochem Biophys Res Commun,* 300**,** 965-71.

WIDRICK, J. J., STELZER, J. E., SHOEPE, T. C. & GARNER, D. P. 2002. Functional properties of human muscle fibers after short-term resistance exercise training. *Am J Physiol Regul Integr Comp Physiol,* 283**,** R408-16.

WIESENER, M. S., JURGENSEN, J. S., ROSENBERGER, C., SCHOLZE, C. K., HORSTRUP, J. H., WARNECKE, C., MANDRIOTA, S., BECHMANN, I., FREI, U. A., PUGH, C. W., RATCLIFFE, P. J., BACHMANN, S., MAXWELL, P. H. & ECKARDT, K. U. 2003. Widespread hypoxia-inducible expression of HIF-2alpha in distinct cell populations of different organs. *Faseb J,* 17**,** 271-3.

WILKINSON, S. B., TARNOPOLSKY, M. A., GRANT, E. J., CORREIA, C. E. & PHILLIPS, S. M. 2006. Hypertrophy with unilateral resistance exercise occurs without increases in endogenous anabolic hormone concentration. *Eur J Appl Physiol,* 98**,** 546-55.

WING-GAIA, S. L., GERSHENOFF, D. C., DRUMMOND, M. J. & ASKEW, E. W. 2014. Effect of leucine supplementation on fat free mass with prolonged hypoxic exposure during a 13-day trek to Everest Base Camp: a double-blind randomized study. *Appl Physiol Nutr Metab,* 39**,** 318-23.

WOLFE, R. R. 1984. Tracers in metabolic research: radioisotope and stable isotope/mass spectrometry methods. *Lab Res Methods Biol Med,* 9**,** 1-287.

WOOD, S. C. & STABENAU, E. K. 1998. Effect of gender on thermoregulation and survival of hypoxic rats. *Clin Exp Pharmacol Physiol,* 25**,** 155-8.

WORKENEH, B. T., RONDON-BERRIOS, H., ZHANG, L., HU, Z., AYEHU, G., FERRANDO, A., KOPPLE, J. D., WANG, H., STORER, T., FOURNIER, M., LEE, S. W., DU, J. & MITCH, W. E. 2006. Development of a diagnostic method for detecting increased muscle protein degradation in patients with catabolic conditions. *J Am Soc Nephrol,* 17**,** 3233-9.

WULFF, T., JOKUMSEN, A., HOJRUP, P. & JESSEN, F. 2012. Time-dependent changes in protein expression in rainbow trout muscle following hypoxia. *J Proteomics,* 75**,** 2342-51.

XIAO, R., FERRY, A. L. & DUPONT-VERSTEEGDEN, E. E. 2011. Cell death-resistance of differentiated myotubes is associated with enhanced anti-apoptotic mechanisms compared to myoblasts. *Apoptosis,* 16**,** 221-34.

YAFFE, D. & SAXEL, O. 1977. Serial passaging and differentiation of myogenic cells isolated from dystrophic mouse muscle. *Nature,* 270**,** 725-7.

YAMADA, N., HORIKAWA, Y., ODA, N., IIZUKA, K., SHIHARA, N., KISHI, S. & TAKEDA, J. 2005. Genetic variation in the hypoxia-inducible factor-1alpha gene is associated with type 2 diabetes in Japanese. *J Clin Endocrinol Metab,* 90**,** 5841-7.

YAMAGUCHI, A., FUJIKAWA, T., SHIMADA, S., KANBAYASHI, I., TATEOKA, M., SOYA, H., TAKEDA, H., MORITA, I., MATSUBARA, K. & HIRAI, T. 2006. Muscle IGF-I Ea, MGF, and myostatin mRNA expressions after compensatory overload in hypophysectomized rats. *Pflugers Arch,* 453**,** 203-10.

YANG, W., ZHANG, Y., LI, Y., WU, Z. & ZHU, D. 2007. Myostatin induces cyclin D1 degradation to cause cell cycle arrest through a phosphatidylinositol 3-kinase/AKT/GSK-3 beta pathway and is antagonized by insulin-like growth factor 1. *J Biol Chem,* 282**,** 3799-808.

YARASHESKI, K. E., BHASIN, S., SINHA-HIKIM, I., PAK-LODUCA, J. & GONZALEZ-CADAVID, N. F. 2002. Serum myostatin-immunoreactive protein is increased in 60-92 year old women and men with muscle wasting. *J Nutr Health Aging,* 6**,** 343-8.

YI, X., LIANG, Y., HUERTA-SANCHEZ, E., JIN, X., CUO, Z. X., POOL, J. E., XU, X., JIANG, H., VINCKENBOSCH, N., KORNELIUSSEN, T. S., ZHENG, H., LIU, T., HE, W., LI, K., LUO, R., NIE, X., WU, H., ZHAO, M., CAO, H., ZOU, J., SHAN, Y., LI, S., YANG, Q., ASAN, NI, P., TIAN, G., XU, J., LIU, X., JIANG, T., WU, R., ZHOU, G., TANG, M., QIN, J., WANG, T., FENG, S., LI, G., HUASANG, LUOSANG, J., WANG, W., CHEN, F., WANG, Y., ZHENG, X., LI, Z., BIANBA, Z., YANG, G., WANG, X., TANG, S., GAO, G., CHEN, Y., LUO, Z., GUSANG, L., CAO, Z., ZHANG, Q., OUYANG, W., REN, X., LIANG, H., HUANG, Y., LI, J., BOLUND, L., KRISTIANSEN, K., LI, Y., ZHANG, Y., ZHANG, X., LI, R., YANG, H., NIELSEN, R. & WANG, J. 2010. Sequencing of 50 human exomes reveals adaptation to high altitude. *Science,* 329**,** 75-8.

YOON, D., PONKA, P. & PRCHAL, J. T. 2011. Hypoxia. 5. Hypoxia and hematopoiesis. *Am J Physiol Cell Physiol,* 300**,** C1215-22.

YOSHIHISA, A., SHIMIZU, T., OWADA, T., NAKAMURA, Y., IWAYA, S., YAMAUCHI, H., MIYATA, M., HOSHINO, Y., SATO, T., SUZUKI, S., SUGIMOTO, K., YAMAKI, T., KUNII, H., NAKAZATO, K., SUZUKI, H., SAITOH, S. & TAKEISHI, Y. 2011. Adaptive servo ventilation improves

cardiac dysfunction and prognosis in chronic heart failure patients with Cheyne-Stokes respiration. *Int Heart J,* 52**,** 218-23.

ZACHWIEJA, J. J., SMITH, S. R., SINHA-HIKIM, I., GONZALEZ-CADAVID, N. & BHASIN, S. 1999. Plasma myostatin-immunoreactive protein is increased after prolonged bed rest with low-dose T3 administration. *J Gravit Physiol,* 6**,** 11-5.

ZHANG, N., FU, Z., LINKE, S., CHICHER, J., GORMAN, J. J., VISK, D., HADDAD, G. G., POELLINGER, L., PEET, D. J., POWELL, F. & JOHNSON, R. S. 2010. The asparaginyl hydroxylase factor inhibiting HIF-1alpha is an essential regulator of metabolism. *Cell Metab,* 11**,** 364-78.

ZHANG, X. J., CHINKES, D. L., SAKURAI, Y. & WOLFE, R. R. 1996. An isotopic method for measurement of muscle protein fractional breakdown rate in vivo. *Am J Physiol,* 270**,** E759-67.

ZHANG, Y., NICHOLATOS, J., DREIER, J. R., RICOULT, S. J., WIDENMAIER, S. B., HOTAMISLIGIL, G. S., KWIATKOWSKI, D. J. & MANNING, B. D. 2014. Coordinated regulation of protein synthesis and degradation by mTORC1. *Nature,* 513**,** 440-3.

ZHAO, M., KONG, Q. P., WANG, H. W., PENG, M. S., XIE, X. D., WANG, W. Z., JIAYANG, DUAN, J. G., CAI, M. C., ZHAO, S. N., CIDANPINGCUO, TU, Y. Q., WU, S. F., YAO, Y. G., BANDELT, H. J. & ZHANG, Y. P. 2009. Mitochondrial genome evidence reveals successful Late Paleolithic settlement on the Tibetan Plateau. *Proc Natl Acad Sci U S A,* 106**,** 21230-5.

ZHAO, S. P. & ZENG, L. H. 1997. Elevated plasma levels of tumor necrosis factor in chronic heart failure with cachexia. *Int J Cardiol,* 58**,** 257-61.

ZHU, X., TOPOUZIS, S., LIANG, L. F. & STOTISH, R. L. 2004. Myostatin signaling through Smad2, Smad3 and Smad4 is regulated by the inhibitory Smad7 by a negative feedback mechanism. *Cytokine,* 26**,** 262-72.

ZIMMERS, T. A., DAVIES, M. V., KONIARIS, L. G., HAYNES, P., ESQUELA, A. F., TOMKINSON, K. N., MCPHERRON, A. C., WOLFMAN, N. M. & LEE, S. J. 2002. Induction of cachexia in mice by systemically administered myostatin. *Science,* 296**,** 1486-8.

ZOU, Q., WANG, X., LIU, Y., OUYANG, Z., LONG, H., WEI, S., XIN, J., ZHAO, B., LAI, S., SHEN, J., NI, Q., YANG, H., ZHONG, H., LI, L., HU, M., ZHANG, Q., ZHOU, Z., HE, J., YAN, Q., FAN, N., ZHAO,

Y., LIU, Z., GUO, L., HUANG, J., ZHANG, G., YING, J., LAI, L. & GAO, X. 2015. Generation of gene-target dogs using CRISPR/Cas9 system. *J Mol Cell Biol,* 7**,** 580-3.

Appendices

Appendix One – Solutions and Buffers

TBS-T 10 × (1 L)

Tris-HCl 1 mol pH 8.0	100 mL
NaCl	87.6 g
Tween	5 mL

Make up to 1 L in dH_2O. Dilute 1:10 in dH_2O for usage. Store at room temperature.

Total protein lysis buffer (1X)

Tris HCl pH 7.4 1 M	400 µL
NaCl 1 M	6 mL
EDTA 100 µL	800 µL
Triton	800 µL

Make up to 40 mL in dH_2O. Store at 4 °C. Add protease and phosphatase inhibitors (1:100) just prior to usage.

Laemmli's loading buffer (4X)

Tris-HCl 1 mol pH 6.8	2.4 mL
SDS	0.8 g
Glycerol	4 mL
β – mercaptoethanol	1 mL

dH_2O	2.8 mL
Bromophenol blue	trace

For use at 4X concentration, do not further dilute. Store at room temperature.

Running buffer 20 × (1 L)

NuPAGE SDS running buffer (20X) (NP0001 – Invitrogen). Store at room temperature.

Dilute 1:20 in dH_2O for immediate usage.

Transfer buffer 10 × (1 L)

Glycine	90 g
Tris	19.3 g

Make up to 1 L in dH_2O. Dilute (1 part 10 ×, 2 parts methanol, 7 parts dH_2O) for usage. Keep 1 × solution at 4 °C.

Appendix Two – Blinded Analysis of Myotube Diameters

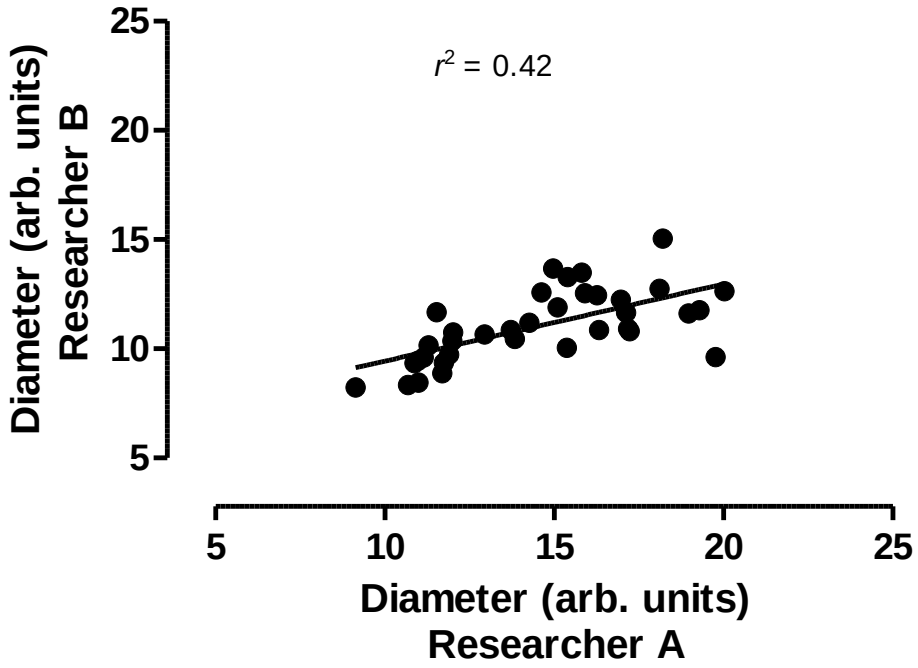

Appendix figure 1: Myotube diameter (arb. units) as measured by researcher B as a function myotube diameter (arb. units) as measured by Researcher B.

A researcher blinded to treatment and time checked analysis of myotube diameters in a matching manner to the doctoral candidate (detailed in Chapter Three). A strong positive correlation was noted between paired myotube diameters as measured by researcher A and researcher B ($r = 0.651$). Pearson's correlation shows this relationship to be significant ($p < 0.001$).

Appendix Three – Ethical Approval of Research Involving Human Participants

Ethical approval for the work described in Chapter Four of this thesis was obtained from the University of Westminster Research Ethics sub-committee (10/11/24) and the University of Brighton Faculty Research and Governance Committee (FREGH/29/09).

Ethical approval for the work described in Chapter Five was provided by the University of Westminster Research Ethics Sub-committee (12/13/46).

Ethical approval for the work described in Chapter Six was provided by the University of Westminster Research Ethics Sub-committee (13/14/22) and the University of California, San Diego Institutional Review Board (131521).

Chapter Four Letter of Approval

UNIVERSITY OF
FORWARD
THINKING
WESTMINSTER

Richard Mackenzie
University of Westminster
School of Life Sciences
115 New Cavendish Street
London, W1W 6UW

14 March 2011

Dear Richard

App. No. 10/11/24 (was previously App. No. 10/11/13)
Richard Mackenzie: School of Life Sciences
Mode: Staff
Dean: Jane Lewis

Melting into thin air: The role of hypoxia in muscle atrophy

I am writing to inform you that your application was considered by the Research Ethics sub Committee at its meeting on 3 March 2011. The proposal was **approved**

If your protocol changes significantly in the meantime, please contact me immediately, in case of further ethical requirements

Yours sincerely

Huzma Kelly
Senior Research Officer (Policy and Governance)
Secretary, Research Ethics sub Committee

cc Dr. John Colwell, (Chair) Research Ethics sub Committee
Prof. Jane Lewis

Chapter Five Letter of Approval

UNIVERSITY OF WESTMINSTER

APP. NO. 12-13-46: Bradley Elliott

PRIVATE AND CONFIDENTIAL
Mr Bradley Elliott
Faculty of Science and Technology
115 New Cavendish Street
London
W1W 6WU

29 August 2013

Dear Mr Elliott

App. No. 12-13-46
Name: Bradley Elliott Faculty: Science and Technology
Mode: MPhil/PhD
Supervisor: Richard MacKenzie

Project Title: The effect of 12 hours hypoxia upon plasma and muscle myostatin

I am writing to inform you that your application has been considered by the members of the Research Ethics Sub Committee using processes to expedite approval due to the absence of a meeting of the revised University Research Ethics Committee until October 2013. The proposal was approved subject to the following comments being addressed to the satisfaction of your supervisor and Keith Redway:

- Biohazard COSHH forms should take account of the fact that ACDP Category 3 pathogens (HIV, Hepatitis B/C) are a possibility in human samples, if slight. They should acknowledge this possibility and refer to Appendix 6 of the Lab safety regs for the code for handling human blood in their risk assessments, including provision of a suitable disinfectant and emergency procedure in the event of a needle-stick injury.
- Documents such as consent forms and the coding list should be scanned and the resultant file saved securely on a server, such as the H drive which is backed up.

Please provide me with the above documentation or clarifications as soon as possible.

Yours sincerely

Dr Bob Odle
Acting Secretary, University Research Ethics Committee

Academic Registrar's Department
101 New Cavendish Street
Cavendish House, University of Westminster
London, W1W 6XH
E: odler@westminster.ac.uk
westminster.ac.uk/research

Chapter Six Letters of Approval

131521

UNIVERSITY OF CALIFORNIA, SAN DIEGO
HUMAN RESEARCH PROTECTIONS PROGRAM

TO: Dr. Peter D. Wagner Mailcode: 0623A

RE: Project #131521
Myostatin signaling during acute hypoxic exposure

Dear Dr. Wagner:

The above-referenced project was reviewed and approved by one of this institution's Institutional Review Boards in accordance with the requirements of the Code of Federal Regulations on the Protection of Human Subjects (45 CFR 46 and 21 CFR 50 and 56), including its relevant Subparts. This approval, based on the degree of risk, is for 365 days from the date of **IRB review and approval** unless otherwise stated in this letter. The regulations require that continuing review be conducted on or before the 1-year anniversary date of the IRB approval, even though the research activity may not begin until some time after the IRB has given approval.

The IRB determined that this project presents no more than minimal risk to human subjects in that the probability and magnitude of harm or discomfort anticipated in the research are not greater in and of themselves than those ordinarily encountered in daily life or during the performance of routine physical or psychological examinations or tests.

Date of IRB review and approval: **12/5/2013**

On behalf of the Institutional Review Board,

/lg
Michael Caligiuri, Ph.D.
Director, Human Research Protections Program
(858) 657-5100

Note: IRB approval does not constitute funding **or other institutional required approvals.** Should your studies involve other review committees such as Office of Clinical Trials Administration (OCTA), Office of Coverage Analysis Administration (OCAA), Conflict of Interest (COI), Protocol Review Monitoring Committee (PRMC), and committees under Environmental Health & Safety (EH&S) such as Institutional Biosafety Committee (IBC), Human Exposure Committee (HERC), and RSSC (Radiation Safety and Surveillance Committee), it is the researchers responsibility to ensure that all approvals are in place prior to conducting research involving human subjects or their related specimens.

Approval release date: 1/21/2014

UNIVERSITY OF WESTMINSTER

APP. NO. 13-14-22 Elliott
UREC 15 May 2014

PRIVATE AND CONFIDENTIAL
Bradley Elliott
c/o Faculty of Science and Technology
115 New Cavendish Street
London

23 May 2014

Dear Bradley

Ethics App.	**No. 13-14-22**
Applicant:	**Bradley Elliott**
Faculty:	**Science and Technology**
Mode:	**Doctoral Researcher**
Supervisor:	**Richard Mackenzie**

Proposal title: Myostatin signalling during acute hypoxic exposure

I am writing to inform you that the decision of the IRB at the University of California San Diago for the supplementary study which will be included in your doctoral research programme considered by the University Research Ethics Committee at its meeting of 15 May 2014. The approval from the UCSD IRB and the subsequent amendments to your PIS and consent form were noted by the Committee.

If your protocol changes significantly in the meantime, please contact me immediately, in case of further ethical requirements. Please read the important notes on the following page.

Yours sincerely

Dr Bob Odle
Acting Secretary, University Research Ethics Committee

cc. Chair, University Research Ethics Committee
Chair, Faculty Research Ethics Committee
Supervisors
UREC Member
Graduate School Registry Manager

Academic Registrar's Department
Quality and Standards Office
101 New Cavendish Street
Cavendish House, University of Westminster
London, W1W 6XH
T: +44 (0) 20 3506 6061
E: R.Odle@westminster.ac.uk
www.westminster.ac.uk/research

Appendix Four – Lake Louse Acute Mountain Sickness Questionnaire

Questionnaire was modified from standard (Appendix figure 2) to exclude the final question regarding sleep patterns, as outlined by Richards and colleagues (2014).

Lake Louise Score (LLS) for the diagnosis of Acute Mountain Sickness (AMS)

A diagnosis of AMS is based on:
1. A rise in altitude within the last 4 days
2. Presence of a headache

PLUS

3. Presence of at least one other symptom
4. A total score of 3 or more from the questions below

SELF-REPORT QUESTIONNAIRE

Add together the individual scores for each symptom to get the **total score**.

Headache	No headache	0	
	Mild headache	1	
	Moderate headache	2	
	Severe headache, incapacitating	3	
Gastrointestinal symptoms	None	0	
	Poor appetite or nausea	1	
	Moderate nausea &/or vomiting	2	
	Severe nausea &/or vomiting	3	
Fatigue &/or weakness	Not tired or weak	0	
	Mild fatigue/ weakness	1	
	Moderate fatigue/ weakness	2	
	Severe fatigue/ weakness	3	
Dizziness/lightheadedness	Not dizzy	0	
	Mild dizziness	1	
	Moderate dizziness	2	
	Severe dizziness, incapacitating	3	
Difficulty sleeping	Slept as well as usual	0	
	Did not sleep as well as usual	1	
	Woke many times, poor sleep	2	
	Could not sleep at all	3	
	TOTAL SCORE:		

Appendix figure 2: Lake Louise Acute Mountain Sickness Questionaire.

Appendix Five – Calculation of Total Protein in the Method of Lowry

Taken from manufactures instructions (Bio-rad DC protein assay).

1) Prepare A^{l}. Add 20 µL reagent S to 1 mL reagent A, mix. Scale amount to required A^{l} total volume.
2) Lysed muscle or cellular extract defrosted to 0 °C on ice
3) BSA standards diluted from stock (1.44 $\mu g.mL^{-1}$) to following concentrations in total protein lysis buffer (0.72 $\mu g.mL^{-1}$, 0.48 $\mu g.mL^{-1}$, 0.36 $\mu g.mL^{-1}$, 0.288 $\mu g.mL^{-1}$, 0.18 $\mu g.mL^{-1}$, 0.09 $\mu g.mL^{-1}$).
4) Samples, standards and blank (lysis buffer only) loaded in triplicate into 96 - well U bottomed plate, 5 µL per well.
5) 25 µL reagent A^{l} added to each well
6) 200 µL reagent B added to each well
7) Cover and seal plate, 15 minutes at room temperature
8) Absorbance quantified, read at 750 nm.
9) Standard graphed for quantification of unknowns

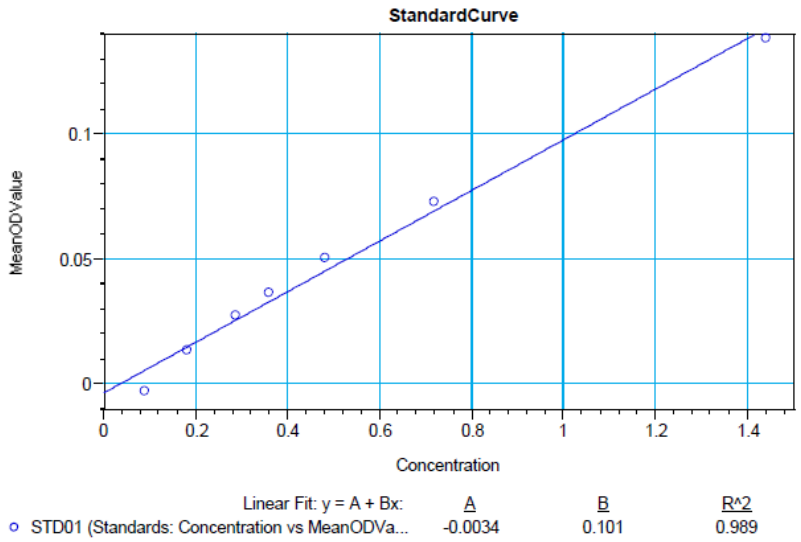

Appendix figure 3: Representative standard curve.

Appendix Six – Extraction of Amino Acids from Muscle and Plasma for Quantification of Label Enrichment by GCMS

Plasma:

1) 500 µL plasma (room temperature), vortex and incubate with 10 µL urease (10 mg.mL^{-1}; U1500-20KU, Sigma), 10 minutes.
2) Precipitated, 10 µL perchloric acid (12 mol), on ice, 15 minutes.
3) Spin, 6000 rpm, 10 minutes, 4 °C.
4) Extract 400 µL supernatant, add 100 µL potassium bicarbonate (1 mol), incubate on ice for 20 minutes
5) Spin, 6000 rpm, 10 minutes, 4 °C.
6) Supernatant extracted, add 10 µL concentrated hydrochloric acid.
7) Dried overnight, 50 °C , rotary evaporator.

Muscle samples:

1) ~ 100 µg powered by mortar and pestle on liquid nitrogen.
2) Resuspended in 0.5 mL ice cold perchloric acid (0.2 mol).
3) Centrifuged, 6000 rpm, 10 minutes, 4 °C.
4) Supernatant 1 incubated in 100 µL 1 mol ice cold potassium bicarbonate on ice, 15 minutes, then 10 µL urease (10 mg.mL^{-1}).
5) Pellet washed in 0.2 mol perchloric acid, spun, resultant pellet and supernatant 1 dried, 50 °C, rotary evaporator, overnight.

For calculation of whole body protein synthesis 250 µL of plasma was brought to room temperature, briefly vortexed and incubated with 10 µL urease (10 mg.mL^{-1}; U1500-20KU, Sigma) for 5 minutes. Samples were precipitated of plasma proteins in 1 mL ice-cold perchloric acid (0.2 mol), on ice for 15 minutes. Purified samples were then spun (6000 rpm, 10 minutes, 4 °C) and subsequent supernatants were extracted and dried overnight at 50 °C in a rotary evaporator. Dried samples

were derivatized with 50 µL pyridine (1 mol) and 50 µL N-tert-Butyldimethysilyl-N-methyltrifluoro-acetamide (MTBSTFA; Sigma, 3948820) at 70 °C for 60 minutes.

Muscle samples from time points -30, 120, 300 and 320 minutes were used for calculation of protein degradation rate post hypoxic exposure. An aliquot of each biopsy (~ 50 mg) were powered by mortar and pestle in liquid nitrogen, then resuspended in 0.5 mL ice cold perchloric acid (0.2 mol) and centrifuged (6000 rpm, 10 minutes). Resultant pellet was washed in 0.2 mol perchloric acid, spun and subsequent pellet run as below. First supernatant was incubated with 100 µL 1 mol ice cold potassium bicarbonate and incubated on ice (15 minutes), after which incubated with 10 µL urease (10 $mg.mL^{-1}$), as above and treated in the same manner as plasma samples.

Dried amino acid samples were resuspended into equal volumes of dH_20 and 12 mol HCl, and heated overnight (100 °C) then read via gas chromatography mass spectrometry (GCMS). Enrichment of samples was determined by gas chromatography-combustion-isotope ratio mass spectrometry for mass fragment peaks of 234 mHz (unlabelled tracee [T]), 235 mHz (^{15}N-Phe tracer) and 239 mHz (D_5-Phe tracer).

$$FSR\ (\%.Hr^{-1}) = \left(\frac{\Delta Et}{[Ep \times (\Delta t)]}\right) \times 100$$

FSR, Fractional synthesis rate (in percent per hour); ΔEt, change in tissue enrichment; Ep mean plasma enrichment; t, time (hours).

Calculation of fractional breakdown rate (FBR) was performed as described by Zhang and colleagues (Zhang et al., 1996) and refined by Phillips and colleagues (Simonson et al., 2015), and is based on the principle of decay of tracer (phenylalanine) to tracee (^{15}N-Phe) in the muscle intracellular pool following termination of isotope infusion.

$$FBR = \frac{E_M(t_2) - E_M(t_1)}{P\int_{t_1}^{t_2} E_A\,(t)dt - (1+P)\int_{t_1}^{t_2} E_M\,(t)dt} \times (\frac{Q_M}{T})$$

FBR, fractional breakdown rate; EM, enrichment muscle; EA, enrichment arterial; t, time; $\int_{t_1}^{t_2} E_X\,(t)dt$ gives area of decay curve of x (muscle or arterial); QM/T, ratio of intracellular free trace verses protein-bound trace content in the sample.

Subsequent net protein balance can be calculated as follows

$$Net\ balance(\%.hour) = FSR\ (\%.hour) - FBR\ (\%.hour)$$

FSR, Fractional synthesis rate; FBR, fractional breakdown rate

Etheridge and colleagues (2011) noted human FSR (%.hour^{-1}) to be ~ 0.02 – 0.1. Thus, expected ranges of ΔE can be proposed, and a standard curve built to examine signal / noise. Simulated ranges of FSR (%.hour^{-1}; Appendix table 1) were examined by spiking samples of phenylalanine (phe) with known amounts of labelled phenylalanine (D5-Phe) to give a known ΔE (% enrichment) calculating resultant % increase over phenylalanine only. Subsequent examination of the increase in D5-Phe over baseline as a function of spiked enrichment (% of total phe) indicates a strong linear relationship (r^2 = 0.9926, Pearson's p < 0.001; Appendix figure 4).

Appendix table 1: Specific peak area under the curve for Phe (234 mHz) and D_5-Phe (239 mHz), resultant enrichment rate and % increase over baseline enrichment. Value of 0 = phe only and 1 = d5-phe only, other values represent ratio of D_5-Phe / Phe.

Simulated FSR (%.hr^{-1})	234 mHz	239 mHz	% enrichment	% increase
0 (phe only)	273226	1096	0.4011	0 (baseline)
0.0125	168945	1850	1.095	0.693898
0.025	315800	5465	1.7305	1.329393
0.05	1137457	34215	3.008	2.606893
0.1	569943	32461	5.6955	5.294349
0.2	213910	25059	11.715	11.31361
1 (D_5-Phe only)	305	62485	100	99.51424

FSR, fractional synthesis rate; Phe, phenylalanine.

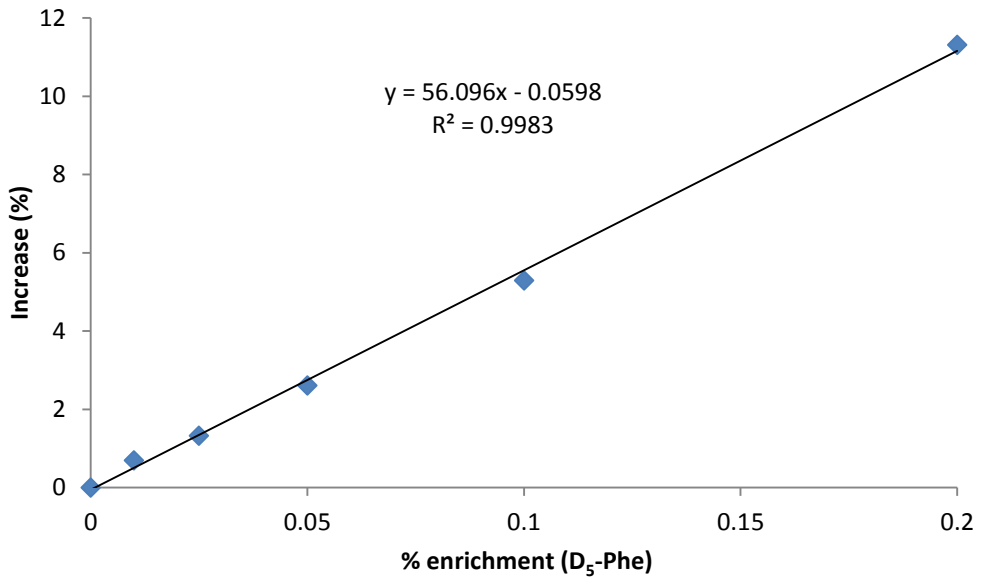

Appendix figure 4: Percentage increase in D_5-Phe over baseline (phe only) for known enrichment amounts, as a function of percent enrichment of D_5-Phe.

Appendix Seven – Detection of Specific Proteins by Western Blot

Before starting:

- Sample total protein content calculated in method of Lowry (Appendix Five)
- **Either -** Samples are pre-diluted 1:4 in Laemmli's loading buffer (4 ×)
- **OR -** Samples are pre-diluted into Laemmli's loading buffer (4 ×) to 2 $\mu g.mL^{-1}$.

Protocol:

1. Boil samples at 95 °C, 5 minutes on plate heater
2. Remove gel(s) from package (Invitrogen - NP0301), rinse in dH_2O.
3. Assemble gel cassette (2 gels, or 1 gel and one blank).
4. Fill cassette with running buffer (Appendix One).
5. Rinse wells in loading buffer with repeated bursts of ~ 100 µL running buffer via loading tip
6. Load: 40 – 60 µg total protein per well (can be varied by expected protein concentration) plus protein ladder and any standards (positive or negative).
7. Run: 30 - 45 minutes, 200 volts, dependent on molecular weight of target protein(s).
8. Transfer: After assembling cassette (Appendix figure 5), transfer 25 V, 60 mA, 3 hours, on ice. Pre-soak all components in transfer buffer (Appendix One), pre-chilled to 4 °C.

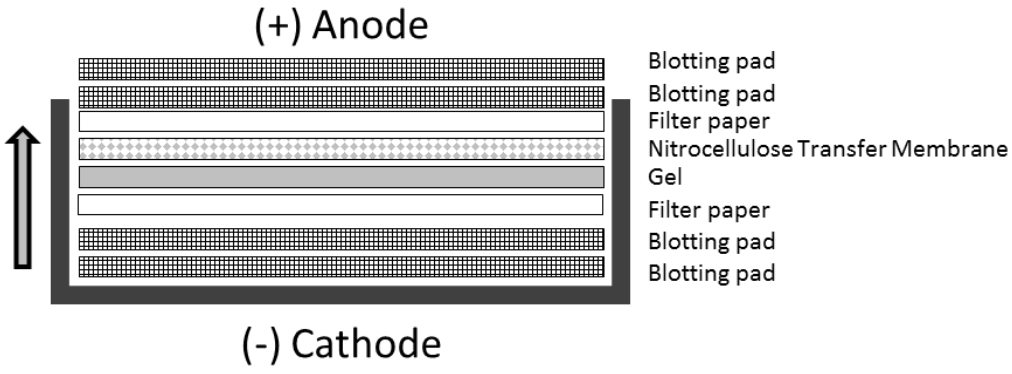

Appendix figure 5: Assembly of transfer cassette for one gel. Repet gel – nitrocellulose – filter paper if needed for two gels.

9. Ponceau s, 1 mL, 2 minutes. Scan and save image for normalization.

10. Block: 5 % BSA or 5 % milk in TBS - T (Appendix One). 1 hour, room temperature, gentle agitation. Gentle agitation.
11. Primary antibody: 1:1000 (or as pre-determined) in protein solution of choice (milk or BSA, 0.5 – 5 %) in TBS - T. Overnight, 4 °C, gentle agitation.
12. Wash – 4 × 5 minutes, ~ 10 mL TBS - T. Gentle agitation.
13. Secondary – 1:10,000 in 0.5 % BSA in TBS - T. 1 hour, room temperature. Anti-rabbit (Cell Signalling, 7074). Gentle agitation.
14. Wash – 4 × 5 minutes, ~ 10 mL TBS - T. Gentle agitation.
15. ECL (20-5000-120, Biological Industries). One part component A and B, approximately 300 mL total volume per membrane for 2 minutes. Immediately expose to film in dark room for 1 – 5 minutes. Develop as standard.
16. Scan and save film digitally. Quantify in ImageJ.

Appendix Eight – Normalisation of Detected Proteins by Ponceau S

For the normalization of total protein loadings per well this work utilizes the method of Romero-Calvo and colleagues (2010). Where traditionally a 'house-keeping' protein has been used, such as β-actin or α-tubulin, Romero-Calvo and colleagues (2010) suggests instead the use of ponceau S stain, as is normally performed for the confirmation of successful electro-transfer during immunoblotting, as it shows greater sensitivity to alterations in loading, is quicker and cheaper than repeated probes and avoids inherent assumptions regarding a lack of change of house-keeping proteins. Most importantly, ponceau S non-specifically stains for any protein, as such directly measures protein transferred, without extrapolating from measures of an individual protein.

Protocol:

1) After transfer stage of Western blot (Appendix Seven) wash membrane (1 min, TBS - T)
2) Ponceau S stain, 1 mL, 2 minutes at room temperature, gentle agitation.
3) Wash briefly (TBS – T, < 1 min)
4) Scan and save digitally each lane of interest, plus at least one blank lane.
5) Quantify lane density and blank lane density, resultant (= lane – blank) gives normalisation value.

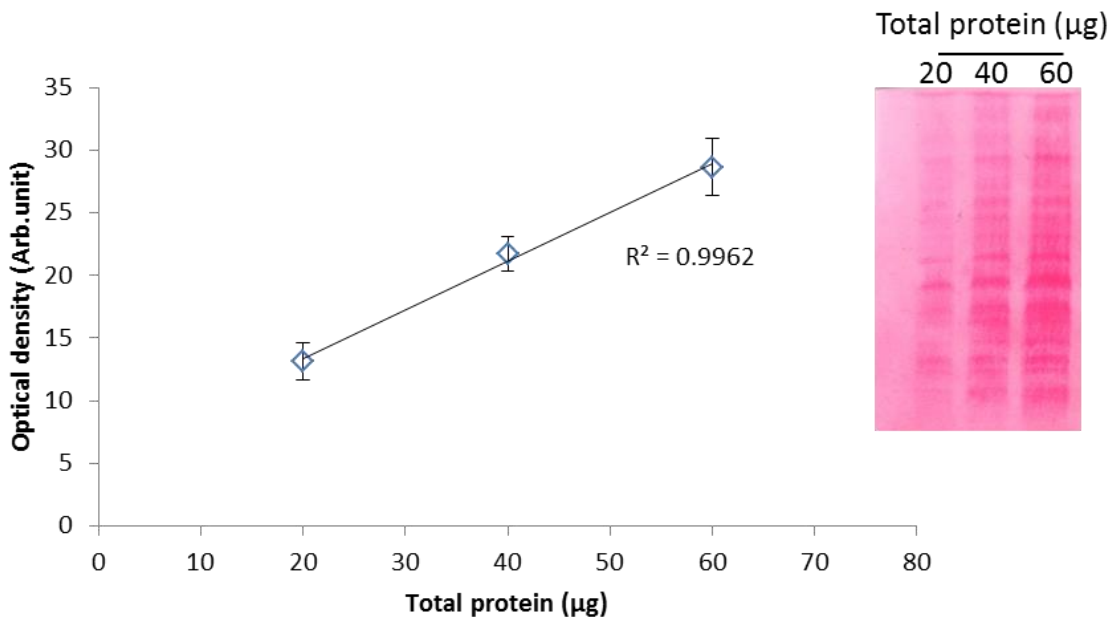

Appendix figure 6: Ponceau S stains in a linear repeatable manner. Total protein (20, 40 and 60 µg).from lysis of C2C12 myotubes was loaded in triplicate into wells, ran and transferred as outlined in Appendix Eight and densitometry quantified in in ImageJ. Error bars represent standard error.

Appendix Nine – Comparison of ELISA kits for the Measurement of Plasma Myostatin

Two commercially available ELISA kits were trialled for the measurement of plasma myostatin. Matching plasma samples from Chapter Four were analysed according to manufacturer's instructions. The kits trialled were provided by R&D (DGDF80, UK) and UCSN (SEB653Hu, China). All samples and standards were run in duplicate. Resultant concentrations of matching samples were directly compared, as were coefficient of variability measures of samples and standards between assays.

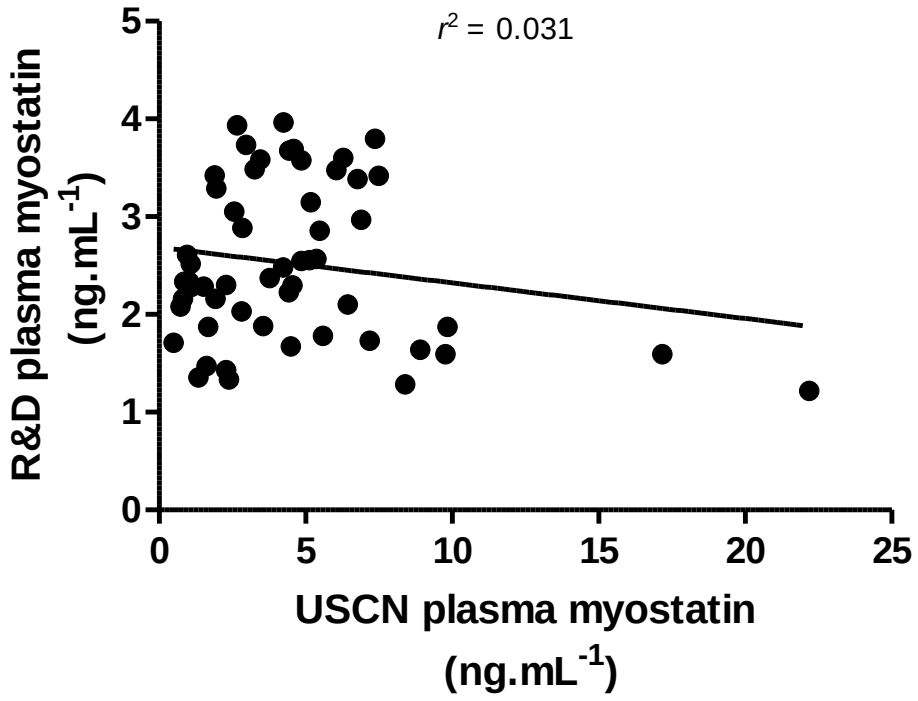

Appendix figure 7: A comparison of commercial ELISA kits from differing manufactures.

A significant lack of similarity was noted in matching measures of plasma myostatin between the USCN and the R&D assay (Appendix figure 7), with no association between matching values (r^2 = 0.031) and no correlation between measures is noted (Pearson's p = 0.20). Data from one

participant is not present on this figure, as concentrations reported by the USCN ELISA kit were consistently below zero, a physiologically unlikely occurrence.

An examination of the coefficient's of variability between assays from data produced in house suggests the R&D ELISA shows greater reliability over the USCN, with the R&D ELISA reporting 3.18 and 13.75 for samples and standards, while the USCN ELISA reports 9.11 and 18.50 for samples and standards, respectively.

The reduced variability of the R&D ELISA combined with the repeated intermittent lack of detection of plasma myostatin with the USCN ELISA resulted in the selection of the R&D ELISA for measurement of plasma myostatin in this thesis.

Appendix Ten – Detection of Myostatin by ELISA

Taken from manufactures instructions (R&D, DGDF80).

1) Samples and standards brought to room temperature.
2) Plasma samples activated (to break myostatin – binding protein links). To 100 µL plasma add 60 µL 1 N HCl, gentle agitation 10 minutes room temperature.
3) Plasma samples neutralized, 40 µL 1.2 N NaOH + 0.5 mol HEPES.
4) Plasma samples (now 200 µL total volume) diluted into 200 µL calibrator diluent (total 1:4).
5) Standards 2000, 1000, 500, 250, 125, 62.5, 31.3 $pg.mL^{-1}$ generated from serial dilution of standard (20,000 $pg.mL^{-1}$) into calibrator diluent.
6) 50 µL assay diluent added to each well.
7) Standards and samples loaded in triplicate into clear U bottom plate.
8) 2 hours room temperature incubation, gentle agitation. Covered with plate sealer.
9) Wash wells, 4 × ~ 400 µL wash solution, with complete removal of wash at each step.
10) 200 µL GDF-8 conjugate added to each well.
11) 2 hours room temperature incubation, gentle agitation. Covered with plate sealer.
12) Wash wells, 4 × ~ 400 µL wash solution, with complete removal of wash at each step.
13) 200 µL substrate solution, 30 minutes incubation, room temperature, protected from light.
14) 50 µL stop solution to each well.
15) Read optical density of each well within 30 minutes at 450 nm, and blank to 570 nm.
16) Calibration curve of known standards constructed (Appendix figure 8).

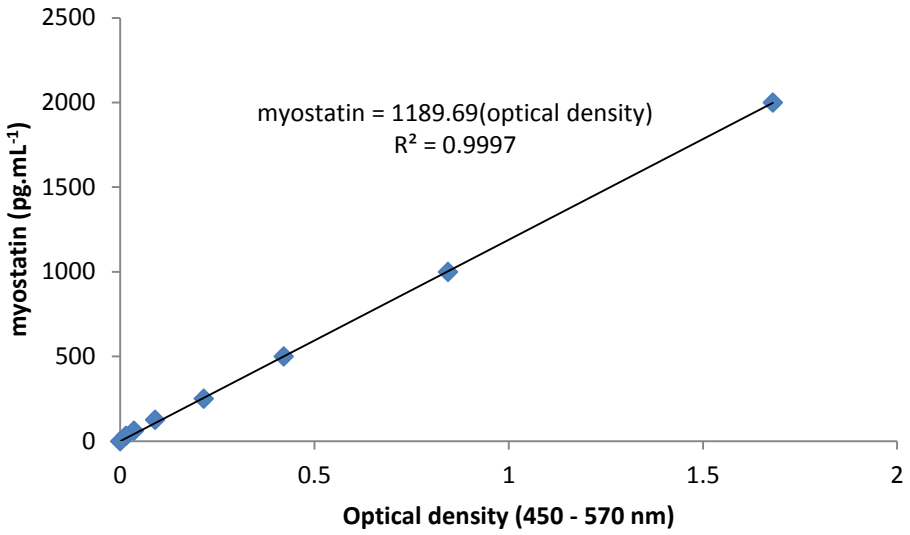

Appendix figure 8: Myostatin ELISA standard curve. Recombinant myostatin (pg.mL^{-1}) as a function of optical density (450 – 570 nm). All samples read in triplicate.

Appendix Eleven – Calculation of Resting Metabolic Rate by Indirect Calorimetry

Protocol modified from the recommendations of Haugen and colleagues (2007). Fasted and rested participants presented to the research laboratory on the morning of testing. Participants were asked to fast for 12 hours, and avoid exercise and active methods of transportation on the morning of testing. Expired gas fractions and volumes were collected for indirect calorimetry (Cortex Metalyzer 3B).

1) Calibrate Cortex for volumes (3 L syringe standard), expired fractions (standards of 17 % O_2 and 5 % CO_2), ambient pressure and temperature.
2) Fit participant with a standard mask, for both fit (seal) and comfort.
3) Record continuous data (V_E, F_EO_2, F_ECO_2) recorded for at least 40 minutes in a darkened, quiet room.
4) Discard first 10 minutes data, giving (at least) 30 minutes continuous data
5) VO_2, VCO_2 and RER calculated as standard.
6) With reference to the tables of Lusk (1924), caloric equivalent per L O_2 determined.

$$Energy\ expenditure\ (kj) = (VO_2\ (L.min) \times caloric\ equilivent)\ \times 4.12$$

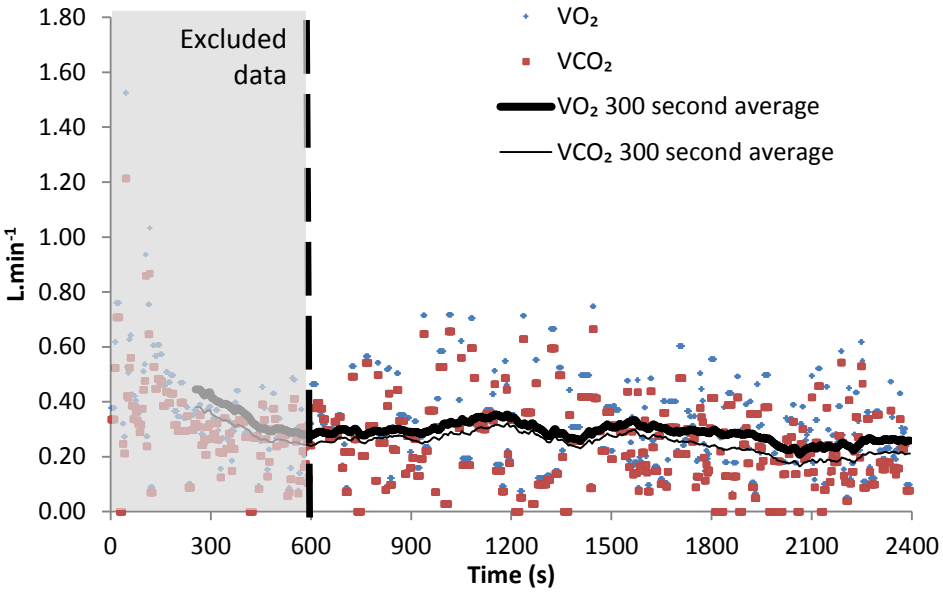

Appendix figure 9: Representative example of indirect calorimetry result. VO_2 ($L.min^{-1}$) in blue crosses, VCO_2 ($L.min^{-1}$) in red squares. Five minute rolling ball average for each group shown (VO_2 thick line, VCO_2 thin line). Vertical dotted line indicates separation between discarded data (0 – 600 s) and data used for calculation of resting metabolic rate (600 – 2400 s, 10 – 40 minutes).

Appendix Twelve – Calculation of Bottled Gas Concentration

For Chapter Five of this work hypoxic gas was mixed from stock solutions and delivered by gas mask system. A calibration curve was determined by atmospheric air, diluted with N_2, and read through an oxygen analyser (Vacuumed – 1760) in duplicate, with analogue output into a chart recorder (Gould, mark 200).

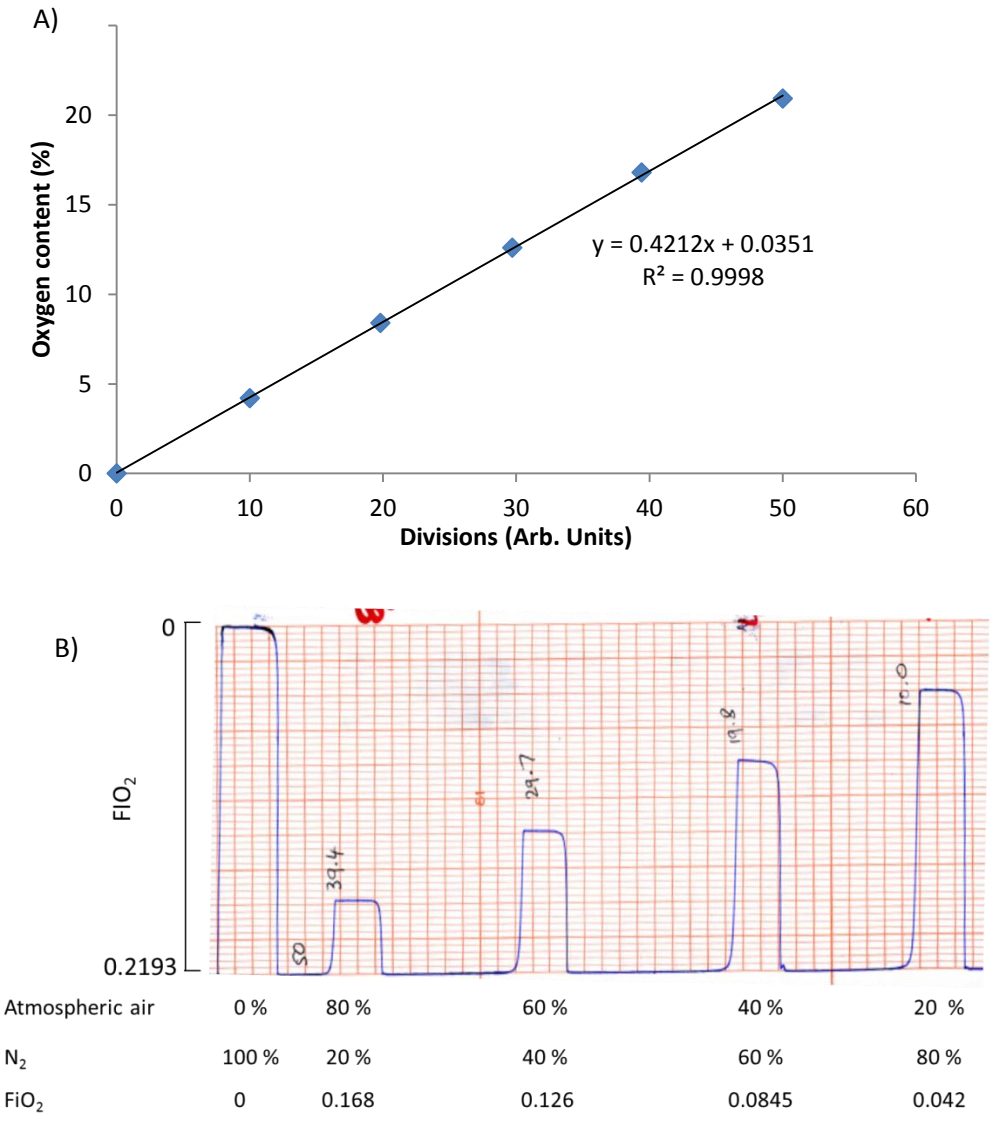

Atmospheric air	0 %	80 %	60 %	40 %	20 %
N_2	100 %	20 %	40 %	60 %	80 %
FiO_2	0	0.168	0.126	0.0845	0.042

Appendix figure 10: Calculation of bottled gas concentration. A) Oxygen content (%) as a function of divisions (Arb. Units) of 100 mL ambient room air. Ambient air was collected into a glass syringe and diluted with 100 % N_2. A Gould chart reader was pre-zeroed to 100 % N_2 [FiO2 of 0 - 0 divisions (Arb. Units)] and 100 % atmospheric air (FiO_2 of 0.2193, 50 divisions (Arb. Units)]. **B)** Representative image of chart output.

Appendix Thirteen – Calculation of Equivalent Altitude from Percentage of Ambient Oxygen Concentration

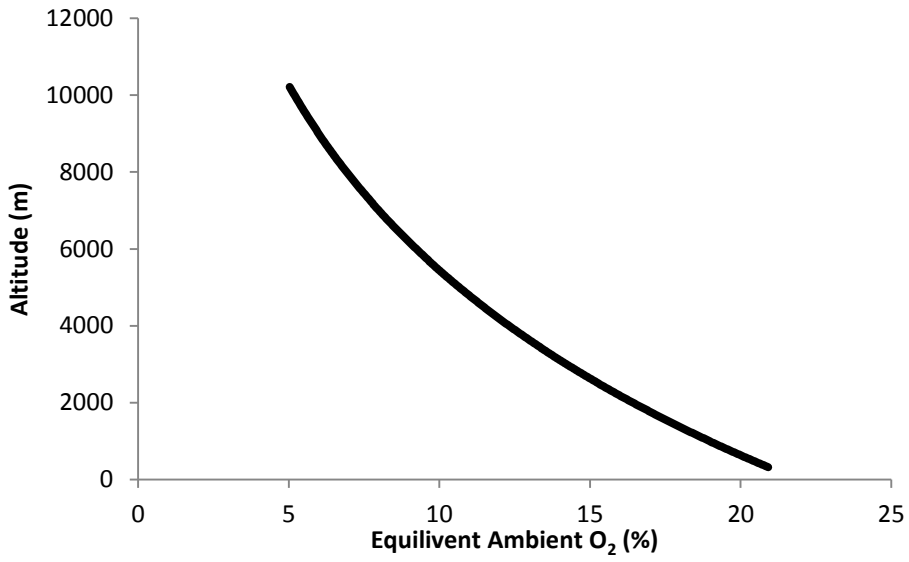

Appendix figure 11: Alterations in barometric pressure (mmHg), PiO_2 and modelled equivalence in F_EO_2 (%) at sea level and increasing altitude. As modelled by Wagner, P (personal communications).

Atmospheric pressure decreases as a function of altitude in a non-linear manner, due to the decreasing force of gravity and subsequent decrease in atmospheric mass applying force below itself. Inspired partial pressure of O_2 (P_iO_2) is a linear function of atmospheric pressure, as given by Daltons Law. Correction for alveolar vapour pressure of water (P_AH_2O), allows for the calculation of equivalence of inspired oxygen (%) as inspired fraction of O_2 (FiO_2).

$$PiO_2 = (P_B - P_AH_2O) \times FiO_2$$

Where PiO_2 represents partial pressure of inspired O_2, PB represents barometric pressure, P_AH_2O the partial pressure of water vapour (47 mmHg at 37 C°) and FiO_2 the fraction inspired O_2.

Two possible checks can be applied. At standard pressure (760 mmHg), standard O_2 content is 20.9 % (FiO_2 = 0.2093), while at an atmospheric pressure of 0 mm Hg, equivalent O_2 content must also be 0 %.

Appendix Fourteen – Comparison of Participant Populations

A comparison of participant descriptive variables is presented below (Appendix table 2). Values are presented here as mean (SD) and are rounded to one decimal place. Direct comparison between Chapters is performed by one-way (Chapter Four, Five, Six) ANOVA, with *post hoc* comparison where necessary in the method of Bonferroni.

Appendix table 2: Comparison of participant descriptors across Chapters.

	Chapter			
	Four	**Five**	**Six**	**p**
Age (years)	26 (2.0)	29.8 (4.7)	27.3 (7.6)	0.386
Height (cm)	178.0 (5.1)	180.3 (7.0)	172.7 (8.7)	0.117
Weight (kg)	72.2 (7.3)	79.0 (9.8)	76.0 (12.3)	0.074
BMI ($kg.m^{-2}$)	22.8 (1.8)	24.2 (1.8)	25.3 (2.6)	0.211
Resting SpO_2	98.0 (0.6)	97.9 (1.1)	98.9 (0.9)	0.102
SpO_2 desaturation (%)^	77.5 (5.5)	84.3 (3.5)	82.7 (7.5)	0.071
Resting HR (bpm)	59.1 (6.9)	71.5 (9.8)	64.3 (9.5)	0.288
O_2 concentration (%)^^	11.9 (0.4)	12.5 (0.3)	12.3 (0.1)	**0.006***

BMI, body mass index; SpO_2, capillary haemoglobin oxygen saturation; HR, heart rate. ^ SpO_2 desaturation represents the mean desaturation over the 2 hours (initial 2 hours in Chapter Five) in 12 % O_2. ^^ Represents mean O_2 % over duration of stimulus (2 hours for Chapters Four, 10 hours for Chapter Five, 2 hours for Chapter Six [12.3 % conditions only]).

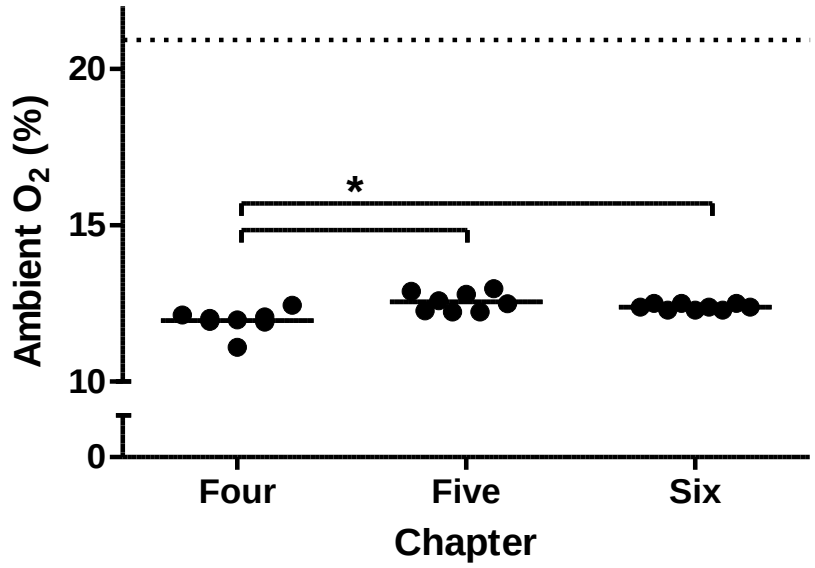

Appendix figure 12: Ambient O_2 exposure (%) for equivalent 12 % conditions by Chapter number (Four, Five, Six). O_2 % over duration of stimulus (2 hours for Chapters Four, 10 hours for Chapter Five, 2 hours for Chapter Six [12.3 % conditions only]). N = 8 individuals for Chapters Four and Five, N = 9 for Chapter Six.